SEDIMENT AND HEAVY METAL DISTRIBUTIONS IN THE AVON-HEATHCOTE ESTUARY, CHRISTCHURCH, NEW ZEALAND

A thesis

submitted in partial fulfilment

of the requirements for the Degree

of

Doctor of Philosophy in Geology

in the

University of Canterbury

by

J.M. Deely

University of Canterbury
1991

TABLE OF CONTENTS

CHAPTER 2

HISTORICAL ANALYSIS OF ANTHROPOGENIC ACTIVITY AFFECTING SEDIMENT AND HEAVY METAL FLUXES TO THE AVON-HEATHCOTE ESTUARY

CHAPTER 4

HEAVY METAL DISTRIBUTIONS IN SEDIMENTS OF THE AVON-HEATHCOTE ESTUARY AND NON-SALINE WATER COURSES DISCHARGING INTO THE ESTUARY

HEAVY METALS IN SUB-SURFACE SEDIMENTS OF THE AVON-HEATHCOTE ESTUARY

CHAPTER 6

METHODS AND QUALITY CONTROL IN ANALYSIS OF SEDIMENT CORES

LIST OF FIGURES

List of Figures continued

List of Figures continued

List of Figures continued

List of Figures continued

LIST OF TABLES

List of Tables continued

List of Tables continued

List of Tables continued

ACKNOWLEDGEMENTS

I would like to thank the following people for there assistance with my thesis: my husband Paul (for patience, and helping with drafting, computing, field work and calculations); Dr J.E. Fergusson (for assistance with methodology, providing laboratory space, chemicals, instruments, and apparatus through the Chemistry Department of the University of Canterbury, proof reading drafts, and typing Table 2.1); Dr S.D Weaver (for approving funds for equipment, providing laboratory space and instrumentation through the Geology Department of the University of Canterbury, and editing drafts); Dr D.W Lewis (for proof reading); Dr J. Robb of the Christchurch City Council (for funding the ^{14}C dating of sediments through the Christchurch Drainage Board, and supplying extensive references and data); Dr M. Matthews of the National Radiation Laboratory (for providing chemicals and apparatus, expertise and instrumentation for the ^{210}Pb study); Dr M. McGlone of New Zealand Department of Scientific and Industrial Research (DSIR, Botany) (for preparation and scientific analysis of pollen diagrams); Mr Len Brown of DSIR (Geology) (for providing data and figures); Professor J.J. Deely (for assistance with statistical analyses); Mr Arther Nicholas, Kerry Swanson and Stephen Brown (for continuous technical assistance throughout the duration of the project); the following students for field assistance: Mark Lawrence (Dr), S. Matthews, D. Barrel, M. Warnes, and John M. Deely; and the following committees who provided scholarships that helped finance travel and living expenses: University Grants Committee (UGC), McKee Trust, Canterbury Branch of the NZ Royal Society, Mason Trust, and New Zealand Royal Society.

ABSTRACT

Shallow cores from the Avon-Heathcote Estuary possess the following four distinct sedimentary units: 1) medium fine sand (Unit A), 2) muddy fine sand (Unit B), 3) slightly sandy mud (Unit C), and 4) muddy fine sand (Unit D).

A combination of historical records, ^{14}C dates, a ^{210}Pb profile, and pollen diagrams disclose the age and sedimentation rates of the units as follows. Unit A was deposited in shallow oceanic waters before the estuary formed and ceased accumulating around 450 years B.P (approximately 1540 AD). Unit B was deposited after the estuary formed at rates of 0.15cm per year (from 1540 AD to 1850 AD) and 0.27cm per year (from 1850 until 1925). From 1925 until around 1950, a mechanical river sweeper swept high quantities of mud from the Avon and Heathcote rivers to the Avon-Heathcote Estuary. During this period Unit C accumulated rapidly (6 to 12 cm per year) in the estuary. Since 1950, Unit D sand has been accumulating at a rate of approximately 0.5cm per year.

X-Ray Diffraction and petrographic analyses of sediments show that individual grain sizes (sand >63μm, silt 4-63μm, and clay 4μm) of all units contain homogeneous mineralogy, which is similar to that in sediments of both the Travis Swamp and Saltwater Creek Estuary. The mineralogical assemblage and grain size distributions indicate that Avon-Heathcote Estuary sediments are derived principally from local deposits of Post-glacial loess, which are in turn derived from the Mesozoic Torlesse rocks (situated along the western edge of Canterbury).

Flame Atomic Absorption Spectroscopy analyses of total heavy metal extracts from the sediments indicate that the urbanisation of Christchurch has had and is having a significant impact on heavy metal levels in the Avon-Heathcote Estuary. A blackened layer of sediment near the top of Unit B (corresponding to the period 1900 to 1925) is moderately enriched in heavy metals and organic matter. At the time this black sediment was deposited, Christchurch was the major "iron-working" district of New Zealand. High quantities of heavy metals and organic matter entered the estuary with industrial and organic wastes, and ash and soot particles carried in river and drain waters.

Unit C sediment is not enriched in either heavy metals

or organic matter despite the high flux of industrial and domestic wastes to the estuary between 1925 and 1950. The rapid sedimentation rate and higher clay content of Unit C diluted heavy metal and organic matter concentrations as the mud accumulated.

Heavy metal and organic matter levels increase from the base of Unit D up to a point corresponding with 1972.

Immediately above the 1972 level, metal and organic matter concentrations drop in the sediments which reflects the sudden removal of most industrial and domestic wastes from the estuary system. Since this brief decline, organic matter concentrations have slowly increased in sediments of most areas of the estuary. The high quantity of algae and nutrients discharged from the Christchurch City Council Sewage Treatment Plant is largely responsible for the high levels of organic matter in the sediments.

The Heathcote Basin is the major sink for Pb, Zn, Cu, Cr, organic matter, and mud derived from the rivers, City Outfall Drain, and sewage ponds.

Zinc and Pb are the most significantly enriched metals in post-1972 sediments of the Avon-Heathcote Estuary. Chromium and Cu are also enriched in some areas of the estuary.

Total heavy metals were analysed (by Graphite Furnace Atomic Absorption Spectroscopy) in suspended sediment and water of the major non-saline water systems entering the estuary. The results reveal that at present the main anthropogenic sources of metals to the estuary are stormwater (Pb, Zn) and the treated sewage effluents (Zn, Cr, Cu).

Generally Fe, Mn, and Ni are not enriched in the Avon-Heathcote Estuary. Some Fe and Mn enrichment near the City Outfall Drain may be due to preconcentration of these metals in sulphide precipitates. A considerable proportion of total Fe in the Avon-Heathcote Estuary appears to be precipitated during estuarine mixing.

INTRODUCTION

Many heavy metals (Fe, Mn, Cr, Cu, Zn, and Ni) are essential to plant and animal life. If heavy metals are undersupplied then biota may become deficient in essential metals needed for metallo-enzymes, such as Fe in haemoglobin. However, high concentrations of some metals (such as Pb, Cu, Cd, and Zn) are toxic to organisms by inhibiting many essential life functions (Nieboer and Sandford, 1984).

Due to the useful physical properties of heavy metals such as electrical conductivity, hardness, and durability they have been extensively utilised in industry, especially since the Industrial Revolution in the late 1800's. Hence, water and sediment metal concentrations have increased markedly over the last 100 years, which has upset many natural aquatic ecosystems (Salomons and Forstner, 1984).

Because estuaries fill with sediment they contain a record of sediment disturbances and changes in drainage brought about by urbanisation of their catchments. In addition, changes in heavy metal fluxes related to anthropogenic activity may be recorded in sediments.

Sediment fluxes are influenced by flooding, land clearing, building, farming, market garden development, and accidental fires. Hence, sedimentation rates vary considerably throughout the history of an estuary (Schubel and Meade, 1977). As a result, heavy metal levels are preconcentrated and diluted to different degrees in an estuary's sedimentary profile depending on the history of **both sediment disturbances and metal-producing activities** in the surrounding area. Therefore, it is impossible to interpret an estuary's history of heavy metal contamination from chemical analyses alone. Knowledge of grain size distributions, mineralogy, sedimentation rates, and anthropogenic activity is essential when studying heavy metals in sediments (Cauwet, 1987).

New Zealand has a low population (3.5 million) and a

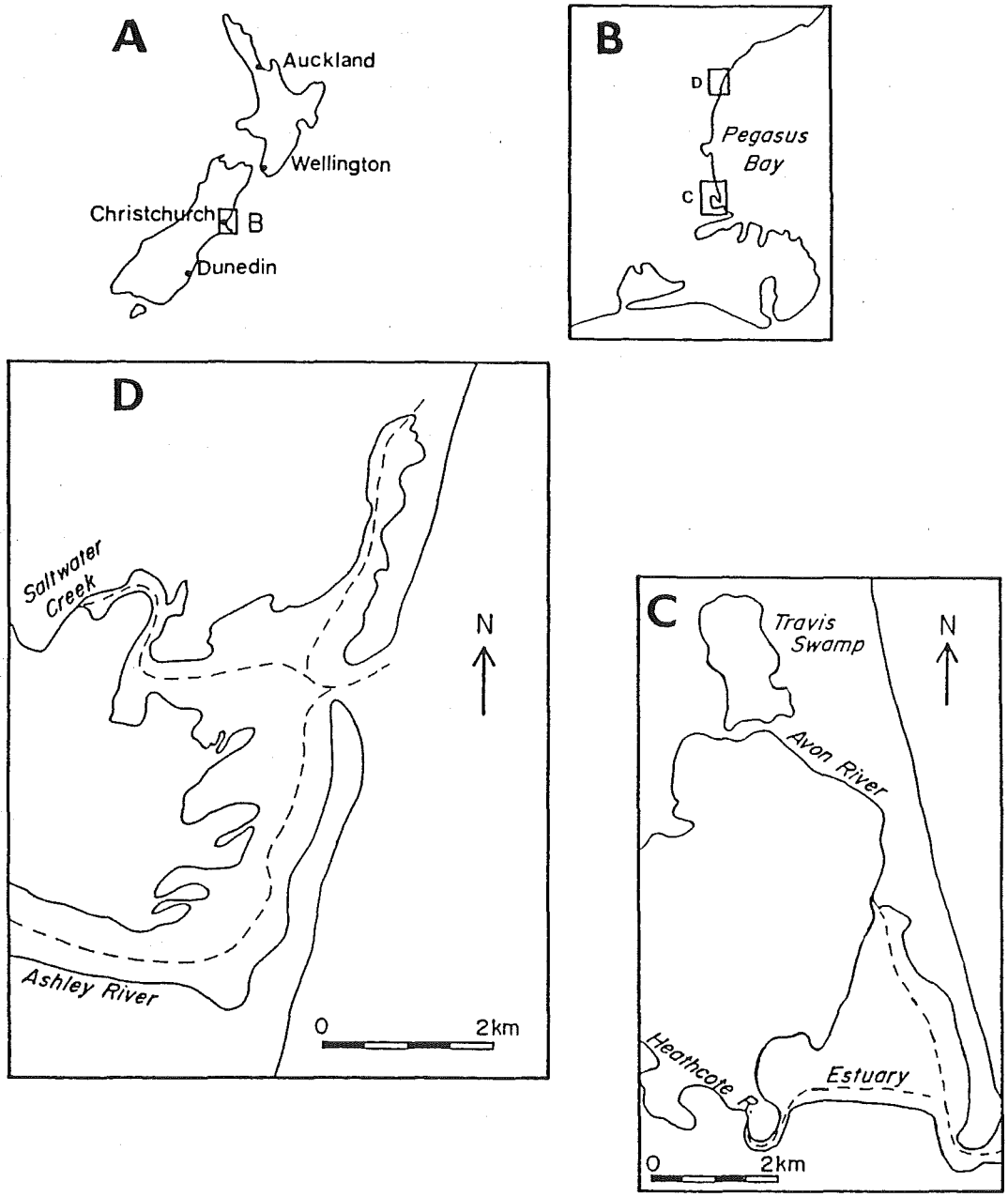

Fig. 1.0a Location Maps. A, New Zealand. B, Pegasus Bay. C, Avon-Heathcote Estuary and Travis Swamp. D, Saltwater Creek Estuary.

land mass about the size of Great Britain, hence heavy metal pollution of harbours, estuaries and rivers is not as serious as in many other countries (Smith, 1986). However, near the major cities, elevated metal concentrations have occurred in localised areas as a result of uncontrolled industrial discharges, geothermal activity, mining, sewage effluents, and urban stormwater discharge.

Christchurch is the third largest city in New Zealand (population 300,000). The Avon-Heathcote Estuary borders the eastern suburbs of Christchurch City and receives non-saline water from the Avon and Heathcote Rivers, a major stormwater drain (City Outfall Drain), and treated effluent from the Christchurch City Council (Christchurch Drainage Board) sewage ponds (Fig 1.0a and b).

Macpherson (1978) established a geochronology of sedimentation in the Avon-Heathcote Estuary. Pre-estuarine ocean sand (Unit A) ceased accumulating in the area of the estuary 1000 years ago. From around 1000 years ago until 1850 slightly muddy estuarine sand (Unit B) was deposited in the estuary. Between 1850 and 1875, approximately 25 cm of mud (Unit C) accumulated throughout the estuary as a result of land clearing by early settlers. According to Macpherson, during this period the tidal compartment decreased by 30%.

After comparing bed level surveys in 1920 and 1962, Macpherson concluded that the estuary bed has lost over 1m of sediment since 1920. Macpherson thought that a combination of rapidly increasing tidal compartment and intense bioturbation eroded sediment deposited during the early period.

Due to a lack of supporting historical data, Macpherson's methods have suffered criticism by more recent workers. Findlay (1984) and Kirk and Findlay (1988) produced data indicating that the tidal compartment of the Avon-Heathcote Estuary has steadily increased since the settlers first arrived. These workers also found no evidence of erosion or deposition at the estuary inlet and

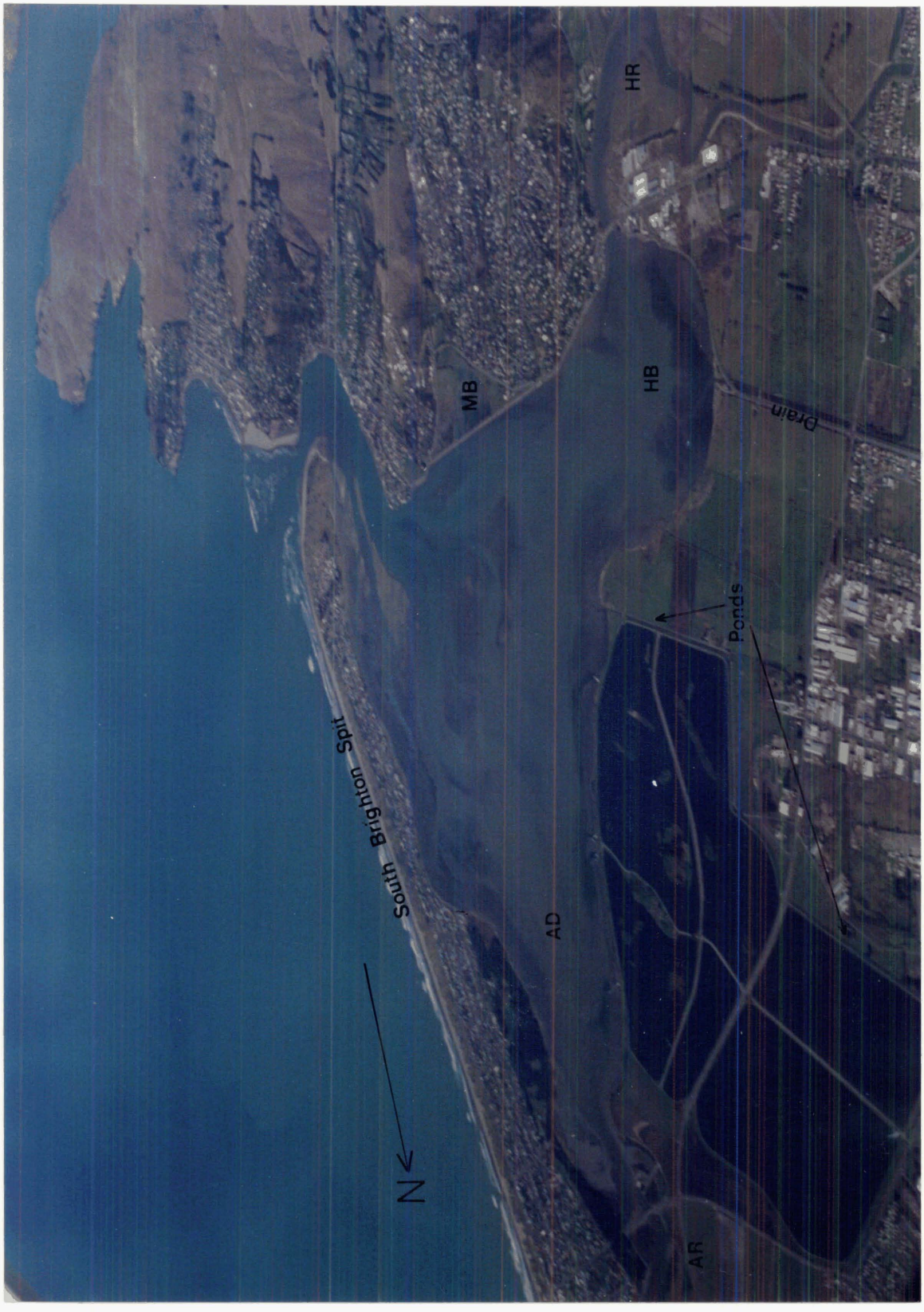
HR
MB
HB
Drain
Ponds
South Brighton Spit
N
AD
AR

Fig. 1.0b View looking southeast across the Avon-Heathcote Estuary at mid tide, April 13 1991 (L.J. Brown N.Z. Geological Survey, pers. comm.). During estuarine mixing the tide prevents mud carried in the river waters from leaving the estuary. Most shoaling can be observed along a band extending from the mouth of the Avon River, across the western shores, to the Heathcote Basin.

AR,	Avon River
AD,	Avon Depository
HR,	Heathcote River
HB,	Heathcote Basin
MB,	McCormacks Bay
Drain,	City Outfall Drain
Ponds,	Christchurch City Council Sewage Oxidation Ponds

the toe of South Brighton Spit before 1920, and little change after 1950. Hence, some doubt has arisen over the geochronology established by Macpherson.

European settlement began in Christchurch in 1850 AD and industrial activity dates back to the 1860's. In fact Christchurch was the main industrial centre of New Zealand at the turn of the century (Morrison, 1948). Many untreated wastes from metal workers were discharged into the Heathcote River at the time. If the estuary is rapidly eroding as claimed by Macpherson (1978), then contaminated sediments deposited before 1900 may be brought to the surface creating a widespread pollution problem. Heavy metal studies to date on surface sediments in the rivers (Anderson, 1985; Hulse, 1983, and Purchase, 1983), City Outfall Drain (Hay, 1988), and estuary (Burgess, 1985; Christchurch Drainage Board (CDB), 1988; Purchase, 1983; and Rodrigo, 1989) generally show moderate to severe contamination adjacent to industrial and stormwater effluent discharge points. However, there is insufficient information available to tell whether or not an ancient contaminated layer is either being exposed by erosion or exists near the surface.

The principal goals of this thesis are to 1) redetermine the geochronology of the Avon-Heathcote Estuary, 2) determine the sedimentary environment of the estuary throughout the history of Christchurch, and 3) investigate the impact that the urbanisation of Christchurch has had and is having on heavy metal and organic matter concentrations in the sediments of the Avon-Heathcote Estuary.

Because Christchurch's history is very recent (less than 150 years), considerable historical data (such as photographs, written documents and observations by elderly people) are available on changes in land use, siltation (rapid mud deposition), and industrialisation of areas adjacent to the estuary. Hence an analysis of historical records is included as part of this thesis.

After a brief review of sediment and heavy metals in estuaries (Chapter 1), a synthesis of **Historical data** is presented (Chapter 2) to establish an accurate base for comparison of **geological and heavy metal data.** Geological analyses of sediment cores from the Avon-Heathcote Estuary, Travis Swamp and Saltwater Creek Estuary are presented in Chapter 3. The following investigations are discussed: grain size distributions, mineralogical studies, ^{14}C dates, a ^{210}Pb profile, and pollen diagrams. These geological studies establish the geochronology and sedimentological nature of the estuarine environment throughout Christchurch's history.

Heavy metal (Pb, Cu, Ni, Zn, Fe, Mn, Cr) and organic matter concentrations in the Avon-Heathcote Estuary sediment profiles (Chapter 4) are interpreted in light of the historical synthesis, sedimentation rates, mineralogy, and grain size distributions presented in chapters 2 and 3.

Analyses of heavy metals in the suspended sediment and water (dissolved phase) of the rivers and drains entering the estuary are also discussed in Chapter 4. This study has determined the main present day contaminant sources.

Two cores from the Travis Swamp and Saltwater Creek Estuary (Fig. 1.0a) are included in geological and heavy metal studies as background references.

A synthesis of the effects of urbanisation on sedimentation and heavy metal distributions in the Avon-Heathcote Estuary is presented in Chapter 5.

Quality control of core studies is assessed separately in Chapter 6.

CHAPTER 1

HEAVY METALS AND SEDIMENTS IN ESTUARIES: A REVIEW

An intricate combination of physical, chemical, biological, and anthropogenic processes affect heavy metal distributions in estuaries. Hence, it is important that scientists studying heavy metals in any estuarine medium (such as biological tissue, sediment, and water), understand the influences of each of the above processes. The first chapter of this thesis presents a review of heavy metals and sediments in estuaries considering anthropogenic, hydrodynamic, chemical, and biological effects. Estuaries are discussed, with regard to 1) hydrography and sedimentation patterns, and 2) heavy metal behaviour from source through transportation, estuarine mixing, deposition, diagenesis, and bioavailability.

1.1 HYDROGRAPHY AND SEDIMENTATION OF ESTUARIES

The slow rise in sea level over recent millennia has caused the sea to invade coastal deposits where wave action and littoral drift have formed bars across river mouths. The resulting embayments are known as estuaries. An estuary is defined as "a semi-enclosed coastal body of water freely connected to the ocean within which seawater is measurably diluted by freshwater runoff from land" (Schubel and Meade, 1977).

Once estuaries are formed, they are filled rapidly with sediments derived from shore, river, wind, sea, and biological activity. Consequently, estuaries have a short life during which they are constantly altered by deposition and erosion of sediments. Estuaries also suffer extreme modification during floods and small changes in sea level. Floods can cause greater river discharge into estuaries in

days than occurs in years under normal conditions (Aston and Chester, 1976). In the past few 100 years the rate of sediment input has increased as a result of human activity; consequently the lifetime of modern estuaries may be shortened considerably.

Sources of estuarine particulate matter include (1) oceans (diatom and foram skeletons, and coastal clay minerals and sand), (2) rivers carrying suspended sediments from the catchment area (oxyhydrates, clay minerals, and organic matter principally from plants), and (3) authigenic precipitates; particulate matter formed during estuarine mixing, such as Fe and Mn oxides (Salomons and Forstner, 1984). These sources introduce trace metals into estuaries in solid, colloidal, and dissolved forms (Aston and Chester, 1976).

The mixing of fluviatile (10^{-3}% salinity) and sea (3.5% salinity) water in estuaries often causes layering of the two water types which influences biological processes and mechanisms of sedimentation, precipitation, and flocculation. In turn, water layering and tidal currents affect the transport characteristics of sediments and hence the sediment grain size distributions.

1.1.1 Fresh and Salt Water Mixing in Estuaries

Mixing in estuaries results from a combination of river, wind, and tidal action. The degree of mixing depends on the magnitude of river flow, tidal flow, and upon the geometry of the basin that contains the estuary. Changes in any of these factors may produce changes in the estuarine circulation pattern, thereby altering the sedimentation pattern. A sequence of estuary types exists from poorly mixed and stratified (layered) to thoroughly mixed and homogeneous. Intermediate types include partially mixed and vertically mixed (Aston and Chester, 1976; Salomons and Forstner, 1984; Schubel and Meade, 1977). Estuaries continually vary in type as conditions

change. At any given time a number of different mixing types may be observed within different segments of the same estuary. An estuary will change from stratified to homogeneously mixed as the magnitude of the tidal flow increases relative to the river flow, or as the width of the basin increases relative to the depth (Meade, 1972).

When the ratio of width to depth is small in an estuary, the ratio of river flow to tidal flow is relatively large and the encroaching seawater forms a wedge under the less dense freshwater. The river-dominated saltwedge estuary exhibits very little mixing of seawater and freshwater. The freshwater flows downstream above the saltwedge, while saline water in the saltwedge flows either upstream or downstream depending on the tide. The net particle movement is landwards. Fine suspended particles that are brought into the estuary by the river settle into the lower saline layer and are brought back upstream by the slow net landward flow of the lower layer and accumulate in the vicinity of the tip of the wedge.

If the tidal flow increases relative to river flow so that the tide is more dominant than the river, the added turbulence provides the mechanism for erasing the saltwedge. Therefore, estuaries grade from saltwedge to homogeneous where tidal flow overwhelms the effect of the rivers. In homogeneous estuaries river movement is more or less symmetrical about the main axis of the estuary with slow net seaward flow at all depths. In such estuaries, there is also an accumulation of fine suspended sediment in the landward reaches between the upstream and downstream limits of the salt intrusion. In mixed estuaries, the concentration of suspended matter is greatest within the turbidity maxima, which is partly due to periodic resuspension of the bottom sediments by tidal scour and estuarine circulation.

The most rapid shoaling in any estuary is normally between the flood and ebb positions at the limit of the salt intrusion or where the upstream flow of the lower

layer is interrupted by an entering tributary (Fig. 1.0b). Fine suspended particles that are brought into estuaries by rivers are carried back upstream to the zone of shoaling by the net landward tidal flow.

In general, for any estuary the sediment trapping efficiency increases as the river flow increases relative to the tidal flow, or as depth increases. Generally most fluvial sediment is introduced when the river flow is high (when the trapping efficiency is greatest). When the river flow subsides and the relative importance of the tidal flow increases, the estuary shifts its circulation pattern toward one of greater mixing and consequently the sediment is redistributed, with losses to open water (Schubel and Meade, 1977).

1.1.2 Sediment Transport Via Rivers

River discharge reflects rainfall in small streams and seasonal changes in large rivers. Sediment transportation parallels this pattern (Burton, 1976; Salomons and Forstner, 1984). The nature and amount of sediment depends on the yield of the catchment area and the carrying capacity of the flow. A river carries sediment from both its catchment area and from erosion in its bed. The different sources contributing to the sediment load of a river during high discharge are also reflected in its trace metal content. During estuarine mixing coarse particles retain their individual sizes while their depositional behaviour is governed by mixing hydrodynamics. Whereas the behaviour of the suspended fraction is modified by processes which cause coagulation and disaggregation of flocculated material.

Dispersed clay particles carried by rivers are unflocculated and negatively charged, and surrounded by a double layer of hydrated cations. In saline waters an increase in the total concentration of ions tends to decrease the thickness of the double layer; hence,

destabilising it (with possible charge inversion) allowing flocculation (Aston and Chester, 1976; Forstner and Wittmann, 1981). Flocculation occurs at varying salinity, which partly depends on the concentration of the suspended sediment. Other factors that contribute to flocculation include (1) adsorption of positively charged particles, (2) compression of the electrical double layer, (3) formation of interparticle bridges by adsorbed material, and (4) enmeshment of clay and hydroxide particles. The different clay minerals vary in their tendency to coagulate. The order of clay mineral settling is usually determined by grain size with the coarsest minerals settling first. The order is frequently kaolinite followed by illite, chlorite, and montmorillonite respectively (Burton, 1976; Horowitz, 1985).

1.1.3 Human Impact on Estuarine Sedimentation

Forest clearing, by settlers, over the last few centuries has contributed enormous sediment loads to rivers, which has caused estuaries and deep harbours to fill (Fyfe, 1984; Lush, 1984).

Conversion of forest to farmland can increase sediment runoff by a factor of 1000, while forest fires can increase erosion up to 7000 times, and changing grasslands to crops can lead to a 100 fold increase in erosion (Fyfe, 1984). Hence, soil cultivation is estimated to be responsible for 95-99% of erosion in agricultural areas (Forstner and Wittmann, 1981).

During periods when houses and highways are constructed, the soil is distributed and left exposed to wind and rain. When storms occur, flushing of loose soil causes sediment concentrations, in water systems, 100-1000 times higher than yielded by undisturbed soil. Mining and dam construction also increase sediment loads.

Anthropogenically accelerated drainage and water flow affects estuaries by 1) changing sedimentation rates, 2)

shifting locations of erosional versus depositional zones, 3) altering the relative proportion of the different types of particulates that settle, and 4) increasing tidal prisms, hence upsetting flushing regimes (Lush, 1984).

In addition, agricultural runoff and municipal sewage effluents contribute nutrients to streams and estuaries. These nutrients promote the growth of microscopic animals and plants. Shells of dead organisms persist and become deposited which enhances sedimentation rates (Schubel and Meade, 1977). Such increased sedimentation rates, necessitate frequent dredging of estuaries to maintain navigation channels.

1.2 SOURCES OF HEAVY METALS

1.2.1 Natural Sources of Heavy Metals

The major source of heavy metals to estuaries is geological weathering of rocks in the catchment area of the rivers that enter estuaries (Leenaers, 1988).

Transition elements such as Cr, and Ni may substitute for Fe and Mg in rocks such as gabbros and basalts. Occasionally Pb may replace K in feldspars whereas Mn, Zn, Cr and Cu may replace Fe, Mg, and Al in iron silicates such as biotite. Zinc commonly replaces Fe and Mn in biotite and amphibole, whereas Cu is more likely to be enriched in olivine and pyroxene. The concentrations of Ni and Cr in mafic rocks can be 100-1000 times higher than granitoids, whereas granites are enriched up to 50 times in Pb compared with ultramafic rocks due to the high feldspar content. The above substitutions are possible because of the similar ionic radii of the different metals (Drever, 1982; Salomons and Forstner, 1984). (Heavy metal bonding in detrital sediments is discussed in Appendix 1.0, Section A1.1.3.1)

Metal concentrations are also naturally elevated in areas which contain mineralised zones (characterised by

metal ores) and geothermal areas. Oxidation of metal sulphide minerals in low pH waters may release significant concentrations of Zn, Pb, Cu, Cd, As and Hg into streams (Hendy, 1988).

It is important to note that the bulk of detrital trace metals never leaves the solid phase from initial weathering to ultimate deposition. In fact, 60-98% of total Zn, Cu, Pb, Cr, and Ni are held detritally in sulphitic and oxidic minerals (such as magnetite, pyrite, ilmenite, malachite, and chromite) and ferromagnesial silicates (such as amphibole, chlorite, pyroxene, and garnet (Hem,1989; Salomons and Forstner, 1984). Hence, detrital heavy minerals from magmatic, metamorphic, and sediment source rocks, which are generally resistant to weathering, may significantly enrich the heavy metal composition of uncontaminated estuarine sediments.

1.2.2 Anthropogenic Sources of Heavy Metals

1.2.2.1 Industrial Wastes

The main anthropogenic sources of heavy metals to estuaries include; industrial wastes, sewage sludge, and stormwater runoff from cities and towns adjacent to the estuaries (Angelidis and Grimanis, 1989; Bordalo Costa and Penedo, 1989; Drever, 1982; DeLaune et al., 1989; Finney and Huh, 1989; Forstner and Wittmann, 1981; Hamilton, 1989; Malm et al, 1989; Stoffers et al, 1986). These sources also carry aerosol particles which contribute to their heavy metal loads.

The multipurpose usage of heavy metals often leads to difficulties in tracing the source of water pollution (Nriagu and Pacyna, 1988). The main industrial sources of heavy metals are summarised in Table 1.1.

Table 1.1 Main Industrial Sources of Heavy Metals

1.	Pulp, paper and board mills: Cr, Cu, Zn, Pb, Ni.
2.	Organic petrochemicals: Cd, Fe, Cr, Pb, Zn.
3.	Fertilisers: Cd, Cr, Cu, Fe, Pb, Ni, Zn.
4.	Basic metal foundries: Cd, Cr, Cu, Fe, Pb, Ni, Zn.
5.	Motor vehicles: Cd, Cr, Cu, Ni, Pb.
6.	Flat glass, cement, asbestos works: Cr and others.
7.	Textile production: Cr.
8.	Leather tanning: Cr.
9.	Steam generation power plants: Cr.
10.	Steel manufacture: Fe, Cr, Mn.
11.	Fuel (such as coal burning): Cu, Ni, Cd, Zn, Mn, Fe.

Globally the most important single industrial source of heavy metals is the electroplating industry, which is often responsible for input of wastes containing 10-100's ppm (μg/g, part per million) Cu, Cr, Ni, Zn, and Cd into estuaries and harbours (Forstner and Wittmann, 1981). Leather tanning and textile production are an important source of Cr, whereas battery manufacturer is a significant source of Pb (Smith, 1986; Stoffers et al, 1986). Two other important sources often ignored are disposal of ash residue from coal combustion and refuse incineration (Nriagu and Pacyna, 1988).

Mining processes release metals by breaking up sulphide minerals, allowing oxygen attack. Oxidation of sulphide ions releases heavy metals. Metals are often leached from such deposits into groundwater, where they find their way into estuaries via rivers (Drever, 1982).

1.2.2.2 Domestic Effluent

Although industrial wastes contain large quantities of heavy metals, domestic effluent is the largest single source of elevated metals to estuaries by virtue of its

shear volume (Forstner and Wittmann, 1981).

Table 1.2 Average Heavy Metal Composition of Sewage Sludge Compared to Crustal Values (μg/g)

Metal	Sludge (s)	Average crust (c)	Ratio S/C
Ni	60	80	0.8
Cr	240	200	1.2
Cu	700	45	15
Pb	450	15	30
Zn	1800	65	40
Cd	10	0.2	50

(Forstner and Wittmann, 1981; Nriagu and Pacyna, 1988)

Generally, Ni and Cr are not elevated in sewage sludges, whereas Cu, Pb, Zn, and Cd may be highly enriched (Table 1.2). Heavily contaminated rivers may contain as much as 30% sewage particles (Forstner and Salomons, 1980).

1.2.2.3 Stormwater Runoff

Urban stormwater is a major source of heavy metals. During heavy rainfall stormwater often contains shock loads of contaminants 100-1000 times higher than other wastewater. Stormwater is affected by street dust, climate, season, and land use. During storm periods atmospheric emission deposits (such as Pb from petrol, and Cr, Mn, Cd, Cu, and Zn from coal combustion) are washed from surfaces into stormwater. De Laune et al, (1989) found Pb levels as high as 1000 ppm in Lake Capitol Sediments (Louisiana) at sites which receive runoff from interstate highways. Also, corrosion of Cu, and Zn roof fittings are an important source of metal enrichment to stormwater (Drever, 1982).

In densely populated areas a considerable amount of

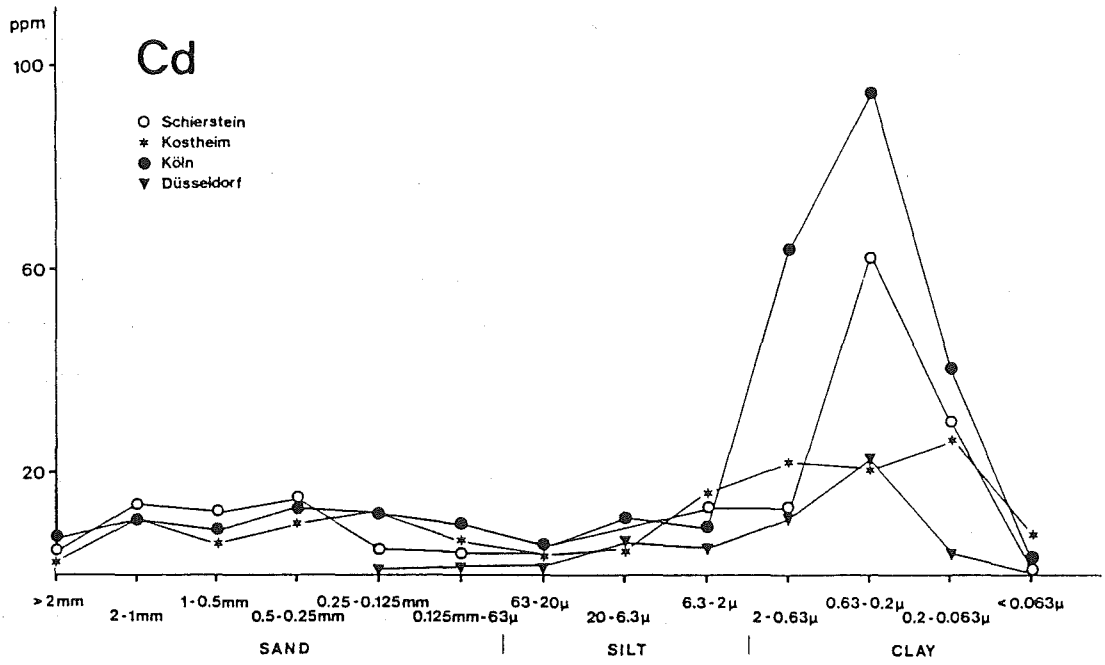

Fig. 1.1 Cadmium Concentration versus Grain Size in West German Rivers (Forstner, 1980).

atmospheric precipitation of heavy metals may also enter estuaries via the sewage system, thus rendering a clear differentiation between the influence of direct sewage and stormwater runoff impossible (Malm, et al 1989).

In general the current atmospheric flux of Cu, Pb, Zn to water systems in developed countries is lower than in 1975 due to clean up measures such as the general reduction in the consumption of Pb-rich gasoline (Nriagu and Pacyna, 1988).

1.3 GRAIN SIZE DISTRIBUTION OF HEAVY METALS

The major part of the fluviatile sediment entering an estuary arrives in the suspended grain size range (<63μm). Marine sediment typically shows a bimodal grain size distribution which peaks at around 2μm and 10-20μm (Horowitz, 1985). The 10-20μm fraction is normally the predominant grain size range but contributes approximately 10% of the total heavy metals (Ackermann et al, 1983; Horowitz, 1985). The less than 2μm fraction usually represents <20% of the bulk sediment and has the highest concentration of heavy metals and organic matter (Fig.1.1). Figure 1.1. shows Cd concentrations found in different grain sizes of various studies in (West) Germany (Forstner, 1980). The curves show uniform Cd levels in the coarse fractions with a 10 fold increase in the less than 2μm fraction. The high concentrations of heavy metals in the fine fraction suggests that heavy metals are transported under conditions of relatively low discharge and are deposited in low energy areas of estuaries (Forstner, 1989).

The phenomenon of heavy metal concentration and organic matter content increasing with decreasing grain size is a well documented relationship (Ackermann et al, 1983; Cauwet, 1987; Forstner, 1989; Forstner and Salomons, 1980; Forstner and Wittmann, 1981; Glasby et al, 1988; Horowitz, 1985; Hornung et al, 1989; Krumgalz, 1989;

Nicolaidou and Nott, 1989; Scoullos, 1986; Stoffers et al, 1986; and Taylor, 1986). A decrease in grain size corresponds to an increase in surface area. Generally, sand and silt sized quartz, feldspar, carbonate, heavy minerals, and rock fragment grains are more or less rounded. Sands and silts of this nature have surface areas of 10-100 cm^2/g and 100-1000 cm^2/g respectively, whereas clay minerals have surface areas of the order of 10-100m^2/g (Horowitz, 1985). While detrital sand and silt grains are rounded in shape, most fine grained clay minerals have a flat platy structure, which is responsible for their extremely high surface charge and cation exchange capacity. The high cation exchange capacity is governed by broken chemical bonds around the edges of minerals and charge imbalances caused by Al^{3+} substitution for Si^{4+} (Appendix 1.0, Section A1.1.3.2).

Fine grained Mn and Fe oxides, and humic substances also have large surface areas of around 300 m^2/g and 1900 m^2/g, respectively, and are negatively charged under normal conditions in estuaries. Hence, these substances frequently adsorb heavy metals and may be, in turn, adsorbed onto the surfaces of clay minerals. More often the Fe and Mn oxides and organic substances attached to the clay minerals are the sites of heavy metal adsorption (Forstner, 1989). (Heavy metal bonding in clay minerals, Fe and Mn hydroxy compounds, and organic matter is discussed in detail in Appendix 1.0, Section A1.1.3)

There is a decrease in heavy metal content in very small grains, below 0.2μm (Fig.1.1), which is not fully understood. It is thought to relate to reduced metal adsorption on partially crystallised and amorphous minerals (Forstner and Wittmann, 1981).

Occasionally high heavy metal concentrations are found in the fine sand and silt fractions, which is usually caused by heavy mineral enrichment (Drever, 1982). On rare occasions high concentrations of trace metals and organic matter are found in the medium coarse sand fraction (>250

μm). The cause is often agglomeration of fine grained material, which formed during drying procedures (Krumgalz, 1989).

1.4 HEAVY METAL BEHAVIOUR DURING SEA AND RIVER WATER MIXING IN ESTUARIES

There are three main processes operating in estuaries during mixing. These include, (1) precipitation of dissolved iron as $Fe(OH)_3$, (2) metal release from solid phases (e.g. organic matter) to solution and (3) uptake of released metals onto solid phases (Balls, 1989; Burton, 1976; Forstner and Wittmann, 1981; Glegg et al, 1988; Morris, 1986; Salomons and Forstner, 1984; and Windom et al, 1988).

Iron (II) from rivers is oxidized to Fe (III) with increasing salinity and precipitates colloidally as $Fe(OH)_3$ as the pH increases above 7.5. Depending on the hydrodynamics of the estuary, $Fe(OH)_3$ colloids will either deposit or escape to the open ocean. Manganese is also precipitated as hydroxides but to a lesser extent.

During estuarine mixing, rapid flocculation and oxidation of organic matter leads to large-scale removal of sorbed heavy metals. Metals are desorbed due to dilution effects (diffusion from high metal concentration to low metal concentration) and complexation with chloride and other anions. In addition, Na and Mg ions from sea water may exchange with trace metals adsorbed on the surfaces of suspended matter. The order of desorption is Cd>Zn>Mn>Co>Cu>Cr.

At the same time that metals are desorbed from suspended matter, the slightly rising pH (due to the influence of the more alkaline seawater) encourages metal hydroxide precipitation (or co-precipitation with $Fe(OH)_3$). There is an increase in suspended matter at the turbidity maximum due to landward movement of bottom sediments by incoming tides (Fig. 1.0b). This resuspended estuarine

sediment rapidly adsorbs the heavy metals released from riverborne particulates. Consequently, the desorption of heavy metals from incoming particulates is often cancelled by uptake on resuspended sediments and Fe hydroxide precipitates (Balls, 1989; Morris, 1986).

After sediment and precipitated $Fe(OH)_3$ and $Mn(OH)_3$ are deposited they may enter a reducing environment where heavy metal remobilisation and further concentration may occur (see section 1.6). The metals released into overlying water may be washed by the tide to the turbidity maximum.

Metal remobilisation is also important when waste water is discharged to estuaries or rivers. In such cases surface desorption of metals occurs during oxidation of waste organic matter and metal sulphides. The high dilution ratio influences metal desorption. Subsequent uptake by Fe hydroxides and suspended sediment often results in metal enrichment in front of sewage outlets.

In summary: the degree of trace metal desorption and uptake by sediments, and hydroxides varies depending on differences between estuaries in (1) estuarine hydrodynamics (2) chemical composition of seas and rivers, (3) concentration of flocculated colloids, (4) release and uptake of dissolved trace metals by bottom sediments, (5) degree of organic matter decomposition in sediments and the subsequent release of trace metals into overlying water, (6) biological uptake of trace metals, (7) quantity of waste effluent discharged into the system and (8) other parameters such as pH, Eh, salinity, turbidity, and water flow.

1.5 HEAVY METAL DISTRIBUTIONS IN SURFACE SEDIMENTS

Generally speaking, surface sediment metal variation across estuaries and along river courses acts as a guide to local pollution centres (Forstner and Wittmann, 1981).

In recent years organic matter levels have risen in estuaries due to increased runoff containing nutrient rich

substances such as fertilizers, detergents, and sewage effluents. These substances are high in nitrogen and phosphorous, which has resulted in an increase in organic life (eutrophication (Lush, 1984)). Actively feeding algae and zooplankton concentrate relatively large quantities of heavy metals adsorbing what they require and excreting the remainder as faecal pellets. Hence, deposition of faecal pellets and decaying organic tests has led to 1) elevated heavy metals in sediment, and 2) an increased demand for oxygen in the surface sediment (Lush, 1984; Valenta et al, 1986).

The decline in heavy metal and organic matter content observed in a seaward direction from estuary heads to ocean entrances is due to a combination of (1) remobilisation of metals from surface sediments and transport upstream with tidal currents, (2) mixing of high metal bearing fluviatile silts and clays with increasing quantities of low metal bearing coarse sediments in a seaward direction, and (3) some loss of adsorbed metals from fluviatile solid particles in transit through the turbidity maximum before deposition, and (4) location of point sources of metal entry from municipal and industrial sewers normally near estuary heads (Fernex et al, 1986; Nicolaidou, 1989; and Salomons and Forstner, 1984).

1.6 EARLY DIAGENESIS IN ESTUARINE SEDIMENTS

1.6.1 Heavy Metal Remobilisation

Early diagenesis in estuarine sediments is characterised by highly complex interactions of metal ions, organo-metallic complexes, sulphide compounds, and organic and inorganic solids. Heavy metal concentrations are often 100 times more concentrated in interstitial waters than overlying waters (Aston and Chester, 1976; El Ghobary and Latouche, 1986; Fernex et al, 1986; Salomons and Forstner, 1984). The interstitial water is the medium for heavy metal

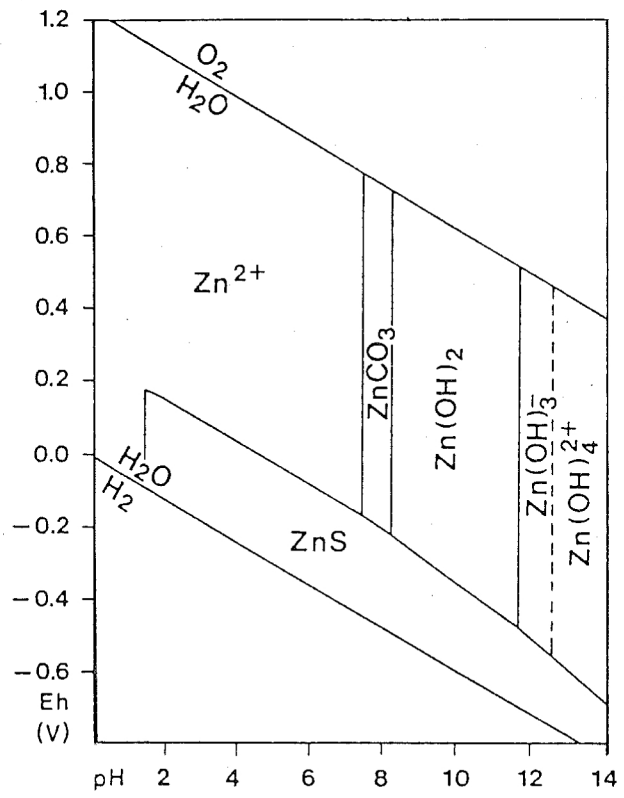

Fig. 1.2 Eh-pH Stability Fields of Zn at 25°C, 1 atmosphere pressure, 96mg/l SO_4^{2-}, and 61mg/l HCO_3^- (Forstner and Wittman, 1981).

transportation within deposited sediments. Metals move by diffusion, both within the sediment column and across the sediment water interface. The exchange between the overlying water and the sediment surface leads to characteristic gradients in dissolved species in the upper 30 cm of sediment deposits. Hence, estuarine sediments may act as sources of heavy metals to overlying water which may upset aquatic ecosystems and pollute drinking water supplies (Drever, 1982).

Heavy metal remobilisation is enhanced by (1) elevated salt concentrations whereby alkali and alkaline earth cations compete with metal ions sorbed onto solid particles, (2) redox changes such as decreasing oxygen potential, (3) lowering of pH which leads to dissolution of carbonates and hydroxides, as well as increasing desorption of metal cations due to competition with hydrogen ions, (4) presence of natural and synthetic complexing agents which form soluble complexes, and (5) biochemical transformation processes.

Organic matter decay (or biologically catalysed oxidation of organic matter) is the driving force behind the downward depletion of oxygen in sediments (Drever, 1982; Farmer and Lovell, 1984; Forstner and Wittmann, 1981; Finney and Huh, 1989; Gonzalez et al, 1985). Most diagenetic reactions are influenced by micro-organisms such as aerobic heterotrophs, denitrifiers, fermenters, sulphate reducers, and methanoic bacteria. Hence, micro-organisms essentially drive the diagenesis process which succeeds, with depth, as follows, 1) oxidation of organic matter, 2) aerobic transpiration, 3) denitrification (oxic), nitrate reduction (post oxic), 4) sulphate reduction (sulphidic), and 5) methane fermentation (methanoic) (Table 1.3). Bacterial action leads to a decrease in pH and Eh with depth and hence increases the solubility of heavy metals (demonstrated in Figs 1.2, 1.3 and 4.29 (Chapter 4), and Table 1.3). Mobile heavy metal-organic complexes result. Consequently, the sediment pore water environment becomes

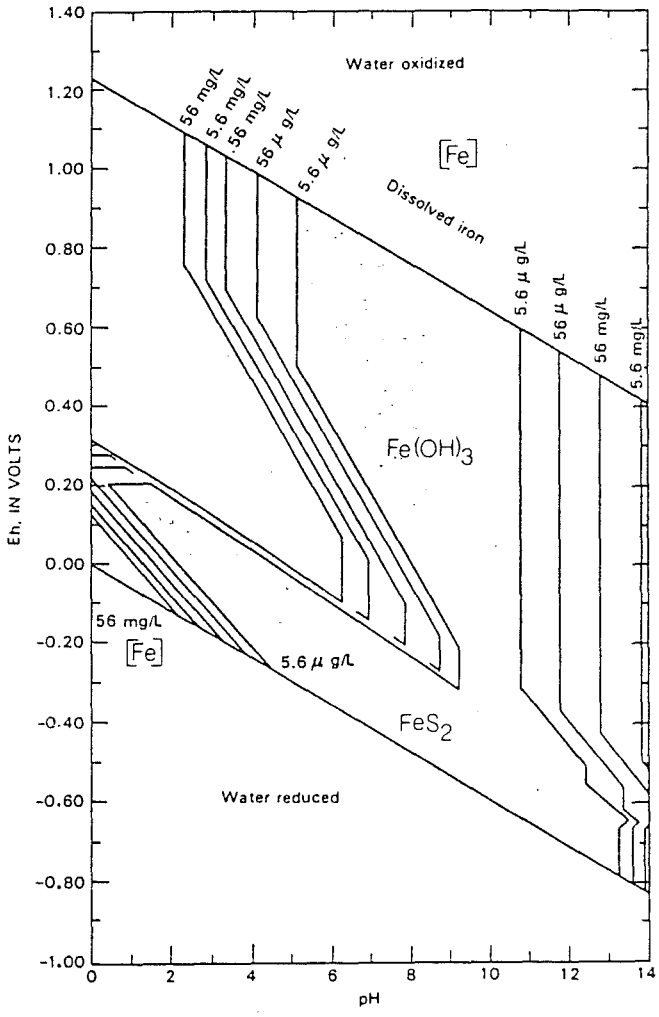

Fig. 1.3 Eh-pH Stability Fields of Fe at 25°C, 1 atmosphere pressure, 96mg/l SO_4^{2-}, and 61mg/l HCO_3^- (Hem, 1989).

strongly reducing with depth (Drever, 1982; Scoullos, 1986; Salomons and Forstner, 1986).

Table 1.3 **Possible Systems Operating in Flooded Sediment as a Function of Redox Potential at pH 7** (Sikora and Keeney, 1983).

System	Redox Potential (V)	Micro-organisms	
oxygen disappearance	+.500 to +.350	aerobic	1)
nitrate disappearance	+.350 to +.100		
Mn^{2+} formation	below + .400	faculative	2) & 3)
Fe^{2+} formation	below + .400	anaerobic	
Sulphide Formation	0 to -.150	obligate	4)
Hydrogen, methane formation	below -.150	anaerobes	5)

1) to 5), category in text.

Fe and Mn hydroxy compounds are stable under oxic and post-oxic conditions which usually persist within 10 cm of the sediment surface. Metals derived from overlying water or from upward migrating pore solutions are often sorbed or co-precipitated on Fe and Mn oxides. As depth increases oxygen is depleted and Fe(III) and Mn(IV) hydroxy compounds are dissolved and reduced to Fe^{2+} and Mn^{2+}. Manganese (II) ions and Fe^{2+} diffuse upwards out of the reduced zone to the oxic zone where they are re-precipitated as Fe(III) and Mn(IV) hydroxides and hydrous oxides (Fernex et al, 1986; Finney and Huh, 1989; Forstner and Wittmann, 1981; El Ghobary and Latouche, 1986). The dissolution and reprecipitation of Fe hydroxides tends to occur at Eh values of approximately 0.2V, whereas Mn oxides precipitate at Eh values above 0.4V. Hence Mn^{2+} persists in the pore water longer than Fe^{2+} and is precipitated, as oxides, closer to the surface. As sedimentation increases the Fe and Mn hydroxide horizons become upwardly displaced, thus remaining at the same relative depth. An increase in chlorinity in the surface sediment layers may cause a decrease in the

oxidation rate of Mn.

With reduction of hydrous Fe and Mn oxides sorbed metals will be released and may be precipitated as sulphides. Microbial reduction of sulphate to sulphides does not occur until all the oxygen has been consumed. Conversion of Fe oxides to sulphides generally causes a sediment colour change from red-brown to black or grey. At neutral pH mackinawite or an amorphous equivalent is normally the first Fe sulphide to form. Pyrite will form if the pH is below 6.5 (Forstner and Wittmann, 1981). At lower pH ranges, H_2S may diffuse upwards and redissolve hydroxide layers. When the pH is 7 or above, HS^- forms rather than H_2S and reacts with heavy metal ions such as Pb^{2+}, Co^{2+}, Ni^{2+}, Hg^{2+}, Ag^+, Cu^{2+}, and Zn^{2+} to form solid sulphides (Fig. 1.2). The reaction controlling sulphate reduction to sulphides is probably $SO_4^{2-} + 9H^+ + 8e \rightarrow HS^- + 4H_2O$ (Smillie, et al, 1981). The HS^- species itself is capable of heavy metal reduction. The methanic fermentation zone will only be reached when the source of sulphide ions is depleted (Forstner et al, 1986). Methanoic and sulphitic environments typically contain a lot of organic matter.

Because early diagenesis is generally controlled by humic substances, organic pollution (related to effluent discharges) greatly enhances metal remobilisation and concentration in sediment pore waters (Salomons and Forstner, 1984). Occasionally microbial decomposition produces intermediate compounds which may act as metal chelators. Many authors have shown that the stability of metal humics is greater than that of metal-inorganic complexes. Sometimes the metal chelate components migrate upwards faster than sulphide ions and other metal complexes. By this means metals may escape the sulphidic zone to be either co-precipitated with Fe and Mn hydroxy compounds or escape to the surface. Copper, Zn and Cd are the metals most likely to escape this way (Calmano et al, 1988).

Generally in estuaries when oxic waters overlie anoxic sediments maximum metal remobilisation occurs at the

sediment water interface. In contrast, mildly reducing conditions in slowly accumulating sediment allows the development of a well defined oxic zone, where remobilised metals may be trapped and greatly concentrated over natural levels. If the sedimentation rate is high, and the sediment rich in organic matter, then anaerobic conditions occur in both the interstitial water and in bottom waters. Such sediments are black in colour and early diagenesis is controlled by sulphate reduction (Marten and Goldhaber, 1978; Blatt et al, 1980). Recycling of metals near the surface in these conditions favours the long-term stability of sulphide and organic complexes and will minimise the release of metals.

1.6.2 Other Influences on Diagenesis

1.6.2.1 Bioturbation and Compaction

Bioturbation causes (1) pumping of enriched interstitial water out of the sediment, (2) brings in water rich in oxygen, (3) actively transports particulate material to the surface and into deeper layers, and (4) discards faecal pellets onto the surface, which may be enriched with heavy metals.

The major function of bioturbation is the release of dissolved metal compounds into the overlying water, which is particularly important in the top 5-15 cm of the sediment. Bioturbation may be several orders of magnitude greater than the sedimentation rate, and because most burrowers live near the redoxicline they move particulate matter from reducing environments to oxidizing environments near the sediment water interface (Rice and Whitlow, 1985; Salomons and Forstner, 1984).

Compaction may also contribute to the upward migration of heavy metals in the sediment column. Freshly deposited sediment contains 40-80% water, which is extruded upwards as deeper sediments are compacted. The upward moving water

enhances the upward chemical gradients in the pore waters (Drever, 1982).

1.6.2.2 Sedimentation Rate

Sedimentation rate is important because it controls the amount of time during which organic matter can undergo decomposition in oxygenated water at or near the sediment water interface (Drever, 1982).

If sedimentation rates are low then there is enrichment of solid Fe and Mn oxides at a depth of a few cm below the surface. In contrast in an anoxic area with extremely slow sedimentation, the surface layer may be almost devoid of Mn that has migrated into the overlying water (Fernex et al, 1986). Frequently the interstitial water of large areas of estuarine sediments is anaerobic because the sedimentation rate is high and organic matter has not had time to decompose as it falls through the water column. Consequently, such sediments are black, green, or grey in colour and may contain pyrite (El Ghobary and Latouche, 1986; Harbison, 1986). This is particularly common in the vicinity of outfalls.

1.7 BIOAVAILABILITY OF HEAVY METALS

Sediments in estuarine waters generally adsorb heavy metals rapidly from the dissolved phase thereby detoxifying the waters. However, once the sediment is deposited part is bioavailable. The metal associated with the crystal lattice can be considered unavailable whereas that attached to the surface is more readily available. The degree of bioavailability of heavy metals in sediments depends on (1) the types of organism, (2) the physico-chemical properties of the interstitial water (pH, Eh, salinity and dissolved oxygen), (3) type of metal-sediment interaction bond, and (4) speciation of metals in interstitial water (Calmano and

Forstner, 1983; Horowitz, 1985; Smith, 1986).

Heavy metals will enter benthic dwellers by either food (sediment or decaying organic material) or water (interstitial). Most studies indicate that the degree of bioavailability of sediment bound heavy metals is inversely related to the strength of the metal particulate bond. Heavy metals that can be removed from sediment by weak acid solutions are considered to be easily released in the gut of most organisms that inhabit the sediment. Such metals are normally adsorbed onto the surface of ferromanganese compounds and organic matter attached to the sediments. Frequently the surfaces of these substances are the deposition sites for heavy metals derived from anthropogenic sources (Wu Yuduan et al, 1988). (Chemical partitioning and bonding of heavy metals on surface sediments is discussed in detail in Appendix 1.0, Sections A1.1 and A1.2.)

In pore waters, the metal species is very important. Hydrated metal ions, alkylated metal ions, and organo-metallic complexes derived from the breakdown of organic matter and subsequent diagenesis are the most readily available forms of heavy metals to benthic organisms, because they can be ingested directly from the pore waters (Calmano et al, 1988; Salomons and Forstner, 1984). The organic matter content of sediments is one of the most important factors in determining bioavailability. The higher the organic matter levels, the more attractive the area is as a food source for bottom dwellers. Unfortunately the highest levels of organic matter are often found in the vicinity of sewage outfalls, which are also potential sources of heavy metals. Hence, these are localities where bioavailability of heavy metals to benthics is highest.

CHAPTER 2

HISTORICAL ANALYSIS OF ANTHROPOGENIC ACTIVITY AFFECTING SEDIMENT AND HEAVY METAL FLUXES TO THE AVON-HEATHCOTE ESTUARY

2.1 INTRODUCTION

2.1.1 Geological Setting of Canterbury

The Canterbury Plains are over 50 Km wide and 160 Km long, extending from Timaru in the south to the Waipara River in the north, and east to Banks Peninsula. The Plains comprise a series of overlapping glacial outwash and alluvial fans which were progressively built during the late Quaternary by eastward flowing rivers emerging from the Southern Alps (Fig.2.1, Brown and Wilson, 1988; Suggate, 1958, 1968; Wilson, 1976, 1986). River catchments consist of highly indurated Mesozoic sandstone and mudstone of the Torlesse Supergroup. These rocks have been intensely folded and faulted during two major orogenies. Subsequent fracturing and jointing during the fluctuating climatic conditions of the Quaternary has led to mechanical weathering of the rocks. The clasts derived from Torlesse rocks are extremely durable and have survived many episodes of transport and deposition.

On the east coast at the seaward edge of the Plains, a late Miocene Volcanic Complex forms Banks Peninsula, which probably originated as an island. During the late Quaternary, alluvial deposits infilled the shallow seaway separating the mainland from the island. Yellow loess, tens of metres thick, covers the northern and western flanks of Banks Peninsula.

The geological events related to the present study commenced approximately 14,000 years ago at the end of the

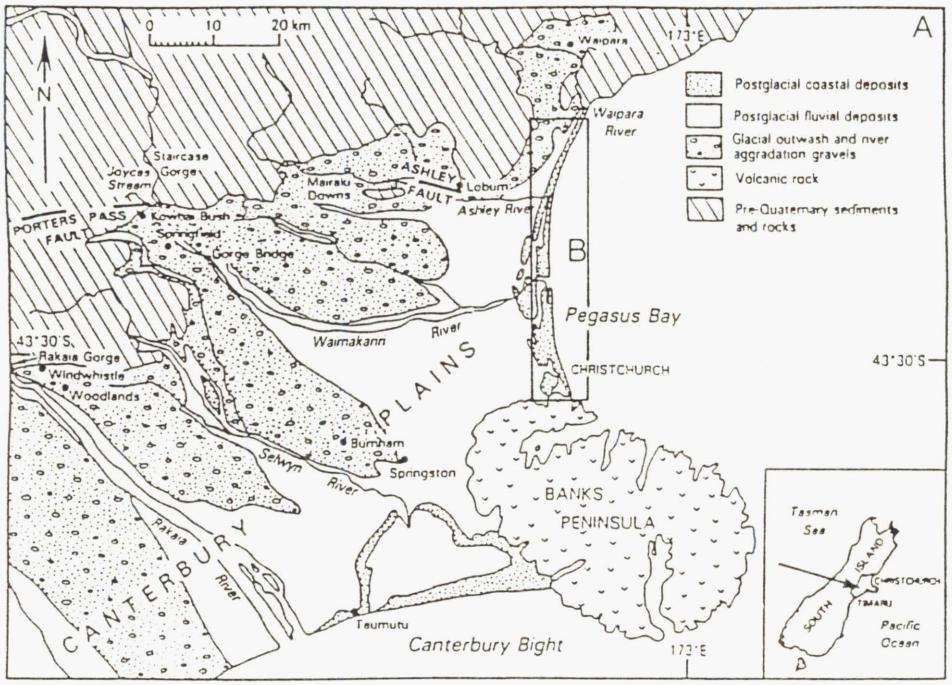

B

Fig. 2.1 Location Maps. A, Canterbury Plains (Brown and Wilson, 1988). B, View north of Banks Peninsula, 1) Avon-Heathcote Estuary, 2) Christchurch City Council Sewage Ponds, 3) Travis Swamp, 4) Saltwater Creek Estuary (L.J. Brown, pers comm.)

last glaciation. During the following 7-8000 years, a marine transgression encroached onto the South Island from the east. The sea reached the present coastline around 10,000 years ago and continued to move inland until it arrived at the localities occupied by Riccarton and Kaiapoi, approximately 6000-7000 years B.P. (Figs 2.2 (pocket of thesis) and 3.11). Beach and associated estuarine, lagoonal, dune and swamp deposits of the Christchurch Formation were laid down during the transgression (Fig. 2.1). Contemporaneously, fluvial gravels, sands, and silts of the Springston Formation were deposited to the west. Locally, Springston Formation sediments are derived from the Ashley and Waimakariri Rivers (Fig. 2.1). Following the marine transgression, the sea level stabilised and over the last 6-7000 years the shoreline has slowly prograded. Coastal progradation of Pegasus Bay, in contrast to coastal erosion south of the Peninsula, occurs because Banks Peninsula protects northern river mouths from the effects of the major northward flowing longshore currents (Blake, 1964; Wilson, 1976).

More recent Springston and Christchurch Formation sediments, indicative of progradational sedimentation, progress eastwards from inland peat and swamp remnants, alluvial gravels sands and silts, aeolian dunes, to modern beach deposits. Considerable interfingering of deposits makes it difficult to differentiate between sediments of the two Formations. Sediments being actively deposited today are not included in either Formation (Brown and Wilson, 1988). Coastal progradation and southward drift (as a result of near shore currents) over the last 1000 years has contributed to the formation of the Saltwater Creek Estuary, the Travis Swamp, and the Avon-Heathcote Estuary (Fig. 2.1b).

The Avon-Heathcote Estuary and Travis Swamp lie within the Kairekei Dunes which are thought to have formed in the last 500-2000 years (Blake, 1964; Deely, 1987; Macpherson, 1978; Millward, 1975). The Avon and Heathcote Rivers derive

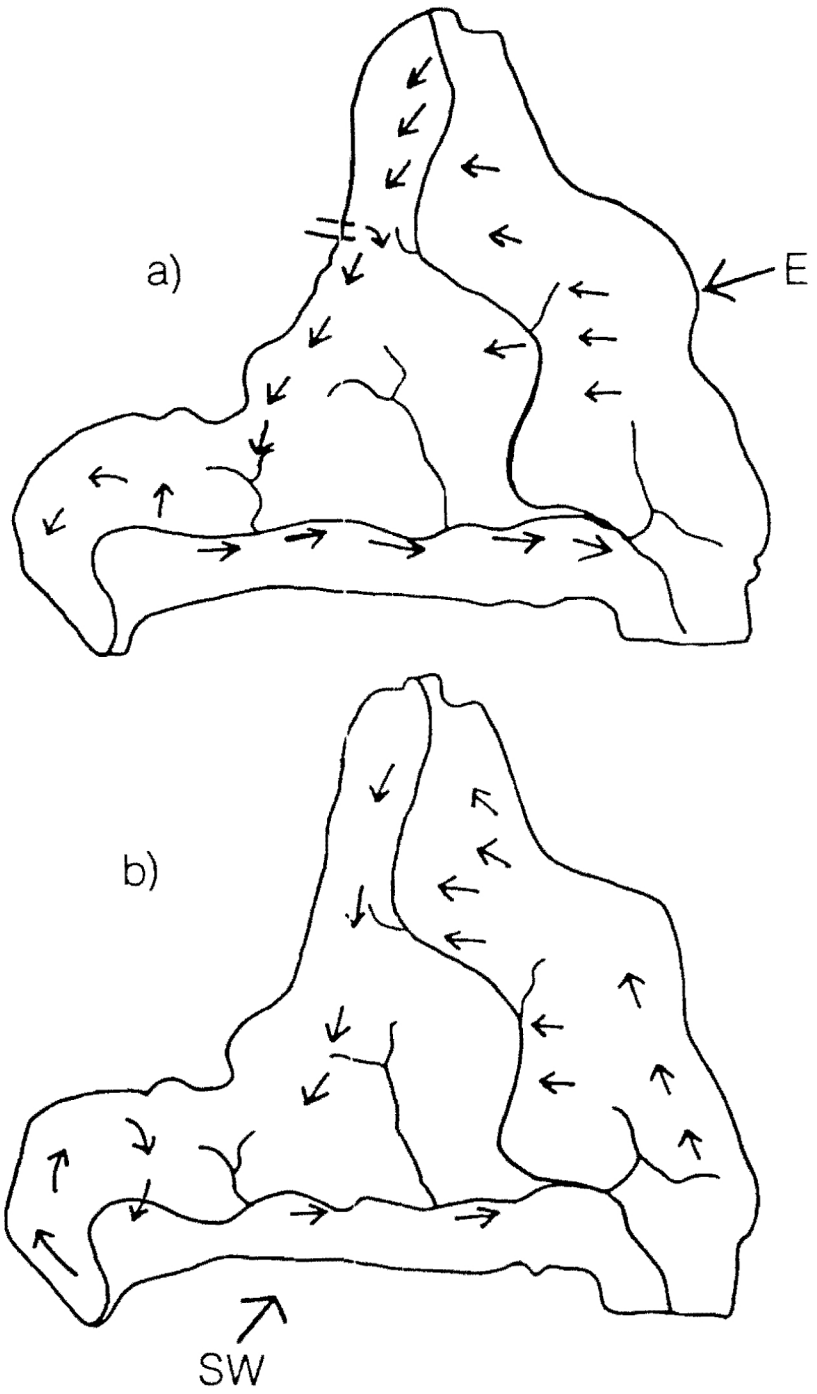

Fig. 2.3 Water Flow Patterns in the Avon-Heathcote Estuary during Easterly and Southwesterly Winds (Macpherson, 1978). a) Easterly Wind b) Southwesterly Wind

their water from underground springs emerging as seepage from the Waimakariri River. The Avon River probably once discharged out to sea near the Travis Swamp. As the New Brighton Spit prograded southwards, the Avon River would have migrated in a similar direction until further migration was prevented by the resistant volcanic rocks of the Peninsula, whereupon ponding of the Avon and Heathcote Rivers formed the estuary (Deely, 1987).

2.1.2 Hydrology of the Avon-Heathcote Estuary

The Avon-Heathcote Estuary is small and micro-tidal (0-2m tidal range), containing tide and wave built features. Because of its shallow character, the estuary varies from "salt-wedge" to "well mixed" (Millward, 1975). The Coriolis force has negligible effect on the Avon-Heathcote Estuary because of the estuary's small size (Knox and Kilner, 1973). In calm conditions, a two-layer water flow develops with pronounced vertical stratification from 34.8ppt (parts per thousand) near the estuary bed to 4.3ppt at the surface. During windy conditions the water salinity is almost vertically homogeneous (Knox and Kilner, 1973). Predictably salinity increases steadily from the head of the estuary to the mouth, oscillating from 4ppt to 32ppt with tidal movement. Saltwater extends up the Avon and Heathcote Rivers as far as the Bexley and Radley Street Bridges respectively (Fig. 2.2). At low tide, interstitial water salinities remain high due to evaporation.

The tides range from 1.1m (4 feet, neap tides) to 2.1m (6 feet, spring tides) and vary with river velocity and volume. Flood tides generally run 4-5 hours at each bridge, whereas ebb tides run 7-8 hours. The wind influences the length of tidal movement.

The most common winds are from east-north-east (34-56%) followed by west-south-west (28-32%) and northwest (16-25%). Westerly winds tend to have more energy than the commoner easterly winds (Macpherson, 1978). Dominant

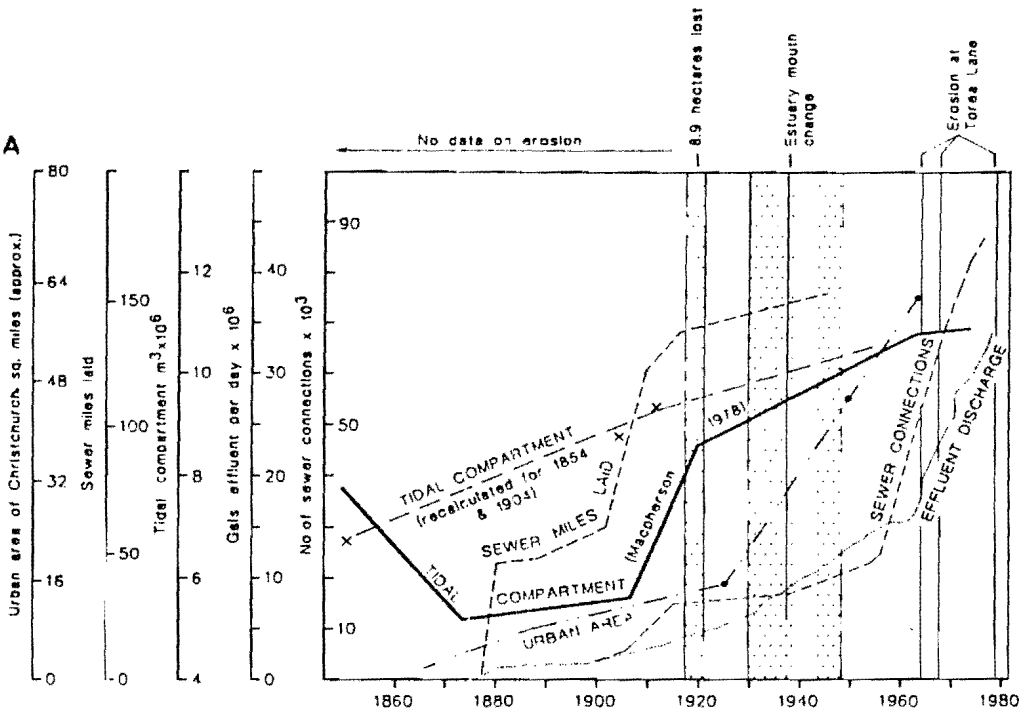

Fig. 2.4 Tidal Compartments calculated for the Avon-Heathcote Estuary by Findlay (1984) and Macpherson (1978), together with miles of sewers, number of sewer connections, and urban area (Findlay, 1984).

sedimentary processes are wind and wave induced within the estuary and tidally induced at the mouth (Macpherson, 1978).

Both Knox and Kilner (1973) and Macpherson (1978) studied water movement in the Avon-Heathcote Estuary. Knox and Kilner used aerial observations of dye movement whereas Macpherson observed movement of treated sewage effluent as it discharged from the Christchurch Drainage Board Treatment Plant. Both studies found that just after high tide during moderately strong easterly winds water entering the estuary from the southern pond outlet (Fig.2.3a) flows south along the western shore of the estuary and enters the Heathcote channel at the eastern edge of the Heathcote Basin. On calm days the plume flows across the western flats and generates currents along the western shore of the estuary. During east and southwest winds, the Avon River is pushed across the western intertidal flats in the north (Fig.2.3b) and the Heathcote River tends to be ponded in the Heathcote Basin. At the same time suspended sediment from the eastern flats flows across the estuary in a westward direction by advection. The above water circulation patterns are enhanced by the incoming tide.

2.1.3 Changes in the Tidal Compartment of the Avon-Heathcote Estuary

There is much debate regarding changes in tidal compartment, bed levels, and sedimentation of the Avon-Heathcote Estuary.

Macpherson (1978) used the Furkert-Heath relationship (Heath, 1975) to calculate changes in the tidal compartment (volume of water at high tide minus the volume at low tide) of the Avon-Heathcote Estuary throughout historical times. This method assumes that there is a linear relationship between cross-sectional area of the inlet and the tidal compartment. Macpherson felt that this was a more accurate method than calculating the tidal compartment using

existing depth soundings (particularly soundings from early surveys). Findlay (1984) and Findlay and Kirk (1988) disagreed with Macpherson and believed that the numerous depth soundings from early surveys are accurate enough to determine the tidal compartment. Both Macpherson's and Findlay and Kirk's tidal compartment curves are presented in Figure 2.4.

Macpherson's results suggested that the tidal compartment decreased considerably (30%) between 1850 and 1875, increased rapidly around 1909, and increased at a slower rate after 1920. In contrast, Findlay and Kirk's curve shows the tidal compartment increasing steadily from 1850 to 1915, then increasing at a slower rate after 1920.

An anomaly in Findlay and Kirk's curve is the decelerating tidal compartment growth after 1920, which coincides with rapid urban growth and changes recorded at the inlet in the 1920's and 30's (Findlay and Kirk, 1988; Knox and Kilner, 1973; Macpherson, 1978; Penney, 1982).

The discrepancies between the two tidal compartment curves in Fig. 2.4 suggest that either the early depth soundings used by Findlay and Kirk are in error or the Furkert-Heath relationship is invalid in this case.

Macpherson observed a massive homogenous mud layer (labelled Unit C), averaging over 25cm in depth, in over 40 2m deep cores from the estuary (Subsurface sediments are discussed in detail in chapter 3.). Unit C mud covers the whole estuary and occurs in areas where mud does not normally accumulate. Macpherson concluded that Unit C deposited quickly, between 1850 and 1875, under conditions of unnaturally rapid sedimentation, which caused the decrease in tidal compartment observed in Fig. 2.4. During this period there was considerable land clearing as the population of Christchurch increased from 100 to 11,000. However, the population of Christchurch increased to 22,000 by 1878 and 75,000 by 1906 (Scott, 1963), which is a more rapid growth than between 1850 and 1875. These figures suggest that runoff should have increased significantly

between 1875 and 1906, resulting in a further decrease in the tidal compartment.

Macpherson (1978 and 1979) suggested that since the establishment of the Christchurch Drainage Board in 1875 drain laying has led to an ever increasing water flux to the estuary, which is eroding Unit C sediment. Findlay and Kirk agreed with Macpherson in that water flows have increased since early times, but point out that most sewers were connected after 1950 and the growth of the urban area did not accelerate until after 1925 (Fig.2.4). This information suggests that major erosion of Christchurch area may have occurred after 1925 and not in the early period (1850 to 1875) as concluded by Macpherson.

A closer examination of the Furkert-Heath relationship indicates that it may not apply to the Avon-Heathcote Estuary. The relationship was originally established by comparing tidal compartments and cross-sectional areas of major harbours and estuaries in New Zealand (Heath, 1975). Amongst these harbours were Wellington, Whangarei, Dunedin, Akaroa, and Lyttelton, all of which are deep (over 20m) and the distances across the inlets in most cases are over 1km. In contrast the Avon-Heathcote estuary is extremely shallow (<3m high tide) and the distance across the inlet is of the order of 1-200m. As discussed earlier Macpherson's bathymetric and sediment studies show that the Avon-Heathcote Estuary and inlet are strongly affected by wind and tidal induced currents, which have negligible influence on deeper harbours. In fact, single events have been recorded at the inlet where the channel has moved, laterally, up to 150m. In addition, historical observations show that the inlet channel changed position on a daily basis in the 1920's and 1940's, and at times there was more than one ebb channel at Shag Rock (Penney, 1982). These observations indicate that wind and wave action are more important than the tidal compartment in determining the cross-sectional area of the Avon-Heathcote Estuary inlet. Hence, the Furkert-Heath

relationship, based on large harbour inlets, may not apply to small estuaries such as the Avon-Heathcote Estuary. In fact Macpherson's 1964 tidal compartment calculation is 55% less than the area determined from the Royds and Sutherland Survey in 1964. Macpherson corrected all his results assuming that a 55% error applied. This error is unlikely to be uniform over the last 100 years if wave and wind action have continually altered the cross-sectional area of the inlet.

The degree of error associated with the early depth soundings (Pandora, 1854; and Lyttelton Harbour Board, 1904) used by Findlay and Kirk is unknown. Hence, there is also some doubt over the accuracy of the early portion of their tidal compartment curve.

All the discrepancies discussed above indicate that tidal compartment changes may not have had as significant an influence on the estuary bed and inlet as previously thought and perhaps changes in sedimentation rates may have had some effect.

2.1.4 Changes in Bed Levels in the Avon-Heathcote Estuary

Another area of debate on historic changes in the Avon-Heathcote Estuary is in bed level data. Macpherson (1978 and 1979) concluded that the estuary bed is undergoing net erosion, and has been since around 1900. Harrison (1976) and Millward (1975) also claimed large scale erosion in recent years, but their evidence is confined to the perimeter of the estuary (Fig. 2.5).

Macpherson (1978) compared bathymetric data collected during surveys of the estuary in 1920 (Lyttelton Harbour Board, LHB), 1962 (Royds and Sutherland; Christchurch Drainage Board), and 1975/77 (Christchurch Drainage Board) and concluded that the intertidal zone of the northern half of the estuary lost up to 1m thickness of sediment between 1920 and 1962. He thought that losses continued between 1962 and 1975 but at a slower rate. In addition, minor

Fig. 2.5 Erosion of the Avon-Heathcote Estuary Perimeter near Sandy Point on the Western Slopes (Harrison, 1976).

accumulation was found, during the latter period, near the river entrances and in front of the oxidation ponds. Macpherson assumed that this pattern applied to the whole estuary and attributed erosion between 1920 and 1962 to the increasing tidal compartment. Macpherson suggested that slight adjustment in subtidal channels is responsible for erosion and deposition after 1962.

The changes in bed levels were derived by extrapolating the 1920 data on to the grid line of the more recent surveys. Each survey line was 200m apart and Macpherson assumed that sediment levels on each line were characteristic of areas 100m either side. He also assumed that the sea level in the estuary has remained constant over the last 150 years and that there have been no changes in the non-tidal flows.

The Lyttelton Harbour Board's 1920 bed level data were collected by boat at high tide, and the grid used was at low angles to the later grid established by Royds and Sutherland in the 1960's (D. Carver (Surveyor) pers comm., Christchurch Drainage). The 1920 bed levels were measured by soundings and corrected to a general tidal curve and are much less accurate than later surveys, which were completed on ground at low tide using accurate reference points. Derek Carver suggests that the original survey may be inaccurate because the calculations do not take into account tidal fluctuations, wave movements, and wind currents which are important in the Avon-Heathcote Estuary. In addition: 1) the exact position of the 1920 survey reference point is unknown, 2) data discussed above (Fig. 2.4) indicate that the tidal compartment has at least doubled in the last 50 years, and 3) the sea level has risen approximately 16cm since 1895 (D. Carver, pers comm.). The above information indicates that the 1920 survey is too inaccurate to compare with the later surveys.

Macpherson's sedimentological analyses of Unit C indicate that this mud layer accumulated during a major

silting phase in recent times. Accurate dating of this layer is required to determine whether or not 1) anthropogenic activity influenced the deposition of Unit C, and 2) a major period of erosion followed Unit C deposition.

Radiometric dating techniques are often inaccurate when applied to sediments less than 150 years because 1) most nuclide detection limits are older than the sediment of interest, 2) the concentration of the nuclides in the sediment may be enhanced or depleted as a result of industrial pollution, 3) bioturbation frequently reworks ten's of centimetres of sediment producing homogeneous nuclide concentrations with depth, and 4) nuclides may be remobilised in contaminated anaerobic sediments (Hume, et al, 1989). As a consequence, historical knowledge is essential in dating modern sediments. Stratigraphic datum levels need to be located. Examples of stratigraphic markers include layers of wood, shell, and coal particles, as well as changes in sediment texture, pollen type, and contaminant levels. These reference layers are identified using historical records. Once marker beds have been located, contaminated sediment layers can be directly correlated with periods of industrial pollution.

The remainder of this Chapter is a synthesis of changes in sedimentation, flora and fauna, and industrial activity related to the Avon-Heathcote Estuary and its rivers. The synthesis has 1) helped identify stratigraphic marker beds in cores from the Avon-Heathcote Estuary, which have in turn provided reference ages for calculations of ^{210}Pb profiles, and assisted in calculation of sedimentation rates (Chapter 3), and 2) yielded <u>new</u> information on historical sedimentation patterns in the Avon-Heathcote Estuary, which helped solve the scientific discrepancies discussed in the previous two sections.

Table 2.1 Historical Observations Relating to Sedimentation and Heavy Metal Changes in the Avon-Heathcote Estuary

Date AD	Pre-European Events
1200	First Polynesian settlers arrive in Canterbury (25)
13-1400	Major burnoff of native bush by Polynesian settlers in Canterbury (24) (50% of area deforested by 1850)
1500	Many Polynesian camp sites among sand dunes surrounding estuary (24)

Date AD	Drainage	Heathcote River	Avon River	Estuary	Flora and Fauna	Estuary mouth	Industries on banks of Heathcote River
1850	1858 Two storm water drains (1)	1850-67 Over 240 vessels drawing up to 3 m travelled to Wilson's bridge (7)	1840 W. Deans introduced water-cress (7) 1858 Withels Cutt (11)				1853 All land in lower Heathcote taken up by farms (5) 1858 Iron foundry, brewery, sawmill (5)
1860			1869 Schooners sailed regularly up river (5)				1864 36 builders, 2 brickmakers, 2 foundries, 5 iron mongers, a moulder, 6 tinsmiths, 2 zinc works, 7 blacksmiths, 6 breweries, and many more (5) 1867 Railway opened through, Lyttelton tunnel (5, 13)

2.2 CHRISTCHURCH AREA BEFORE 1850 AD

Table 2.1 presents a summary of the anthropogenic activity that affected sedimentation and heavy metal levels in sediments of the Avon-Heathcote Estuary. By referring to Table 2.1, the timing of drainage and sedimentation changes on land, in the rivers, and in the estuary can be compared and the order of events leading to "silting" (deposition of Unit C) in the estuary will be disclosed. In addition, the timing of silting can be compared with periods of industrial activity which most likely caused heavy metal contamination of the estuary sediments.

The Canterbury area was first settled around 800 years ago by Polynesian (Maori) people from North Pacific Islands. Soon afterwards large areas of forest land were burnt-off. There was a large encampment on the sand hills just south east of Moa Bone Point Cave, one at Bromley, and another on the north banks of the Avon River. By about 500 years B.P., the Maori population had grown to a size where their food gathering habits were having a deleterious affect on the environment. At the time, thousands of hectares of native bush were burned-off in the Canterbury area; subsequent cover was scrubby vegetation such as bracken and grass (McFadgen, 1989; McSaveney and Whitehouse, 1989; Trotter in Penney, 1982). Devegetation reduced natural resources considerably. Hence, the Polynesian settlers were forced to change to a hunter-gatherer life style, and many of their camp sites are known amongst the dunes which run between the Avon-Heathcote Estuary, New Brighton and Canterbury.

Sediment profiles from lakes and swamps often show an influx of sediment at the same time that pollen and charcoal records indicate deforestation of the catchment areas (600-700 years B.P.; McGlone, 1989). The 600-700 year B.P. burning of the Canterbury plains, together with later camping among the sand dunes probably affected coastal

Table 2.1 continued

Date AD	Drainage	Heathcote River	Avon River	Estuary	Flora and Fauna	Estuary mouth	Industries on banks of Heathcote River
1910	Economic depression (5)	1912-14 Development of market gardens in the Heathcote Valley causing serious soil erosion and silting of river (1)	1912 Silting more serious (9, 12) 1915 Problem of silting of Avon spreading to lower reaches of river	1912 Ship entering estuary (15) **1914-18 Photograph Ferrymead bridge at low tide (Fig 2.7b) showing water extending to outer perimeter of Heathcote Basin** (7) David Barr used to sail into Humphreys drive area in 1 m skimmer at low tide during World war I (9)	The eelgrass *zostera* abundant all over the estuary before 1920 (7, 19)	1916 Channel cut across Sumner bar by navy (15)	1913 Electricity slowly introduced into factories and houses (5)
1920	1923 Amalgamation of outer suburbs complete (5) 1925-29 Many stormwater drains and sewers laid to outlying areas (1)	Early 1920's River became restricted by willow growth trapping silt and rubbish (1) **1925-26 "River sweeper" cleared large areas of river** (1,7) 1929 Further river sweeping (1)	1920-25 Silting problem continuing and further restriction due to willow growth (12) **1927-29 River swept from Barbadoes St. to Bridge St.** (12)	1920 Deep channel at junction of Avon and Heathcote rivers (15) 1922 Syklark Is completely disappeared (14) **1928 Photograph, (Fig 2.7c) Heathcote Basin mud flats exposed at low tide** (7) **1929 Entire surface of estuary is mud and riddled with burrows** (16)	1929 *Zostera* grows sparsely (16)	1918-22 Severe erosion of spit toe (14) 1921 Christchurch yacht club re-staked channels, Moncks Bay (11) 1921 Build up of sand Clifton Beach (14) 1929 New mouth opened up alongside naval reserve (15)	1920 Soap and candle factory in HumphreysDrive replaced by starch factory (6) 1926 Tar became available from Christchurch Gas Works; roads sealed rapidly after this time (21)

Date AD	Drainage	Heathcote River	Avon River	Estuary	Flora and Fauna	Estuary mouth	Industries on banks of Heathcote River
1870	1874 City Outfall Drain (2) 1875 Christchurch Drainage Board commissioned (3) 1878-80 Six stormwater drains (1)		1874 River becoming choked with weeds (12)				Woolston is industrial centre of Christchurch 1874 8 woolscours, 7 tanneries, 1 soap and candle factory, several glue and carpet builders, breweries, wharfringers, 2 foundries and more (5)
1880	1882 Sewage farm commenced operation (1) 1885 Christchurch water table lowered (4)	1880's Sailing ship Minnie near Radley bridge (Fig 2.6) (7) **1880's Silting river** (8)	1886 Willow choking river (2) **1887 Water cress problem, silting problem** (12) 1887 No longer lakes on land surface after rain (12)				1884 11 woolscours, 8 tanneries, 1 glue works, 2 limekilns, flax mill, many iron and brass foundries (5)
1890	1890-1920 Economic depression (5)	Ships still sailing up to Radley bridge (5) Hill erosion causing silting of river (9)	1894-99 'Avonia' steamer employed to cut weeds in river (12) Problem of silting worsening (12)				Sydenham major industrial centre of Christchurch
1900	1903-23 Amalgamation of Christchurch and suburbs (5) Economic depression (5)		1900-03 Silting worsening further, but weed problem in check	Keel boats (3 m) moored at Ferrymead bridge (9) 1907 Construction of causeway across McCormacks Bay			1903 Christchurch the chief industrial centre of new Zealand, principal iron working district

Table 2.1 continued

Date AD	Drainage	Heathcote River	Avon River	Estuary	Flora and Fauna	Estuary mouth	Industries on banks of Heathcote River
1950	1952-62 The number of house and business connections to sewers tripled (2)	1951 Severe hill erosion and silting of Heathcote River, 1954-55 All sediment removed by river sweeper and dragline (1) 1956-57 Deepening and clearing especially below Radley St (1,9)			1952 *Zostera* rare, blue green algae *Ulva* and *Enteromorph* abundant (18), yellow green slime *Euglena* common near outfalls (6)	1950's Spit toe has consolidated and vegetated (14)	Serious spill from Christchurch Gas Works into Heathcote River at Bell's Creek (22) (spills high in coal and coke in addition to heavy metals)
1960	1962 Secondary treatment brought into operation at Bromley Treatment Plant (2) 1963 Effluent from ponds contributing 30% freshwater to estuary (1) 1968 Redcliffs, Moncks Bay, St Andrews Hill, Mt Pleasant and Ferrymead effluent diverted to Treatment Plant (2)	1960's Occasional river clearing (9)			1964 *Zostera* beds increasing along Avon channel (19) 1969 *Zostera* increased to areas near Causeway (20) 1969 *Euglena* abundant south and west shores (6)	1960's Minor erosion and deposition events, channels unchanged (14)	1968 Provita starch factory in Humphreys Drive closed (6) 1969-72 Bulk of industrial effluent diverted from Heathcote River to CDB treatment plant (except for gasworks) (6)

Date AD	Drainage	Heathcote River	Avon River	Estuary	Flora and Fauna	Estuary mouth	Industries on banks of Heathcote River
1930	1931 Area sewered and drained tripled since 1914 (1,2) 1932 More stormwater drains laid (1)	1936-41 River cleared below Cashmere Bridge, also straightened and deepened (1)	1933 Rat Is filled on Bromley side (13)	1935-36 Estuary still silting up (11)		1930 Erosion spit toe (14) 1933 Re-direction of ebb channel (14) 1934-36 Ebb channel migrated East (14) 1936 Channel confined to south side Moncks' Bay 1938 Ebb delta migrated north from Cave Rock to its present position (14)	Sydenham still major industrial area of Christchurch, but many industries that prospered in iron working days are gone. Now, 1 tannery and fewer iron and brass foundries (22)
1940	1941-45 Deepening of major stormwater drains and extensions to other drains (2)	1940's Tremendous amount of silt carried down rivers during floods (10) 1948-50 Drag line used to clear river, Charlesworth St. to Tunnel Rd. Bridge (1)	1947-52 River widened using dragline (10) 1949-50 Cut, Kerr's Reach (1)	1944 Bed estuary described as fairly compacted (12) 1944 Erosion clays, Ferrymead bridge caused by crabs burrowing (12) 1948 Silting still a problem in the estuary (15)	1944 First documentation of sea lettuce algae and *Euglena* slime (17)	1940-49 Severe erosion of spit toe 1947 Main flow permanently transferred to south Moncks Bay (14) 1949 Erosion ceased after groyne fences constructed at spit toe (14)	Most roads sealed by 1940's (22)

Date AD	Drainage	Heathcote River	Avon River	Estuary	Flora and Fauna	Estuary mouth	Industries on banks of Heathcote River
1970 - 1990	1973 Pond 5 brought into operation (6) 1973 Treatment plant stopped discharging effluent over outgoing tide (6) 1970's-1980's Sewered areas extended to include Belfast and Sumner (2)	1970 Severe loess runoff during period of land development in upper reaches (10) 1970's River stopped receiving stormwater runoff (9) 1986 Woolston cut ()	1970's-1980's River periodically cleared (9)	1970's Minor shifts in channel positions (23)	1972 *Zostera* spreading on both sides of Avon channel (20) 1970's Algae abundant to almost nuisance levels (6) 1981 *Zostera* grows continuously over intertidal area of estuary (20) 1980's Marked decrease in density of *Euglea* along southern shores and Heathcote Basin (8)	1970's Minor erosion and deposition events (14) channels unchanged	1981 Christchurch Gas Works closed down (22)

References: 1 Scott 1963; 2 Wilson 1989; 3 Hercus 1949; 4 Hoben 1914; 5 Morrison 1948; 6 Knox & Kilner 1973; 7 de Thier 1976; 8 Robb, Christchurch Drainage Board (CDB) 1990; 9 Barr 1990; 10 McWilliam 1990; 11 Penney 1982; 12 Lamb 1981; 13 Greenaway 1976; 14 Findlay & Kirk 1988, 15 Penney 1982; 16 Thompson 1930; 17 Linzey 1944; 18 Bruce 1952; 19 Webb 1965; 20 Gibb 1981; 21 Dobson 1930; 22 Pollard 1990; 23 Macpherson 1978; 24 McFadgen 1989; 25 Penney 1982.

sedimentation patterns including that of the Avon-Heathcote Estuary.

When the Europeans arrived in 1850, the Polynesian population had dwindled as low as 400-500. At that time, the Christchurch area consisted of large swamps interspersed between sand-dune ridges and shingle lobes (Hercus, 1948; Morrison, 1948; Millward, 1975; Macpherson, 1978; Wilson, 1989). The sand dunes occurred in rows along the coast. The older inland dune complexes were covered with grasses and manuka, whereas the youngest eastern most dunes were unvegetated and semi-artesian with tidally influenced groundwater (Scott, 1963). Low-lying swampy areas between the sand dunes were vegetated with rushes, flax, and ferns. Open areas of grassland were interspersed between the swamps and sand hills. Originally the estuary extended 50 to 100 m further north and west at the entry zones of the Avon and Heathcote Rivers respectively (Millward, 1975).

2.3 AN OUTLINE OF THE HISTORY OF DRAINAGE OF CHRISTCHURCH AREA, 1850-1990

2.3.1 1850 to 1875

The early settlers found Christchurch difficult to drain because the area was low lying, with the city centre only 5m above sea level (Fig. 2.2; Wilson, 1989; Scott, 1963). Initially the natural drainage system provided by the Avon and Heathcote Rivers and tributaries was utilised, and no drains were constructed before 1858 (Hercus, 1948; Morrison, 1948). During 1858, two stormwater drains were constructed; one leading into the Avon River via Fitzgerald Avenue and the other leading into the Heathcote River via Ferry Road and Radley Street (Table 2.1). However, due to the swampy nature of Christchurch, these first two drains had little affect and in 1861 many parts of Christchurch were still impassable due to accumulation of surface water

and mud in street-side channels, drains and gullies. In 1862, the Canterbury Provincial Government constructed a few open drains and roadside ditches in an attempt to remove water to the Avon and Heathcote Rivers.

Despite this effort, the water levels were so high that in 1865 and 1868 major floods brought over 1m of water to the centre of Christchurch (Hercus, 1948; Anderson, 1949; Scott, 1963). By 1867 most of the major swamps were still undrained (for example Halswell, Hagley Park, Papanui). In 1871 the Fitzgerald Avenue and Ferry Road drains were blocked so the provincial government commenced building a large stormwater drain, from Tuam Street, along Fitzgerald Avenue, and Linwood Avenue to the estuary at Canal Reserve. The City Outfall Drain as it is now called was completed in 1874 (Fig. 2.2; Hercus, 1948; Wilson, 1989). But even this drain was not adequate and a substantial area of Christchurch remained continuously waterlogged (Scott, 1963).

2.3.2 1875 to 1900

With the commission of the Christchurch Drainage Board in 1875, plans were immediately prepared to lower the water table and sewer the Christchurch area. The first stage of drain laying did not commence until 1877. Unfortunately the situation deteriorated in the meantime, as households and factories continued to cast refuse into side channels and swampy areas, and by 1880 the rivers themselves were polluted (Morrison, 1948).

Between 1878 and 1880 the Christchurch Drainage Board constructed seven large stormwater drains to the Avon and Heathcote Rivers as well as making improvements to the City Outfall Drain and the Ferry Road Drain (Table 2.1). Hence, by 1885 low lying areas of Christchurch were no longer permanently water-logged (Scott, 1963; Wilson, 1989). At the same time many sewers were laid and the sewage farm was completed at Bromley in 1882.

The treatment of sewage originally involved pumping raw sewage to sand hills, and settling of solid matter in tanks which were cleared periodically. Subsequently, the sewage was applied to 17 paddocks where it filtered through sand before being channelled out to the estuary at a location near the northern outlet of pond 6 (Figs 1.0b and 2.2; Scott, 1963).

These initial stormwater drains and sewage systems were effective in clearing up the problem of contaminated surface water. Unfortunately, throughout the 1880's and 1890's New Zealand suffered a financial depression, hence very little work was undertaken during this period. Consequently, many roads and streets were not curbed or channelled, and the Richmond and St. Martins areas were still largely swamp.

2.3.3 1900 to 1950

Between 1900 and 1925 the area of the Christchurch Drainage Board's jurisdiction expanded from Christchurch City proper (Fig. 2.2; area between Fitzgerald Avenue, Moorhouse Avenue, Rolleston Avenue and Bealey Avenue) to include St. Albans and Linwood (1903), Beckenham (1907), Richmond (1914), Opawa (1916), Avonside and St. Martins (1917), Woolston and Spreydon (1921), Bromley and Papanui (1923) (Hoben, 1914; Morrison, 1948). However, it was not until after the first world war that Christchurch emerged from economic depression.

During 1925 and the early 1930's sewers and stormwater drains were extended to these outer suburbs, while the rivers and older drains were deepened and cleared. Additional drains were laid in areas not previously drained such as Fendalton, Bryndwr, Northcote, and Riccarton. During this period the drained and sewered areas of Christchurch were more than tripled (Table 2.2).

Table 2.2 Growth of Sewered Area of Christchurch

Year	Increment in Years	Total area Sewered (ha)	Increment in area sewered (ha)	City Growth rate per 10 year (ha)
1884		680	680	
1903	19	979	299	157
1910	7	1520	541	
1914	4	1560	40	528
1931	17	5265*	3705	2179
1956	25	7709	2444	978
1989	33	14422	6713	2034

* Total sewered area tripled between 1914 and 1931 (Scott, 1963; Wilson, 1989)

Throughout the rest of the 1930's, 40's and 50's drains and sewers were extended and cleared as necessary (Hercus, 1948; Scott, 1963; Wilson, 1989).

2.3.4 DRAINAGE OF CHRISTCHURCH AFTER 1950

By the 1950's not only was treated effluent from the Bromley Treatment Plant entering the estuary but also untreated domestic sewage from the septic tanks of St. Andrews Hill, Mt. Pleasant, Redcliffs, Moncks Bay, and Ferrymead (Fig. 2.2). At times there was more effluent than the paddocks at Bromley could hold, and some was run into a ponding area where it underwent secondary treatment before entering the Avon-Heathcote Estuary through the southern outlet. The secondary treatment involved oxidation and bacterial action (Bruce, 1952; Knox and Kilner, 1973; Scott, 1963).

There were minor stormwater extensions and maintenance during the 1950's and 60's. After 1950 there was an unexpected population growth of Christchurch. As a result, between 1952 and 1962 the number of sewer connections tripled from around 20,000 to 60,000 (Wilson, 1989).

Consequently, it was necessary to upgrade the treatment works at Bromley.

In 1962 the upgraded treatment process involved primary treatment using mechanically cleared screens, grit removal by aerated tanks, primary sedimentation with scum collection, trickling filters, anaerobic digestion of solids, and lagooning of the digested residue. Secondary treatment included biological oxidation in an oxidation pond series prior to discharge from pond 6 to the Avon-Heathcote Estuary (Knox and Kilner, 1973). This treatment process is largely unchanged today, and has improved the character of the effluent discharged to the estuary since 1962.

During 1968 the Redcliffs, Moncks Bay, St. Andrews Hill, Mt. Pleasant, and Ferrymead effluents were all diverted to the Bromley Treatment Plant. In addition, between 1968 and 1972 10 million litres per day of industrial waste was diverted to the treatment plant from the Woolston area. The industrial effluent had formerly discharged directly into the Heathcote River (Knox and Kilner, 1973). Consequently it was necessary to bring all 6 ponds into use in 1973. The treatment plant was extended further in the 1970's and 80's to accommodate the wastes of the outlying Sumner and Belfast areas.

The growth of the Christchurch area and diversion of untreated effluents into the treatment plant has resulted in a gradual increase in the quantity of effluent discharged to the estuary along the western slopes (Table 2.3).

Table 2.3 **Average Daily Flow of Treated Effluent from the Christchurch Drainage Oxidation Ponds to the Avon-Heathcote Estuary**

Year	Volume (1000 m^3/day)	(million gallon/day)
1929	36.7	8.1
1958	73.0	16.1
1963	77.1	17.0
1965	101.6	22.4
1966	96.2	21.4
1967	98.9	21.8
1968	105.7	23.3
1969	99.8	22.0
1970	100.7	22.2
1971	115.2	25.4
1972	128.8	28.4
1986-89*	140.0	31.0

(Knox and Kilner, 1973; *J. Robb pers.comm, Christchurch Drainage)

Before 1968, approximately 10% of the non-tidal water entering the Avon-Heathcote Estuary was in the form of untreated polluted wastes derived from septic tanks along the southern shores, industrial effluent entering the Heathcote River (10 million litres/day), and a Starch Factory effluent (Humphreys Drive area). The rest of the non-tidal budget consisted of 20% from treated sewage effluents along western shores, 59% from the Avon River, and 18% from the Heathcote River. In addition, the effluent from the ponds was discharged continuously throughout the tidal cycle, which resulted in considerable organic enrichment and eutrophication of the estuary and lower reaches of the Avon and Heathcote Rivers (Knox and Kilner, 1973).

Several workers attempted to calculate the efficiency of tidal removal of effluent from the Avon-Heathcote Estuary. Bruce 1952 estimated using salinity variations that 32 to 41% of the effluent that left the estuary in 1 tidal cycle returned in the next. Knox and Kilner's dye study indicated that the effluent may take several tidal cycles to completely leave the estuary and as little as 15%

may leave in a single tidal cycle. Both studies contain many assumptions and generalisations in their calculations. Nevertheless in 1973, the Christchurch Drainage Board discontinued effluent release during the flood tide (as recommended by Knox and Kilner, 1973). Today the effluent is discharged only during the first half of the ebb tide and removal to the open ocean is more effective (Jones, 1978).

At present the effluent from the ponds makes up about 30% of the non-saline water discharging into the estuary. In addition, since 1972 all the untreated wastes have been diverted to the treatment plant eradicating much of the localised organic pollution problems that existed along the southern shores and in the Heathcote Basin.

2.4 CHANGES IN SEDIMENTATION PATTERNS IN THE AVON AND HEATHCOTE RIVERS

The Avon and Heathcote Rivers drain through swampy terrain of the Christchurch area. Both rivers originally had many tributaries, most of which have now been channelled and piped as stormwater outlets. The river courses today are virtually permanent due to urbanisation of their catchments (Macpherson, 1978). Both rivers are spring fed with water derived from the Waimakariri River.

2.4.1 Avon River

The Avon River (Fig. 2.2), is 21 km long and uprises in Avonhead (Christchurch Drainage Board, 1988). The watershed of its catchments is 84.3 km^3 and its average flow is 2.7m^3 sec.

Schooners used to carry freight up as far as the Barbadoes Street Bridge in the early days (Morrison, 1948). Passengers were still being ferried from the Colombo Street Bridge to New Brighton in the 1880's in the 14m long passenger steamer "Diamond". However, in the late 1880's

the Avon River started to "silt up". In 1840 W. Deans introduced watercress, which by 1880 was trapping debris, and had spread to the point of choking many areas of the Avon River. With the construction of Horners Stormwater drain in the late 1870's, the river Catchment was reduced by 16.2 km^2 as some of its natural watershed was diverted to the Styx River further north of Christchurch. At the same time (1878-80) 6 major stormwater drains were constructed, 3 of which emptied in the Avon River (Fitzgerald Avenue, Madras Street, Riccarton Main Drain). Other small drains were also constructed that terminated in the Avon River.

Prior to the 1880's, whenever there was heavy rain Christchurch was "studded all over with lakes" but after the construction of the main stormwater drains "every place was free from water within half an hour" (Mr. Walkden, City Surveyor, 1887, in Lamb, 1981). The flushing of side channels by heavy rains resulted in an enormous amount of sediment entering the Avon River. The sediment became trapped in the river bottom vegetation (Greenaway, 1976). A steam dredge the "Avonia" was employed by the Christchurch Drainage Board between 1894 and 1899 to cut weed in the Avon River throughout the city area (Greenaway, 1976, Lamb, 1981). The river was polluted by domestic sewage and rubbish at this time. The dredge was successful in cutting weeds and clearing the city area of sediment which unfortunately blocked the river below Fitzgerald Avenue. In the early 1900's the Avon River was only 3-4 inches deep in many places where it had formerly been 10-20 feet. In addition, great banks of silt were forming in the lower reaches. The Christchurch Drainage Board was suffering from the general economic depression in New Zealand, hence no improvements were undertaken. By 1915 the mud was so thick that at low tide swans could walk across the river near the Fitzgerald Avenue Bridge (Lyttelton Times 20 January 1915). There is some evidence that silting may have started to reach the head of the estuary by 1915

(Greenaway, 1976). But generally, the incoming tide prevented the silt from travelling beyond the area of the river mouth. By 1920 the silting problem was enhanced by willow growth in the river-bed (Press, 18 January 1921; Record New Brighton Council, 13 November 1920; Scott, 1963).

In 1925 the Christchurch Drainage Board purchased a river sweeper which commenced work in July 1927 at Carlton Bridge and worked downstream. After 3 months it was downstream of Wainoni Bridge and by 1930 it was 1 km upstream of the estuary (Lamb, 1981). The sweeper swept a 3-4 feet high mound of mud in front as it progressed down river. At the time it was impossible for launches to get upstream of the mass of mud (Greenaway, 1976; D. McKenzie, pers. comm.; Lamb, 1981). Almost all the sediment swept down the Avon River in the late 1920's and 1930's entered the Avon-Heathcote Estuary (Greenaway, 1976; D. McKenzie, pers.comm.). In the 1940's and 50's, the Christchurch Drainage Board purchased dragline equipment for clearing the rivers and after 1950 most sediment was removed onto adjacent land (J. Pollard, pers.comm.). This method was used to widen the Avon River near the estuary (Seaview Road) in 1947-48 (Scott, 1963). Kerrs Reach cut was formed in 1949-50. After 1950 the river was cleared and widened as necessary, but has never become as deep as it was in the 1800's.

2.4.2 Heathcote River

The Heathcote River (Fig. 2.2) is spring-fed from Wigram and flows slowly (1.1 m^3/sec) through its catchment (103.4 km^3) around the northern perimeter of Banks Peninsula (Christchurch Drainage Board, 1988). Many small rivers running from the Port Hills make up a third of the river catchment (Scott, 1963). The Heathcote River has a low flow but normally contains high suspended loads when in flood (Millward, 1975).

Originally the lower reaches consisted of swampy terrain. By 1853 this area had been converted to dairy farms and orchards (de Thier, 1976; Morrison, 1948). In the early days, clearing of the Port Hills for farming caused severe erosion, but there is no record of siltation in the Heathcote river before the 1880's. In fact, between 1850 and 1867 over 240 vessels ranging from 10-120 tons and drawing up to 8 feet of water were employed on route up to Wilsons Bridge (de Thier, 1976; Penney, 1982).

As mentioned earlier, throughout the late 1870's a number of major stormwater drains were constructed in Christchurch. Drains entering the Heathcote River included Waltham Road Drain, Ferry Road Drain, and Wilderness Drain, as well as a number that followed natural stream courses such as Jacksons and Bells Creek. In addition to carrying stormwater, many of these drains also carried untreated industrial effluent (Wilson, 1989).

By the 1880's and early 1890's the Heathcote River was also "silting up" as a result of stormwater runoff. In addition, the Woolston area of the river was so polluted that virtually no plant life existed (Hercus, 1948; Robb, pers. comm.).

Siltation was particularly noticeable after the construction of the present day market gardens in the Heathcote Valley area, between 1912 and 1914. Soil erosion greatly increased after the small holdings were taken up and much of the soil was removed by tunnel-gully erosion during heavy rain storms (Scott, 1963). The eroded soil was deposited on slopes of less than 3° and washed away during heavy rains.

In the 1920's, willow growth within the river was trapping silt and rubbish, which resulted in serious flooding during 1925. In 1925 the river sweeper purchased by the Christchurch Drainage Board was used to clear the Heathcote River from Ford Road to Long Street (Fig. 2.2; all the Woolston area). Between 1936 and 1941, the river was also swept below Cashmere Bridge and straightened and

deepened (Scott, 1963). Nearly all the silt swept during the early period ended up in the Avon-Heathcote Estuary (de Thier, 1976; P. McWilliam, pers.comm.). Draglines were used to widen and deepen the Heathcote River during the period 1945-1959 in the lower reaches from Radley Street Bridge downstream. This later method was more successful at removing sediment onto the land than the earlier sweeping technique (H. Page, ex Christchurch Drainage Board, pers. comm.). Many deep channels were dug to trap silt in the 1950's. During this time major floods brought much silt from the Port Hills which had to be removed by river sweeper and dragline during 1954-55 (Scott, 1963).

In recent years (since the 1950's) clearing and widening of the rivers has been undertaken less frequently because tar sealing of roads has reduced runoff considerably (J. Pollard, pers. comm.).

2.5 HISTORICAL OBSERVATIONS THAT INDICATE CHANGES IN SEDIMENTATION RATES IN THE AVON-HEATHCOTE ESTUARY

An extensive survey of the historical literature has revealed no record of sedimentation or water level changes in the Avon-Heathcote Estuary prior to 1920 (Table 2.1). Neither are there any significant changes reported at the estuary inlet prior to 1920 (Findlay and Kirk, 1988).

In 1907 the tram causeway was constructed across McCormacks Bay (Fig. 2.2). At the time Skylark Island, which was vegetated and grazed, existed just north of McCormacks Bay. After construction of the Causeway, the Island began to erode as the Heathcote channel was diverted northward. By 1922 Skylark Island was reduced to mud flats (Findlay & Kirk, 1988). Erosion was enhanced by burrowing crabs (Penney, 1982). It was during 1921 that George Andrews of the Christchurch Yacht Club had to restake the channels in Moncks Bay and the first major erosion occurred at the tip of Brighton Spit (Findlay and Kirk, 1988). It can be inferred that erosion of Skylark Island, brought

Fig. 2.6 Painting of a large sailing vessel the "Minnie" near Radley Street Bridge in 1880 (de Thier, 1976).

about by the construction of the causeway, contributed to changes in the channels in Moncks Bay and erosion at the spit end during the early 1920's.

2.5.1 Photographic Records

In 1850 the Heathcote River channel was the deeper of the 2 channels that flowed out through the Avon-Heathcote Estuary, hence was the preferred route for trade (Penney, 1982). Fig. 2.6 shows Captain P.J. Messervey sailing a large vessel the ("Minnie") near the present Radley Street Bridge in 1880 (de Thier, 1976). There is no mention of water level problems in the estuary or rivers at this time. The only problem ships suffered was negotiating the tight bends in the Heathcote River.

Several lines of photographic evidence demonstrate that the estuary did not "silt up" substantially prior to 1920 (Figs 2.7a, b, c, from de Thier, 1976). Figure 2.7a provides a scale for Fig. 2.7b (see Fig. caption). Figure 2.7b is a view looking west across Humphreys Drive from the Ferrymead Bridge during the first world war (1914-18). Water can be seen right out to the edge of the Heathcote Basin at low tide. This photograph was taken by David Barr (89 year-old resident of Redcliffs), who can remember sailing into the Humphreys Drive area in a 34 foot skimmer at low tide before World War 1. Mr. Barr remembers that there was a deep channel in the Heathcote depository at this time and boats with 12-15 foot keels used to moor at the Ferrymead Bridge.

Figure 2.7c dates 1927-28 (de Thier, 1976). This photograph looks south-east across the Heathcote Basin at low tide to the former Mortens Jetty below St Andrews Hill (Fig. 2.2). The photograph shows no sign of the deep channel of the Heathcote River and the mudflats are fully exposed. Figure 2.7c contrasts with Fig. 2.7b, which shows the mud flats covered with water at low tide. The 2 photographs reveal that rapid sedimentation of the

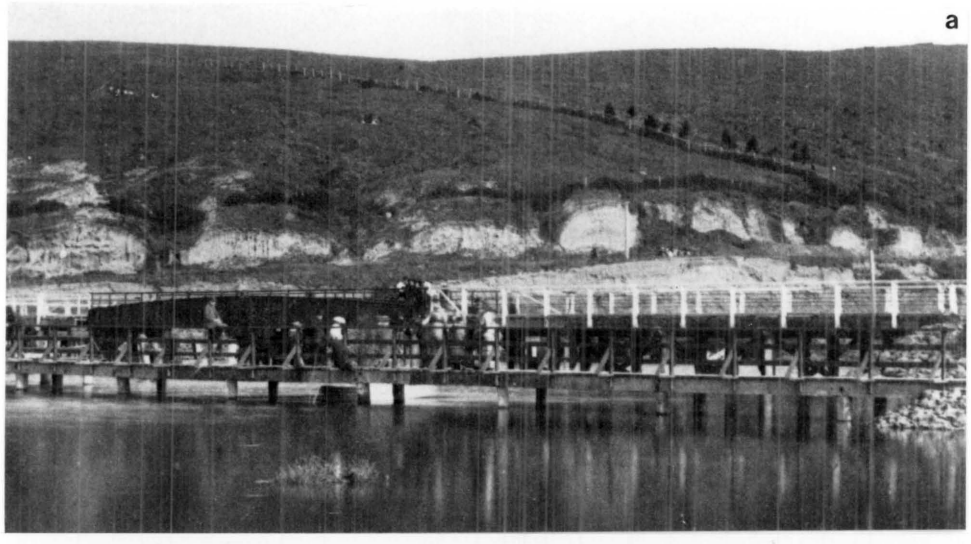
a

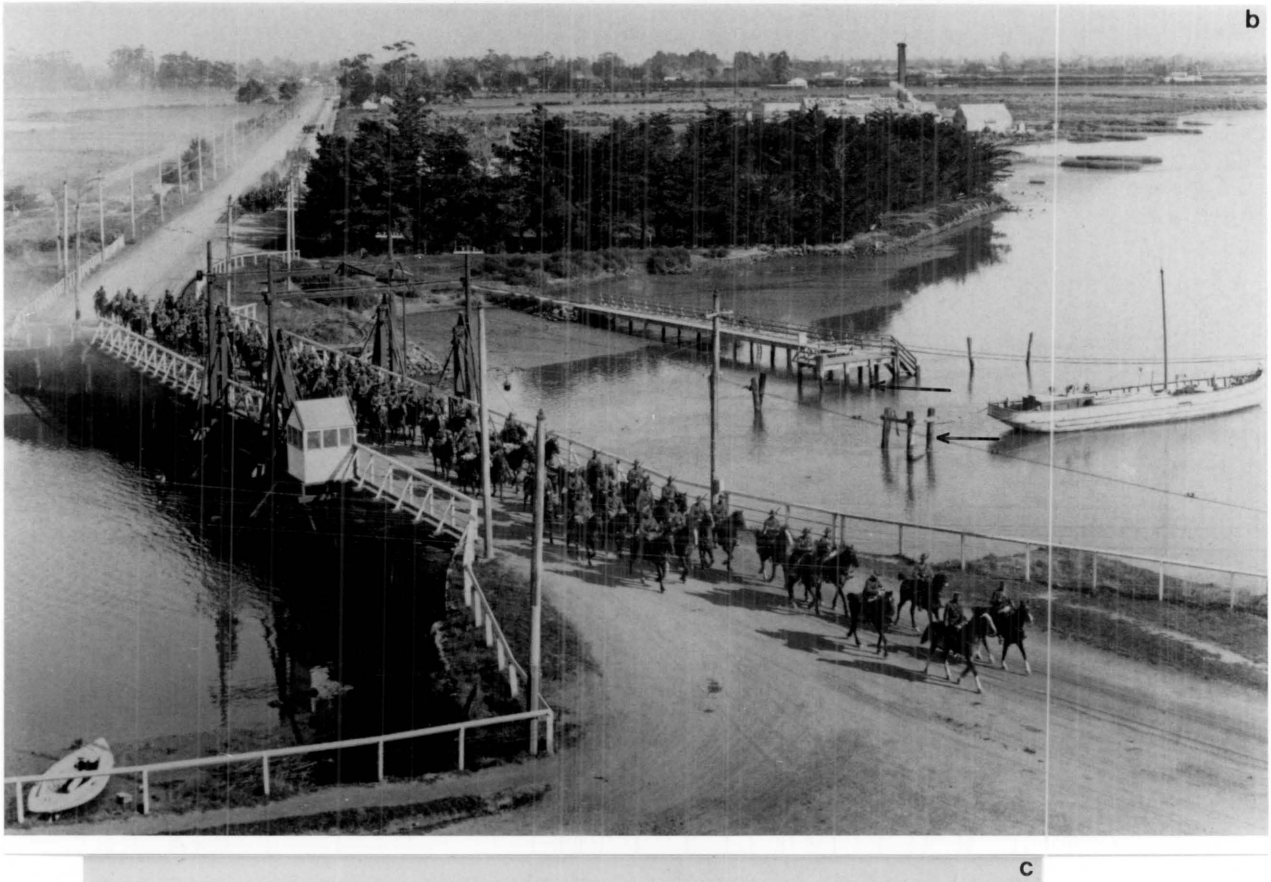
b


c

Fig. 2.7 Photographic Record of "Silting" in the Heathcote Basin between 1918 and 1928.

a) Jetty formerly located north of Ferrymead Bridge in 1880 (de Thier, 1976). This photograph provides a scale for Fig. 2.7b. The piles holding up the jetty are as wide as the adults walking on the jetty (ie over 1 foot wide). The jetty has long since dissappeared.

b) A view looking west across Humphreys Drive from Ferrymead Bridge during the First World War (1914-1918). Water extends right out to the edge of the Heathcote Basin at low tide. The same jetty as in Fig. 2,7a is in the middle of the picture. In Fig. 2.7b the piles holding up the jetty contain water marks 4 to 5 feet above the water surface (judging by the 1 foot thickness of the piles), which indicates that the tide is almost completely out. Similar water marks are also visible on the piles where the boat is moored (D. Barr, pers. comm.).

c) View looking southeast across the Heathcote Basin at low tide to the former Mortens Jetty below St Andrews Hill in 1927-28 (Fig. 2.2). This photograph shows the mud flats fully exposed, which is in contrast to Fig. 2.7b (Sumner Historical Society).

Heathcote Basin occurred between 1918 and 1928.

2.5.2 Observations by Local Residents

Walter de Thier lived in the vicinity of the Avon-Heathcote Estuary all his life and was a pioneer in development of the dry lands of Banks Peninsula, Port Hills, Sumner, Mt. Pleasant, and St. Andrews Hill. In his book (de Thier, 1976) he writes about his own observations of silting in the estuary during the late 1920's and 30's. In 1921 Mortens Jetty was built directly below St. Andrews Hill Quarry (Fig.2.2). In the early 1920's the beach surrounding the jetty was composed of blue clay and sand. At this time the Heathcote channel extended right into Humphreys Drive before taking a loop back to the site of the jetty (loop 1, Fig.2.8a). De Thier describes the disappearance of the meander loop as the Heathcote River brought silt down from the Port Hills and works at Woolston. De Thier explains how, during 1926, the river sweeper "sluiced 60 years of accumulated mud and filth" from the Avon and Heathcote Rivers into the estuary. The mud carried effluent and waste from industries along the banks of the Heathcote River to the estuary. As sediment filled the loop, the channel was diverted towards the jetty. De Thier states that "black banks were formed and channels were blocked, as the ebb and flood tide met, such a bank built up opposite Mortens Jetty which forced the stream over and the break work and steps were undermined."

George Andrews was a well known yachtsman sailing on the estuary between 1895 and 1952. In page 2 of his notes (held by Dr J. Robb, Christchurch Drainage) he writes "The greatest change that has come over the upper part of the estuary has been the disappearance of the seagrass, the lowering of the mud flats, and silting up of the channels. I estimate the lowering of the mud flats has been from 1-2 feet over the greater part. The old channels have almost

entirely silted up and shallow new ones acting as drains and taking a more direct course to the outlet, have in part taken their place." This statement mentions lowering of the mud flats, which indicates major erosion as alleged by Macpherson. However, Andrews clarifies this point on page 3 of his notes: "Without going into figures, it can be concluded that 1½ feet more water over the whole estuary would be a tremendous increase in the volume of water going in and out each side of high water. Changes with a sandy outlet were bound to happen." Hence, Andrews is more likely referring to an increase in the tidal compartment, than erosion of the estuary bed.

It is not known exactly when George Andrews notes were written, but it must have been after 1940 because he mentions the straightening of the channels, which was not apparent until well into the 1940's (see, later discussion).

Referring back to Kirk and Findlay's tidal compartment curve (Fig. 2.4) an increase of approximately 35% occurred between 1850 and 1940 which corresponds to a water depth increase of about 2 feet (assuming the average high tide level is 5 feet above the low tide level). In addition, the sea level rose about 8cm between 1850 and 1940 (D. Carver, Christchurch Drainage, pers. comm.).

David Barr noticed that rising water levels during the 1930's and 1940's caused considerable erosion at Beachville. During that time the retaining wall at Beachville was extended upwards to prevent serious damage to property (Fig.2.2). David Barr also had a bach (holiday home) at Rockinghorse Road on the Southshore (Fig.2.2), and remembers erosion problems in the area around 1940. Barr claims that silting of the estuary was mainly confined to the channels and that most other changes to the estuary were related to channel movement.

Another elderly resident of the area, Joan Ritchie, remembers sailing from Moncks Bay to the jetty at Jellicoe Park in 1920 and that a deep channel (Jellicoe Loop) swung

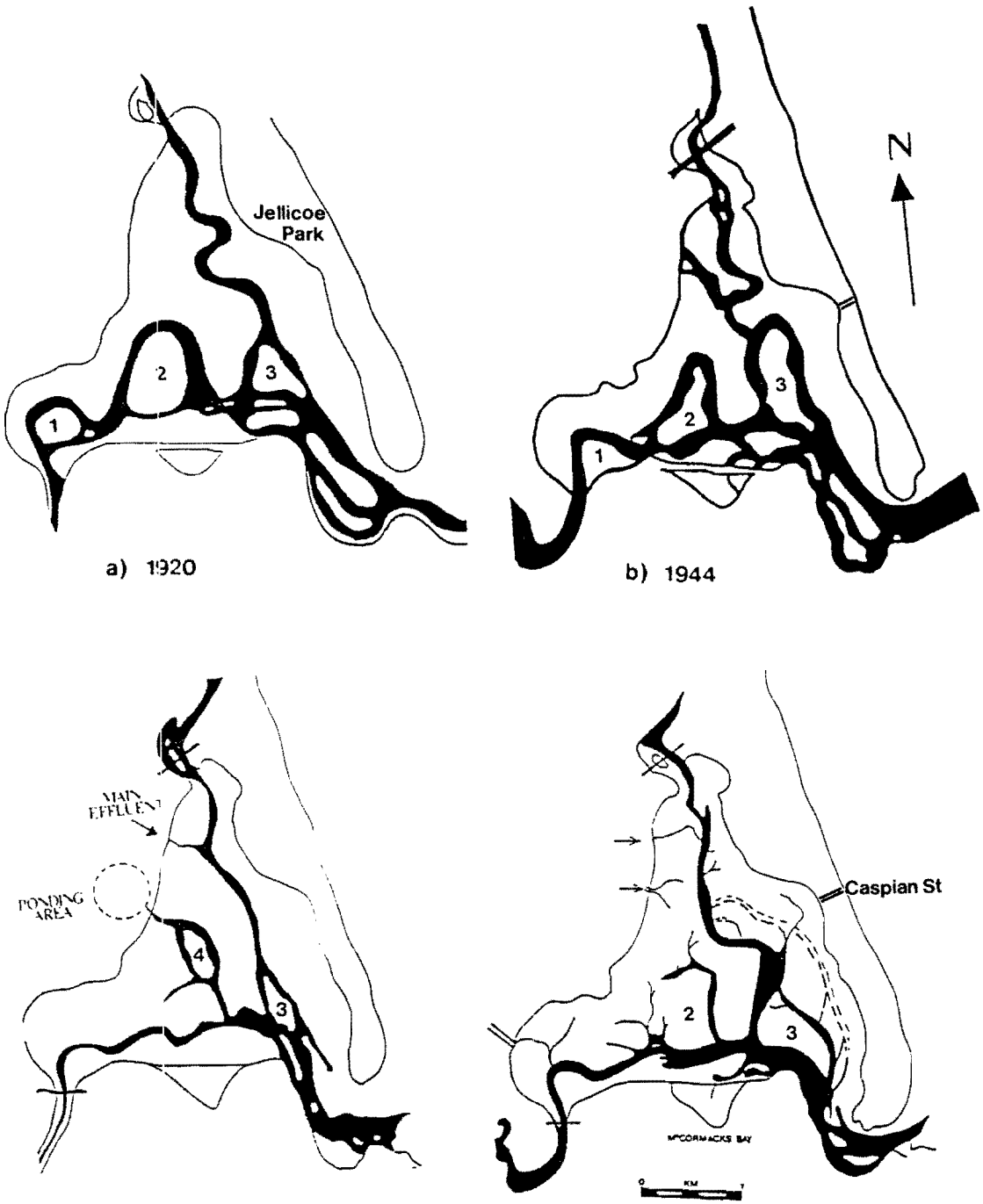

Fig. 2.8 Changes in the Configuration of the Channels in the Avon-Heathcote Estuary from 1920 to 1988 (Bruce, 1952; Christchurch Drainage Board (CDB), 1988; Knox and Kilner, 1973; Linzey, 1944; Macpherson, 1978; and Webb, 1965).

eastward in front of the park (Fig. 2.8a). At the time of the First World War, large sailing vessels with deep keels tied to the Jetty.

During 1935-36 the shallowing and silting problem in the estuary seriously hindered yachtsmen of the Pleasant Point Yacht Club (Penney, 1982).

By 1948 the continued shallowing of the estuary was causing further problems for yacht races (Penney, 1982).

Stan Rule (Sumner Historical Society) was involved with drain laying in the mud flats of former Skylark Island around the 1960's and has noticed since then that about 1m of erosion has exposed the pipes. Mr Rule stated that the erosion appears related to channel movement.

2.5.3 Scientific Observations

Thompson (1930) made a full biological survey of the Avon-Heathcote Estuary during 1928-1929 and described the sediment as follows, "Near the channels, except for extensive sand in Moncks Bay, the mud is soft and heavy, grey on top and a black evil smelling substance below....nothing but heavy mud occurred at low water and this merged into clay at the high water mark". Thompson describes the shores as soft mud banks riddled with the burrows of the crab Helice crassa.

Linzey (1944) made a hydrographic survey of the estuary in 1943 and describes the bed of the estuary as "fairly compacted" except around the outlets of the sewers. He mentions that the clay banks near the Heathcote River were suffering serious damage between the tide marks caused by crabs burrowing. Linzey's survey shows a large loop in the Heathcote channel across the western flats in front of the Sewage Farm (loop 2; Fig.2.8b). At the same time the Avon channel formed a large meander in front of Jellicoe Park (Jellicoe loop); and the channel split in two opposite Caspian Street (see Fig. 2.2 for location), one branch flowing over the eastern flats to Moncks Bay, the other

branch flowing south to join the Heathcote channel opposite the eastern end of the causeway across McCormacks Bay. Linzey describes the surface sediments of the estuary as more or less homogeneous mud with material on higher slopes generally coarser than nearer the channels. Sediment near the sea is described as coarser than nearer the head.

The map of Bruce (1952, Fig. 2.8c) shows that loop 2 had disappeared (in the Heathcote Channel) except for a small arm extending west below a new loop 4 formed by effluent discharge from the more southern outlet of the sewage ponds. Loop 1 had also decreased in size since 1944. It is clear that the two river channels straightened between 1944 and 1952. By 1952 the Avon meander in front of Jellicoe Park had almost disappeared and the split in the channel had migrated a considerable distance south towards Moncks Bay. The straightening of the channels corresponds with the sediment accumulation in the channel meanders described by Andrews, Barr, and de Thier. These two maps (Fig. 2.8b and 2.8c) also show that between 1944 and 1952 that the three channels in Moncks Bay migrated south forming a large single channel.

The positions of the channels from 1962 to 1988 are shown in Fig. 2.8d. The positions have changed little since 1952, except the Avon channel has migrated westward in the northern area of the estuary. By 1988 the northern margins of the subtidal channels in front of the ponds had almost closed reforming the old loop 2. Also a small subtidal channel of the Avon River has formed along the eastern shores (Christchurch Drainage Board, 1988). The relative stability of the channel positions from 1962-1978 indicates that sometime between 1952 and 1962 the water and sediment budget to the Avon-Heathcote Estuary stabilised and the period of rapid mud deposition ended.

Millward (1975) described the surface area of the estuary consisting of fine sand and mud with the highest percentage of mud near the river entrances, on the western and eastern shores adjacent to the old meander loops.


a


b

Fig. 2.9 Southward View of the Mactra ovata Shell Beds adjacent to the Avon River channel near Pleasant Point (Fig. 2.2). Fig. 2.9a was taken in 1975 (Harrison, 1976) and Fig. 2.9b in 1988. Comparison of the two photographs indicates that the Avon River has eroded less than 1m westward into the shell beds over the period 1975 to 1988.

(Slight differences between the two views include: 1) Fig. 2.9b was taken standing at approximately the position where the shell beds cross the black horizontal line in Fig. 2.9a, hence the small channel is behind the photographer, 2) the tide is slightly further in (by about 0.75m) in Fig. 2.9b than in Fig. 2.9a; the arrow marks the position of the channel, 3) the photographer probably knelt while taking Fig. 2.9a, whereas the author stood while photographing Fig. 2.9b, and 4) Fig. 2.9a was taken using a wide angle lens, hence the background is enlarged relative to the foreground in Fig. 2.9a which slightly distorts a clear comparison between the two photographs.)

Millward observed a sand layer beginning to cover the eastern shores. Macpherson (1978) made similar observations but observed a reduction in the size of the muddy area on the eastern shores. Macpherson concluded from surface sediment studies that in most areas, sediment is being actively deposited in the Avon-Heathcote Estuary, under the influence of tide, wind, and wave action, but intense bioturbation is causing slow sediment removal from the estuary.

The photographs in Fig.2.9a and b are taken about 100m south of Bridge St bridge looking south along the Avon Channel. The first photograph (Fig. 2.9a) was taken by Harrison (1976) and the second photograph (Fig. 2.9b) by myself in 1988. The two pictures have been scaled to equivalence (horizontally and vertically) using the hills in the background. Taking the differences into account (noted in the Figure caption), a comparison shows that in the last 12 years the Avon River has cut less than 1m westward into the Mactra Ovata shell beds. The shell beds are 5 cm thick and the shells are in life position. Harrison reported the same thickness in 1975, which indicates that insignificant surface erosion or deposition has occurred in this part of the estuary over the last 12 years. These findings suggests that the estuary has stabilised in recent years except for slight shifting in the channels.

Today the surface sediment of the Avon-Heathcote Estuary consists mainly of muddy sand with only small areas of over 50% mud, which include the Avon and Heathcote depositories and zones near the channels.

The observations of changes in 1) sedimentation and 2) channel positions strongly suggest that the estuary was filled with a blanket of mud between 1925 and about 1952. This blanket of mud is probably Unit C sediment of Macpherson (1978) (see Chapter 3 for discussion of subsurface sediment). The disappearance of the loops in the Avon and Heathcote channels and the straightening and

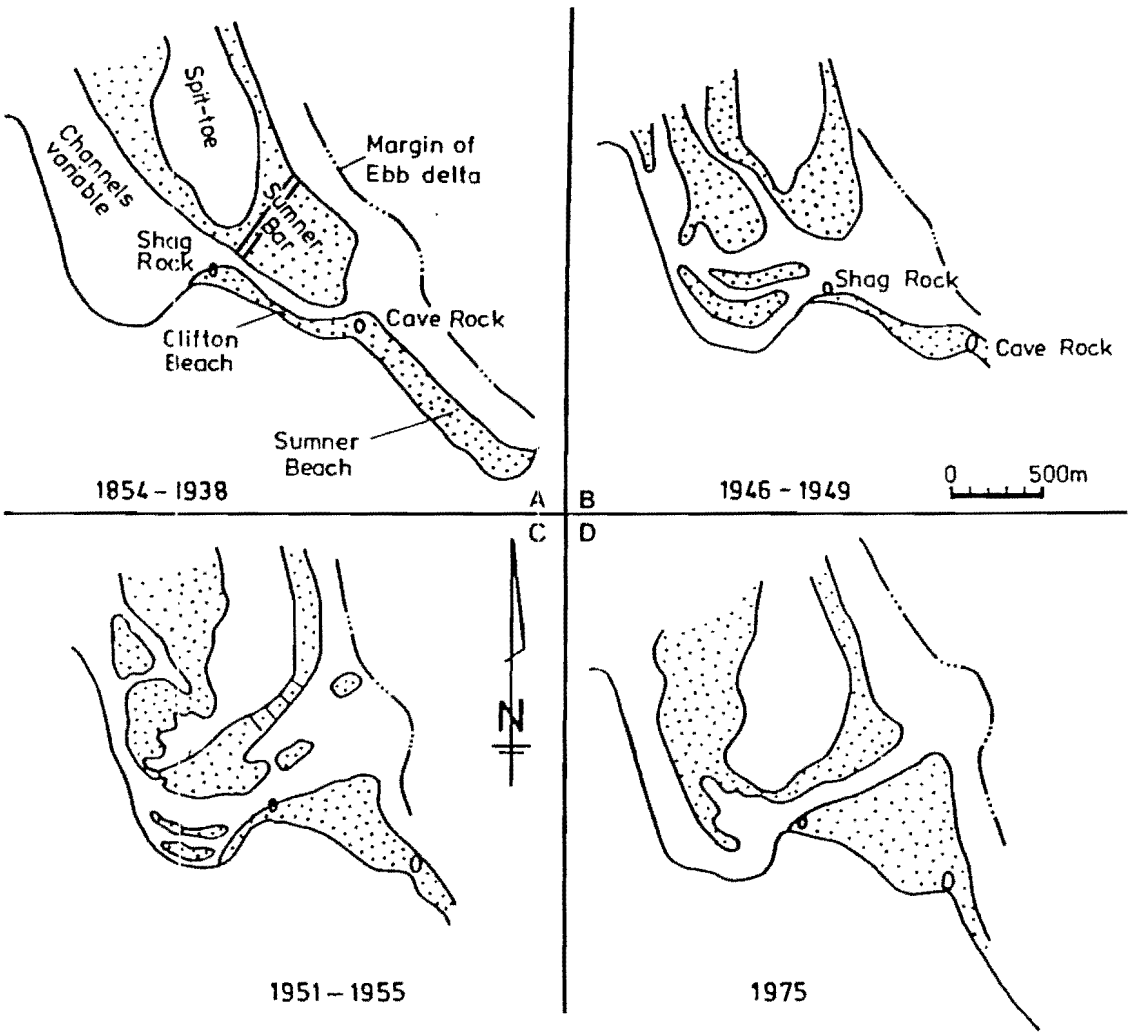

Fig. 2.10 Summary of changes to the estuary mouth between 1854 and 1978 (Findlay and Kirk, 1988). ═══ , channel cut by Navy in 1916.

widening of their courses corresponds with 1) the increasing tidal compartment and 2) the gradual build up of silt on the eastern and western shores, and Avon and Heathcote depositories. Somewhere between 1952 and 1962 the mud deposition slowed and estuary conditions stabilised, as indicated by the uniform pattern of the channels between 1962 and 1978. Recently, further stabilisation of the estuary is suggested by the gradual formation of meanders near the former channel loop positions.

2.6 HISTORICAL CHANGES TO THE ESTUARY MOUTH 1850-1988

Detailed historical records of changes to the estuary inlet are presented by Macpherson (1978), Findlay (1984), Kirk and Findlay (1988). The historical records show very little change to the estuary mouth between 1847 and 1910 (Table 2.1). During this period there were three channels in Moncks Bay, their position variable. The main channel discharged to sea just north of Cave Rock (Fig.2.10a). A large sand bar (Sumner Bar) extended south east off the toe of the spit.

During World War I a channel was cut across the Sumner Bar by the Navy (Penney, 1982). Between 1918 and 1922, during the time that Skylark Island was eroding (Section 2.5), there was a large build up of sand at Clifton Bay and 22 acres of land was eroded from the toe of the spit.

In the late 1920's more significant changes commenced at the estuary mouth. Firstly, in 1929 a new mouth opened up beside the Naval Reserve channel across Sumner Bar, and severe erosion occurred in late 1930 to the toe of the spit. While Clifton Beach was prograding in 1929-33 the ebb channel was gradually re-directed across the bar (George Andrews; Findlay and Kirk, 1988). By 1936 the ebb channel had moved north 150m, after the spit hook formed. The spit hook interfered with the northern most Moncks Bay channel, because by 1936 the flow was confined for a period to the southern side of Moncks Bay. During 1938, the main ebb

delta migrated north from Cave Rock to its present position where it has remained (Fig.2.10b). This event was followed by severe erosion to the spit tip between 1940-49. Around 1947, the main flow was transferred permanently to the southern most channel in Moncks Bay.

The spit end and its hook consolidated and stabilised after the construction of fences and drum groynes during 1949-50. During 1964-70 there has been slight progradation of the spit with minor erosion episodes. The 1970's and 80's has also seen minor erosion and accretion of the spit. However at the present time the spit's configuration is similar to that of 1975 (compare Fig. 2.10d and Fig. 2.11).

Findlay and Kirk (1988) and Macpherson (1978) concluded that the changes in the estuary inlet between 1920 and 1950 were initiated by the increasing tidal compartment. These workers believed that when the tidal compartment reached a level beyond the pre-European high of 8×10^6 m^3, the inlet changed its configuration to accommodate the increasing flow.

Findlay and Kirk suggested that the changes at the mouth may have been initiated by the erosion of Skylark Island between 1910-20. These authors view Christchurch as a continuous area containing uniform proportions of unsealed to sealed surfaces and noted that the growth of the urban area of Christchurch parallels the growth of the tidal compartment until 1925 when urban growth rapidly accelerates. They suggest that during the 1920's and 30's the estuary reached a size beyond which the inlet was forced on it the change, from a bar dominated configuration to a mixed tidal and bar dominated configuration, to accommodate the increased flow. Post 1950 accretion and stabilisation is interpreted to indicate that the inlet has fully adjusted to the 1940-50 tidal compartment.

The construction of groynes and fences at the end of the spit probably had a marked affect on spit stabilisation over the last 40 years despite the rapidly increasing tidal

compartment (Fig. 2.4).

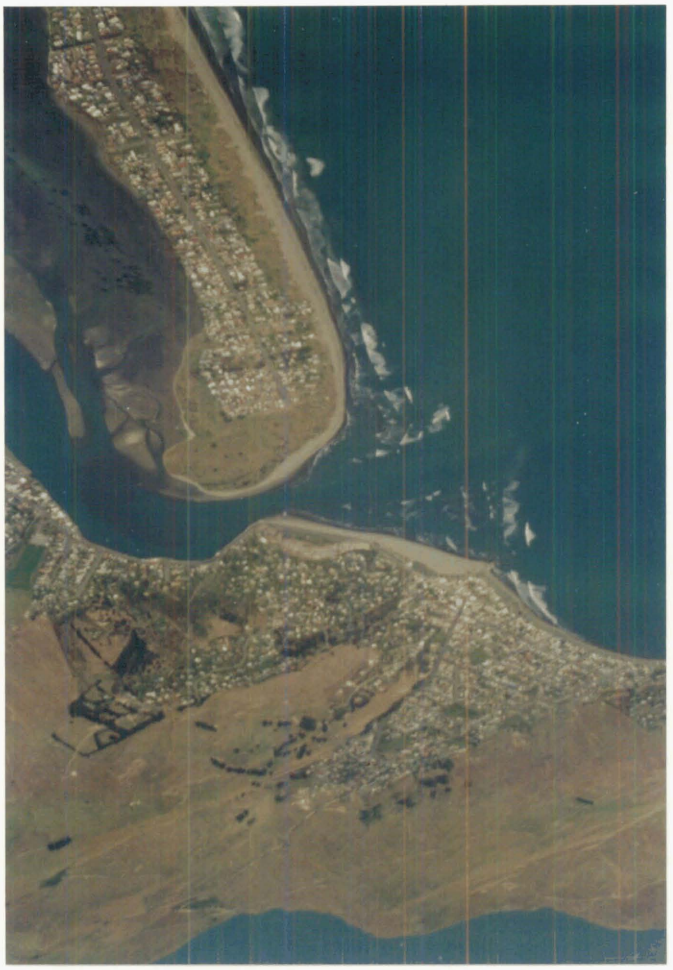

Fig. 2.11 The estuary mouth, 13 April 1991 (I.J. Brown, N.Z. Geological Survey pers. comm.). In 1991 the positions of the channels and bars are similar to those in 1975 (Fig. 2.10d) indicating that the spit toe is stable.

2.7 OBSERVED CHANGES IN FLORA AND FAUNA OF THE AVON-HEATHCOTE ESTUARY

2.7.1 Eelgrass (Zostera nana)

The eelgrass (or seagrass) Zostera nana grew prolifically throughout the estuary prior to 1928 (David Barr and Joan Ritchie pers. comm.). Before the causeway was built in 1907, Zostera grew lushly in deep channels in McCormacks Bay, where eels could be seen feeding (de Thier, 1976). Around 1910 about 10 families made their living by collecting shrimps from the eelgrass beds around the Avon-Heathcote Estuary (Gibb, 1981; Ogilvie, 1978). A local resident, David Barr, has a photograph dated 1910 showing the eelgrass growing in thick patches along the banks of the low tide channel near Beachville Road. George Andrews mentions that the eelgrass grew everywhere between the channels and the shoreline except for a small patch, 1km radius, down stream of the Heathcote River Bridge. Andrews describes near the channel edges, an anaerobic black layer of mud existing beneath the plant beds, above a soft puggy clay. George Andrews noticed that Zostera disappeared at the same time channel erosion commenced.

In 1928-29 Thompson (1930) recorded Zostera growing very sparsely and could not see any particular reason for dwindling plant numbers, because at the time Zostera was growing well in others areas of New Zealand. By 1952 Zostera had almost completely disappeared and was found growing only in small areas near South Brighton Bridge (Bruce, 1952). South Brighton Bridge, incidently, was one of the most organically polluted areas in the estuary at the time. However, by the 1960's Zostera numbers were increasing in abundance and were recorded, in addition to New Brighton Bridge, along the Avon channel and near the causeway (Gibb, 1981; Webb, 1965). Observations by Cameron (1971), Knox and Kilner (1973) and Macpherson (1978) reveal Zostera numbers were vastly higher in the 1970's. By then

Zostera had extended to dense patches on both sides of the Avon and Heathcote channels and other central parts of the estuary. In 1981 Gibb recorded the eelgrass growing continuously and densely over most of the tidal area of the estuary.

The cause of the disappearance of Zostera from the Avon-Heathcote Estuary has received much debate over the last 40 years. Other varieties of Zostera began to disappear from river and estuary beds in North America and Europe in the 1930's and re-established again in the 1950's (Marger and Milne, 1951). Some of the disappearance has been traced to attack by fungi and parasites, while others were thought to be related to industrial pollution and silting. In the mid 1930's, Zostera beds in Hobson Bay Estuary, Auckland Harbour, were destroyed by rapid sand deposition (Hounsell, 1935). Macpherson (1978) found large clumps of Zostera leaves in Unit C sediment in many of his cores.

It seems unlikely that the Zostera beds of the Avon-Heathcote Estuary were attacked by fungi because (1) Zostera was widespread in other areas of New Zealand (Parenga Harbour, Stewart Island), and (2) there is no record of Zostera beds attacked by fungi in the Southern Hemisphere at the time. Domestic and industrial pollution is also unlikely to be the cause of Zostera disappearance because, in 1952, surviving plants were in the most polluted area of the estuary near the northern outlet of pond 6.

The disappearance of Zostera beds correlates closely in time to the silting of the estuary, and changes to the inlet, between 1927 and 1952. Hence it seems likely that the Zostera beds were silted up in the early 1930's at the same time other changes occurred in the estuary.

2.7.2 Algae

2.7.2.1 Ulva and Enteromorpha

Blue green algal blooms are frequently associated with "cultural" eutrophication of estuaries (Knox and Kilner, 1973). Sewage effluents are normally rich in nitrogen and phosphorous compounds which stimulate algal growth. When high numbers of algae die they increase in the level of organic detritus in the sediment, which is the principal source of energy for most benthic dwellers. Hence, the numbers of crabs, mud-flat snails, shellfish, worms, and shrimps rapidly multiply. In addition, organic matter decay leads to oxygen depletion in sediments. In the resulting anaerobic environment, heavy metals are remobilised from sediment surfaces, and become preconcentrated in the pore waters (Chapter 1). Such conditions increase the bioavailability and toxicity of heavy metals.

The algae species Ulva lactuca (sea lettuce) and Enteromorpha were practically absent from the Avon-Heathcote Estuary before 1946 (Thompson, 1930; Bruce, 1952). Both species were abundant in 1949, however, and increased dramatically between 1950 and 1960 (Knox and Kilner, 1973).

Knox and Kilner studied the ecology of Ulva and Enteromorpha and attributed their rapid spread to an increase in 1) nutrient input to the estuary from the sewage effluent, 2) summer temperatures, and 3) numbers of cockle shells. During the winter, these drift algae survive as reduced water plants attached mainly to cockle shells, where they remain dormant until spring. During spring the algae grow and become buoyant enough to float. Their distribution patterns are related to water circulation patterns. Knox and Kilner's report contains photographs showing 100% algae cover of Humphreys Drive area and McCormacks Bay in the early 1970's.

The blue green algae are still extremely abundant in the Avon-Heathcote Estuary. When these species die their

decomposition commonly causes high levels of organic matter in the Humphreys Drive and McCormacks Bay areas.

2.7.2.2 Green Slime (Euglena)

A yellow green slimy flagellate is found on the surface sediment in front of the outlets of the sewage ponds on the western slopes of the Avon-Heathcote Estuary. Euglena is a particularly sensitive indicator of pollution because it thrives in environments high in organic matter and nutrients (Knox and Kilner, 1973).

From the early 1950's to early 1970's, very dense populations, up to 700,000/cm^3, occurred in front of effluent discharges from the Provita Starch Factory (Humphreys Drive), and septic tanks from St. Andrews Hill, Ferrymead, Mt. Pleasant, Moncks Bay and Sumner; as well as in front of the oxidation ponds, and at the entrances of the two rivers.

When Euglena is present it deprives the sediment of oxygen resulting in anaerobic black sediment rich in H_2S. After the Starch Factory closed (1968) and the Ferrymead to Sumner effluents were diverted to the treatment plant, Euglena numbers decreased markedly in these areas (Knox and Kilner, 1973; J. Robb, pers.comm.). Since the ponds stopped discharging during the flood tide, effluent is no longer swept up the rivers, and Euglena numbers have also decreased in sediments at the river entrances.

2.7.3 Shellfish

The muddy reaches of the Avon-Heathcote Estuary are rich in macro-invertebrates particularly the mud snail (Amphibola crenata), cockle (Stutchyburyi sp) and crab (Helice crassa). These three invertebrates have greatly increased in abundance since 1930 due to an increase in the organic, nutrient and mud content of the sediment (Knox and Kilner, 1973). These shellfish are particularly abundant in the Heathcote Basin area and in front of the sewage ponds.

A death assemblage of a burrowing bivalve Mactra ovata is exposed within Unit C sediment at Pleasant Point (Fig.2.9). Macpherson (1978) suggested that this assemblage was killed by rapid deposition of Unit C. Unit C also lacks all other species of ostracods that are found in sediment above and below the unit, except Callistocythene reoplana, which thrives during conditions of rapid sedimentation. Macpherson suggests that the rapid sedimentation of Unit C may have caused mass mortality of many micro and macro invertebrates, which have recently recolonised.

2.8 INDUSTRIAL ACTIVITY ALONG THE BANKS OF THE HEATHCOTE RIVER

From 1860 to 1973 the Heathcote River was severely polluted by industrial activity along its banks (Hercus, 1948; Knox, and Kilner, 1973; Morrison, 1948; Wilson, 1989).

During the 1850's few industries had developed (Table 2.1). At the time there was 1 iron foundry, several breweries, a sawmill, and few other shops.

By 1860 coal was being brought in by ships to the Railway at Ferrymead. As a consequence industries thrived. In 1864 the Woolston area housed 36 builders, 2 carriage builders, 2 brick makers, 4 carriers, 2 iron foundries, sawmills, 5 iron mongers, a moulder, 6 tinsmiths, 2 zinc works, 7 blacksmiths, 1 fellmonger, a brewery and other industries. All industries discharged untreated wastes directly into the Heathcote River (Hercus, 1948; Morrison, 1948)..

Industries developed further by 1874 to include 8 wool scours, 7 tanneries, 1 soap and candle factory (located in the Humphreys Drive area, which discharged wastes directly into the Avon-Heathcote Estuary), and several glue factories.

By 1884 there were 8 tanneries, 2 lime kilns, and many iron and brass foundries making implements for agricultural

purposes.

In 1903 Christchurch (Woolston and Sydenham) was the principal iron working district and chief industrial centre of New Zealand (Hercus, 1948; Hoben, 1914; Morrison, 1948). At the time there were 10 tanneries, and a large population employed in making railway rolling stock and agricultural implements. "As a commercial centre the city drained the trade of one fifth of the population of New Zealand" (Hercus, 1948). Over 4½ million litres of industrial effluent discharged to the Heathcote River each day (Dr. J. Robb, Christchurch City Council, pers. comm.). However, "many industries such as small tanneries, lime kilns, and wool works were very short lived" (Morrison, 1948), and by 1915 Bowrons Tannery was the only tannery operating.

During the booming industrial period, coal was the principal fuel burned to generate steam. The atmosphere, particularly in the industrial area, was described as "very dark and murky with black soot covering many buildings" (Hercus, 1948).

Electricity was introduced after 1913, but most industries continued to burn coal as their main fuel. One of the most prolific coal burning industries was the Christchurch Gas Works. There have been many spills from the gas works since the 1860's, with serious spills in the 1950's emptying coal, coke and tar grit into the Heathcote River at Bells Creek. The Christchurch Drainage Board's dredge removed 100-1000's of tons of black sediment from the Heathcote river during the late 1950's (David Bar, pers comm.; Knox, and Kilner, 1973; J.Pollard (ex Christchurch Gas Works), pers comm.). Spills from the gas works and other industries caused the Heathcote River to deteriorate ecologically between 1956 and 1968. During this period the river bed between Bells Creek and the Tunnel River Bridge was described as black glutinous mud which released H_2S when disturbed (Cameron, 1970). The river water in this area was devoid of oxygen and the sediment absent of animal life (Christchurch Drainage Board, 1988).

Before 1971, over 10 million litres per day of effluents from over 150 firms discharged directly into the Heathcote River. Around this time, a battery factory effluent entering the river frequently contained Pb concentrations 10-8400 μg/ml (Christchurch Drainage Board, 1988). Between 1971 and 1973, after the construction of the Woolston Industrial sewer, all such effluents were pumped directly to the Christchurch Drainage Board Treatment Plant. (Knox, and Kilner, 1973; Dr J.Robb, pers comm., Christchurch City Council). One of the few remaining effluents was that of the Christchurch Gas Works, which continued discharging into the Heathcote River, via Bells Creek, until it closed in 1981 (J.Pollard, pers comm.). Since the industrial effluents were removed from the river in 1973, the water and sediments have shown considerable improvement and shellfish are slowly recolonising the area (J. Robb, Christchurch City Council, pers comm.).

The types of contaminants most likely to have affected the bed of the Heathcote River and the Heathcote Basin area of the estuary over the years 1860 to 1973 include As, Cr (from tanneries), Pb (from battery factories), HCl (from glue works), acids, alkalis, and sulphur compounds (from woollen mills), calcium bisulphate (from wool scours), acid, and heavy metals such as Pb, Cu, Zn, Cr, Ni, Fe, (from metal works), tars and oils (from the gas works), and atmospherically derived coal and coke particles (from coal burning).

2.9 SYNTHESIS OF HISTORICAL DATA

The historical analysis of changes in sedimentation patterns in and around the Avon-Heathcote Estuary has yielded no data on the estuary proper prior to 1910 (Table 2.1). However, during this early period major industrial activity in the Woolston and Sydenham areas most likely supplied heavy metals to Heathcote River and Avon-Heathcote Estuary sediments.

The first changes in sedimentation patterns were confined to the area near the mouth of the estuary. The construction of the causeway across McCormacks Bay in 1907 diverted the Heathcote channel across Skylark Island. The disappearance of the Island between 1918 and 1922 corresponds with channel changes in Moncks Bay, severe erosion at the spit end, and a build up of sand on Clifton Beach.

The events that lead to the major "silting" phase in the estuary started during the early urbanisation of Christchurch. Between 1875 and 1880 7 major stormwater drains were built all leading to the Avon and Heathcote Rivers, except the City Outfall drain which emptied directly into the estuary. These drains successfully lowered the water table of Christchurch. However, during heavy rain and floods large quantities of surface soils were carried with stormwater into the rivers. As a result, the rivers shallowed rapidly. The construction of the City Outfall Drain in 1874 may have initiated "silting" in the Heathcote Basin area of the estuary; however there is no supporting evidence in the given review.

The ongoing coal burning and industrial activity centred in the Woolston area would have increased heavy metal and coal particle fluxes to the Heathcote River after 1860. However, the rapid mud deposition may have diluted the levels of many contaminants in the Heathcote River.

The rapid sedimentation of the rivers continued until 1925 when the Christchurch Drainage Board purchased a river sweeper. Between 1900 and 1925 silting of both rivers increased markedly. The causes were 1) tripling of the area drained by storm sewers, which followed the amalgamation of Christchurch suburbs (1914-1931), and 2) soil erosion in the Heathcote Valley (1912-1914), where market gardens were being developed.

The river sweeper commenced work on the Heathcote River in 1925, 2 years before it worked on the Avon River. Therefore, mud deposits in the Heathcote Basin are likely

to be several years older the Avon Depository, especially if the City Outfall Drain had an affect prior to 1900.

The period of the river sweeping as well as the photographic, historical, and scientific records (including the disappearance of Zostera) strongly suggest that the Avon-Heathcote Estuary filled with mud rapidly from 1925 to the early 1950's. The evidence suggests that the thickest silt deposits accumulated in the channels.

Sediment swept from the lower reaches of the Heathcote River was probably contaminated with heavy metals. However most of the sediment entering the estuary, between 1925 and 1950, was derived from uncontaminated areas, such as Port Hills Loess, the Avon River bed, and the Heathcote River bed many kilometres upstream of the Woolston district. Hence, such contamination may be diluted by large quantities of "clean" sediment.

All historical and scientific evidence of erosion presented here relates to bioturbation and erosion of either the channels or the periphery of the estuary (such as Fig. 2.5). Considerable erosion has been reported during the period of rapid sedimentation between 1925 and 1950. The erosion of the channels seems to be related to 1) intense bioturbation, 2) infilling of old channels, and 3) the disappearance of the Zostera beds. The increase in benthonic shellfish is a result of 1) higher mud content of the sediment and 2) eutrophication of the estuary. The eutrophication has been brought about because nutrients and organic matter introduced to the estuary from sewage effluents have caused the expansion of all organic life commencing at the bottom of the food chain with algae species such as Ulva and Euglena (Knox and Kilner, 1973). The silt accumulation in the early channel loops correlates with the disappearance of the Zostera beds. Zostera is a well known sediment binder in estuaries throughout the world (Knox and Kilner, 1973). As the plant disappeared from the Avon-Heathcote Estuary, new sediment deposited near the main channels would have been unstable and easily

re-eroded.

Erosion around the circumference of the estuary clearly relates to increasing water levels throughout the history of Christchurch. Rising water levels were caused by 1) increasing tidal compartment, and 2) rapid infilling of channels with sediment.

The growing tidal compartment is a direct result of drain laying in the Christchurch area after 1875, which has accelerated stormwater runoff. To a lesser extent, discharge of sewage and industrial effluent would have enhanced the water volume prior to 1950. However, after 1950 the massive increase in effluent discharging on the western slopes probably had a greater affect on tidal compartment volumes. The higher volume of sewage effluent discharged to the estuary after 1950 was due to 1) the rapid growth of Christchurch, 2) extensions of the CDB treatment plant, and 3) the diversion of all industrial effluents to the treatment plant. The findings of this analysis suggest that the tidal compartment increased fairly rapidly from the time the early settlers arrived, which agrees with the tidal compartment curve of Findlay and Kirk (1988).

While rapid sediment deposition may slightly decrease the volume of water entering and leaving an estuary during a tidal cycle, it would also lead to elevated water levels. Water would be expected to spread upwards and outwards in a small shallow estuary, such as the Avon-Heathcote Estuary. The erosion reported around the perimeter of the estuary supports such water movement.

The water level increase observed by George Andrews suggests that the tidal compartment growth was so rapid that the period of silting caused only a slight deceleration in its growth rate. Such a deceleration is suggested by the change in slope of Findlay and Kirks tidal compartment curve after 1920 (Fig.2.4).

There is little historical evidence for or against large scale erosion between 1950 and 1960. The intense

bioturbation of unstable channel edges (partly due to the absence of Zostera) may have resulted in some sediment loss. However, the stabilisation of the spit combined with the ever increasing tidal compartment suggests no major loss of material from the bed of the estuary.

Macpherson's bed level data show some loss of sediment from the intertidal flats between 1962 and 1975. Figure 2.5 shows that, at this time, there was also considerable losses from the perimeter of the estuary.

The stable channel positions in Figs 2.8d and 2.9 suggest that the estuary has stabilised in the last 20 years with minimal losses from the channel edges, where Zostera plants have now recolonised. There remains some sediment erosion around the circumference of the estuary, but most areas are now adequately stop banked.

From 1860 to 1973, contaminants (such as heavy metals) were entering the Avon-Heathcote Estuary from industries adjacent to the Heathcote River, the City Outfall Drain, and the septic tanks surrounding the estuary. During the period of rapid mud deposition, contaminant levels in sediments were probably diluted. However, after 1950 concentrations probably rose rapidly as sedimentation slowed. Following the early 1970's, contaminant levels should have dropped abruptly after all untreated effluents were removed from the rivers and estuary.

CHAPTER 3

GEOLOGY OF THE AVON-HEATHCOTE ESTUARY, TRAVIS SWAMP, AND SALTWATER CREEK ESTUARY

The most important factors that influence heavy metal distributions in sediments are 1) grain size distributions, 2) mineralogy, 3) sedimentation rates, 4) biological activity and 5) anthropogenic activity (Cauwet, 1987).

As discussed in Chapter 1 the fine clay grain size (<4μm) contains higher trace metal concentrations than the coarser sand (>63μm) and silt (4-63μm) size fractions (Forstner, 1989; Horowitz, 1985). As grain size decreases, increasing mineral surface areas and surface charges allow greater adsorption of heavy metals (Appendix 1). In addition, clay minerals exhibit high cation exchange capacities, and therefore readily exchange major ions for heavy metals in the aquatic environment. (Clay mineral chemistry is discussed in Chapter 1.0, Section 1.3, and Appendix 1.0.) Heavy metal grain size distributions are also affected by sediment reworking, which may increase or decrease the fine grained component of the sediment. Hence sediment reworking may alter heavy metal distributions in sediments. For the above reasons it is important to account for grain size distributions when studying heavy metals in sediments.

In industrially polluted water systems, where sedimentation rates are slow, bottom sediments may have high concentrations of heavy metals. In contrast, when sedimentation rates are high, a large sediment surface area is available for metal adsorption which may dilute metal concentrations, even in contaminated bottom sediments (cauwet, 1987). Hence, knowledge of sedimentation rates is important when evaluating the extent of heavy metal pollution in an area.

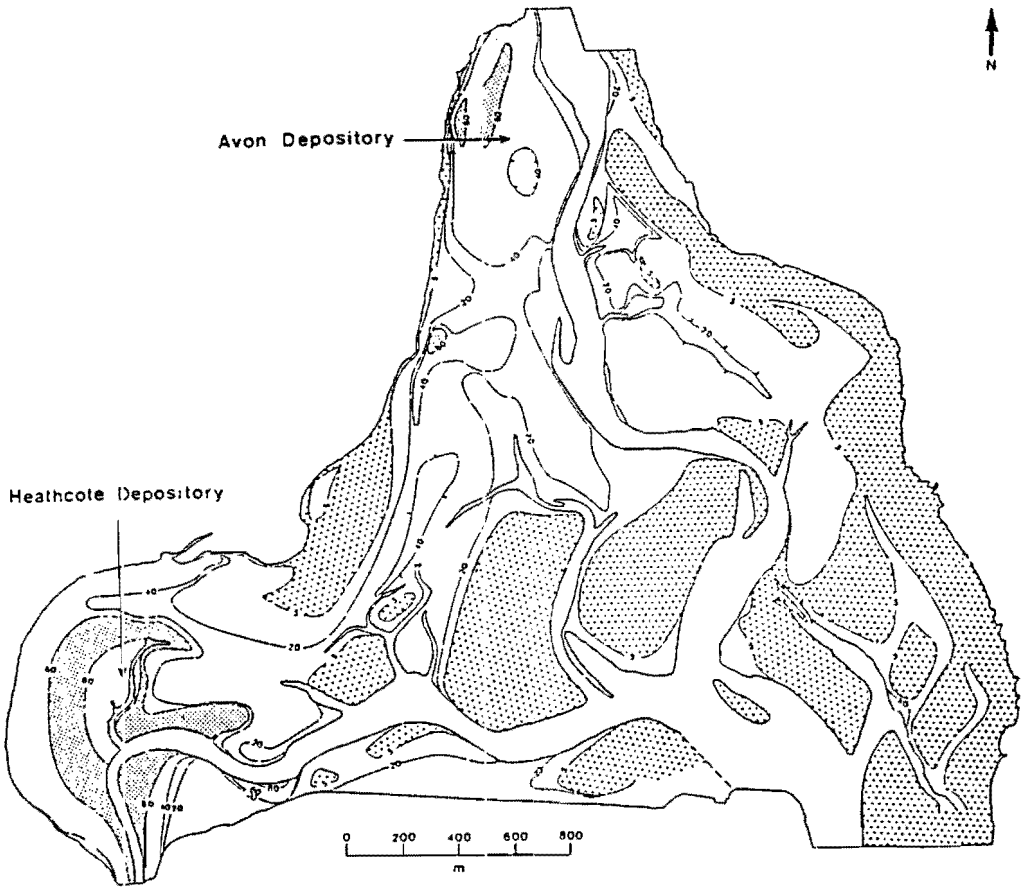

Fig. 3.1 Muddiness of Avon-Heathcote Estuary surface sediment, contoured at 5%, 20%, 40%, 60%, and 80%. Large dots <5% mud; small dots>60% mud (Macpherson, 1978).

Heavy minerals and clay minerals naturally contain higher concentrations of heavy metals than minerals such as quartz, calcite, and feldspar. Therefore, an understanding of mineralogy is important when comparing heavy metal concentrations between sediment cores, units, and locations.

The affects of anthropogenic activity on sediment supply and heavy metal fluxes to the Avon-Heathcote Estuary are reviewed in Chapter 2.

The present chapter examines Avon-Heathcote Estuary sediment cores for grain size distributions, mineralogy, and sedimentation rates. The contacts between the sediment units (A, B, C, and D) have been dated accurately using a combination of ^{14}C ages, ^{210}Pb curves, pollen profiles, and knowledge disclosed in the history review.

A few cores from the Travis swamp and Saltwater Creek Estuary, have also been studied to evaluate their suitability as baseline sites.

3.1 SEDIMENT DISTRIBUTIONS IN THE AVON-HEATHCOTE ESTUARY

3.1.1 Surface Sediment Distributions in the Avon-Heathcote Estuary

Sediment studies of the Avon-Heathcote Estuary have been undertaken by Knox and Kilner (1973), Millward (1975), Harrison (1976), Macpherson (1978), and Christchurch Drainage Board (1988). All these studies show uniform sediment accumulation over the last 20 years, with most areas of the estuary showing coherent patterns of sediment deposition.

Mud is deposited close to the river entrances and the channels, whereas the sand component increases towards the mouth. Over 80% of the mud entering the estuary annually (approximately 12000 tons) is deposited in the Avon and Heathcote depositories (Fig. 3.1, Macpherson, 1978). The Heathcote Basin is 2.5 times the size of the Avon

depository and 10% muddier, which reflects the higher sediment load carried by the Heathcote River. Areas on the western slopes of the estuary are also high in mud. Sediment deposition in this area is influenced by the Avon River, the pond outfalls, and wind circulation. Sandier sediment occurs on the eastern slopes than the western slopes because dominant easterly winds tend to divert the Avon River in a westerly direction. Macpherson suggested that the general absence of mud above the medium tide level, except near the river mouths, indicates that wave energy exerts the principle control on mud deposition.

The majority of the active surface sediment in the Avon-Heathcote Estuary is in equilibrium with the physical environment. However, Macpherson (1978) maintained that intense bioturbation by dense populations of crabs, snails, and shellfish is causing net erosion of sediment from the estuary. Historical records (Chapter 2) suggest that some erosion has occurred near the channels and around the periphery of the estuary, but no evidence was found for widespread erosion from the bed of the estuary.

3.1.2 Subsurface Sediment in the Avon-Heathcote Estuary

Macpherson (1978) studied the sedimentology of more than 40 1-2m deep sediment cores from widely spaced localities in the Avon-Heathcote Estuary. He recognised three main stratigraphic units below the modern sediment horizon.

3.1.2.1 Unit A

The basal unit, A, is a massive, dark grey, fine to medium sand; it is uniformly well-sorted containing less than 3% mud (Fig. 3.2a and 3.2b). Sparse wood and shell debris is present. Because of the similarity between Unit A and the monotonous marine sand found in wells around Christchurch, Macpherson correlated Unit A with the Christchurch Formation of Suggate (1958). Unit A is

a

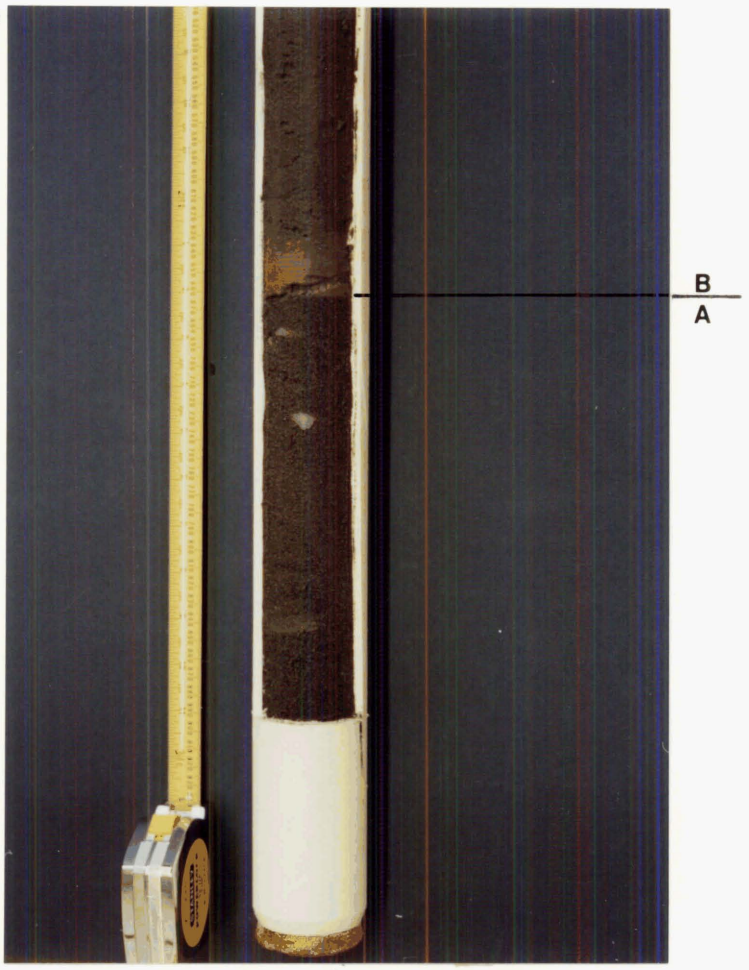

b

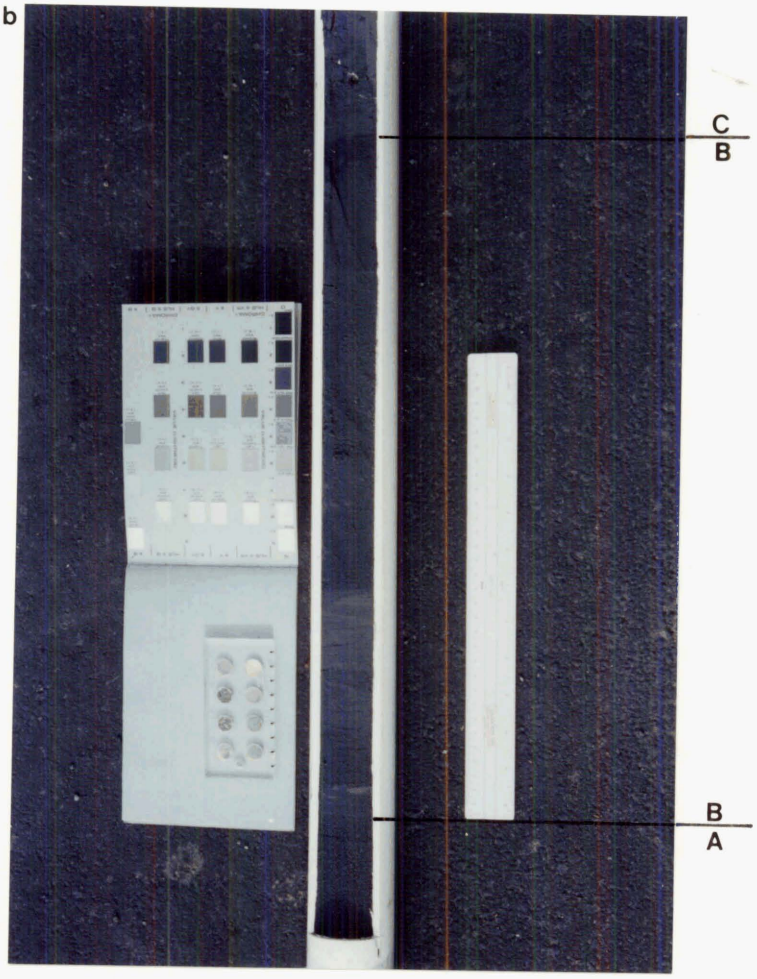

Fig. 3.2 Sections from cores AHE/1a and AHE/3a showing the contacts between sediment units A and B, and B and C.

a) Contact between units A and B in core AHE/3a.

b) Contacts between units A and B, and B and C in core AHE/1a.

interpreted to represent material deposited in shallow oceanic conditions before the estuary evolved. The contact between Unit A and overlying Unit B is always sharp and abrupt.

3.1.2.2 Unit B

Unit B is a muddy very fine sand, plane laminated in places. Decimetre fining upwards sequences are common, grading from clean fine sand to very fine sand with greater than 50% mud. Coarsening upwards sequences also occur. The laminated sequence is frequently overlain by massive uniform muddy sand (Fig. 3.2b). Macpherson's grain size and bathymetric level studies show that Unit B is similar to sediment actively accumulating in the estuary today. Unit B is interpreted to have been deposited after the Avon-Heathcote Estuary was separated from the open ocean and to represent material deposited under similar conditions to those which prevail today.

3.1.2.3 Unit C

Unit C ranges from an olive grey plastic mud to a very fine sandy mud which is generally massive and monotonous in appearance (Fig. 3.2b and 3.3). Coarse leafy organic debris (Zostera leaves) is abundant in Unit C, while laminated zones are rare. Unit C averages 40-80% mud, is poorly sorted, has a mean thickness of 25 cm, and a remarkably uniform appearance throughout the estuary.

The contact between Unit C and underlying Unit B is either sharp and abrupt with a major textural discontinuity, or gradational with interbedded sand and mud grading up through sandy mud to mud.

The greatest thickness of Unit C mud occurs in the Avon and Heathcote depositories. Unit C accumulated as a thin blanket of mud throughout the estuary, and is found in places where mud is normally absent. Macpherson found no relationship between Unit C sediment properties and water depth. The evidence suggests that this mud accumulated

a

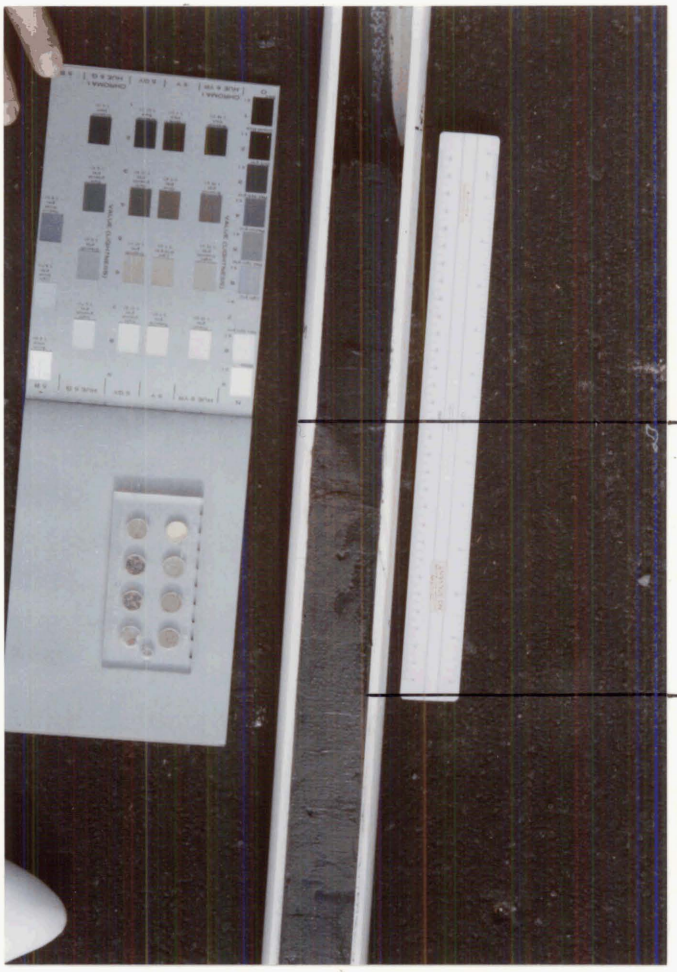

b

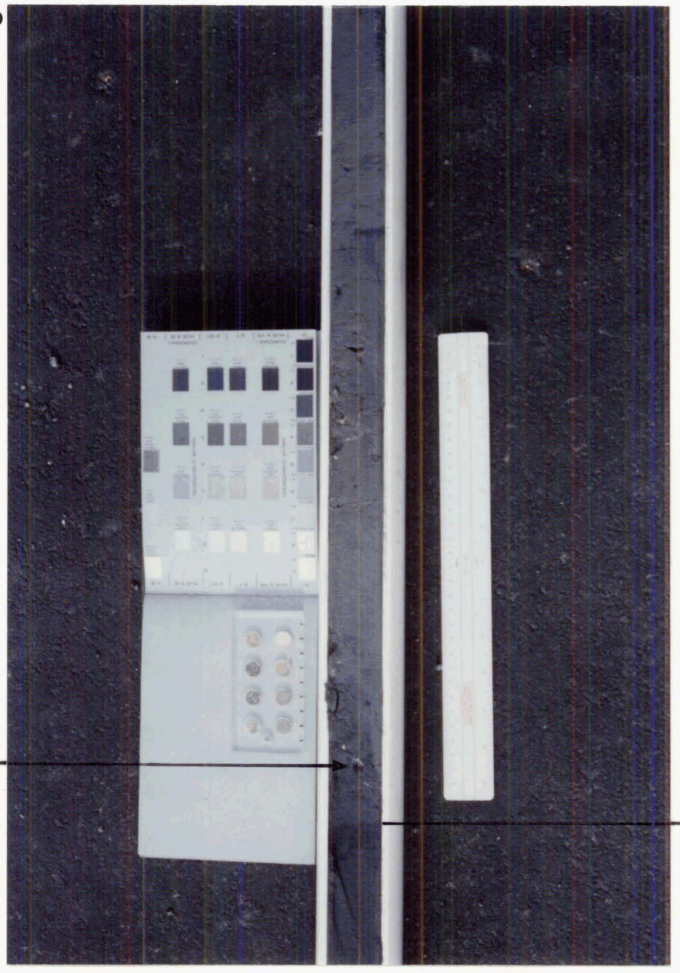

Fig. 3.3 Sections from core AHE/1a showing the contacts between units B and C, and C and D.

a) Contact between units C and D.

b) Contact between units B and C.

rapidly, during a period of higher than normal suspended load, and at uniform rates. Macpherson concluded that Unit C was deposited as a direct result of rapid erosion of the Christchurch area during the early settlement between 1850 and 1875. The historical synthesis in Chapter 2 supports such an origin. However, the evidence indicates that initially sediment was deposited in the Avon and Heathcote Rivers, and that Unit C sediment did not reach the estuary until a period of mechanical river sweeping, after 1925.

3.1.2.4 Modern Subsurface Sediment (Unit D)

In many cores Macpherson found that Unit C sediment has an intensely burrowed upper contact. The overlying sediment is a massive sand, containing abundant living or coarsely fragmented bivalves (Fig. 3.3a). Locally there are strips and pods of soft plastic mud derived by bioturbation of Unit C. Muddy horizons are intensely disturbed and consist of a few streaky remnants surrounded by sand. The modern layer is labelled Unit D for convenience in this study.

The benthic dwellers that bioturbate Unit D include polychaete worms, cockles (Chione stutchburyi), mud flat snails (Amphibola crenata), and crabs (H. crassa and M. hirtipes). During the excavation and feeding of these organisms, sediment is extruded on to the surface in the form of faecal strips and mounds. The density of mud flat snails and crabs is so high that Macpherson concluded the majority of the sediment is reworked in less than 2 weeks.

Macpherson mentioned a modern active layer occurring as a thin skin (1-2cm) on top of the subsurface bioturbate zone. The active layer reflects contemporaneous physical processes which may be different from the underlying sediment. Beneath the active layer, the bioturbation zone consists of a homogeneous mixture of constituents reworked from above and below.

Macpherson suggested that the Avon-Heathcote Estuary

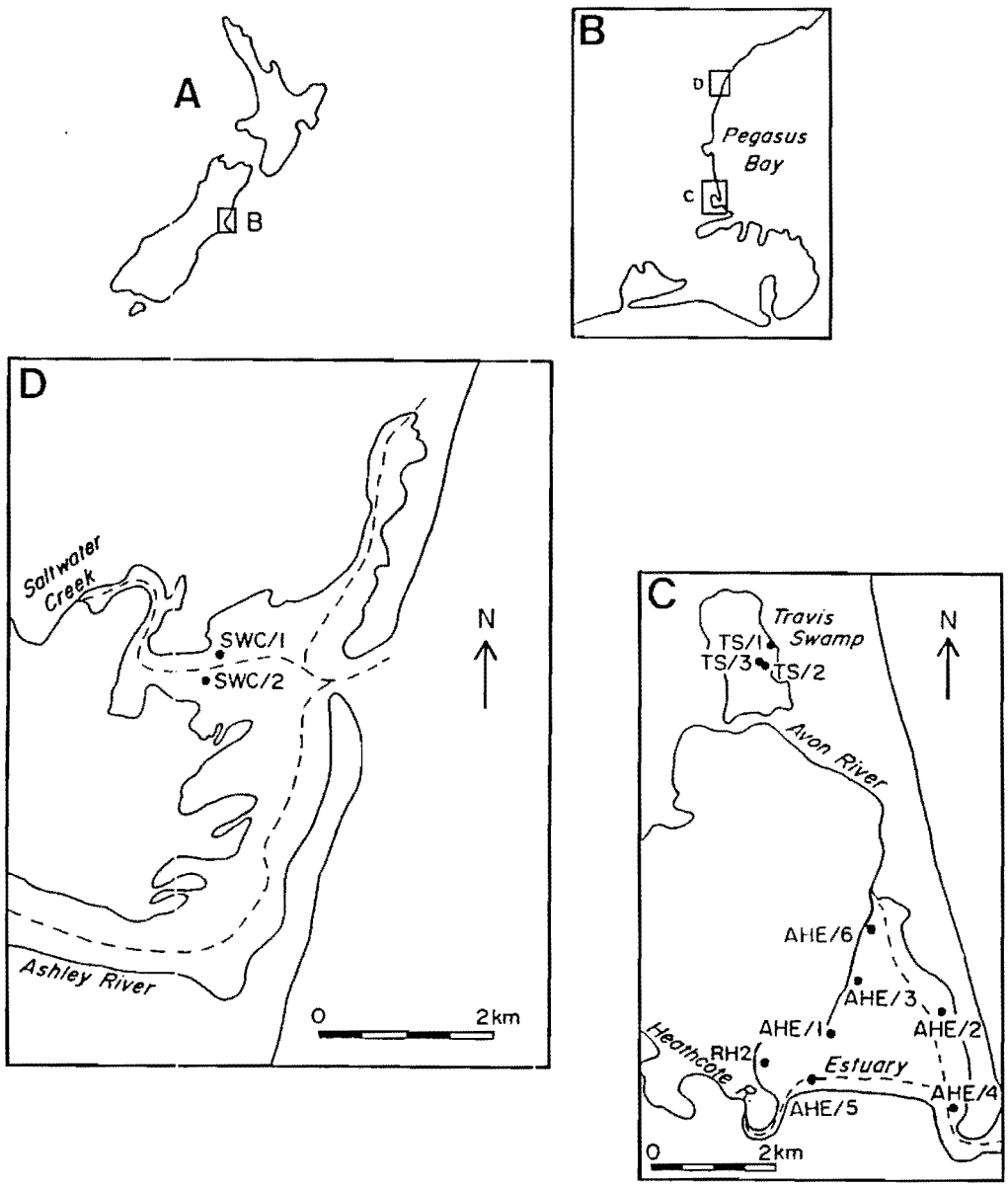

Fig. 3.4 Maps showing locations where sediment cores were collected in this study. A New Zealand, B Pegasus Bay, C Travis Swamp and Avon-Heathcote Estuary, D Saltwater Creek Estuary (core RH2 is from Hay, 1988).

is experiencing ongoing net erosion and that the sediment water interface is continually deepening as the inhabitants of the bioturbate zone "eat" their way downward into progressively older sediment. During this process, the suspendible fraction is added to the water column and washed out of the estuary with the tide.

Macpherson predicted that eventually a layer of uniformly clean sand will blanket the estuary when the biologically available virgin mud is worked out to a uniform depth and that the sand will act as a buffer between the ancient muddy Unit C sediment that remains and the modern environment.

Results of the historical survey in Chapter 2 indicate that bioturbation was intense before and during Unit C deposition. The estuary appears to be in equilibrium with respect to bioturbation. Most erosion is restricted to the channel edges and the perimeter of the estuary.

3.2 DESCRIPTION OF SEDIMENT CORES FROM THE AVON-HEATHCOTE ESTUARY, AND TRAVIS SWAMP

3.2.1 Avon-Heathcote Estuary

3.2.1.1 Method of Coring and Subsampling

Six cores were collected during the course of this study from the locations given in Fig. 3.4c. Cores AHE/1, AHE/2, and AHE/3 were duplicated. Cores were collected in acid washed 5cm PVC pressure piping using the method adopted by Macpherson (1978). Each core was hammered into the sediment with a sledge hammer, tightly capped, and retrieved by loosening the surrounding ground with a spade, allowing the cores to be pulled free. The cores were opened by cutting a slice of plastic from opposite sides with an electrical band saw, leaving a thin layer which was subsequently cut through with a knife. Once cores were open, the top part was lifted off, exposing an almost

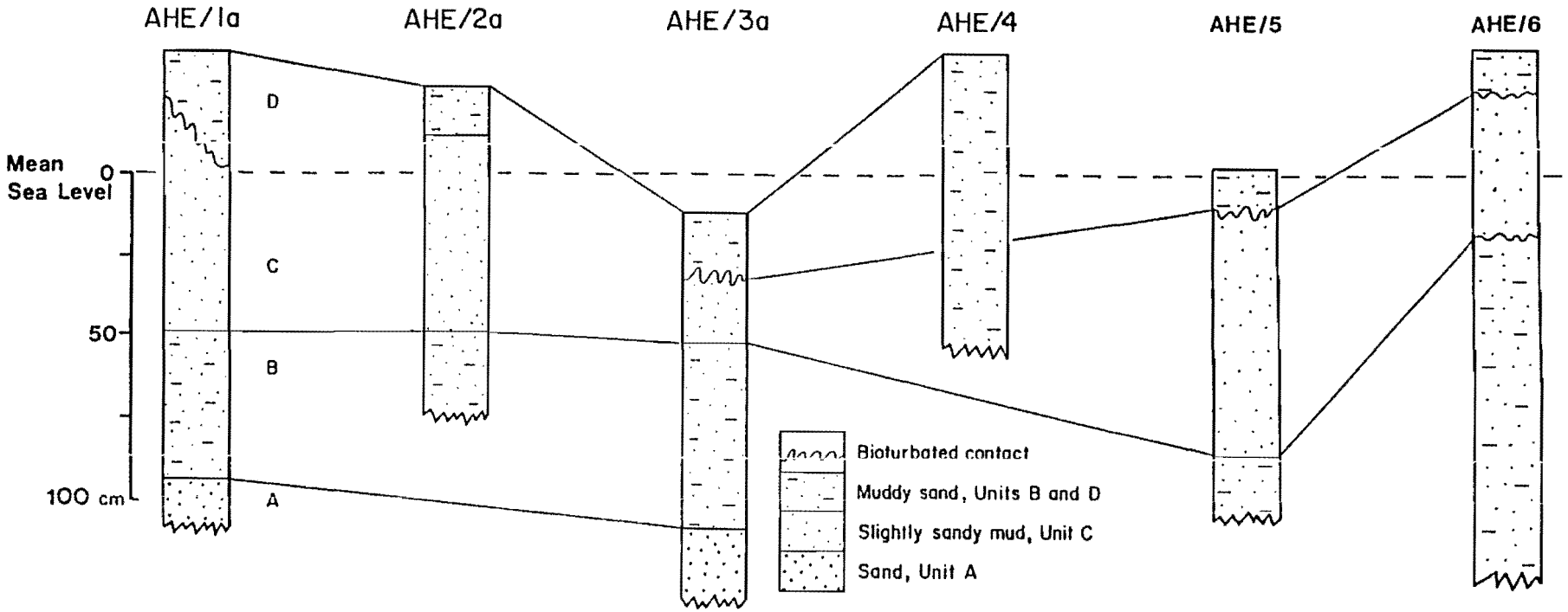

Fig. 3.5 Summarised Stratigraphy of cores from the Avon-Heathcote Estuary (for location see Fig. 3.4).

undisturbed sequence of sediment for description and analysis. The sediment sequence was compressed by about 5% during coring.

All sample handling and laboratory procedures were carried out at the cleanliness levels required for trace analysis of sediments (Chapter 6, Section 6.2).

Once the cores were open and the stratigraphy recorded, the sediment was subsampled at 2-4cm cuts. To avoid smearing and contamination affects, samples were removed from the tube, leaving a 0.5cm sediment skin around the edge. Each subsample was dried, then crushed ready for analysis.

3.2.1.2 Descriptions of Sediment Units

Full core descriptions are given in Appendix 2.0, (Section A2.1) whereas the summarised stratigraphy is presented in Fig. 3.5.

The units observed are named the same as those of Macpherson (1978). All 6 cores contained units A-D except AHE/4 from the mouth of the estuary. Core AHE/4 consisted of homogeneous fine sand, similar to Unit B, from the base to top. Photographs of parts of cores AHE/1a and AHE/3a are presented in Figures 3.2 and 3.3.

Additional observations of the cores of value to this study are discussed below.

Unit B

A black coloured zone 1-2cm thick was observed at the top of Unit B in most cores but distinctly in cores from the Heathcote Basin (Fig. 3.2b and 3.3b). Core AHE/5 from the southern edge of the Heathcote Basin contains black streaky layers near the top of Unit B (Appendix 2.0). Coal particles occur near the top of Unit B in Core AHE/2a (Fig. 3.19) and in Unit C of AHE/1a (Fig. 3.3). A core RH2 taken by Hay (1988) in front of the City Outfall Drain contains a black coloured zone near the contact of units B and C

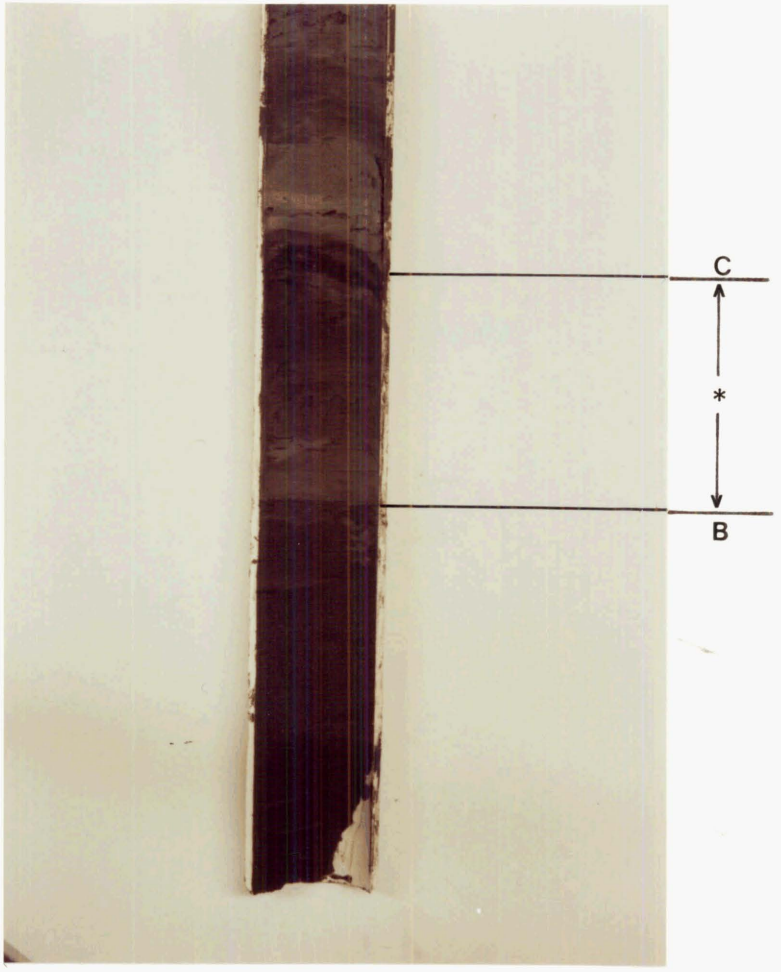
C
*
B

Fig. 3.6 Section from core RH2 (Hay, 1988), which is from directly in front of the City Outfall Drain (see Fig. 3.4 for location). The Unit C-B contact is 1874 to 1925 (Chapter 2). The black organic rich layer corresponds with peak industrial activity between 1900 and 1925.

* Diffuse zone: As the City Outfall Drain became blocked with sediment in the late 1880's, the sedimentation rate in the estuary adjacent to the drain would have slowed down before Unit C was deposited. The upwardly increasing sand content, in the diffuse zone, reflects the decreasing mud flux to the estuary as the drain became blocked.

(Fig. 3.6). These dark layers containing coal and coke particles are probably derived from atmospheric emissions during early industrial activity (1860's to 1930's), particularly along the banks of the Heathcote River, which involved large scale coal burning (Chapter 2, section 2.8).

All Unit B sediment is saturated in slightly saline ground water (salinity, 6-10 parts per thousand (ppt)) at pH 7-7.5, dissolved oxygen (DO) 2-2.6mg/l and Eh -3.0 to -0.4V. The ground water is semi-confined by the overlying thick puggy Unit C mud. When the cores were retrieved and the base of Unit C punctured, ground water quickly filled the holes from where the cores were collected (Figs 3.7 and 3.8).

Unit C

Zostera leaves 10cm long were observed in Unit C of core AHE/1b (Appendix 2.0). Clumps of partly decayed organic matter, probably Zostera, occur in Unit C (Fig. 3.7) of core AHE/2a, and near the base of core AHE/4. These observations support the historical records of mass mortality of the Zostera beds during rapid silting of the estuary (Chapter 2, section 2.7.1).

Unit D

The active layer is slightly lighter in colour than sediment beneath, otherwise sediment properties are the same.

Unit D sediment is extremely black and anaerobic in cores from the Heathcote Basin (AHE/1a, AHE/1b, AHE/5, and RH2 (Hay, 1988), and the Avon depository (AHE/6). A slightly greener colour was observed in cores AHE/3a and 3b from in front of the sewage ponds. The modern sediment in core AHE/2a from the Southshore is medium grey and contains a black layer 6-8cm beneath the surface (Fig. 3.7a).

Surface sediment Eh values decreased rapidly with depth at all locations. The most reducing conditions were found near the entrances of the two rivers and along the

a

b

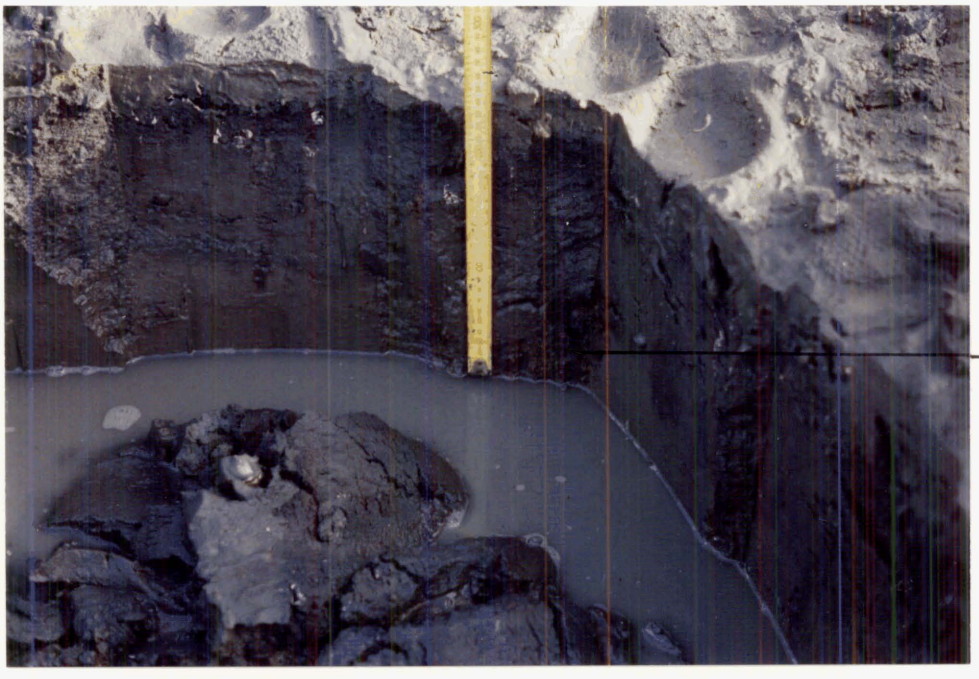

Fig. 3.7 Photographs of the hole remaining after core AHE/2a was retrieved from the Southshore (see Fig. 3.4 for location). The water levels rose quickly after the base of Unit C was penetrated. Both photographs were taken within 10 minutes of digging the hole.

DPM: Decaying plant matter (Zostera).

Black Zone: The black zone in Fig. 3.7a is most likely an Fe/Mn sulphide precipitation zone.

a

b

Fig. 3.8 A hole dug in the Heathcote Basin to measure the groundwater chemical environment.

a) a water pump is removing the groundwater as it upwells.

b) dissolved oxygen reading being taken in the uncontaminated flow as the water upwells.

western slopes. At low tide, Eh values in the top 1cm of sediment were -0.095V, directly in front of the City Outfall Drain, -0.101V near the locality of Core AHE/5, -0.230V at surface where Core AHE/6 was collected, and -0.328V at locations where cores AHE/3a and 3b were collected. The pH readings at all locations remained consistently between 7 and 7.4. These anaerobic conditions at neutral pH favour the precipitation of black Fe and Mn sulphides (Figs 1.2 and 1.3, Chapter 1), which explains the extremely black and greenish black colouration of Unit D sediments from the Avon depository, along the western slopes to the Heathcote Basin. Negative Eh values correspond with areas high in organic matter reported by Christchurch Drainage Board (1988), and Knox and Kilner (1973). Hence, reducing conditions are probably caused by high levels of decaying organic matter in the sediments. The causes of organic enrichment are most likely a combination of 1) the high mud content of sediment at the head of the estuary (which has a greater potential to trap organic matter than coarser sediment), and 2) the daily release of nutrient rich (N and P) effluents from the sewage ponds, which has encouraged growth of all levels of organic life (Chapter 2, Section 2.7). In these areas the decay of large quantities of dead plant and animal matter deprives the sediment of oxygen, thus lowering redox levels (Chapter 1, Section 1.6.1).

At the location of AHE/2a, surface sediment Eh values were -0.04V at the surface, decreasing to -0.240V at the black horizon 6-8 cm below the surface. The pH was 7 along the black zone. Hence, the black zone is probably also a Fe and Mn sulphide precipitate layer rather than a hydroxide precipitate (which requires Eh values well above zero).

The +0.05V Eh value at the surface near the location of core AHE/4 indicates that oxidising conditions increase towards the mouth of the estuary.

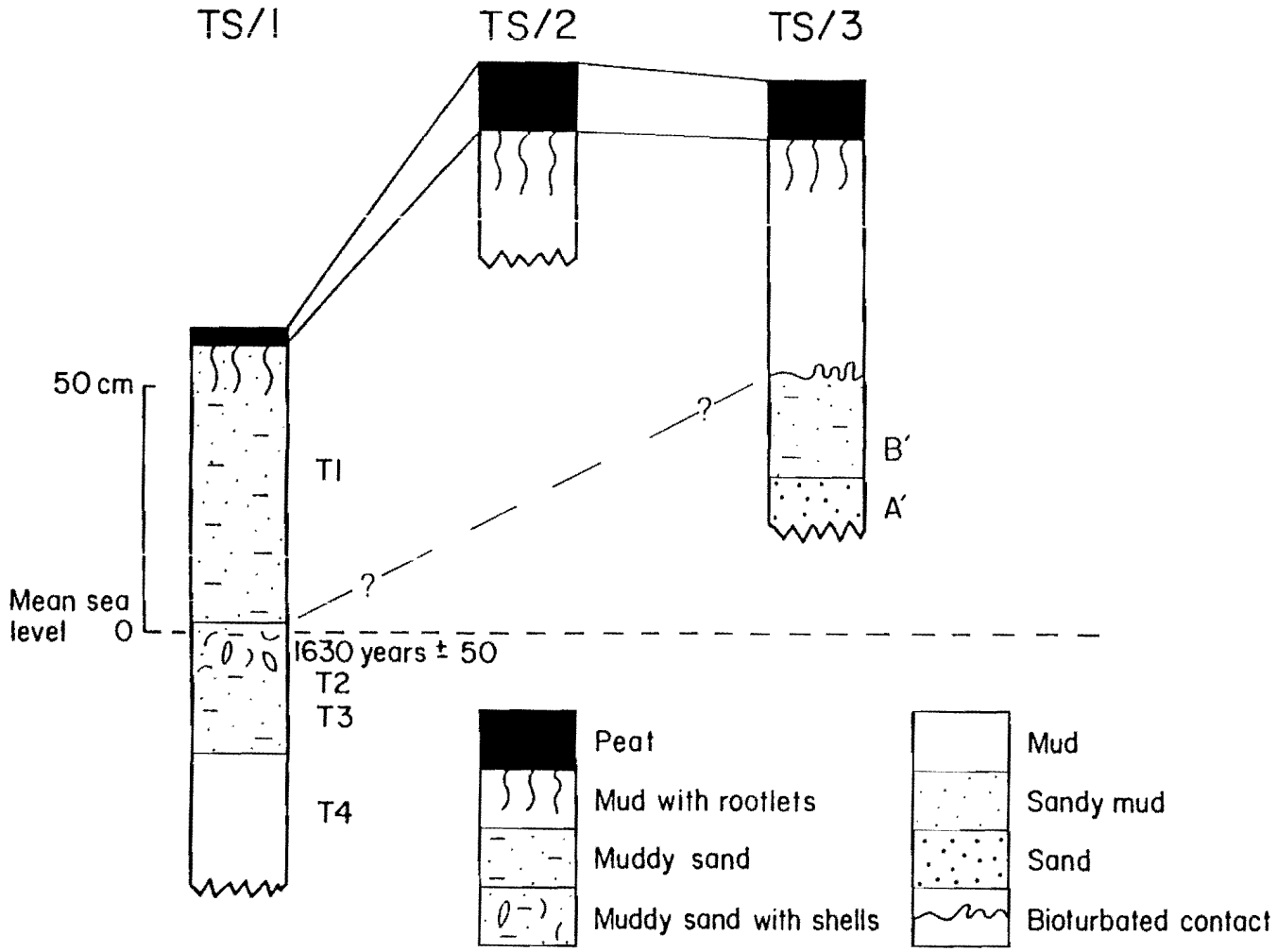

Fig. 3.9 Summarised stratigraphic columns from Travis Swamp cores (see Fig. 3.4 for location).

3.2.2 Travis Swamp

The Travis Swamp is located 4km north of the Avon-Heathcote estuary (Fig. 3.4C), and prior to 1990 had changed little since Europeans arrived in 1850.

Three cores were collected from the locations given in Fig. 3.4c, and by the methods given in Section 3.2.1. Simplified stratigraphic columns are given in Fig. 3.9; detailed descriptions of each core are given in Section A2.1 of Appendix 2.0. Only core TS/1 and TS/3 are discussed in this dissertation.

Core TS/1 is from the edge of the swamp and shows a progradational sequence progressing upwards from oceanic mud through estuarine sands to sandy swamp sediment. The basal unit T4 of TS/1 consists of soft, light blue-grey, very plastic mud, which lacks sand. Units T2 and T3 consist of light brown silty estuarine sand. The only difference between the two units is that Chione shells are sparse in T3 and abundant in T2. A sample of Chione shells (M35/f25) from the shell layer of T2 was ^{14}C dated at 1650 years B.P. by the Institute of Nuclear Sciences (INS, Lower Hutt, N.Z.[+]). Unit T1 is brown fine silty sand containing numerous rootlets.

Core TS/3 is from deeper in the swamp. The basal Unit A' is a clear sand similar in texture to Unit A of the Avon-Heathcote Estuary (Fig. 3.10). Unit A' sand is overlain by a dark grey slightly muddy fine sand Unit B' which is similar in texture to units T2 and T3, of TS/1, and Unit B of the Avon-Heathcote Estuary. Unit B' is intensely bioturbated and mixed with sediment from the overlying olive coloured sandy mud (similar to Unit C of AHE). The olive grey mud fines upwards, and contains extensive rootlets in the top 10cm. This swamp mud is probably a lateral equivalent of Unit T1. The mud is overlain by 12cm of peat.

The blue mud Unit T4 has been exposed by builders currently developing the western part of the Travis Swamp.

[+] C^{14} laboratory data s in the back pocket of the thesis.

Fig. 3.10 Section from core TS/3 showing the contact between units A' and B'.

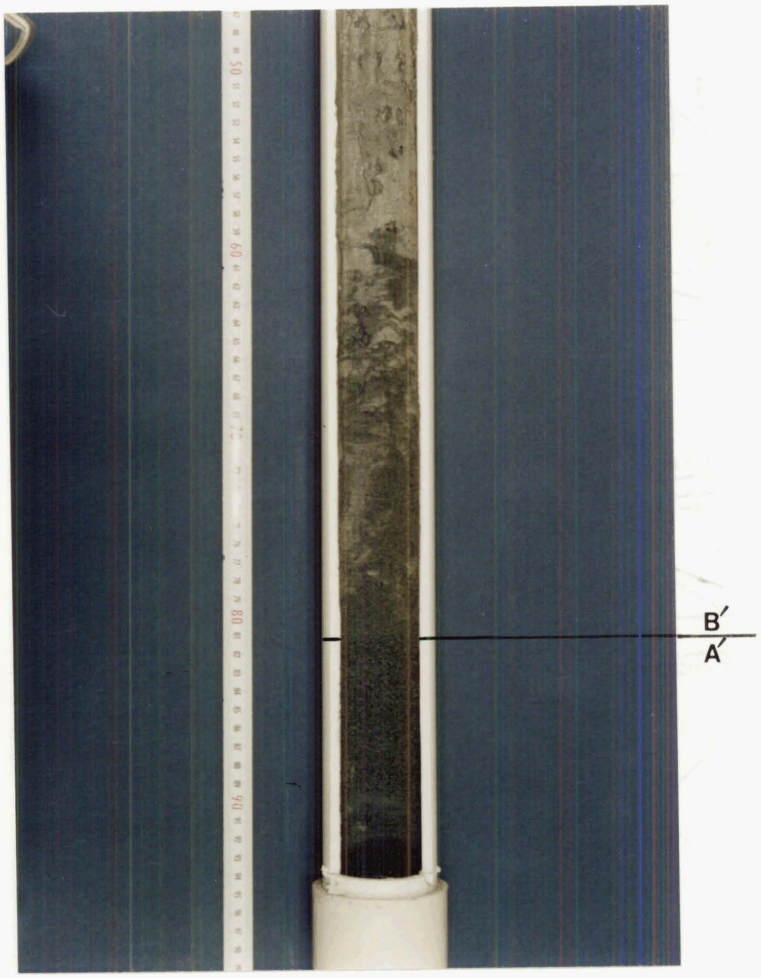
B′
A′

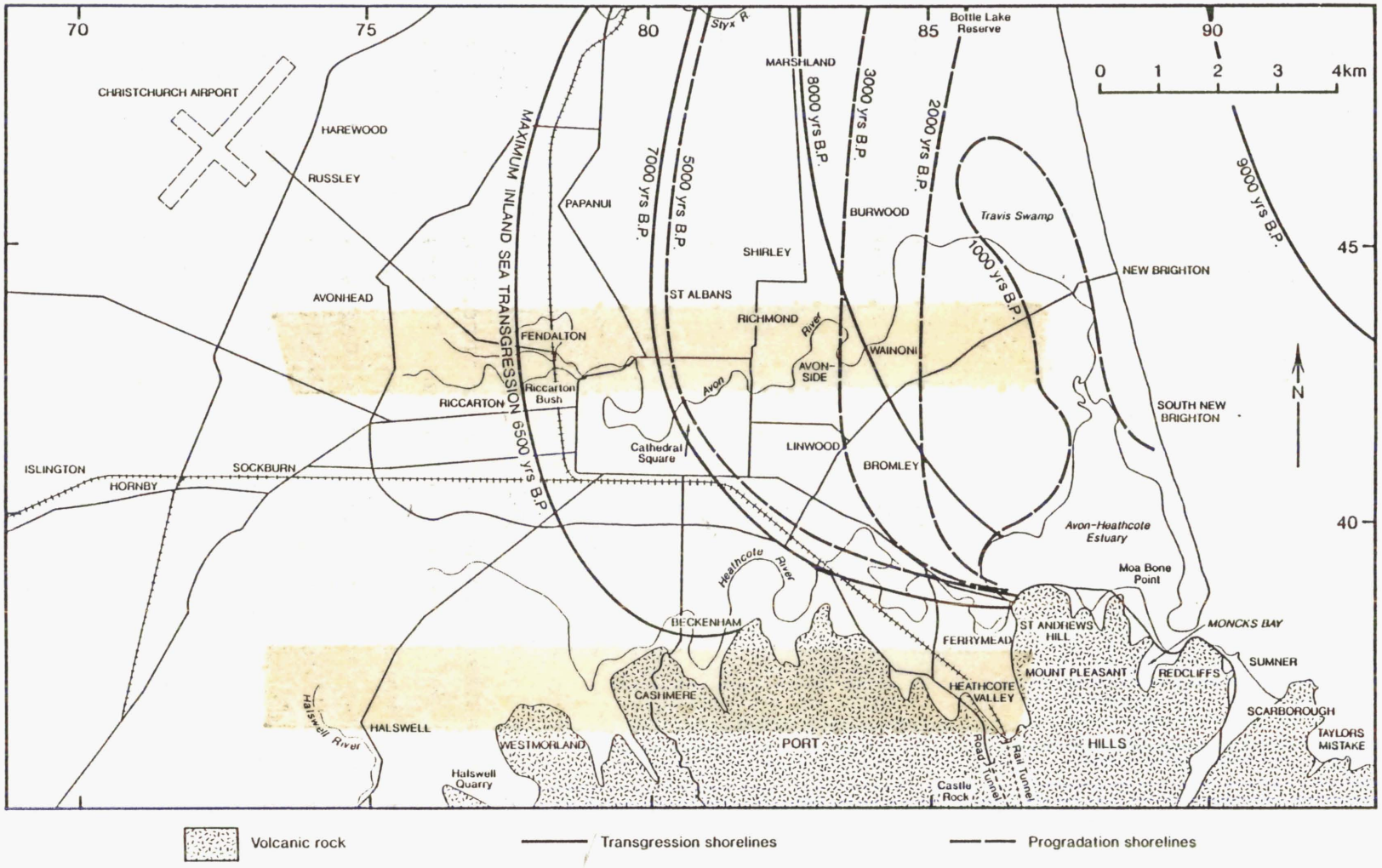

Fig. 3.11 POSTGLACIAL MARINE TRANSGRESSION AND PROGRADATION SHORELINES
(Brown and Weber, in press)

Drainage Board workers also exposed it north east of the swamp in 1986 when laying sewers. The blue mud is considered, for the purposes of this discussion, the basal sediment beneath the swamp. Unit T4 was probably deposited in a sheltered bay about 2000 years ago. The more inland location of the, younger, shallow marine sediment Unit A' suggests that when the estuary (units T2, T3, and B') formed, the inlet was located southwest. Today sediment similar to Unit A (and A') is found inside the inlet of the Avon-Heathcote Estuary and also on the beach at Clifton Bay.

A map showing ancient shoreline positions is presented in Fig. 3.11 (Brown and Weber, in press). The position of the shorelines have been determined using carbon-14 dates from water wells in the Christchurch area. The 1000 year B.P. shoreline traces a long thin bay-estuary traversing the areas of the Travis Swamp and Avon-Heathcote Estuary. Contours drawn by Macpherson (1978) on the upper surface of Unit A show that just before the Avon-Heathcote Estuary formed a shallow ocean channel flowed south from the bay-estuary into the area of the Avon-Heathcote Estuary, meeting another channel flowing out from the Heathcote River. These channels were probably formed by the Avon and Heathcote rivers discharging directly into shallow offshore waters, eroding the surface sediment (Units A and A'). Units T2 and T3 would have been deposited in the northern quiet part of the bay-estuary, while Units A and A' were deposited near the entrances and slightly off shore. As the spit migrated further south the swamp sediments (Unit T1) would have replaced the estuarine sediments in the vicinity of Travis Swamp. Hence, units A' and B'(T2, and T3) are early lateral equivalents of units A and B of the Avon-Heathcote Estuary.

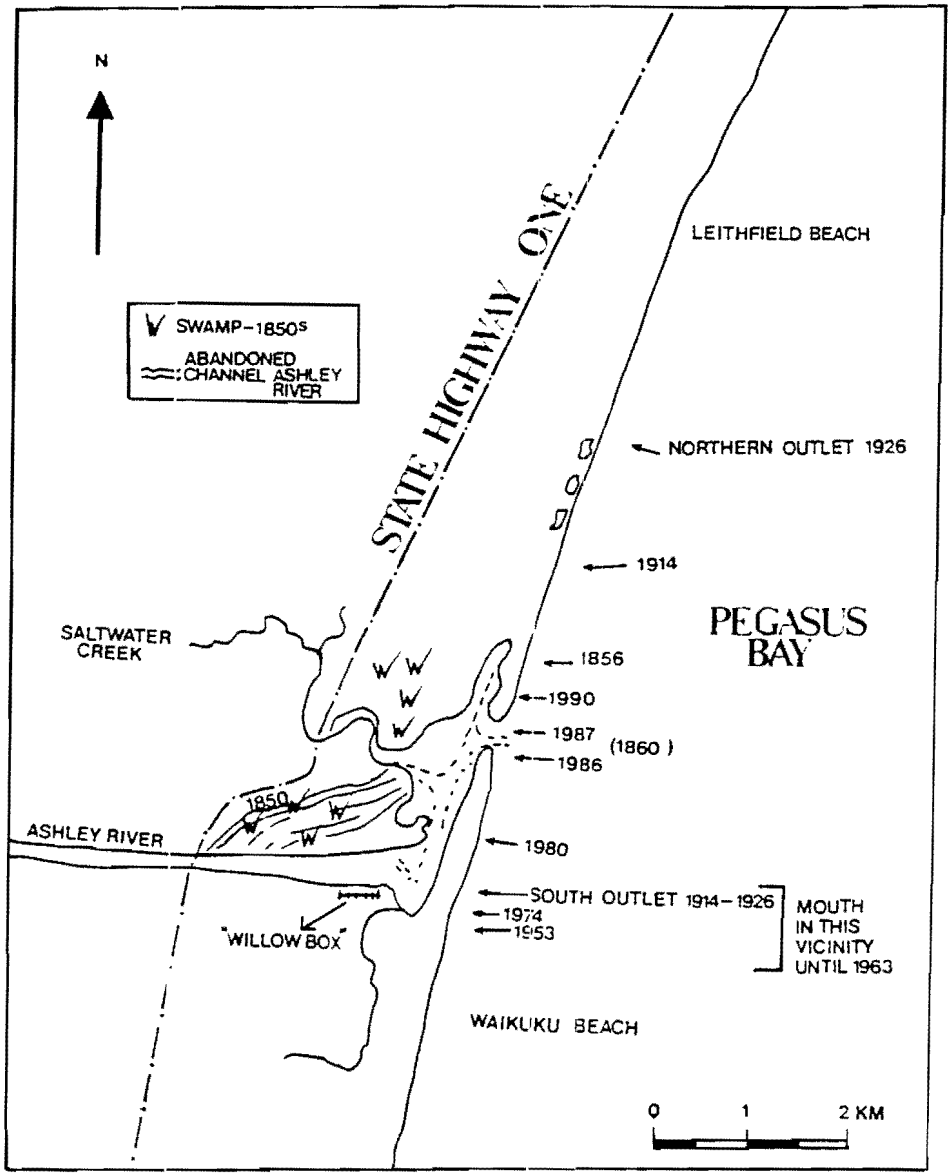

Fig. 3.12 Map showing the positions of the Saltwater Creek Estuary mouth over the last 140 years (Carson, 1986).

3.3 GENERAL GEOLOGY AND CORE DESCRIPTIONS FROM THE SALTWATER CREEK ESTUARY

3.3.1 Introduction

The estuary of the Ashley River and Saltwater Creek; known as Saltwater Creek Estuary is located amongst the Kairekei dunes (500-1000 years) and the modern Ohuan dunes (<500 years old; Blake, 1964; Millward, 1976). The Swift Ashley River drains an area of 1000km^2 before entering the Saltwater Creek Estuary (Figs 2.1, and 3.4d, Wilson, 1986).

The Saltwater Creek Estuary differs from the Avon-Heathcote Estuary in that it is a major river-mouth estuary formed as a result of a change in the position of the Ashley River. The estuary has formed in an abandoned channel of the Ashley River. Shingle deposits are common in abandoned channels at Saltwater Creek. The position of the river mouth has shifted up to a dozen times over the last century due to the dynamic nature of the river (Fig. 3.12). Frequent floods influence the position of the mouth.

3.3.2 A Brief History of the Saltwater Creek Estuary

During 1850, the Ashley River followed a course parallel to the road and joined Saltwater Creek about 200m further inland (Fig. 3.12; John Mathers, great grandson of early settler, pers. comm.). At this time the mouth of the estuary was 2m deep at low tide and quite navigable.

The area was used as a port in 1859 and the township of Northport sprang up in the 1860's west of State Highway one between the Ashley River and Saltwater Creek (Hawkins, 1957). The town survived for about 8 years servicing trading between North Canterbury farms and Lyttelton.

In the 1860's the Ashley River mouth had migrated 1km south (near its present position). The channel was over 5m deep, enabling ships to enter easily during this period. Nevertheless, farming activities upstream were causing

rapid silt deposition in the estuary. As a result, in 1863, a ship sank just inside the bar. Subsequently, the channel was cleared every year at the beginning of the wool season (Hawkins, 1957).

By 1870 the estuary had silted to a point where it was almost impossible to bring ships safely into the estuary. As a consequence, shipping ceased and the township closed.

After 1900 the mouth of the Saltwater Creek Estuary continued to migrate north, until around 1914 when flooding caused the Ashley River to breach the dunes directly opposite the main channel, resulting in two mouths (Blake, 1964; M. Ashworth, descendant of early settler, pers comm.). A lagoon was formed between the two inlets behind the coastal sand bar. It is uncertain whether the southern inlet remained open or closed. Meanwhile the northern inlet continued to migrate north until reaching the northernmost position in 1926. A major flood recorded in 1923 may have re-opened the southern inlet (North Canterbury Catchment Board, 1986). By 1940 the northern mouth had closed and both the river and creek were discharging out to sea directly east of the main channel in the Ashley River (Blake, 1964). Resulting sand encroachment filled most of the northern lagoon. A large flood recorded by the North Canterbury Catchment Board in 1936 may have influenced the permanent transfer to the southern opening.

Between 1942 and 1974 the estuary mouth remained opposite the main channel of the Ashley River. However, there were slight variations in the shape of the spit and position of the main channel over this period. The inlet started to migrate north in 1950 but was halted during a major flood. Southward migration of the spit was prevented by the construction of a "Willow Box" groyne in 1953 by the North Canterbury Catchment Board (NCCB).

In the late 1970's and early 1980's the inlet commenced its present northward migration (NCCB, 1986). The inlet continued to migrate north until its current position was reached in 1990 about 2Km north of the centre line of

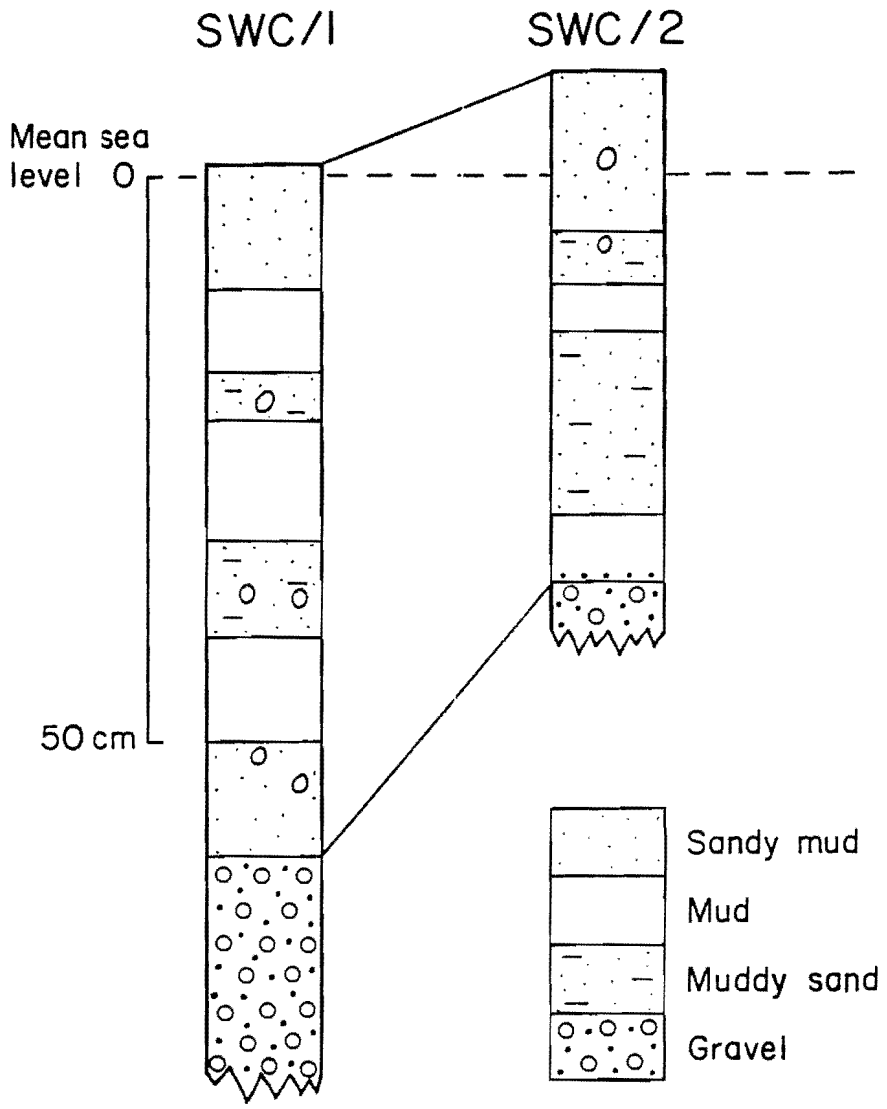

Fig. 3.13 Summarised stratigraphy of sediment cores from the Saltwater Creek Estuary (see Fig. 3.4 for location).

the Ashley river (Fig. 3.12). Carson (1986) suggested that the current northward migration is due to unusually low peak flood levels since 1979, combined with a slight northward migration of the main braid of the Ashley River. At present the channel is flowing north east parallel to the southern spit as the river discharges to the sea.

3.3.3 Stratigraphy of Cores from the Saltwater Creek Estuary

Two 1m cores were collected from the localities shown in Fig 3.4d. Complete core descriptions are given in Section A2.1 of Appendix 2.0. The stratigraphy is summarised in Fig. 3.13.

The basal unit from each core consists of poorly sorted gravel which coarsens upwards. The gravel is overlain by alternating decimeter scale beds of poorly sorted coarse sand with granules, and mud beds with shells. These sequences reflect the migrating positions of the Ashley River mouth and will be discussed further, in section 3.6.3.2.

Sediments are aerobic which is evident from the orange-brown layers in core SWC/2 (Fig. 3.14). The precipitation is probably Fe oxide (goethite or limonite). In contrast modern Avon-Heathcote Estuary sediments are black and anaerobic.

3.4 GRAIN SIZE ANALYSIS OF SEDIMENTS

Grain size distributions are useful to sedimentary geochemists because they yield information on mode of sediment transportation, environment of deposition, and natural causes of heavy metal variation.

Normally grain size statistics are discussed in terms of phi (ϕ) rather than diameter in mm or μm. The phi scale is the logarithmic transformation of the Udden-Wentworth scale, where $\phi=-\log_2 d$, and d = diameter in mm (Blatt et al,

Fig. 3.14 Section from core SWC/2 showing alternating mud and sand layers (stained orange-brown by Fe oxides).

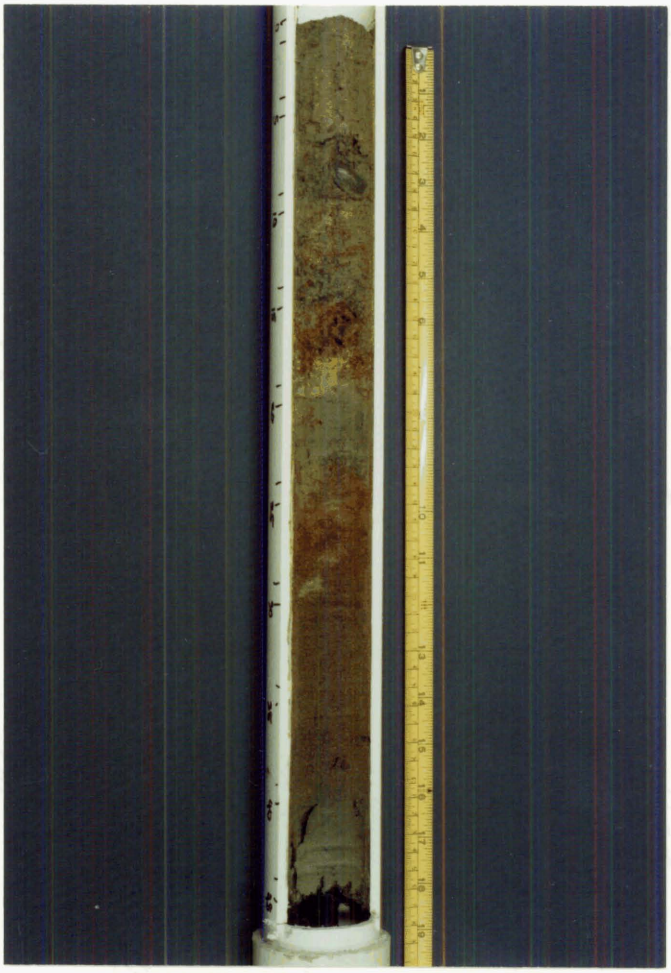

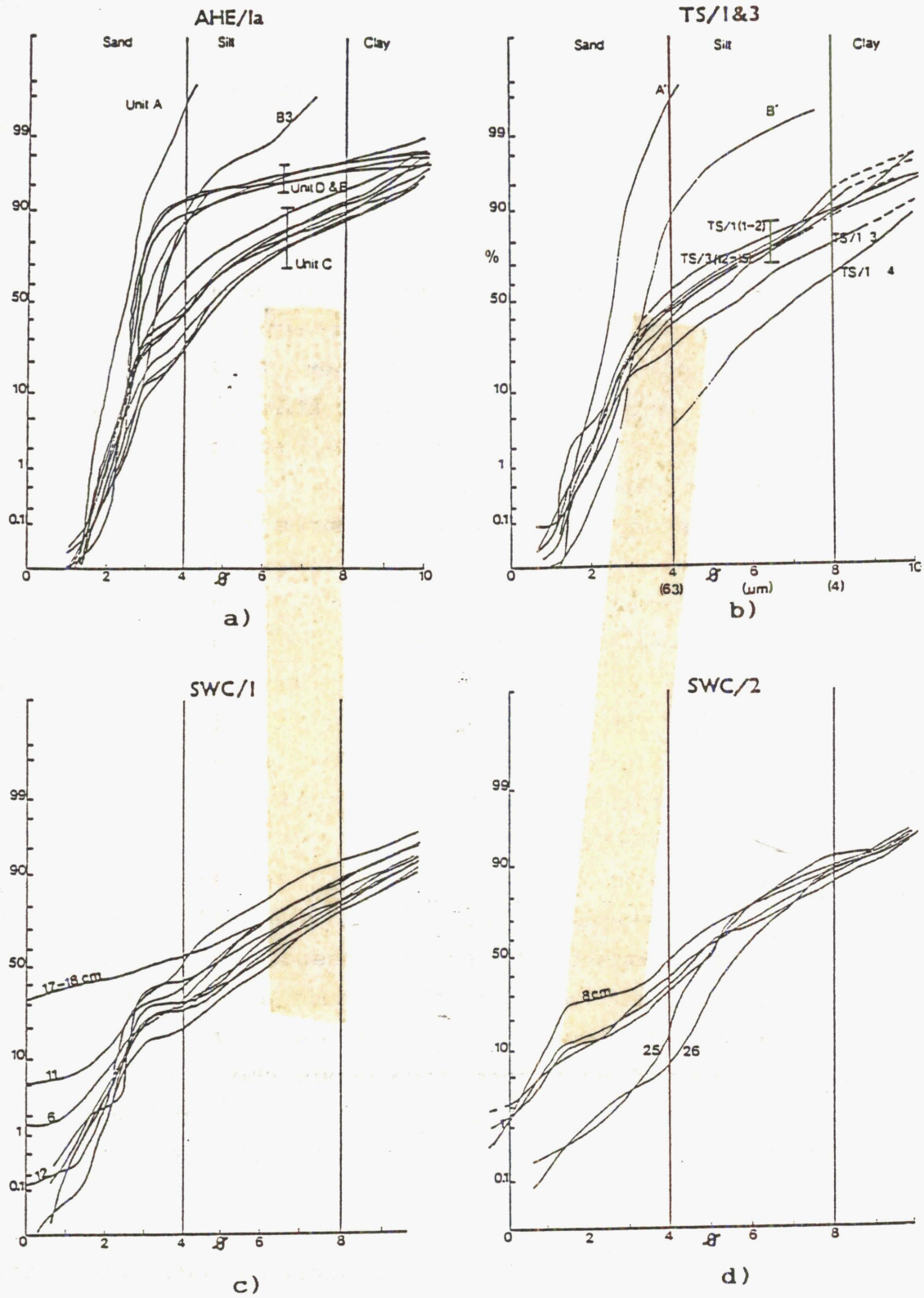

Fig. 3.15 Cumulative Grain Size curves of sediments from cores AHE/1a, TS/1&3, SWC/1, and SWC/2 (silt + clay = mud).

1980; Lewis, 1982). The phi scale is convenient because it involves whole numbers. The large grain sizes which are conventionally plotted on the left by geologists become negative and smaller than fine grain sizes which are plotted to the right (Fig. 3.15).

Grain size distributions are normally described using cumulative curves, where straight line segments represent normal distributions of individual grain size populations (Blatt et al, 1980; Allen, 1971; Visher, 1969). The overall curve shapes are described using standard statistical parameters, such as the mode, mean, standard deviation (SD), skewness, and kurtosis.

In this study the graphic measures of Folk and Ward (1957) were used (see discussion in Lewis, 1982).

Beach sands are commonly well sorted (low SD) negatively skewed (absence of fines), bimodal (2 dominant grain sizes) and platykurtic (more or less equal mixture of 2 populations; Cronan, 1972). In contrast, fluviatile sands are often positively skewed (higher concentration of suspended matter), and less well sorted (large SD; Allen, 1971; Visher, 1969).

One of the problems with grain size analyses is that the same processes occur within a number of environments and the consequent textural response is similar. Fortunately the sediments of this study are modern. Hence, knowledge of the surrounding geological environments, all of which remained unchanged throughout the last 500 years (such as location of rivers, swamps, dunes, and beaches), allows realistic interpretations of depositional conditions.

Macpherson (1978) accurately measured the grain size distributions of all Avon-Heathcote Estuary sediment units. However, it was considered necessary to repeat a few analyses in order to compare Avon-Heathcote Estuary grain size statistics with those of the Travis Swamp and Saltwater Creek Estuary.

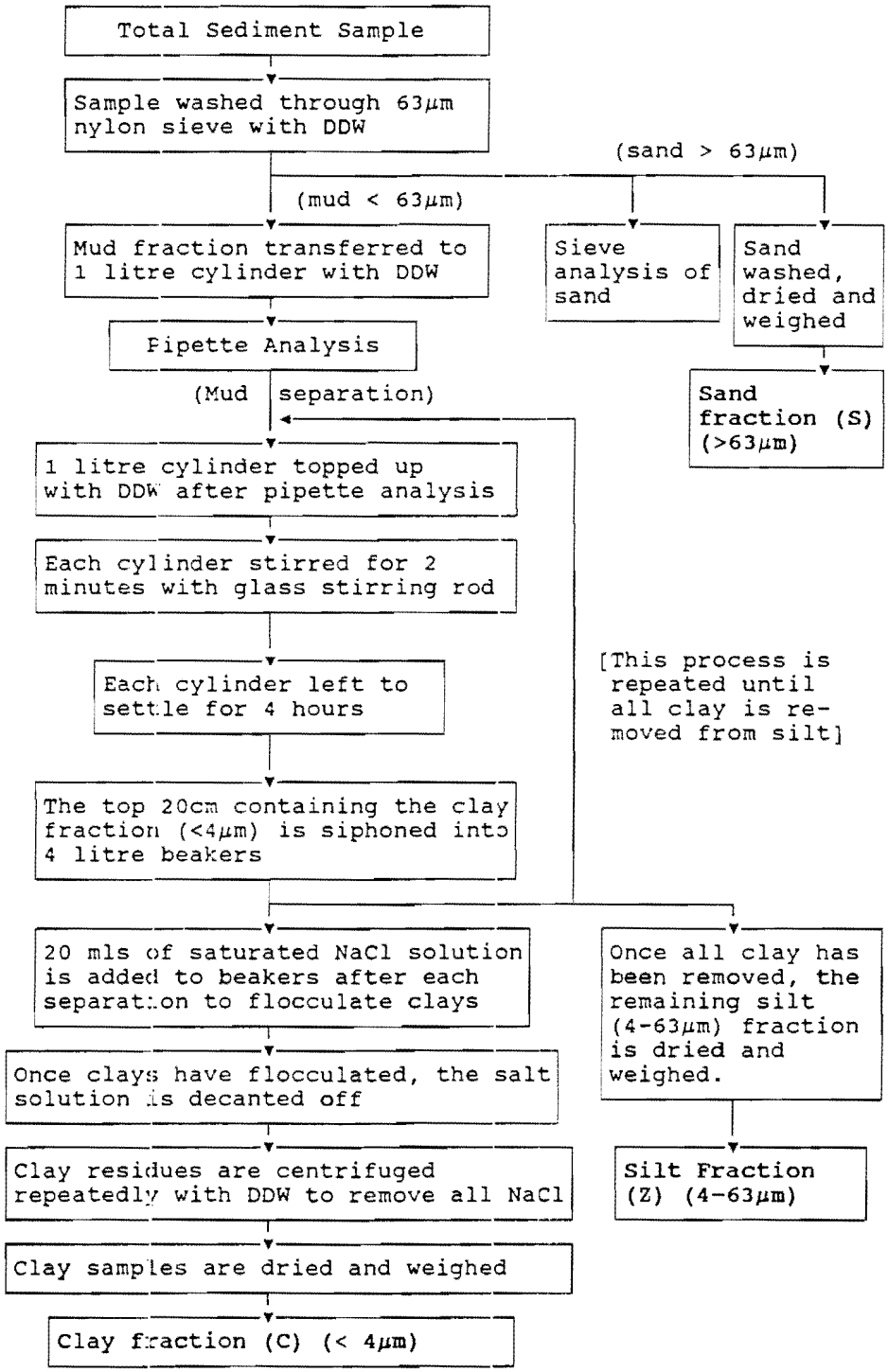

Fig. 3.16 Flow diagram illustrating steps in the sand (S), silt (Z), and clay (C) separation procedure.

3.4.1 Method of Grain Size Analysis and Separation

Small subsamples (25 to 30g) of the 4cm samples sectioned from each core were wet sieved through a 63μm nylon sieve to remove sand (S) (Fig. 3.16). The sand fractions were then resieved through nylon sieves with pore diameters ranging from 63μm to 250μm to determine the grain size distribution of the sand. The mud that passed through the original 63μm sieve was transferred to a measuring cylinder and made up to 1 litre with double distilled water. No dispersant was required as the mud particles disaggregated readily and did not flocculate.

The silt (4-63μm) and clay (<4μm) concentrations were determined in the columns using the standard pipette analysis technique (Lewis, 1982). The technique involved removing samples of mud, with a pipette, at specific times and depths from the stirred 1 litre columns. The weight of each dried pipetted fraction represented the proportion of the total size fraction remaining in the suspension above a specific depth at a specific time. Hence, by weighing dried samples the quantity of each grain size, in each sample, was measured.

Once grain size analyses were complete, the 1 litre columns were topped up with double distilled water (DDW), and the clay and silt fractions were separated by the method outlined in Fig. 3.16. The method is as follows: After stirring, the columns were left to settle for 4 hours. Subsequently, the top 20cm containing the clay (C) fractions were siphoned into 4 litre beakers. This procedure was repeated up to 10 times, until all clay was removed from the silt (Z) (Hulse, 1983). Following each separation, about 20ml of saturated NaCl solution was poured into the clay suspension to flocculate the clay minerals. After the liquid was decanted off, the final flocculated clay suspensions were centrifuged with repeated washings of DDW to remove all NaCl. Once prepared, clay and silt fractions were dried at 50°C to determine their total

grain size content. (The potential for heavy metal contamination and loss during grain size separation is discussed in Chapter 6, Section 6.2.1.)

3.4.2 Grain Size Distributions of Avon-Heathcote Estuary Sediments

Unit A

All grain size curves are presented in Fig. 3.15. The basal sediment Unit A is entirely sand with near symmetrical skewness and peaked unimodal kurtosis (Fig. 3.15a). The dominant grain size is 3ϕ (125μm). The grain size analysis produced almost identical results to those of Macpherson (1978). The sediment is similar in texture and mineralogy to sediment studied by Reed (1951) in 1-2 feet of water from the inlet area of the estuary, and just offshore from Brighton Beach. The results support Macpherson's conclusion that Unit A is a shallow ocean sand.

Unit B

Grain size analysis of a few Unit B samples shows the sediment to be moderately sorted near symmetrical to finely skewed, leptokurtic (predominately fine sand), muddy very fine sand. The sediment contains 80-90% sand and 4-7% clay. Unit B sediment textures are similar to the modern sediment Unit D. The grain size curves support Macpherson's interpretation that Unit B was deposited after the Avon-Heathcote Estuary separated from open ocean conditions, and to represent material deposited under conditions essentially similar to those which prevail today.

Unit C

Unit C consists of a very poorly sorted, very finely skewed, mesokurtic (unimodal, almost normally distributed) sandy silt. The sediment averages 45% sand, 45% silt, and 10% clay, which varies depending on locality. The average

grain size is 3ϕ. The findings of this study support Macpherson's interpretation that Unit C accumulated during a short period of unnaturally high sedimentation.

Unit D

Unit D sand is a massive well sorted, very finely skewed, extremely leptokurtic fine sand. The sediment is similar to the massive fine sand found in Unit B of cores 1a, 2a, and 3a. Unit D sediment contains 70-90% sand, 10-30% mud (including 3-5% clay). The grain size distributions of units B and D are bimodal, consisting of two fine sand saltation populations with the dominant grain sizes 2.5ϕ (180μm) and 3.5ϕ (90μm). Each of these populations is well sorted and probably result from swash and backwash as the tide comes in and out of the estuary, and resorting due to wave action. The fine tail represents the suspension population, which is derived from a combination of fines brought down by the rivers and redistribution of fines brought to the surface by bioturbating animals.

3.4.3 Grain Size Distributions in Travis Swamp

The grain size distributions of Travis Swamp sediment are similar to units A, B, and C of the Avon-Heathcote Estuary (Fig. 3.15b). Units T1 and T2 of TS/1, and T12-15 of TS/3 are similar to Unit C except slightly muddier. Units B' and A' contain almost identical grain size distribution to Avon-Heathcote Estuary units B and A respectively.

Units T1 and T2 from TS/1 contain 45% sand, 45% silt, around 7% clay, and are very poorly sorted, very finely skewed, and platykurtic (equal mixture of fine and coarse sediment). These silty sands accumulated in swamp (T1) and estuarine (T2) conditions where the supply of mud is high.

Subsamples 12/13/14/15 from TS/3 parallel units T1, T2 of TS/1 in that they are very poorly sorted, finely skewed, mesokurtic (unimodal) containing 38-56% sand, 35-44% silt,

9-16% clay. These sediment units were either deposited during similar conditions to Unit C, or belong to the same source (ie are the source).

Unit T4 consists of <3% sand, 62% silt, 35% clay, has near symmetrical skewness, and is platykurtic. This mud probably accumulated in a low energy environment with limited circulation. The shoreline data of Brown and Weber (in press) indicate that Unit T4 is an offshore sediment. Hence, Unit T4 probably accumulated in quiet bay conditions as the shoreline started its southern recurve around 2000 years B.P (Fig. 3.11).

3.4.4 Grain Size Distributions in Saltwater Creek Estuary

The grain size distributions of the Saltwater Creek sediments are unlike either the Avon-Heathcote Estuary or Travis Swamp sediments except in the fine silt and clay parts of the curves (Fig. 3.15c and d). Sediments range from finely skewed to near symmetrical, and from platykurtic to leptokurtic and mesokurtic. All sediments are poorly sorted sandy silts. Sediment concentrations range 7-49% sand, 35-78% silt, and 7-21% clay. Most curves contain many inflexion points; the grain size distributions are polymodal, and difficult to interpret by conventional percentile statistical parameters. Knowledge of the area and the history of the Ashley River mouth, Saltwater Creek Estuary, together with the grain size data, suggests that the coarse tails rich in pebbles reflect the traction population of the Ashley River. Neither the tide or Saltwater Creek would have enough energy to transport such large pebbles.

The varied grain size distributions reflect changes of the Ashley River in 1) the position of the mouth, 2) water volume, 3) flow rate, and 4) suspended load. Polymodal distributions suggest a combined influence of the dynamic Ashley River, the slow meandering Saltwater Creek, and tidal reworking of sediments.

Most sediment in the Saltwater Creek Estuary has accumulated under swift and more turbulent conditions than in the Avon-Heathcote Estuary.

3.4.5 Comparison of Grain Size Distributions of Sediments in this Study with Loess Deposits of Canterbury.

Unit C and Travis Swamp mud samples have similar grain size distributions to both Late Pleistocene and Post-glacial loess (Table 3.1). Saltwater Creek samples are also similar except much richer in coarse sand, which indicates an additional source of coarser sediments, such as gravel beds up river. Unit A, A', B and D are unrelated to the loess deposits as far as grain size is concerned. The coarser composition of units A and A' is probably related to offshore reworking of sediments. Units B and D (B/D) show similar very coarse range to Post-glacial loess, but are enriched in medium sand and coarse silt and depleted in fine silt and clay. This pattern is indicative of selective deposition in an estuarine environment.

The similar grain size distributions between the two loess deposits and Unit C, the Travis Swamp, and Saltwater Creek Estuary sediments suggests that the loess is the source of sediments in this study.

Table. 3.1 Comparison of Average Grain Size Distributions of Sediments from this Study with Pleistocene and Post-glacial Loess (Ives, 1973)

	V.Coarse sand (>200μm)	Sand-silt (200-20μm)	Silt-clay (20-2μm)	Clay (<2μm)
Loess (%)				
Late Pleist.	0	40-69	22-37	8-23
Post Glacial	1-4	45-68	24-35	7-18
Sediment (%)				
TS/1 (T2&T3)	1-4	65-69	21-29	2-14
Unit C	0.5-3	65-80	12-32	3-8
SWC	1-42	32-74	21-35	5-13
Unit B/D	1-3	93-97	3-7	0-3
Unit A	20%	80	0	0
Unit A'	18	82	0	0

3.5 MINERALOGICAL STUDIES

Some minerals have a greater capacity to adsorb organic matter and heavy metals than others (Forstner, 1989). Hence, differences in mineral proportions cause natural heavy metal variation. Therefore, it is important to identify the mineral components of sediments when assessing the degree of metal contamination.

3.5.1 Clay Mineralogy

The most abundant clay mineral groups are illite, kaolinite, chlorite, vermiculite, and smectite, which are frequently interstratified (Wilson, 1987). Generally in marine sediments, illite is the most common group, and is the second most reactive after smectite (Blatt, et al, 1980; Drever, 1982; Wilson, 1987).

Smectite layers expand during adsorption of water or organic material (such as ethylene glycol), whereas most other common clays are unaffected. In nature, the expansion of smectite particles leads to 1) breakdown of large clay mineral agglomerates to smaller ones, which increases surface areas, and hence the heavy metal adsorption capacity, and 2) greater adsorption of phases rich in heavy metals such dissolved organo-metallic complexes.

In addition to clay minerals the clay fraction contains clay sized quartz, feldspar, Fe and Mn hydroxy compounds, and organic material.

Macpherson (1978) studied the clay mineralogy of 80 samples from the Avon-Heathcote Estuary and found that most samples contained approximately 60% illite, 40% chlorite, and a trace of smectite. No stratigraphic or locational preferences were detected. However, it was necessary to carry out an additional mineralogical study to cover aspects important to this study that were not determined by Macpherson. These aspects include 1) quartz and feldspar concentration (high concentrations of these minerals may

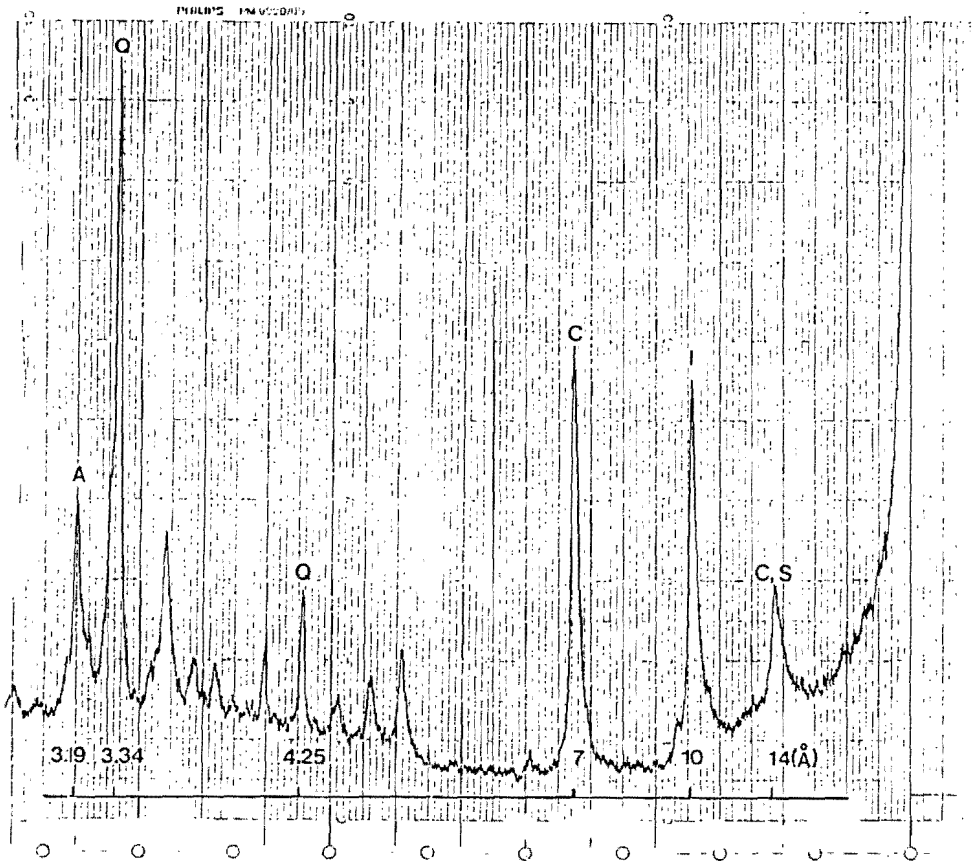

a)

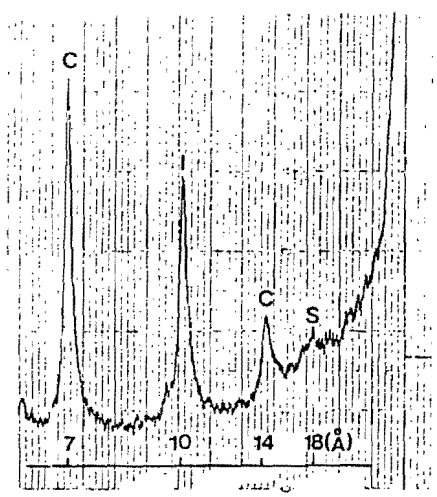

b)

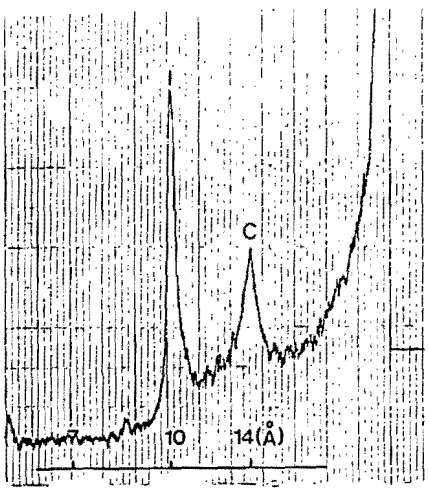

c)

Fig. 3.17 X-Ray Diffractograms of sample C10 (clay fraction) from core AHE/5.
a) Untreated orientated mount.
b) Glycolated orientated mount.
c) Heated (550°C) orientated mount.
C chlorite, S smectite, I illite, Q quartz, A albite.

lead to heavy metal dilution), and 2) the clay mineralogy of the Saltwater Creek Estuary and Travis Swamp sediments (to assess their compositional similarity to the Avon-Heathcote Estuary clays).

3.5.1.1 Method of Clay Analysis

The clay mineralogy was determined by X-Ray Diffraction (XRD) using CuKα radiation.

Samples were prepared for XRD analysis by standard methods (Brindley and Brown, 1980; Whitton and Churchman, 1987). About half a gram of each clay sample was dispersed in 5ml of double distilled water with a few drops of Na_2CO_3, stirred and left overnight. The suspensions were restirred the following morning and orientated mounts were prepared by pipetting solution onto glass slides and leaving to dry. Each slide was X-rayed from 2-46 2θ and the general mineral assemblages were determined using the X-Ray Powder Diffraction Data Files.

After the initial scan the slides were treated with a few drops of ethylene glycol and rescanned in the low angle range 2-10 2θ.

All slides that showed layer expansion after glycolation (from 14Å to 18Å) were heated to 350°C for 1 hour to test for smectite layer contraction to 10Å.

All slides that showed 7Å peaks were heated to 550°C for 1 hour to distinguish between kaolinite and chlorite.

Samples that contained smectite peaks were treated with saturated LiCl and glycolated to test for montmorillonite (Greene-Kelly, 1953; Whitton and Churchman, 1987).

3.5.1.2 Results of Clay Analyses

(i) General Mineral Assemblage

The most noticeable feature of the X-ray traces was

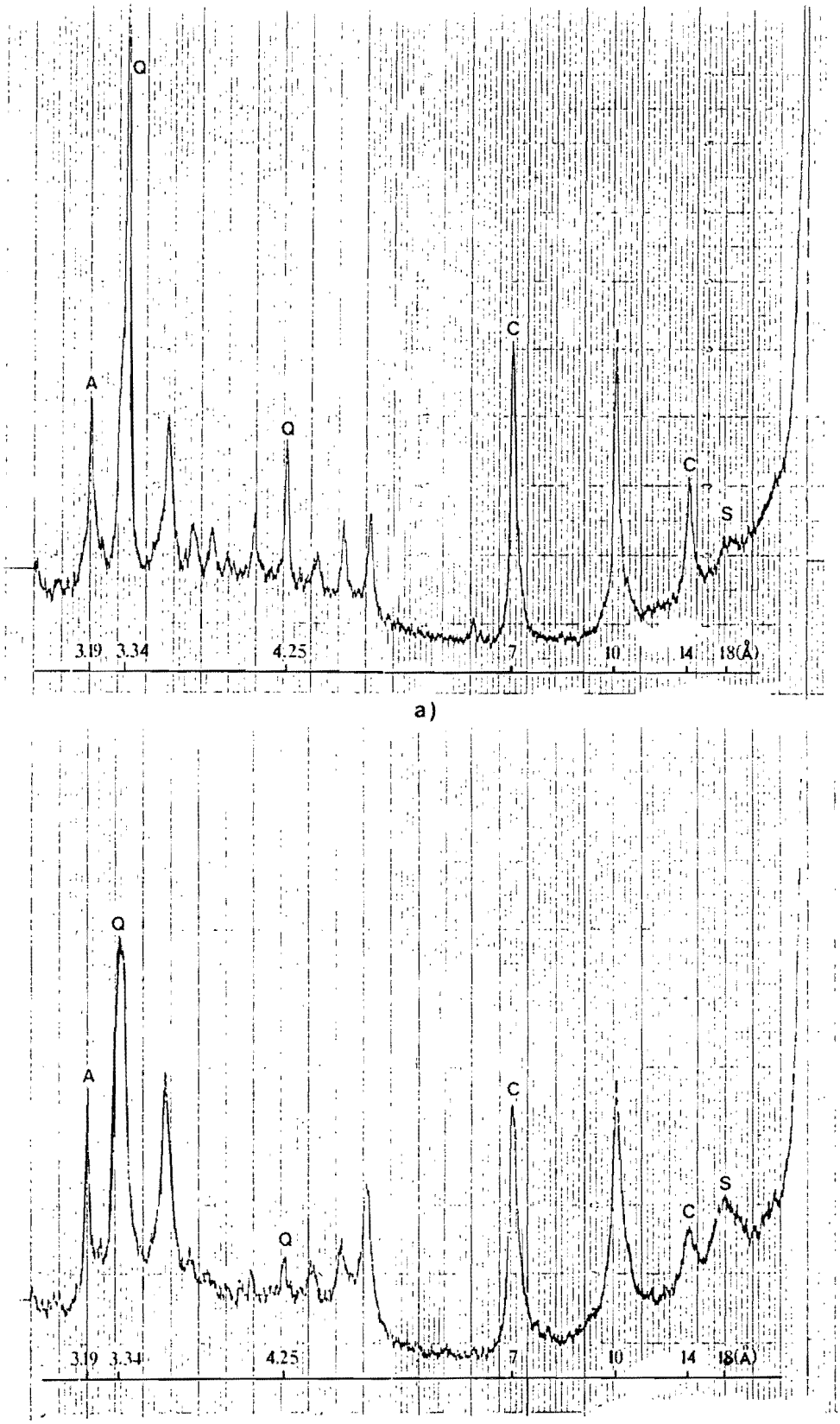

Fig. 3.18 Glycolated X-Ray Diffractograms of sample 10 (clay fraction) from core SWC/1. a) <4µm fraction. b) <0.5µm fraction. C chlorite, S smectite, I illite, Q quartz, A albite.

the uniformity between all the samples regardless of unit or locality (Fig. 3.17b and 3.18a). The following characteristics were used to identify the minerals present.
1) All non glycolated samples produced strong sharp X-ray Diffraction maxima at 14Å (chlorite, smectite), 10Å (illite), 7Å (chlorite, kaolinite), 4.25Å (quartz), and 3.34Å (quartz), and 3.19Å (feldspar; albite identified from overall peak assemblage) (Fig. 3.17a).
2) Most glycolated samples produced small broad peaks around 18.5Å (smectite) and slightly smaller 14Å peaks (chlorite only) (Fig. 3.17b), and smaller 10Å peaks indicating slight interstratification of illite and smectite.
3) Lack of expansion of glycolated peaks after LiCl treatment indicated that montmorillonite is the dominant smectite species. The 14Å position of the unexpanded 001 smectite peak suggests that the exchangeable cations are Ca^{2+}, and Mg^{2+}. These cations are probably present in 2 layers of water (Hume and Nelson, 1982).
4) The 7Å peak disappeared for almost all samples heated to 550°C whereas the 14Å peak remained intact indicating that chlorite is present rather than kaolinite (Fig. 3.17c). In addition, slow scanning across the 3.5-3.6Å range revealed 1 peak present at 3.54Å (chlorite) and no peak at 3.58Å (kaolinite).
5) Heating samples to 350°C resulted in the disappearance of 18Å peaks and slight thickening of 10Å peaks on the low angle side supporting the smectite identification.

(ii) Grain Size Analysis of Clay Minerals

Selected samples were separated into 2-4μm, 1-2μm, 0.5-1μm, and < 0.5μm fractions by centrifuging (Hume and Nelson, 1982; Jackson, 1956). Orientated mounts were prepared and X-rayed as above. All samples exhibited the same behaviour. As grain size decreased the relative size of the quartz peak gradually diminished, whereas the size of the glycolated smectite peak at 18Å increased. The major

quartz peak is significantly diminished in <0.5μm fraction compared to the <4μm fraction (compare Fig.3.18a and b). These results reveal the increased concentration of smectites in the very fine grain size and the diminishing presence of quartz. However in the <0.05μm fraction, quartz and albite are still relatively abundant compared with the clay minerals.

(iii) Quantitative Analysis of Clay Mineral Fractions

Mineral proportions in samples (12 from AHE Unit D, 14 Unit C, 4 Unit B, 4 TS/1, 5 TS/3, 5, SWC/1, 3 SWC/2) were determined separately for 1) quartz and albite, and 2) clay minerals.

Quartz and Albite

Pure quartz and albite minerals were milled to obtain fine grained consistency of approximately <4μm. Three tests were carried out to find the most precise method of quantifying quartz and albite. The tests are discussed in Appendix 2.0, Section A2.2. The method adopted involved direct comparison of standard peak heights with sample peak heights. Samples were X-rayed as dry packed powder mounts in aluminium holders (random orientation).

This technique is semi-quantitative because the accuracy was not determined. The accuracy may be low due to interference from other minerals.

The peaks used were quartz 4.25Å and albite 3.19Å. Ten diffractograms were run for each standard to obtain the average peak heights. The average standard peak heights were directly compared to average sample peak heights (after 3 analyses of each sample). The results are summarised in Table 3.2.

Table. 3.2 Mean Clay Fraction Compositions of Avon-Heathcote Estuary, Saltwater Creek Estuary, and Travis Swamp Sediments

	Organic*	Quartz	Albite	Smectite	Illite	Chlorite
AHE						
Unit D	7.2	11.8	8.6	0.9	44	29
Unit C	5.9	11.4	8.9	1.0	44	29
Unit B	5.9	11.6	9.0	1.0	44	28
TS/1	5.0	13.0	9.8	0.8	45	2 7
TS/3a	4.7	12.6	9.4	0.8	44	2 9
SWC/1	6.0	10.5	8.2	1.4	49	25
SWC/2	6.0	9.7	7.8	6.2	48	25

(4% error on the mean values, CI=95%; * Organic matter content was determined by weight loss on ignition, see Chapters 4 and 6)

Generally speaking quartz and albite concentrations are uniform within and between the Avon-Heathcote Estuary, Saltwater Creek Estuary, and Travis Swamp. The organic matter content is tabulated for comparison, but will be discussed in Chapter 4.

Clay Minerals

Pure illite, chlorite, and smectite samples were not available for this study, consequently a different approach was required. A number of authors have quantified the proportions of minerals present, assuming that the relative heights of the mineral peaks are proportional to the amount of each constituent present (Churchman, 1980; Biscaye, 1964; Whitton and Churchman, 1987; Macpherson, 1978; Johns et al, 1954; Weaver, 1961). Such an approach is not accurate but as long as the samples are prepared in an identical manner a high degree of precision can be obtained. It was decided for comparison to use the same method as Macpherson (1978), which is adopted from Biscaye (1964), Johns et al (1954), and Weaver (1961). The method involves direct comparison of peak heights using the following weighting factors: 18Å x 1 (smectite), 10Å x 4

(illite), 7Å x 2 (chlorite). The traces from glycolated mounts were used to obtain separate montmorillonite (18Å) and chlorite (14Å) peaks. The results are summarised in Table 3.3.

Table 3.3. Percentage Clay Mineral in the Clay Mineral Portion of the Clay Size Fraction.

	Smectite	Illite	Chlorite
AHE	1.5	60	39
TS	1.1	60	39
SWC/1	1.9	65	34
SWC/2	7.8	61	32

(error of mean is 3% at CI=95%)

The Avon-Heathcote Estuary and Travis Swamp results (60% illite and 39% chlorite) are in close agreement with Macpherson's findings of 60% illite and 40% chlorite. Macpherson ignored the contribution from smectites. The Saltwater Creek Estuary clays are slightly higher in smectites and lower in chlorite.

Discussion

The higher mean organic matter level found in Unit D (Table 3.2) reflects the eutrophication of the estuary in modern times due to the release of nutrient (nitrogen and phosphorous) rich effluent from the sewage ponds (Chapter 2, Section 2.7.3). The behaviour and significance of organic matter is discussed in detail with the heavy metal distributions in Chapter 4.

The clay mineral content is generally similar between the three localities. However, both cores from Saltwater Creek Estuary contain slightly less chlorite and slightly more illite than either the Avon-Heathcote Estuary or Travis Swamp. In addition, smectite levels are significantly elevated in Saltwater Creek Estuary core 2 (Table 3.3).

Smectites, illite, and chlorite are ultimately derived from rock weathering. Examples of source minerals include:

1) micas and feldspars (illite), 2) ferromagnesium minerals such as olivine, pyroxene, amphibole (chlorite), and 3) volcanic glass and olivine (montmorillonite) (Blatt et al, 1980; Lewis, 1982; Weaver, 1958). Transformation from one clay mineral to another commonly occurs as a result of chemical changes during transportation, deposition, and compaction (Churchman, 1980). The general similarity between all samples of this study in the shape of mineral peaks (all clear and sharp indicating good crystallinity) suggests that the minerals are detrital in origin. Therefore, the slight compositional differences between the Saltwater Creek Estuary and the Avon-Heathcote Estuary are most likely caused by differences in proximity to source, and sediment reworking.

The general similarity between the Avon-Heathcote Estuary and the Travis Swamp in grain size distributions and clay mineralogy suggests that the Travis Swamp clay minerals are excellent baseline samples for heavy metal analyses of the Avon-Heathcote Estuary sediments.

3.5.2 Sand Mineralogy

The mineralogy of sands and silts from the three sites was analysed to determine the provenance (origin) of the sediments.

3.5.2.1 Method of Sand Analysis

A portion of the sand fraction 2.5-3.5ϕ (88-180μm) of 6 Avon-Heathcote Estuary samples, 1 Travis Swamp sample, and 2 Saltwater Creek samples were separated into light and heavy minerals fractions by stirring in sodium polytungstate (specific gravity (SG), 2.89-2.96) in separating funnels. After settling, the heavy fractions were poured into preweighed filter paper, washed free of sodium polytungstate with distilled water, dried and weighed before petrographic examination.

The mineral proportions in the heavy mineral fractions were calculated semi-quantitatively. Individual minerals were counted in 10 fields of view for each sample, and adding the total of each mineral for all fields. The percentage, of each mineral, was then calculated by dividing into the total number of grains counted for the sample.

Quartz and feldspar concentrations in the remaining light fraction were determined petrographically and by XRD (in the manner outlined in the clay section above). The organic matter percentage was measured by weight loss on ignition. The quantity of rock fragments was determined by counting minerals petrographically.

3.5.2.2 Results of Sand Analyses

Table 3.4 Percentage Composition of Sand Fractions

Sand sample	Quartz	Albite	Heavy Minerals	Rock Frag.	Organic Matter
AHE/1 D	44	16	2.7	5-10	1.0
AHE/1 C	43	19	0.8	5-10	1.6
AHE/1 B3	42	18	0.8	5-10	1.3
AHE/1 A1	44	18	1.1	5-10	1.0
AHE/6 B22	44	17	0.7	5-10	1.3
TS/1 2&3	45	19	1.1	5-10	1.4
SWC/1	68	15	2.0	5-10	0.9
SWC/2	52	16	1.1	5-10	1.0

Petrographic examination of the light fractions showed that quartz and feldspar together formed 85 to 90 % of the mineral component, whereas the XRD analyses yielded approximately 60% quartz and feldspar. Hence, the quantitative XRD method used here is not accurate and produces low results.

All sand fractions contained similar quantities of each mineral (Table 3.4). Again the general Avon-Heathcote Estuary suite is almost identical to the Travis Swamp

samples. These results, provide further support for the interpretation that the Travis Swamp estuary deposits are an older lateral equivalent of the Avon-Heathcote Estuary.

The two Saltwater Creek samples are higher in quartz than either the Avon-Heathcote Estuary or the Travis Swamp. The Saltwater Creek sediments are either derived from a source higher in quartz than the Avon-Heathcote Estuary, or have followed a different transportation and sorting history. The differences in the hydrodynamics of the two systems could explain the discrepancy.

Petrographic analysis of all sand fractions showed mainly subangular to subrounded glassy or white quartz and feldspar, rock fragments, and occasional dark green oval shaped glauconite grains and rounded quartz. The rounded grains have probably been derived from an offshore source.

All Avon-Heathcote Estuary samples except Unit A contained red brown crusty sub-metallic matter that stained many of the minerals. This material was identified as Fe oxide possibly goethite. Similar material, except yellower, is associated with Saltwater Creek sand. This material may have a slightly different composition (limonite rather than goethite) in the Saltwater Creek Estuary. Iron oxide was not observed in the Travis Swamp samples.

Some Fe oxide in the Avon-Heathcote Estuary could be derived from weathering of volcanic minerals such as olivine and pyroxene. However most Fe oxide coated aggregates of coarse organic debris (grass like material, ash, and twigs), silt, and clay particles, which suggests authigenic precipitation during estuarine mixing. Hence, Fe oxide is probably precipitated in both estuaries during estuarine mixing (Chapter 1, Section 1.4). However, the anaerobic conditions in the Avon-Heathcote Estuary sediments do not favour long term stability of Fe oxide. Hence, the coatings observed on the Avon-Heathcote Estuary sand grains probably formed, after sample collection, by oxidation of anaerobic authigenic Fe compounds (such as sulphides, and carbonates). In contrast the red brown

Table. 3.5 Heavy Mineral Concentrations in Sand Fractions (%)

Mineral	AHE/1 D	AHE/1 C	AHE/1 B3	AHE/6 B22	AHE/1 A	AHE/4 8	TS/1 B/C	SWC/1	SWC/2	Torlesse	K-T
Ilmenite	3.3	2.3	.8	.8	1	1	1	1.4	3.3	27.3	44.5
Magnetite	1.1	.3	.1	.4	.5	.4	.5	.4	2.5	.6	2.2
Rock Fragment	35.6	26.4	33	25.9	29.5	32.7	32.5	20.2	33.2	27.4	10.2
Biotite	.3	10	13.4	18.6	3.7	10.2	8.6	1	2.1	12.4	.8
Chlorite	1.6	5.7	3.3	11.1	.7	2.8	3.5	1	1.7	2.7	3.2
Garnet	3.6	2.1	.3	.7		.4	1			2.9	1.7
Zircon	3	5.7		.7		2.8	1.5	2	1.3	3.1	7.3
Titanite	2.3	1	2.2	.4	1.5		.5		.4	3.3	1.1
Epidote	8.2	4.7	4.4	2.5	5.9	8.6	4	6	12.4	12.3	9.2
Clinozoisite	4	3.6	4.1	1.4	2.9	5.5	4.6	2.5	3	3.1	10.8
Tourmaline	.3	1		.4			.5	1		.2	1
Pumpellyite	26	26	35	30.7	45	30	33	52	37	1.4	.7
Hornblende	1.3	2.6				1.6		1		.8	5.3
Apatite	1.6	3.6		2.1	1.5	.8	2	4.5	.9	2.3	1.3
Allanite	.3			.7						-	-
Augite	6.3	1.6	1.6	1.1	5.2	2.8	3	5	.4	-	-
Muscovite	1.3		1.1	2.5	2.9	.8	3		1.3	-	-

K-T; Cretaceous-Tertiary Sediments
-, no data

colouration was present when the Saltwater Creek cores were opened (Fig. 3.14).

The organic matter and Fe oxide coatings may be a major sink for heavy metal ions in each estuary.

3.5.2.3 Heavy Mineral Analyses

Table 3.5 contains the results of the heavy mineral analysis of this study together with the average heavy mineral content of 72 samples from the Mesozoic Torlesse Terrane, and 171 samples from Cretaceous-Tertiary sediments examined by Smale (1988). The Torlesse rocks consist of slightly metamorphosed quartz arenites which are derived from schists forming the Southern Alps west of Canterbury (Fig. 2.1). The Torlesse rocks lie to the east of the Southern Alps along the foothills bordering Canterbury and Southland. The Cretaceous-Tertiary sediments are eroded Torlesse sediments and are common all over Canterbury (Smale, 1987 and 1988).

Initial examination of the Avon-Heathcote Estuary, Travis Swamp, and Saltwater Creek Estuary suites suggests either igneous or metamorphic source rocks. Minerals derived from either geological environment include biotite, augite, apatite, hornblende, ilmenite, magnetite, and muscovite (Milner, 1963; Shelley, 1982). However, a Banks Peninsula volcanic origin appears less significant because 1) titanite, zircon, tourmaline, and garnet, are more commonly associated with metamorphic or plutonic igneous terranes, 2) Banks Peninsula volcanics are devoid of biotite, ilmenite, and muscovite (Dr S.D. Weaver, per. comm.), and 3) pumpellyite, clinozoisite, epidote (together with chlorite) are diagnostic of low grade metamorphic rocks. In addition, pure albite (which is common in all grain sizes of this study) is indicative of metamorphism to the higher grade amphibolite facies (Shelley, 1982). Nevertheless, some chlorite, plagioclase feldspar, and most of the less durable augite and apatite, are probably

derived from the Banks Peninsula volcanics.

The semi-opaque debris (or rock fragments) are more informative than the individual minerals themselves. The rock fragments are generally white, yellow, or blue green in colour. These fragments are unlikely to be derived from the Bank Peninsula volcanic rocks because fine grained volcanic matter is usually grey to opaque in colour (Smale, 1988). The rock fragments are diagnostic of a Torlesse source for the sands, consisting of combinations of epidote-pumpellyite, muscovite-pumpellyite, quart-pumpellyite, chlorite-pumpellyite, chlorite-epidote, and zircon-epidote. These combinations are definitive of saussuritisation (plagioclase alteration) of basic igneous rocks by low grade metamorphism (Whitton and Brooks, 1972). However, some apatite-pumpellyite rock fragments may be derived from local volcanic rocks.

Consequently it is concluded that the heavy mineral suites of the Avon-Heathcote Estuary, Saltwater Creek Estuary, and Travis Swamp are dominated by sediments derived from Torlesse and Cretaceous-Tertiary rocks. The lower concentrations of heavy ilmenite (SG 4.8) and magnetite (SG 5.1), together with the higher concentrations of lighter pumpellyite (SG 3.2), found in the samples of this study, suggests that these modern sands are predominately derived from aeolian deposits (which were themselves derived from the older rocks). Locally the most likely sources are Post-Glacial and Late Pleistocene Loess deposits covering the Canterbury Plains and flanking Banks Peninsula.

3.5.3 Mineralogy of Silt Fractions

The silt compositions were determined by XRD with quantitative analysis of quartz, albite, illite, chlorite using the same methods as described in Section 3.5.1. The organic matter and rock fragment concentrations were determined in the manner described in Section 3.5.2.

Table 3.6. Percentage Composition of Silt Fractions

Silt sample	Quartz	Albite	Illite	Chlorite	Organic Matter
AHE/3a D	33	19	7	4	2.2
AHE/3b D	30	19	6	2	2.6
AHE/2 C12	32	18	7	4	2.4
AHE/5 C10	35	19	9	5	2.0
AHE/6 C3	35	21	9	5	1.7
AHE/3a B	36	19	7	6	2.2
AHE/5 B2	30	22	7	4	2.0
AHE/6 B22	34	16	9	4	2.2
TS/1 2	35	22	10	4	1.8
SWC/1 10	33	16	6	3	1.8

The silt compositions presented in Table 3.6 are relatively uniform for the Avon-Heathcote Estuary, Travis Swamp, and Saltwater Creek Estuary. There is no significant depth or locational preference for any mineral. The silt fractions contain approximately 10% less quartz than the sand fractions, which is balanced by addition of a little over 10% clay minerals, and a slight increase in organic matter.

3.5.4 Discussion of Mineralogy

The mineralogy and grain size distributions indicate that the sediments of the Saltwater Creek Estuary, Avon-Heathcote Estuary, and Travis Swamp are derived principally from, 1) Quaternary loess deposits, and partly from Quaternary fluviatile deposits. Both of these sources were themselves derived from the Torlesse Supergroup sediments located along the foothills of the Southern Alps.

Quaternary loess deposits are widespread over the Canterbury area and are over 8-9m thick on the northern flanks of Banks Peninsula (Griffiths, 1973; Ives, 1973; Raeside, 1964). The loess was deposited in two stages 1) Late Pleistocene, ceasing about 10,000 years ago and 2) Post-glacial, with deposition continuing today along the banks of many braided rivers in the region. The loess

mineralogy is similar to Torlesse sandstones and Cretaceous-Tertiary sandstones (quartz and feldspar constituting 90%), except some minerals have weathered to clays which make up about 20% of the sediment. The grain size distributions of these aeolian sediments parallels Unit C and Travis Swamp deposits.

The results of the Chapter 2 indicate that Unit C was derived from the loess deposits covering the Christchurch area and the Port Hills, during a period of river sweeping between 1925 and the 1950's. The carbon date from the Travis Swamp shows that similar estuary sediment accumulated 1000 years earlier. Hence, the Travis Swamp mud probably belongs to the source of Unit C sediment.

Reed (1951) examined the mineralogy of sands near the mouth of the Avon-Heathcote Estuary and found an almost identical heavy mineral and light mineral assemblage to that examined in this study. In addition, shallow offshore sands showed identical grain size distribution to Unit A. Reed found the mineralogy of sands at the mouth of the Waimakariri similar to sands near the inlet of the Avon-Heathcote Estuary. These finds indicated that sediment in Pegasus Bay south of the Waimakariri river is derived ultimately from weathering of Torlesse quartz and feldspathic sandstones in the catchment area of the Waimakariri River. Such deposition patterns must have been predominant for a long time because wells in the Christchurch area do not reach volcanic rocks until depths greater than 60-70m (Brown and Wilson, 1988). The bulk of the medium fine sands in the Avon-Heathcote Estuary are probably derived from shallow marine sediments in Pegasus Bay, which are themselves derived from the Waimakariri River. Coastal transportation explains the presence of a few rounded glauconite and quartz grains in the sands. In contrast the coarse sands in the Saltwater Creek Estuary are derived directly from the Ashley River. The sediments in Saltwater Creek Estuary are most likely also derived from Torlesse rocks.

3.6 DATING OF SEDIMENTS AND ESTIMATION OF SEDIMENTATION RATES

Determining sedimentation rates during historical times is difficult because the most widely used radiometric dating technique (C-14) are not applicable to sediments younger than 250 years. Hence, it is helpful to identify marker beds that correlate with historical events. Stratigraphic marker beds include wood chips from log milling (Hume and Gibb, 1987), and changes in pollen distributions (Hume and McGlone, 1986), while chemical marker beds include contaminants such as heavy metals and organo-chlorine compounds (Hume, et al, 1989). Knowledge of marker beds and other historical data are often incorporated into radiometric dating calculations (such as ^{210}Pb) to obtain accurate age profiles and sedimentation rates.

In the following section all sediment units of the Avon-Heathcote Estuary are accurately dated using a combination of ^{210}Pb profiles, ^{14}C ages, pollen profiles, and the historical records of Chapter 2.

3.6.1 Carbon-14 Dating of Shell Material

The first dating method undertaken was ^{14}C analysis of shell beds. Two composite shell samples (M36/f43 and M36/f44), from a deposit near the base of Unit C in cores AHE/2a-d, were sent to the Institute of Nuclear Sciences (INS), Lower Hutt (NZ) for ^{14}C dating+. A sample of shells (M35/f26) from the Mactra ovata bed along side the Avon channel near Pleasant Point was also dated (Chapter 2, Fig. 2.9).

The position of the shell layer in core AHE/2a is shown in Fig. 3.19. The age of the shell layer is 350±60 years B.P. The historical evidence presented in Chapter 2 suggests that this shell horizon is younger than 1927. Most shells were articulated and in life position, so they cannot have been transported from older sediments. The

+ C^{14} laboratory data is in the back pocket of the thesis.

Fig. 3.19 Stratigraphic Sequence in core AHE/2a. The contacts between units B and C, and C and D are marked by horizontal lines. *, ^{14}C sample; CP, coal particle.

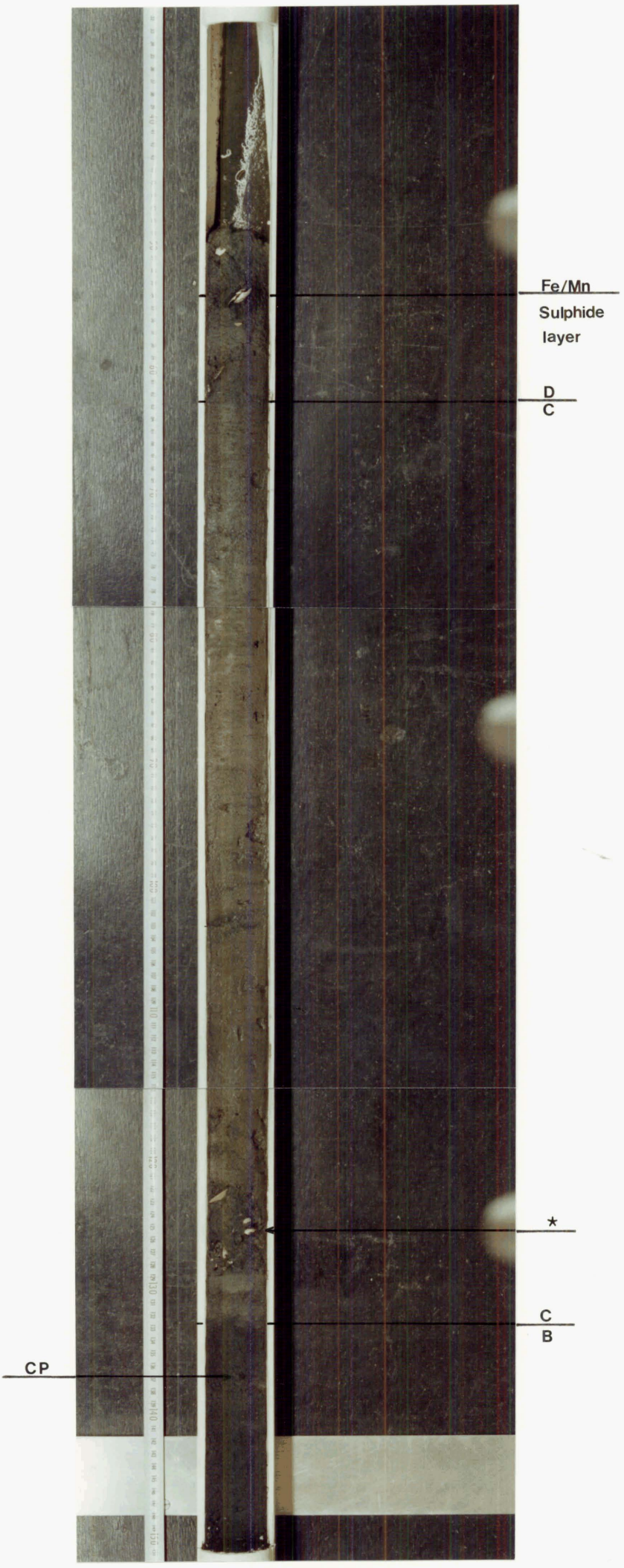
Fe/Mn
Sulphide
layer
D
C
★
C
B
CP

sediment was slightly blackened at the top of Unit B and base of Unit C in most cores. Charcoal and ash occurred in this layer. In fact, a charcoal particle is visible in Fig. 3.19. Such material is most likely derived from burning of fossil fuels during the early period of industrialisation (Chapter 2, Section 2.8). Coal, ash, and lime are high in "dead carbon" isotopes and are therefore low in the young isotope ^{14}C. River transport of coal, ash, and charcoal particles to the estuary bed, during the early period, would have contaminated the benthic environment with dead carbon (Dr J.McKee, INS, pers comm.). Carbon dioxide and carbonate ions derived from lime burning may also have been a source of dead carbon to the sediments. Dead carbon probably became incorporated in the shells of the benthic dwellers during their lives, which explains why such an old age was obtained. This interpretation is confirmed by ^{210}Pb and pollen profiles discussed in Sections 3.6.2 and 3.6.3.

The age obtained for the Mactra ovata shell beds is "Post Bomb", which means the shellfish were alive during or after the nuclear testing in the Pacific from 1945-1972 (Dr J. McKee, (INS), pers comm.). During nuclear testing ^{14}C is released into the atmosphere in large quantities. The 120% ^{14}C value obtained for the shells corresponds with peak nuclear testing during the 1960's (Dr R. Spike, INS, pers comm.).

The 1960's age of the Mactra ovata shell beds and photographic evidence in Fig. 2.9 indicate that, near Pleasant Point, sediment has accumulated very slowly in recent times. In Figs 2.9a and b the shell beds are exposed only where the Avon River channel has cut westward into the mud flats. The small side channel in Fig. 2.9a shows that the shell bed extends beneath sediment to the west of the Avon channel. In other words this shellbed is buried by modern sediment in areas away from the channel. If the estuary was undergoing overall erosion then the shell beds would be fully exposed across the mud flats.

The shellfish may have been killed during a pollution

event (Chapter 2, Section 2.3.4). During the 1950's when Christchurch was undergoing rapid growth, raw sewage frequently entered the estuary along the western slopes, when the treatment plant was overloaded (J. Pollard, pers comm.). Such an incident may have killed the shellfish.

A layer of dead shellfish was found between 45-50cm in core AHE/6 (Appendix 2.0, Section A2.1), which was collected 50m up slope of the shellbed. The shell layer in core 6 may correlate with the shellbed exposed along side the channel. Mactra ovata normally live 20cm below the surface (living assemblages were present in cores AHE/4 and AHE/6). Assuming the two shell layers are the same then the shellfish were flourishing during Unit C deposition and their age (early 1960's) corresponds to that of the sediment 20cm higher up (25-30cm level), which is 10cm below the top of Unit C. Hence, the upper contact of Unit C is probably after 1960 in the Avon depository. A further 25cm of sediment has accumulated in the area since the early 1960's which corresponds to a sedimentation rate of around 0.9cm per year.

3.6.2 Lead-210 Dating of Core AHE/1a

Because the radiocarbon dates of the shell layer at the base of Unit C, are inconsistent with the findings of the historical synthesis, a ^{210}Pb dating technique was developed and tested on core AHE/1a.

3.6.2.1 Introduction

Lead-210 is produced from ^{222}Rn (radon-222) decay through a series of short lived daughter isotopes (Po, Pb, Bi). In sediment and soils mineral bound ^{226}Ra (radium-226) decays to ^{222}Rn its inert gas daughter element. The ^{222}Rn ($t_{½}$=3.8 days) then diffuses out of the soil into the atmosphere where it rapidly decays to ^{210}Pb ($t_{½}$=22 years) which, in particulate form, is subsequently deposited on

the land surface. The rate of deposition of ^{210}Pb has been constant, when normalised for rainfall, throughout recent history (Dr M. Matthews, National Radiation Laboratory (NRL), Christchurch, New Zealand, pers. comm.). Consequently ^{210}Pb has proved to be an important nuclide in the study of sedimentation on a human time frame of approximately 100 years (Chanton et al, 1983; Ivanovich and Harman, 1982; Matthews and Potipin, 1985; Stiller and Imboden, 1986).

Soil and sediment bound ^{210}Pb consists of the following forms: a) mineral ^{210}Pb (^{210}Pb produced by ^{222}Rn decay within the mineral lattice), b) interstitial ^{210}Pb (^{210}Pb adsorbed on mineral particles due to decay of ^{222}Rn after escape from the host particle, before diffusion into the atmosphere), c) fallout ^{210}Pb (produced by ^{222}Rn decay in the atmosphere followed by deposition attached to aerosol particles) (Matthews and Potipin, 1985). Total ^{210}Pb (mineral, interstitial, and fallout) is normally extracted by severe acid attack on sediments, usually involving HF, which breaks down the mineral lattice. Extractable ^{210}Pb (fallout and interstitial) is commonly studied by digestion in dilute HCl or HNO_3 (Chanton et al., 1983; Matthews and Potipin, 1985).

Sources of Error in ^{210}Pb Profiles

Conditions other than radioactive decay which influence ^{210}Pb distributions in sediments include compaction, post-depositional nuclide migration, smearing during coring, variation in sedimentation rate, bioturbation, and grain size distributions (Tanaka et al., 1983). The ^{210}Pb content of the sediments also depends on the proportions of constituents that make up the sediments such as shells (foraminifera), organic matter, and authigenic minerals (such as Fe/Mn hydroxy compounds). Lead-210 may be enriched in organic matter, which often migrates in interstitial waters during organic

decomposition (Ivanovich and Harman, 1982; Sharma et al., 1987).

In estuaries, the majority of fallout ^{210}Pb is transported to sediments attached to particulate matter (particularly clays and organic matter) (Chanton et al, 1983). Stiller and Imboden (1986) studied ^{210}Pb phase relationships in the waters and sediment of Lake Kinneret, Israel, and found 25% of the flux derived from the atmosphere, 55% from river transport on particulate phases, and 20% from decay of ^{222}Rn in the water column. They discovered that 90% of incoming ^{210}Pb from the atmosphere and waters is lost to the sediments of Lake Kinneret. The results of the Lake Kinneret investigation and similar studies (Appleby and Oldfield, 1978) indicate that accelerated deposition will dilute ^{210}Pb activities, because sediment surfaces are buried before adsorbing a significant quantity of the fallout ^{210}Pb.

Often ^{210}Pb concentrations in surface sediments are consistent for 10's of centimetres because of biological mixing. Realistic sedimentation rates may be obtained from bioturbated sediment providing the deposition rate is high and bioturbation is effective only in the first few cm. In some cases where bioturbation is persistent to considerable depths, complex mathematical corrections have produced results comparable with similar undisturbed sediment (Gardner et al, 1987; Ledford-Hoffman et al., 1986; Sharma et al., 1987).

The other important influence on ^{210}Pb profiles in sediments is grain size. Due to the dynamic nature of marine (particularly estuarine) environments, ^{210}Pb studies often yield anomalous profiles. Where the sediment is clearly unbioturbated the cause is usually variation in sand and mud content. Chanton et al. (1983) studied sediment profiles from Cape Lookout Bight, a rapidly changing coastal basin on the Outer Banks of North Carolina (USA). The sediment column grades upwards from coarse grained to fine grained material over a 40 year period due

to changes in the Cape configuration. Consequently, ^{210}Pb distributions are progressively diluted with sand at depth. Sand, silt, and clay fraction analyses revealed the ^{210}Pb activity of clay is 3.2 x silt, and 24.7 x sand. Lead-210 activities corrected for mud content yielded dates confirming the recorded ages of sand layers corresponding to storm events.

3.6.2.2 The Method of ^{210}Pb Extraction

Lead-210 dating depends on the precise and accurate determination of fallout ^{210}Pb. There are several methods commonly used. Some workers prefer analysing fallout ^{210}Pb by dissolution and comparison of total ^{210}Pb and total ^{226}Ra levels with assumptions regarding $^{226}Ra/^{222}Rn$ equilibrium in sediments (Ledford-Hoffman et al, 1986; Moore and Poet, 1976). Simpler methods involve extraction of the ^{210}Pb derivative ^{210}Po (Polonium-210) using dilute acid and auto-plating onto silver discs (Chanton et al, 1983; Farmer, 1978; Finney and Huh, 1989; Robbins and Edginton, 1975: Sharma et al, 1987).

Polonium extraction was used in this study. Dr. Murray Matthews of the National radiation Laboratory, Christchurch (NRL), assisted with method development and supervised the instrumental analysis of the polonium plated discs. The development of methods is discussed in Appendix 2.0, Section A2.3.

Milled 5g samples were boiled for 1 hour, with 1ml of 7.7dpm/ml ^{208}Po tracer, in 1M HCl, with stirring. After extraction the solutions were filtered and diluted with double distilled water to 0.5M HCl. Ascorbic acid (0.1g) was added to complex Fe. Pre-cleaned (see Appendix 2.0, Section A2.3) silver discs were suspended in the solutions, at 80-95°C, for 4 hours to allow the nuclides to self plate on the discs. The radioactivity of the discs was measured using alpha spectroscopy by Dr M. Matthews of the National Radiation Laboratory, Christchurch. It was assumed that the

^{210}Po activity is in equilibrium with ^{210}Pb activity.

3.6.2.3 Analysis of Core AHE/1a

Sediment in the Avon-Heathcote Estuary varies from almost pure sand to greater than 80% mud, and the most recent sediment layer, Unit D, is intensely bioturbated in many places. Thus it was difficult to find a core that contained a thick and undisturbed sediment sequence. Core AHE/1a from near Sandy Point was chosen; the sediment is almost entirely unbioturbated except for a small section across the contact between Unit C and Unit D (Fig. 3.3a).

The subsamples (spanning 4cm) were extracted and plated 2 at a time. The international Reference SD-N-1 (IAEA) was analysed with every third pair of samples, and the results are presented in Table 3.7.

Table 3.7 Lead-210 Results for SD-N-1

Number Analyses	Mean(X) (mBq/g)	Mean(μ) (mBq/g)	Confidence Interval (α=.05)	Yield (X/μ) (%)
4	104±1	138	101-155	75

1Bq = 1 decay (d)/ second, therefore 1dpm=1/60Bq.
X; mean of SD-N-1 analyses.
μ; certified mean (IAEA, 1988).

The count rate of SD-N-1 was 104 mBq/g which is within the confidence interval of IAEA (1988). The precision of the method was greater than 99%. Several blank samples were measured and found undetectable.

Separate sand, silt, and clay samples were analysed, from units D and C, to find the proportion of ^{210}Pb adsorbed in each grain size.

Table: 3.8 Lead-210 Activity in Sand, Silt, and Clay Fractions

Sample	Sand	Silt	Clay (dpm/g)
AHE/1D1	0.588	0.911	3.916
1C1	0.397	0.947	3.794
Average (%)	11	17	72

The results of the grain size analyses reveal that 89% of the ^{210}Pb is entrained in mud particles with 72% held in the clay fraction. This result suggests that the majority of fallout ^{210}Pb is transported to the Avon-Heathcote Estuary attached to clay and silt particles and possibly organic matter associated with clay particles.

Analysis of clay or mud samples alone would produce the best results. However, after heavy metal and grain size analyses, the silt and clay fraction samples left weighed less than 0.5g. Lead-210 analyses attempted on these small samples yielded activities below detection. Therefore, total sediment samples of 5g were analysed and normalised to mud content (<63μm). The results are presented in Table 3.9 and Figs 3.20a and b.

Figure 3.20a contains the ^{210}Pb (^{210}Po) activities for the total sediment not corrected to the mud content. The activities generally increase with depth which reflects the increasing mud concentrations of samples. The same data normalised to the mud content is presented in Fig. 3.20b.

There are two main methods used in the literature for calculating ages from excess ^{210}Pb profiles. The first model assumes a constant initial concentration (CIC) of ^{210}Pb at the sediment surface. This model assumes that the specific activity of the sediment source has remained constant over the period that the sediment was eroded and deposited. The relative age at any depth is calculated using:

$$t=(1/-\pi)\ln(Az/Ao) \qquad 3.1),$$

Table 3.9 Results of ^{210}Pb Analysis of Core AHE/1a

Depth (cm)	Sample	Mud (%)	^{210}Pb (dpm/g) ±6%	^{210}Pb normalised to mud %	^{210}Pb from Fig. 3.20	Age ±10years
4	1D2	7	.799	10.3	10.3	1979-1986
8	1D3	7	.595	7.63	8.3	1971-1981
12	1D4	7	.583	7.48	5.5	1958-1968
16	1D-C/1	25	.818	3.00	3.5	1948 (1954)
20	1D-C/2	46	.841	1.72	2.0	1929 (1936)
24	1D-C/3	35	.879	2.33	1.77	1926 (1932)
28	1D-C/4	34	.771	2.10	1.65	1924 (1930)
33	1C1	57	.972	1.62	1.65	1924 (1930)
37	1C2	73	.905	1.20	1.60	1923 (1929)
45	1C4	55	.748	1.29	1.55	1922 (1928)
53	1C6	54	.886	1.56	1.51	1921 (1927)
62	1C8	77	1.16	1.47	1.50	1921 (1927)
70	1C10	70	.944	1.30	1.49	1921 (1927)
78	1C12	45	1.032	2.15	1.49	1921 (1927)
81	1C13	35	1.162	2.43	1.45	1920 (1926)

Ages are calculated relative to the surface Ao=1988.
Ages in brackets are calculated relative to the base of Unit C (1C13), where Ao=1926 (from historical data in Chapter 2).
Samples 1D-C/1-4 are from the bioturbated zone between units D and C.

where Ao equals the excess ^{210}Pb activity at some horizon of known age (such as the surface) and Az is the excess ^{210}Pb activity recorded at an unknown horizon. The ^{210}Pb decay constant π=0.03114 y^{-1} (Chanton et al., 1983; Ivanovich and Harman, 1982).

The other model commonly used involves the assumption of constant rate of supply of ^{210}Pb to the sediment surface (CRS). The CRS model is normally applied to sediments suspected to vary in sedimentation rate (Appleby and Oldfield, 1978). The calculation for the CRS model is identical to that for the CIC model, except that Ao and Az are derived from the nuclide activity versus mass-depth (g/cm^3) curve rather than the nuclide activity versus depth curve. This calculation assumes that rapidly deposited sediments are less well compacted than slowly deposited sediments. The CRS model should only be applied to homogeneous sediments because muds naturally compact considerably more than sands. Hence, rapidly deposited mud contains greater densities than slowly deposited sands, which would yield erroneous results using this model. The mass densities of Unit D and C sediment are $2.36g/cm^3$ and $2.71g/cm^3$ respectively, which suggests (using the CRS model) that Unit C was deposited at a constantly slower rate than Unit D. The sedimentological and historical data indicates that Unit C was deposited more rapidly than Unit D, hence mass density corrections cannot be implemented in this study.

For the above reasons the CIC model was adopted and relative ages of each sample calculated using equation 3.1 taking Ao as activity at surface (1988), and ages in brackets taking Ao=1926 at the base of Unit C (sample AHE/1C13; Chapter 2).

The core contained a bioturbated zone between subsample 1D-C/1 and 1D-C/4 (17-30cm), which is not included in the sedimentation rate calculations. The presence of this bioturbation zone suggests some loss of sediment between Unit C and D deposition. However, the top

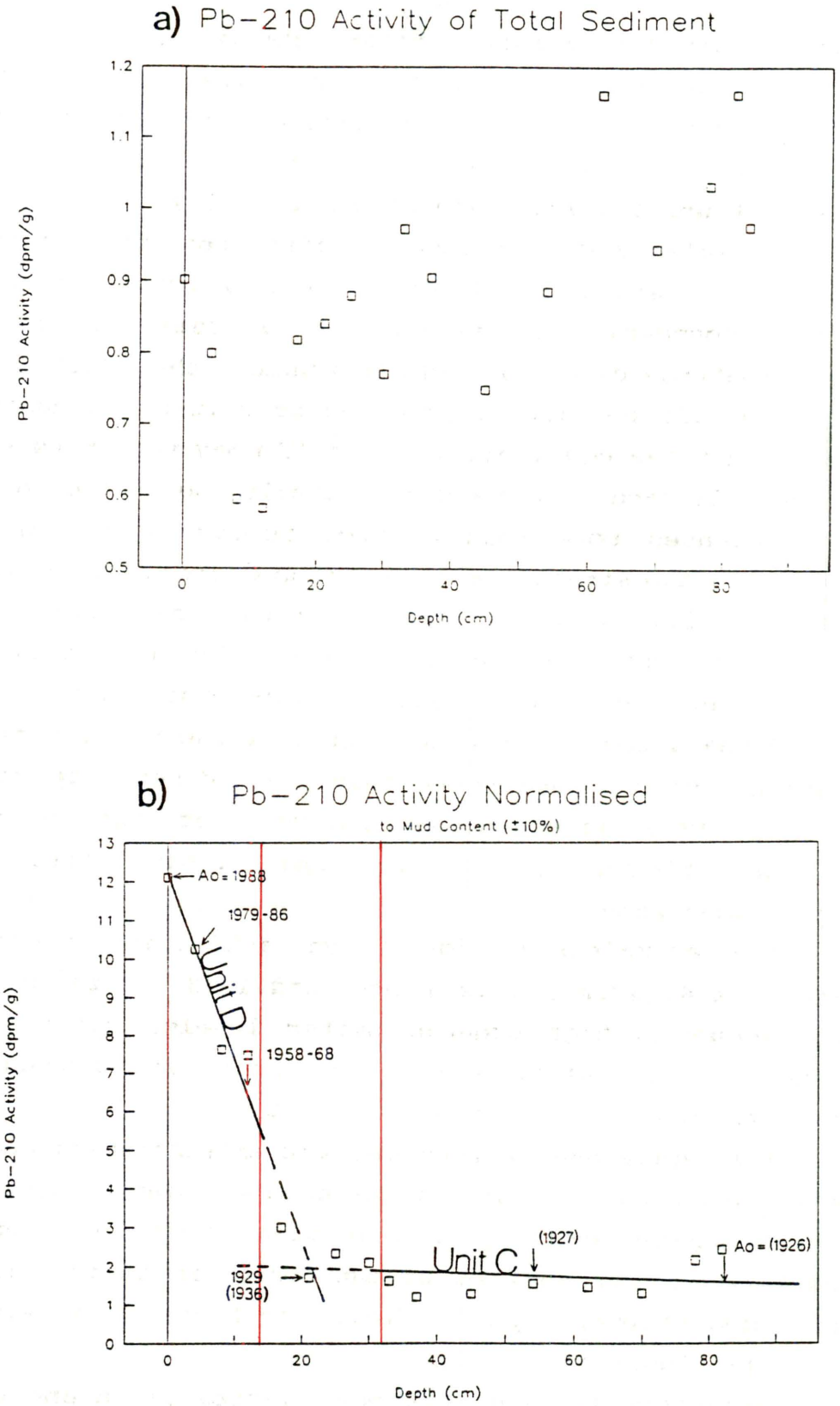

Fig. 3.20 Lead-210 depth profiles: a) in total sediment, and b) normalised to mud (<63µm) content. The red vertical lines mark the bioturbated zone between units C and D.

17cm of Unit D is not bioturbated (Fig.3.3a).

The CIC model assumes that the flux of sediment and ^{210}Pb remains constant at a particular locality with time. However, historical, grain size, and mineralogical data show that units D and C are compositionally dissimilar and have accumulated at significantly different rates. Assuming that Unit C was deposited more rapidly than Unit D, and that atmospheric fluxes of ^{210}Pb remained constant throughout the deposition of both units, then Unit C ^{210}Pb levels should be diluted relative to Unit D. In addition, the $^{222}Rn/^{226}Ra$ equilibrium with ^{210}Pb may vary between the essentially sand Unit D and essentially mud Unit C, because ^{222}Rn escapes more rapidly from porous sand than mud. Hence, the two straight line sections corresponding to each unit, of Fig, 3.20b, will be regarded separately. Unit D dates and sedimentation rates are calculated using the surface as the datum (Ao=1988), and Unit C dates are calculated using the base of Unit C as the datum (Ao=1926, from Chapter 2). Such an approach should not only produce more accurate ages for each layer, but also allow an estimate of the amount of time missing across the bioturbated zone.

The anomalously high ^{210}Po activities found for samples 1D4 (12cm), 1C12 (78cm) and 1C13 (82cm) are most likely due to high organic matter levels, which can be correlated to anthropogenic activity surrounding the estuary. Towards the base of Unit C, the mud content decreases while sand and organic matter (including coal and coke particles) levels increase (see black layer Fig. 3.2b). Organic matter has a tendency to adsorb nuclides from the surrounding environment during transportation and after deposition, which explains the high ^{210}Pb levels in these samples.

Generally speaking the near horizontal shape of the Unit C ^{210}Po activity curve in Fig. 3.20b reflects the extremely rapid deposition of this silt layer in the estuary. Ignoring the bioturbation zone, Unit C spans a

time range of 4 years which corresponds with a sedimentation rate of 12.5cm per year. Extrapolation of the Unit C curve to the middle of the burrowed zone, where the curve crosses the Unit D curve, reveals an age of 1936, using Ao=1926 from the base of Unit C. Further extrapolation to the top of the bioturbation zone reduces Unit C's sedimentation rate to 6.5cm/year and gives the mud layer a 10 year time span.

The Unit D sedimentation rate of 0.43cm/y is considerably slower than Unit C. Therefore, the individual subsamples (4cm) contain 9 years of deposition. Such large subsampling ranges may have resulted in important heavy metal contamination episodes being overlooked in this study. In future smaller divisions (1-2cm) should be studied.

The age calculated where the two curves cross is 1929 using Ao=1988 at the surface. A discrepancy of 7 years exists between dates produced from each curve, which is within the 10 year experimental error of this technique. This result supports the conclusions drawn from the historical analysis (Chapter 2) in that: 1) bioturbation is a natural component of sedimentation in this area of the Avon-Heathcote Estuary, 2) sedimentation is more rapid than reworking by benthic fauna, and 3) bioturbation is more likely responsible for redistribution of sediment in a given area, over a period of time, than erosion leading to sediment removal from the estuary.

The basal Unit C subsample is 1920, using Ao at the surface = 1988, which is only 6 years younger than suggested by historical records. Considering 1) method errors, 2) the dissimilar sediment textures of units D and C, and 3) the differences in sedimentation rate between the two units, the ^{210}Pb profiles show excellent agreement with the historical data in Chapter 2.

Conclusion of ^{210}Pb Analysis

The ^{210}Pb profile of core AHE/1a agrees with the historical evidence that Unit C was deposited after 1925 and not between 1850 and 1875 as concluded by Macpherson (1978, and 1979). The ^{210}Pb ages also support the conclusion that the shells ^{14}C dated, from the base of Unit C, were contaminated with dead carbon from coal and lime burning during the early industrial period of Christchurch (1860 to 1930).

The differences between Figures 3.20a and b show that grain size correction is essential when studying sediments containing large variability in sand, silt, and clay content.

The reasonable agreement between ages where the Unit D and C curves cross, in the bioturbated zone, suggests that little or no sediment has been eroded from the estuary in historical times. This result is in agreement with 1) evidence of continuous sediment deposition disclosed by the carbon-14 age of the Mactra ovata beds at Pleasant Point, and 2) the 1960 to 1977 bed level data of Macpherson (1978), which shows slow sediment accumulation on the western slopes and near the river entrances, with minor erosion near channel edges. The Unit D sedimentation rate of 0.43cm per year is similar to the value (0.9cm per year) estimated from the ^{14}C age of the shells exposed at Pleasant Point (Section 3.6.1).

3.6.3 Pollen Analysis of cores AHE/3a and SWC/1

3.6.3.1 Pollen Profile from Core AHE/3a

Pollen profiles from core AHE/3a and SWC/1 were examined by Dr Matt McGlone of the Botany Division (Department of Scientific and Industrial Research, DSIR). The aim of the pollen study was to identify known stratigraphic datums; 1) Polynesian burn off of the

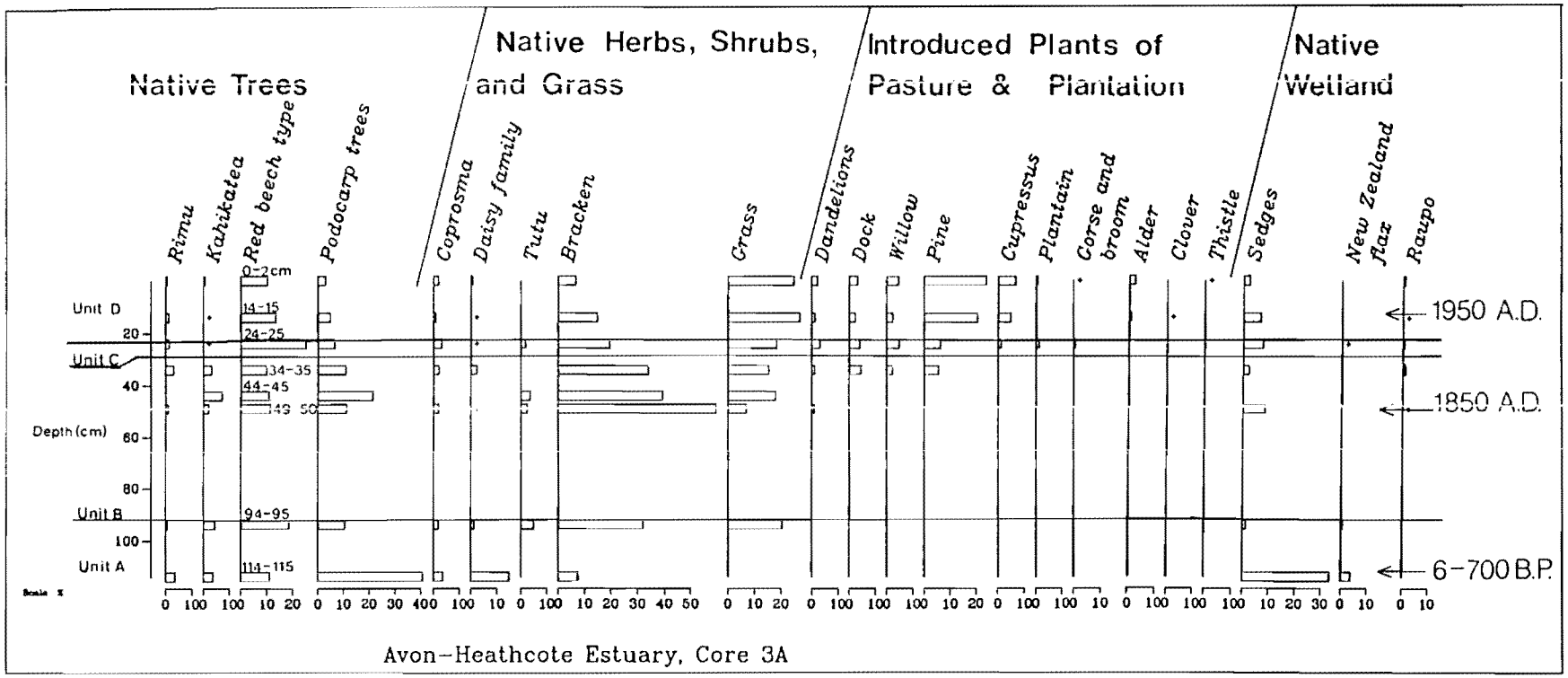

Fig. 3.21 Pollen diagram, core AHE/3a (Dr M. McGlone, Botany Division, DSIR, pers. comm.).

hinterland of Canterbury 700-800 B.P., 2) European arrival around 1850, and 3) major pine tree planting after World war 2 (WW2).

Fig. 3.21 contains the results of the pollen analysis of core AHE/3a. The results are presented as percentage of total pollen excluding the Wetland plants and ferns which are insignificant in number. The basal sample 3a/A4 (114-115cm) of Unit A dates from early Polynesian times, which is based on the high percentage of native podocarp trees, low grass and bracken content, and high concentration of native wetland plants such as sedge. From 115cm to 95cm, the dramatic bracken and grass increase, combined with the sudden decrease in sedges and podocarp tree pollens indicates recolonisation of Canterbury by secondary plants. Dr McGlone has examined pollen profiles from throughout Canterbury, and has found that the sudden increase in bracken and grass is a universal datum that correlates with carbon dates between 400-800 B.P. (depending on locality) (McGlone, 1989; McSaveney and Whitehouse, 1989).

It is an interesting correlation that the sudden increase in secondary plants is found at the top of Unit A, just prior to the formation of the Avon-Heathcote Estuary. Near the end of the period that Canterbury was deforested by Polynesian burning activity (450 B.P.), a major period of coastal dune building commenced (McFadgen, 1989). According to McFadgen, coastal progradation and dune building occur at times when erosion rates are high. The accelerated erosion at the beginning of the Ohuan dune building phase was most likely brought about by the deforestation of Canterbury. The pollen data imply that the Avon-Heathcote Estuary evolved during the Ohuan dune building phase, around 450 years B.P., and hence may have formed as a result of Polynesian activity.

Dr McGlone places the European datum (1850) around 49-50 cm sample 3a B5. This datum is 20cm below the base of Unit C (29cm) and 10cm below the diffuse zone where Units C and B merge (Fig. 3.22). The position of this datum is

Fig. 3.22 Section of core AHE/3a showing the 1850 datum (established by pollen changes) in relation to the contact between units C and B.

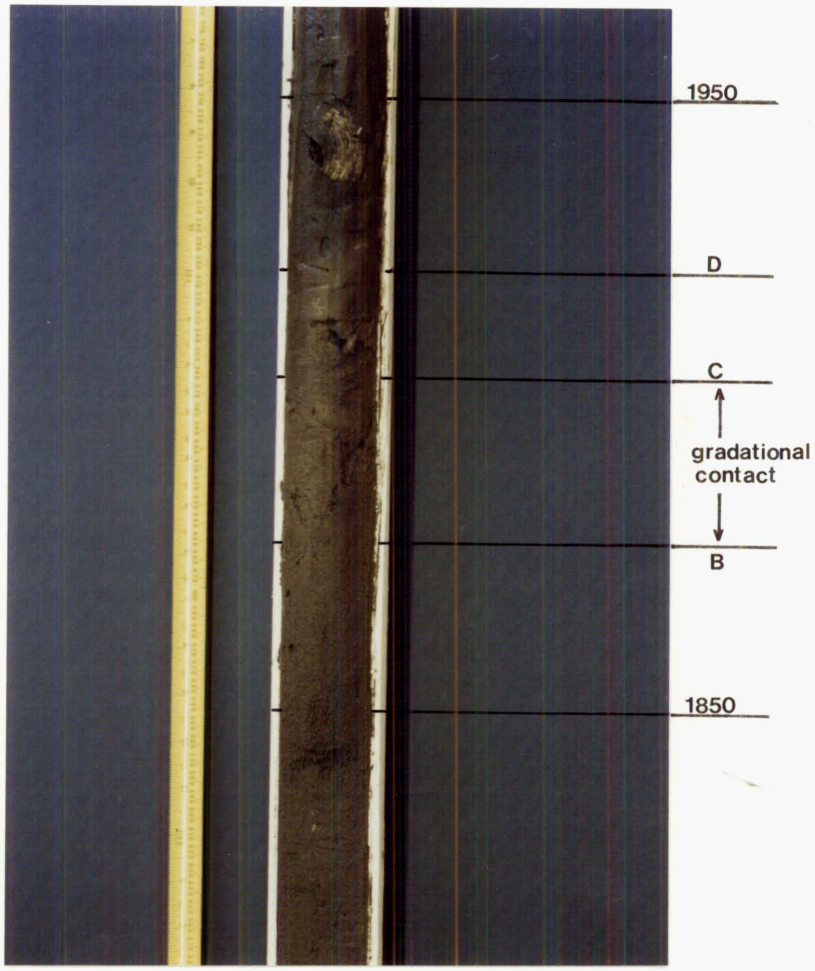
1950
D
C
gradational
contact
B
1850

based on 1) the appearance of dandelion, an introduced flower at 49 cm and 2) the decline in bracken and increase in grass in the overlying sample at 44-45cm, which would become apparent after land was cleared for farming and urban building. Figure 3.22 shows the position of the 1850 datum with respect to the contact between Unit C and B. It is evident from this figure that there has been no bioturbation or any disturbance what so ever in the vicinity of this contact. Taking the base of Unit B to be approximately 450 years B.P., then 45cm of sediment accumulated between 450 B.P. and 1850 A.D. which corresponds to a sedimentation rate of 0.15 cm per year (45cm/300 years). Between the 1850 position and the base of Unit C 20cm of sediment accumulated which corresponds to a sedimentation rate of 0.27cm per year (20cm/75 years). Hence, the early settlement of Christchurch (1850 to 1925) did not have a significant affect on sedimentation in this area of the estuary.

Dr Mcglone suggests that the estuary surrounds must have been well established by the 35cm level (well into the 1900's), because of the high level of pine pollen.

The upper units C-D contact is intensely bioturbated as is evident by the broken shell in Fig. 3.22 (part of a living organism when the core was collected). Bioturbation has most likely caused some levelling out of the pollen in Unit D. All the same, a pattern of increasing pine levels, and decreasing bracken, podocarps, and sedges concentrations emerges in Unit D, which suggests that mixing has only partially affected the pollen distributions.

The 1950 datum occurs at the 15cm level, which is based on substantial pine plantings in the Canterbury area in the 1930's and 40's coming into flower in the 1950's. The sedimentation rate after 1950 is 0.4cm per year (15cm/38 years) based on the position of the 1950 datum. This rate is similar to values obtained for Unit D sediment from other areas of the estuary (0.9cm per years Pleasant

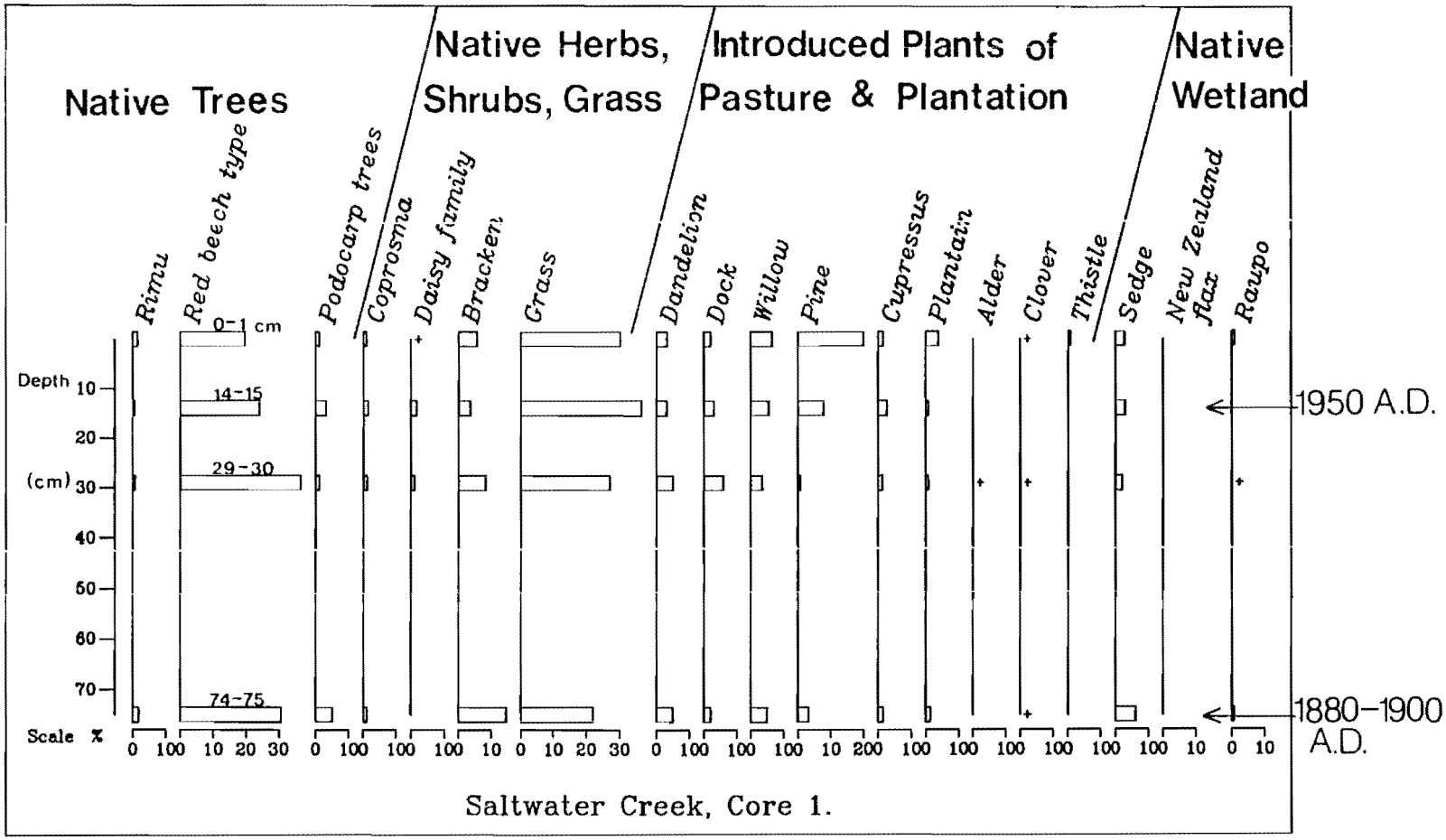

Fig. 3.23 Pollen diagram, core SWC/1 (Dr M. McGlone, Botany Division, DSIR, pers. comm.).

Point (^{14}C method, Section 3.6.1) and 0.43cm per year (^{210}Pb method, Section 3.6.2.3).

The position of the 1950 datum suggests that either some of the top of Unit C has been removed from the area or that Unit C deposition ceased earlier on the western slopes than in either of the two river depositories. The western slopes were intensely polluted during the 1940's and 1950's, and benthic dwellers were sparse (Chapter 2, section 2.7.3), which argues against erosion assisted by bioturbation as suggested by Macpherson (1978).

3.6.3.2 Pollen Profile from Core SWC/1

Figure 3.23 contains the pollen distributions from core SWC/1. The high concentrations of introduced plants at the base of the core indicate that the area was in pasture land. Dr McGlone suggests that the basal sample is around 1880 to 1900 AD in age. This age is also supported by the high levels of grass and low abundance of bracken and native trees and shrubs. The mud bed around 15cm probably dates from 1950, because of the high (10%) quantity of pine pollen. Significant pine planting occurred in Canterbury area around 1930's.

The Saltwater Creek Estuary's history of flooding and inlet change (discussed in section 3.3.2), combined with the pollen profile indicates the following with respect to Fig. 3.13. The basal gravel was deposited either during a serious flood or when the estuary was discharging out to sea 4-5Km north of its present position. At the time the main river channel flowed parallel to the Highway and cut across Saltwater Creek, near the location of these cores. As the mouth migrated north the river bed may have slowly cut further westward across the braided area shown in Fig. 3.12 and progressively coarser material was deposited up sequence. When the river broke through south, in 1914, the main channel would have been quickly diverted south into the present channel position. The poorly sorted coarse

sandy mud layers with pebbles and granules are probably flood deposits corresponding with major floods, in 1923, 1936, and 1951. The mud horizon layers are typical of quiet estuarine conditions which would have existed between flood periods. There was probably also considerable erosion between flood events, which is indicated by the red brown Fe oxide staining of the coarse sandy layers in core SWC/2.

3.7 DISCUSSION OF GEOLOGICAL DATA

The grain size and mineralogical studies show that sediments from all three sites are similar and derived principally from Late Pleistocene and Post-glacial loess deposits covering the Canterbury Plains. The loess itself originated from the Mesozoic Torlesse Terrane sediments that outcrop along the eastern slopes of the Southern Alps. The coarser sand component of the sediments may be derived directly from the source rocks by fluvial transport in the Ashley (Saltwater Creek Estuary sediments) and the Waimakariri (Avon-Heathcote Estuary and Travis Swamp sediments) rivers.

The results of the grain size and mineralogy studies indicate that the Travis Swamp estuary deposits are older lateral equivalents of the Pre-European Avon-Heathcote Estuary sediments. The modern swamp sediment probably belongs to the source of Unit C.

The coarser sediments, aerobic conditions, and the slightly different mineral composition exhibited by the Saltwater Creek Estuary are probably a direct result of the dominant influence of the swift Ashley River on this system. The frequent floods and constant migration of the Ashley River mouth will erode sediments on a regular basis, thus exposing them to a plentiful supply of oxygen.

In contrast, estuarine deposits in the Travis Swamp and Avon-Heathcote Estuary reflect the influence of the meandering Avon and Heathcote streams carrying finer sands

and silts. The coarse fluvial sediment carried by the Waimakariri River is deposited near the mouth of the river or along the coast. Only the medium and fine sand would be transported into the Avon-Heathcote Estuary with the tide. In modern times, the stable position of the Avon-Heathcote Estuary mouth, and the continuous supply of organic and nutrient rich effluents to the estuary, has produced anaerobic conditions. The reduced water circulation associated with swamp environments has also resulted in anaerobic conditions in the Travis Swamp.

The Saltwater Creek Estuary sediments are geologically similar to those of the Avon-Heathcote Estuary. However, the differing redox conditions, between the two estuary beds, suggest that heavy metals are likely to behave differently in each environment. In contrast, the chemical and geological similarity between the sediments of the Travis Swamp and Avon-Heathcote Estuary signifies that the ancient estuary deposits in the Travis Swamp are "ideal" background sediments for heavy metal studies of the Avon-Heathcote Estuary system.

3.8 GEOCHRONOLOGY OF THE AVON-HEATHCOTE ESTUARY

A number of dated horizons have been identified in this study by combining results of various dating techniques with information from the history review in Chapter 2.

Reasonable age ranges for all the sediment units have been established. The estuarine deposit in the Travis Swamp is 1650 years B.P. based on carbon dating of shells. Pollen data shows that sediment in Core SWC/1 dates from the turn of the century, with the mud bed at 15cm deposited around 1950 A.D.

From the results of Chapters 2 and 3, the geochronology of the Avon-Heathcote Estuary is as follows:

1) The contact between Units A and B is 400-500 B.P. (pollen data, Section 3.6.3).

2) 1850 AD age sediments are located between 10 and 20cm beneath the contact between Unit C and Unit B (pollen data, Section 3.6.3).

3) The period around 1900 to 1925 is represented by a black layer rich in coal and ash debris beneath the contact of Units B and C in sediments from most areas of the estuary (historical data, Chapter 2, section 2.8, Fig. 3.6).

4) The contact between Units B and C is 1925-1927 A.D (historical data Chapter 2, Section 2.5, and ^{210}Pb data, Section 3.6.2.3).

5) The contact between Units C and D is not known accurately, but dates between the late 1940's and 1960's (historical data, Section 2.5, ^{14}C age, ^{210}Pb data, and pollen data, Section 3.6).

The geological data presented in Chapter 3 disproves much of the post 1850 geochronology established by Macpherson (1978), and supports the historical synthesis presented in Chapter 2. The results show that the Avon-Heathcote Estuary formed around 450 years B.P., as a result of accelerated erosion caused by deforestation of the Canterbury Plains. Unit B was laid down between 450 years B.P and 1925 at sedimentation rates of 0.15cm per year (450 B.P. to 1850 A.D.) and 0.27cm per year (1850 to 1925). The construction of 6 major stormwater drains in 1878 lead to rapid silting of the Avon and Heathcote Rivers between 1878 and 1925. Between 1925 and the 1950's, mechanical sweeping of both rivers removed the mud to the Avon-Heathcote Estuary, where it was deposited as Unit C at a rate of 6-

12cm per year. Once the river beds were cleared and Christchurch City roads and pavements tar sealed Unit C accumulation ceased. Since the 1950's and 60's modern Unit D sandy sediment has accumulated at around 0.5cm per year.

CHAPTER 4

HEAVY METAL DISTRIBUTIONS IN SEDIMENTS OF THE AVON-HEATHCOTE ESTUARY AND NON-SALINE WATER COURSES DISCHARGING INTO THE ESTUARY

4.1 DISCUSSION OF RESULTS FROM PREVIOUS HEAVY METAL SEDIMENT STUDIES

Sediment heavy metal studies of the Avon-Heathcote Estuary to date have concentrated on surface and near surface distributions (Hulse, 1983; Purchase, 1983; Anderson, 1985; Burgess, 1985; Rodrigo, 1985; Purchase and Fergusson, 1986; Christchurch Drainage Board (CDB), 1988; and Hay, 1988). Table 4.1 presents average results of clay fraction analyses from the Avon and Heathcote Rivers, the City Outfall Drain, and the Avon-Heathcote Estuary. Metal concentrations in possible anthropogenic source materials, Christchurch soils, and the internationally accepted fine grained baseline sediment are also tabulated for comparison. This section discusses and interprets the results of the above studies taking into account possible contaminant sources, and the historical synthesis and geochronology established in Chapters 2 and 3.

4.1.1 Heavy Metals Distributions in the Rivers

Heavy metal sediment studies of both the Avon and Heathcote rivers show Pb, Cu, Ni, Zn, Cr, and organic matter elevated in all grain sizes (Purchase, 1983; Hulse, 1983; Anderson, 1985; Purchase and Fergusson, 1986; and CDB, 1988). Iron and Mn are not enriched relative to baseline (Table 4.1). The low Mn results of most researchers are principally caused by low metal recovery (Chapter 6,Section 6.6.2).

Table 4.1 Potential Sources of Heavy Metals to the Avon-Heathcote Estuary System and Mean Heavy Metal Concentrations in Surface Sediments (<4μm fraction) from areas in and around the Avon-Heathcote Estuary

POTENTIAL SOURCES	Pb μg/g	Cu μg/g	Ni μg/g	Zn μg/g	Fe %	Mn μg/g	Cr μg/g	ORG %	Reference
Christchurch Street Dust									
Garlands Road #	1294	72	-	429	2.39	381	76	15	(1)
Spreydon	887	48	-	850	2.36	399	38	12.6	(1)
Riccarton Road	10700	258	-	365	5.82	399	58	7.2	(1)
Christchurch Soil #	379	17.5	-	135	2	57	36.9	10.1	(2)
CDB Sewage Sludge	359	595	142	2080	-	-	4780	-	(8)
Sewage Sludge (Global Av)	140-480	240-1030	25-110	900-2800	-	220-540	8-550	-	(9)
Coal Fly Ash & Bottom Ash (Global Average)	12-65	25-90	15-75	30-130	-	134-445	40-120	-	(9)
AREA									
Avon River	161	108	520	501	4	235	103	-	(5)
Heathcote River	94	80	39.5	431	4	55	352	7.24	(4)
Heathcote Rr Point Source	55000	200	-	700	-	-	10708	-	(3)&(4)
City Outfall Drain	3296	162	135	6215	6.54	2184	165	16.2	(7)
Estuary near Drain	244	62.7	42.9	528	7.57	1120	202	8.93	(7)
Avon-Heathcote Estuary	42.2	52.3	73.8	180	4	128	193	12.8	(6)
International Baseline (mean Shale, <2μm)	20-30	21-45	32-70	95-120	4-5	600-800	60-90	1.8-3.5	(*)

#; Christchurch Street Dust & Soils are composed of silt (4-63μm) and clay (<4μm) grains.
-, no data; References: (1) Fergusson et al. 1984; (2) Fergusson et al. 1986; (3) Purchase and Fergusson, 1986b; (4) Hulse, 1983; (5) Anderson, 1985; (6) Burgess, 1985; (7) Hay, 1988; (8) Smith, 1985; (9) Nriagu & Pacyna, 1988.
* (Turekian and Wedepohl, 1961; Salomons and Forstner, 1984; Forstner and Wittmann, 1981)
CDB, Christchurch Drainage Board.

Heathcote River

All studies showed significant surface sediment enrichment in Pb, Cu, Zn, Cr, and organic matter, particularly in the Woolston area (Fig. 2.2). Heavy metal enrichment in surface sediments up river of Woolston probably reflect the current stormwater discharge from 3 large drains. Nickel, Mn, and Fe showed no enrichment in Heathcote River bottom sediments.

Hulse (1983) and Purchase and Fergusson (1986b) found most metal concentrations decreased rapidly with depth; baseline values were reached within 20-30cm of the surfaces. With a pollution history going back to the 1860's (Chapter 2, Section 2.8), one might expect to find very high metal concentrations for considerable depth in the Woolston area of the Heathcote River. However river sweeping between 1925 and 1950, has removed most of the contaminated sediment, and only pollution since the 1950's is likely to be recorded in the sediment profile.

In the Woolston area, extremely high levels of Pb (55,000 μg/g), Cu (200 μg/g), Zn (700 μg/g), and Cr (10708 μg/g) were found in zones adjacent to former industrial effluent discharge points, such as near a Pb-acid battery factory (Pb), tanneries (Cr), and rubber manufacturers (Zn) (Purchase, 1983). These results suggest that some factories still occasionally discharge untreated effluent into the Heathcote River. Most serious contamination is localised in sediments near the outfalls. For example, the lead levels of 55,000 μg/g found in front of the battery factory (upstream of the Garlands Road Bridge, Fig. 2.2) dropped rapidly to 1000 μg/g within 100m of the discharge point (Purchase and Fergusson, 1986b). During the course of Purchase and Fergusson's study the Pb levels dropped 60% in the sediment next to the battery factory because the company improved the quality of effluent discharged.

Most cores of Purchase (1983) were rich in ash, coke, and coal particles, and organic matter levels were greater

than 20% in many places. These deposits probably relate to spills from the Christchurch Gas works during the 1950's which were rich in coke, ash, and tar particles (Chapter 2, Section 2.8). The drain from the gasworks is located at Bells Creek upstream of the battery factory. However, some of the ash may have originated as fly ash from the battery factory.

Purchase found a zone high in heavy metals at a depth of 16cm below the surface, which may relate to an early pollution event. Near the battery factory, the surface sediment pH is in the range 5-6, and decreases with depth. Such low pH values favour metal remobilisation into overlying water (Chapter 1, Figs 1.2, and 1.3). Purchase's speciation studies showed that with depth the lead species graded from $PbCO_3$, through $PbSO_4$, Pb, to PbS. These are the types of species predicted by normal pH-Eh regimes, however some $PbSO_4$ correlated with layers rich in ash.

Avon River

Anderson (1985) (Table 4.1) showed that the Avon River surface sediments are generally more enriched in most heavy metals (Pb, Cu, Ni, and Zn) than those of the Heathcote River (excluding the Woolston area). Christchurch Drainage Board (1988) made similar observations, and attributed the results to the significantly higher proportion of stormwater discharged into the Avon River, compared with the Heathcote River. The heavy metal levels dropped rapidly with depth, as in the Heathcote River, indicating also that only recent contamination is recorded in the sediments.

The extremely high average Ni concentration (520 $\mu g/g$) observed by Anderson is problematical. Neither Purchase nor CDB observed any Ni enrichment in either river or the estuary. There are no metallurgy industries discharging into the stormwater drains that empty into the Avon River. In addition, the untreated sewage sludge of the Christchurch Drainage Board Treatment Plant contains

concentrations averaging 142 μg/g (Table 4.1). Hence, leachates from the sludge are not likely to be the source of Ni. The highly polluted stormwater drain (City Outfall Drain) and Woolston area of the Heathcote River contain Ni concentrations 3-4 times lower than reported by Anderson.

The above findings and the historical records of the Avon River (revealing little or no industrial pollution) cast doubt on the Ni results of Anderson (1985).

4.1.2 Heavy Metal Distributions in the City Outfall Drain

Sediment studies of the City Outfall Drain and estuary near the drain show that the drain is seriously contaminated with Pb and Zn, and enriched in Cu, Ni, Fe, Mn, and organic matter (Table 4.1; CDB, 1988; Hay, 1988). The most likely contaminant source is storm water containing 1) Pb from petrol emissions, 2) Cr, Cu, Mn, Fe, and organic matter from coal combustion (domestic and industrial), 3) Cu from water pipes and plumbing fixtures, and 4) Zn from galvanised roof fittings, tyre wear, and paint pigments (Drever, 1982; Hem, 1989; Smith, 1985).

Hay (1988) analysed heavy metals in 0.2g of the drain's surface clay fraction by total digestion in concentrated HF and HNO_3, and obtained average Pb levels of 3296 μg/g. The Christchurch Drainage Board (CDB) analysed total sediment in the drain using dilute acid extraction (0.25M $HClO_4$, and 0.6M HNO_3 on 5 to 10g samples), and obtained Pb concentrations of 1098 μg/g. Despite the significant differences in extraction techniques (and grain size), both studies reveal marked Pb contamination in stormwater drain sediments.

The very high Pb levels (887-10700μg/g) in Christchurch street dust (Table 4.1) indicate that dust is most likely carried into the drain and estuary with stormwater. The street dust is contaminated with Pb from petrol combustion (Fergusson et al. 1984). The high Pb concentrations in some Christchurch soils (379μg/g)

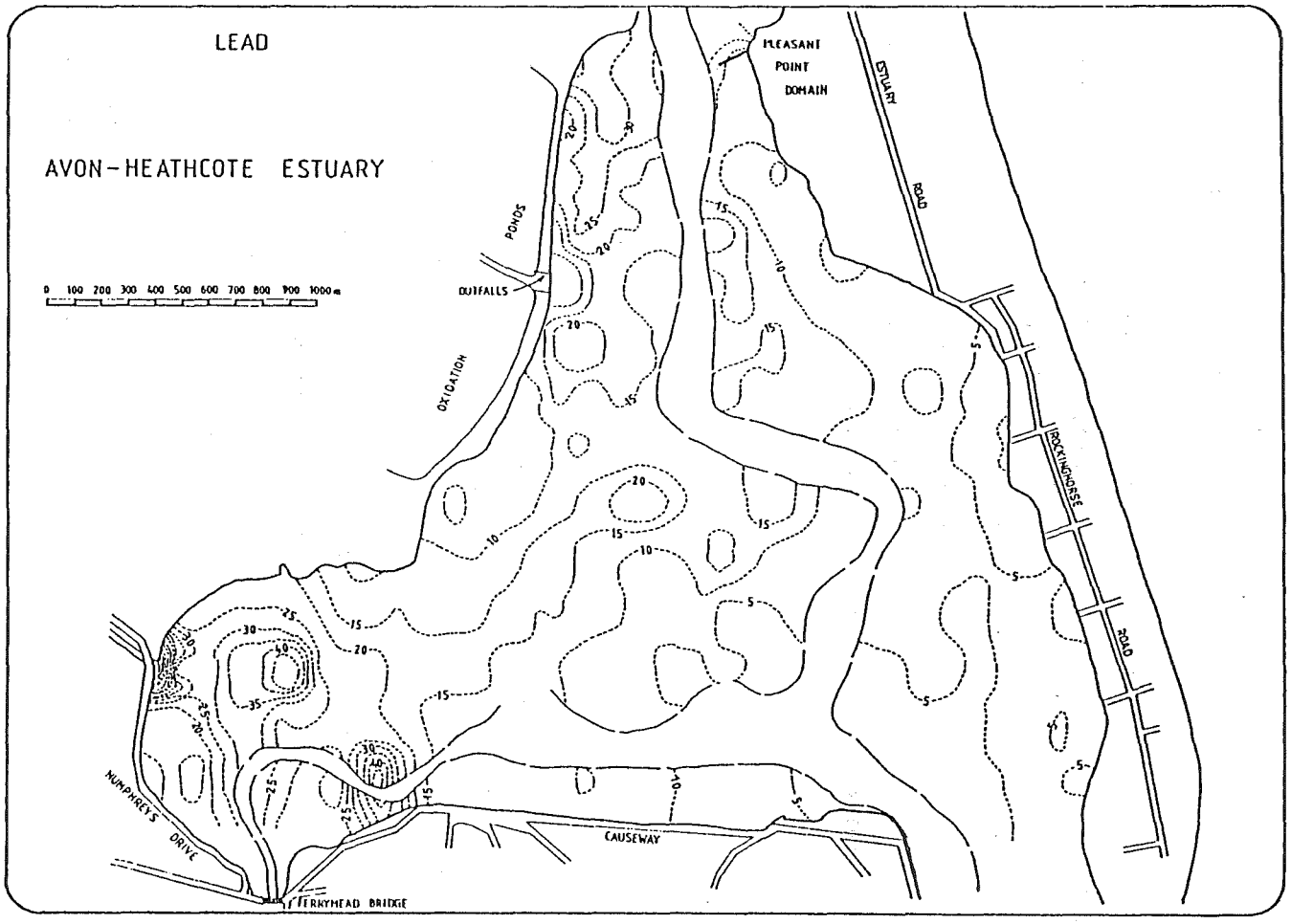

Fig. 4.1 Contours of Pb concentration in <u>total</u> sediment of the Avon-Heathcote Estuary (Christchurch Drainage Board, 1988).

relative to baseline (20-30μg/g) also reflect the generally high atmospheric emissions of Pb in the Christchurch area. (New Zealanders have been slow to adopt the unleaded petrol option. In May 1990, only 15% of all drivers were using unleaded petrol (Mr. M. Petrie, Treasury Department, Wellington, New Zealand).)

The moderately high Zn levels in street dust suggests that stormwater carries some Zn derived from tyre wear. However, Zn concentrations (135 to 850μg/g) in street dust and soil are not high enough to account for all the Zn (6215μg/g) in sediments of the City Outfall Drain. The majority of Zn is most likely washed from galvanised roofing and house paints with rain water, and enters the City Outfall Drain in the dissolved phase, from which it is then rapidly adsorbed onto the sediment.

A proportion of all anthropogenically derived metals may be derived from industrial emissions (fallout and effluents) because the drain's catchment is near the main commercial and industrial area of Christchurch (Fig. 2.2).

The sediments in the drain are black and anaerobic. On field trips to the drain with R. Hay, the author noted that when sediment was stepped on gas bubbles escaped emitting the odour of H_2S. Hence, the high levels of Mn and Fe may result from their pre-concentration and precipitation as metal sulphides. Coal combustion (domestic and industrial) may also be a source of Mn to the drain, but ash metal levels are generally not high enough to be an important source (Table 4.1).

Both CDB (1988) and Hay (1988) found heavy metal enrichment (especially Pb) in estuary sediments adjacent to the drain, with levels decreasing rapidly away from the drain (Fig. 4.1), showing that most contamination is localised.

Hay (1988) analysed a core, RH2, from the estuary adjacent to the stormwater drain (Chapter 3, Section 3.2.1.2). All grain sizes (sand, >63μm, silt 4-63μm, and clay 4μm), showed marked heavy metal and organic matter

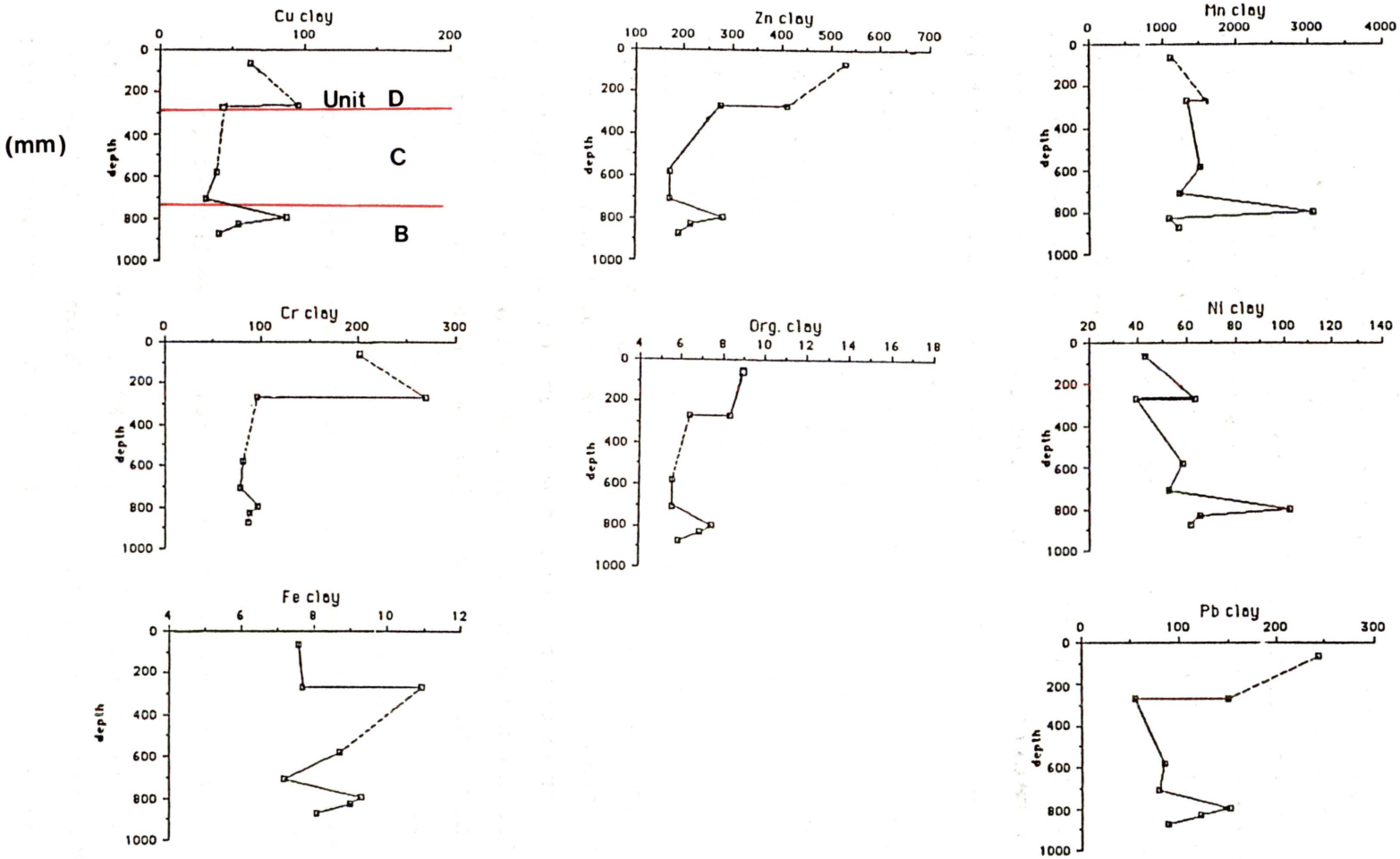

Fig. 4.2 Heavy Metal and Organic Matter Concentrations with Depth in the Clay Fraction of Core RH2 (Hay, 1988).

increase in two horizons, one at a depth of 30cm, and another at 80cm. This pattern was particularly noticeable in the clay grain size (Fig. 4.2). The 30cm peak occurs within Unit D, while the 80cm peak occurs in the blackened zone across the diffuse contact between units C and B (Fig. 3.6). In the absence of dating information Hay did not offer an interpretation for the metal behaviour. The present study has dated the Unit C-B contact at 1925 in the Heathcote Basin (Chapter 3.0, Section 3.8), with a diffuse contact in core RH2, spanning the age range 1874 to 1925 (due to silt discharge from the drain shortly after it was dug in 1874, before the major silting period, 1925-1950's). The black stratified sediment, high in heavy metals, near the top of this diffuse zone correlates with the early period of industrialisation ("Iron working days") around 1900 to 1925 (Chapter 2, Section 2.8)), when coal burning and heavy metal discharge was prolific.

The 30cm metal and organic matter peak in Unit D may represent a pre-1972 high related to industrial and domestic effluent discharge directly into the estuary and Heathcote River. Such a high would have occurred after 1950 when the silt flux to the estuary slowed (when river sweeping ceased), before all industrial and domestic wastes were removed from the river and estuary in 1972 (Chapter 2, Section 2.8). Both the Unit B and D peaks also occur in the cores of this study, which will be discussed later in Section 4.4.1.

4.1.3 Heavy Metal Distributions in the Avon-Heathcote Estuary

Heavy metal studies of <u>total</u> surface sediment in the Avon-Heathcote Estuary showed Pb to be the most significantly enriched metal followed in order by Zn, Cr, and Cu (CDB, 1988; Rodrigo, 1985; Purchase and Fergusson, 1986; and Hay, 1988). Most metal and organic matter enrichment is confined to the Heathcote depository,

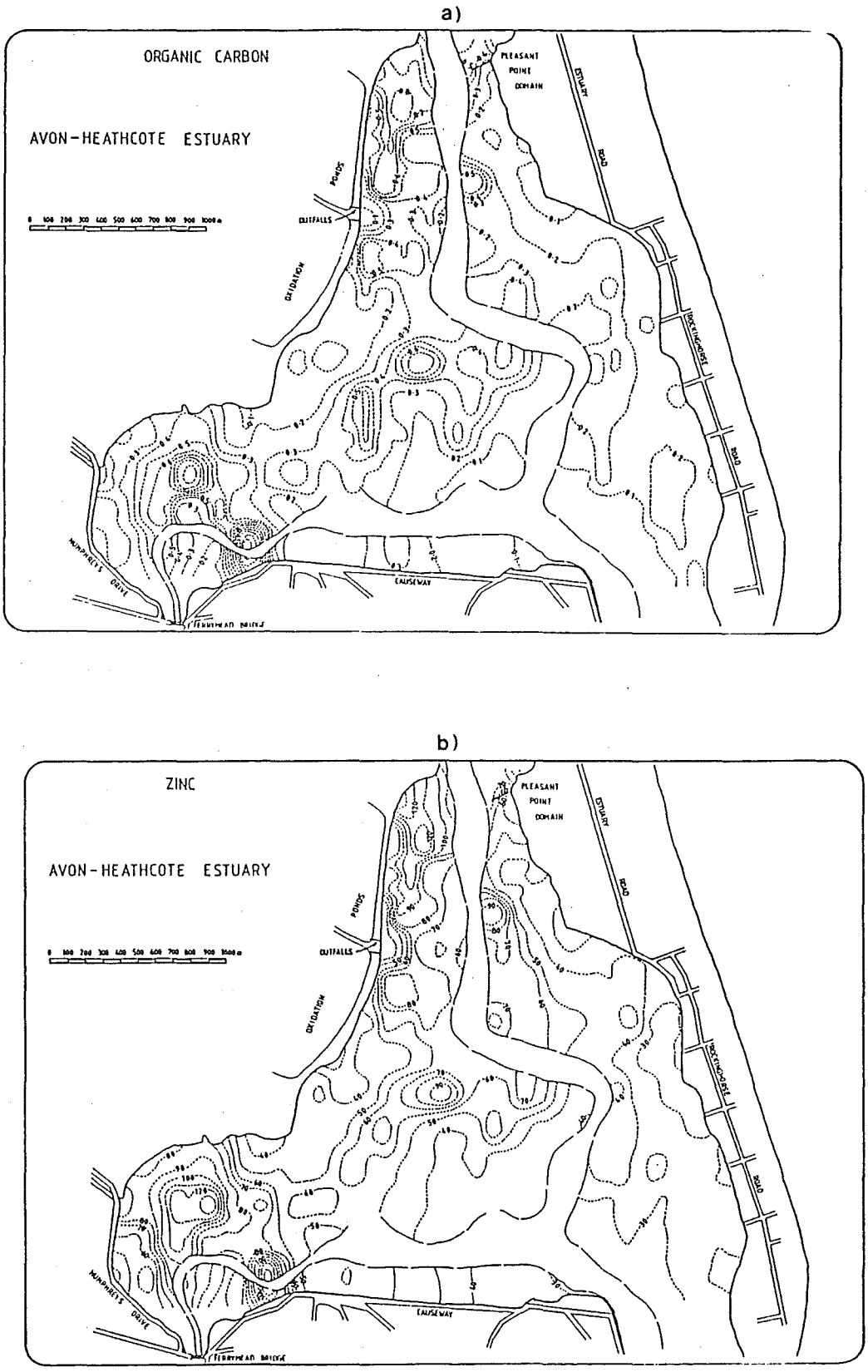

Fig. 4.3 Contours of Zn (b) and Organic Matter (a) concentrations in <u>total</u> surface sediment of the Avon-Heathcote Estuary (Christchurch Drainage Board (CDB), 1988).

particularly near the City Outfall Drain, and to the area along the western slopes, in front of the sewage ponds towards the Avon depository (Figs 4.1 and 4.3). These are not only the muddiest areas in the estuary, but are also affected by discharges from the ponds and the City Outfall Drain.

The clay fraction results of Burgess (1985) show that most metal enrichment in the estuary sediments is due to an increase in the clay component, except in the Heathcote Basin and immediately adjacent to the outfalls (Table 4.1). However, Burgess obtained low heavy metal recoveries compared to other workers (Chapter 6, Fig. 6.7) and hence may not have exposed important metal contamination. Nevertheless, both Burgess and CDB found Cr enrichment on the western slopes. The extremely high levels of Cr (4780μg/g) in the sewage sludge (Table 4.1) suggests that discharge from the ponds is the source of Cr in these sediments.

Burgess also found a horizon rich in heavy metals at a depth of 12-16cm below the surface in a core collected along the western slopes. This horizon may correlate with the enriched horizons found by Purchase (1983) in sediments of the Heathcote River, and by Hay (1988) in front of the City Outfall drain (core RH2). This peak probably represents levels reached around 1972 before all industrial and domestic wastes were removed from the Avon-Heathcote Estuary system.

The Christchurch Drainage Board (1988) studied heavy metal surface sediment (total sediment) distributions in the Saltwater Creek and compared the results to the Avon-

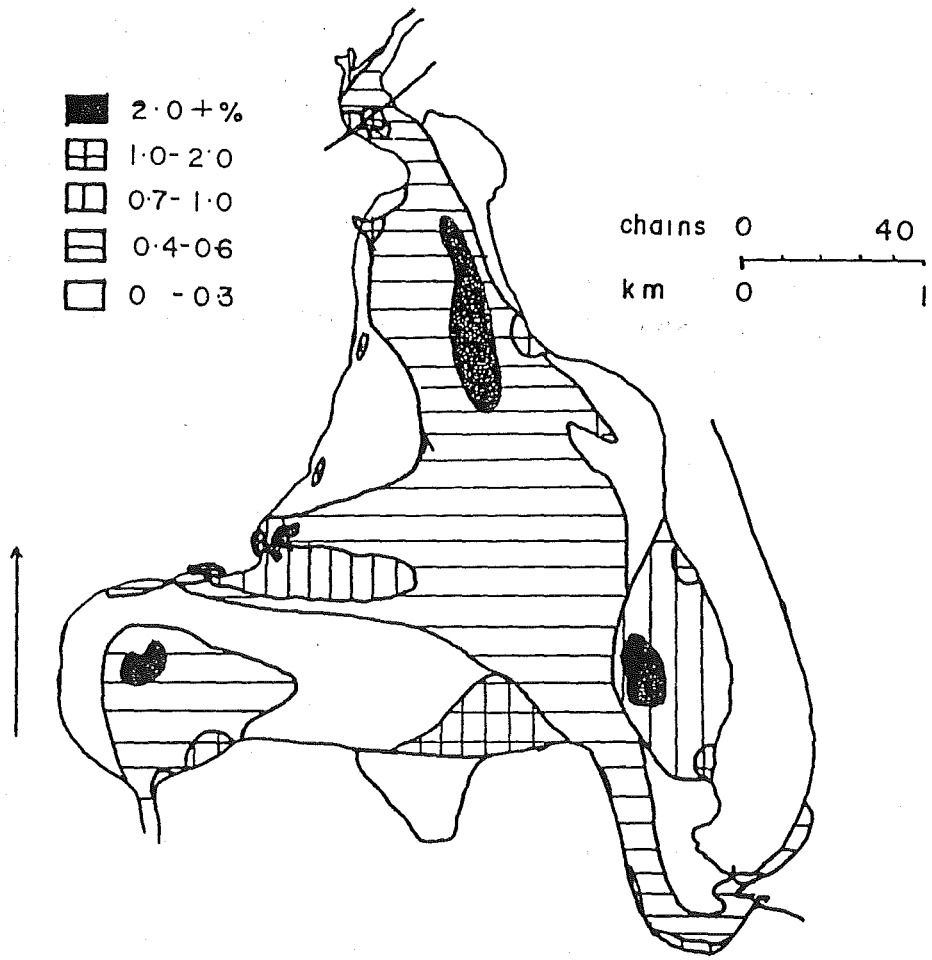

Fig. 4.4 Iron oxide in surface sediment of the Avon-Heathcote Estuary (Millward, 1975).

Heathcote Estuary. Copper, Cr, Ni, Zn, and Pb showed consistent spatial distribution in the Saltwater Creek Estuary. When comparing similar sediment, Pb, Zn, and Cr were elevated 3, 2.3, and 2 fold respectively in the Avon-Heathcote Estuary relative to the Saltwater Creek Estuary, whereas Ni exhibited similar levels in both estuaries.

Millward (1975) measured Fe oxide distributions in surface sediments of the Avon-Heathcote Estuary and found the highest concentrations near the mouths of both rivers and the estuary entrance (Fig 4.4). The Fe oxide maxima near the head of the estuary also coincide with 1) the areas highest in mud and organic matter observed by CDB (1988), Knox and Kilner (1973), and Macpherson (1978), and 2) the areas of muddiest (brownest) water photographed during mid tide (estuarine mixing) in April 1991 (Fig. 1.0b). Although the general anaerobic conditions in the Avon-Heathcote Estuary sediments do not favour long term stability of Fe oxide (Chapter 2), the lighter colour of the thin active surface sediment indicates that oxidised species may be present at the very surface. The Fe oxide distributions reported by Millward probably locate the positions of the turbidity maxima, where Fe oxide is precipitated during estuarine mixing in each tidal cycle. After precipitation, Fe hydroxy compounds would be deposited at the sediment surface, where they rapidly transform into sulphide or carbonate species. The thin oxidized film would be maintained by the continuous supply of oxides and hydroxides to the sediment surface during each tidal cycle. The high organic matter and mud content near the areas high in Fe oxide support such an interpretation.

Table 4.2 Methods of Correcting for Grain Size Effects

Method		Reference
(A)	Extrapolation of Grain size distribution	
(1)	normalised to <63 μm fraction	Araujo et al, 1988; Forstner and Salomons, 1980; Taylor, 1986.
(2)	normalised to <20 μm fraction	Horowitz, 1985; Scheider and Weiler, 1984.
(B)	Metal Concentration versus Surface Area	Donazzalo et al, 1984; Forstner and Wittmann, 1981.
(C)	Grain Size Separation	
(1)	<63 μm fraction	Araujo et al, 1988; Horowitz, 1985; Forstner and Salomons, 1980; Forstner and Wittmann, 1981; Salomons and Forstner, 1984.
(2)	<20 μm fraction	Ackermann et al, 1983; Glasby et al, 1988; Nicolaidou and Nott, 1984; Stoffers et al, 1986.
(3)	<2 μm fraction	Forstner and Salomons 1980; Forstner and Wittmann, 1981; Horowitz, 1985.
(D)	Treatment with Dilute Acid	Forstner and Wittmann, 1981; Salomons and Forstner, 1984.
(E)	Inert Mineral Correction	
(1)	Quartz	Forstner and Salomons, 1980; Forstner and Wittmann, 1981; Salomons and Forstner, 1984.
(2)	Carbonate	Horowitz, 1985.
(F)	Conservative Element Correction (Al, Fe, Cs, Sc, Rb, Sm, Th, Ti)	Araujo et al, 1988; Ackermann et al, 1983; Finney and Huh, 1989; Forstner and Salomons, 1980; Forstner and Wittmann, 1980; Hornung et al, 1989; Horowitz, 1985; Nicolaidou and Nott, 1989; Salomons and Forstner, 1984.
(G)	Relative Atomic Variation (RAV)	Ackermann, 1980; Forstner and Wittmann, 1984.

HEAVY METALS IN SUB-SURFACE SEDIMENTS OF THE AVON-HEATHCOTE ESTUARY

4.2 METHOD OF HEAVY METAL EXTRACTION

Samples of sand (>63μm), silt (4-63μm), and clay (<4μm) from all cores were analysed for Pb, Cu, Ni, Zn, Fe, Mn, Cr, and organic matter using the following procedure. Initially all samples were oven dried at 105°C, overnight to remove any water. The dried samples were ignited for 8 hours at 550°C allowing organic matter to burn off. The weight loss was noted after ignition, and presumed to represent the quantity of organic matter burned off. The ignited samples were digested in 6-12 ml of 40% HF and 3-6ml of 16M HNO_3 (depending on sample size), filtered, made up to 20-25mls with double distilled water, and analysed by Flame Atomic Absorption Spectroscopy. A reagent blank, standard reference (SD-N-1, IAEA 1988), and secondary reference were analysed with each batch. Accuracy varied between 80-90% depending on the metal, whereas precision was 85-90% for all metals. Throughout the course of this study quality control was an important consideration at all stages of sample handling, including grain size separation and heavy metal analyses. Hence, the quality control related to core analyses is discussed separately in Chapter 6.

4.3 GRAIN SIZE DISTRIBUTION OF HEAVY METALS

Heavy metal studies on bulk sediment samples may give false information as to the extent of contamination in an estuary, because contaminated fine grained sediment may be diluted to different degrees throughout an estuary by low metal bearing coarse grained sediment (Nicolaidou, 1989). Hence, trace metal analysis of total sediment samples is meaningless without some form of grain size correction.

Table 4.2 lists the common methods of correcting for

Table 4.3. Heavy Metal Concentrations in Sand, Silt, and Clay Size Fractions

Sample	Pb µg/g	Cu µg/g	Ni µg/g	Zn µg/g	Mn µg/g	Fe %	Cr µg/g	ORGANIC %
AHE/5D 1								
Sand	6.68	4.18	7.97	27	33.9	1.08	23.2	.86
Silt	10.6	16.8	12.4	73.1	79.4	2.1	43.4	2.32
Clay	92	74.4	61	303	297	4.02	118	6.98
TS/1 T3								
Sand	2.57	5.72	6.15	22.3	32.4	1.36	17.1	1.03
Silt	UD	6.34	13.9	20.5	25.6	1.44	28.5	1.31
Clay	36.6	16.4	40.9	109	231	5.48	85.3	4.39
SWC/1 10								
Sand	1.58	4.85	8.21	17.9	37.8	1.32	22.8	1.34
Silt	3.2	7.2	10.7	25.4	17.6	2.22	31.8	1.8
Clay	9.68	35.1	37.5	110	256	4.71	91.9	6.53

UD; Undectable

grain size used in the literature. The more commonly used techniques are discussed further in Appendix 3.0, Section A3.1. All these methods reduce the fraction of sediment that contains insignificant proportions of heavy metals (such as quartz, feldspar, and carbonate) relative to the proportion of fine grained minerals that are enriched in metals. More information can be obtained by combining several of the correction techniques (such as treatment with dilute acid to determine the mobile fraction and standardization with conservative elements). Most correction techniques ignore the contribution of heavy metals from the coarse grained fraction. This is normally not important because almost all anthropogenically derived heavy metals are held in fine grained material (Forstner, 1989).

The grain size correction method employed will depend largely on (1) the equipment available, (2) the grain size distribution of the sediments and (3) the time and money available for the study. In this study the sand (>63μm), silt (4-63μm), and clay (<4m) size fractions were separated (Chapter 3, Section 3.4.1) to make results comparable to previous studies. Contamination affects during grain size separation are discussed in detail in Chapter 6 (Section 6.2.1).

4.3.1 Grain Size Distributions in this Study

Both heavy metal and organic matter concentrations increased in all samples as grain size decreased, with clay fractions containing up to 5 times higher metal concentrations than in the silt fractions (Table 4.3). Metal levels in most silts are only slightly above those observed for sands. Burgess (1985), Hulse (1983), Anderson (1985), and Hay (1988) found similar distributions in sediments from the rivers, drain, and estuary.

As discussed in Chapter 1, the reason for heavy metal levels increasing with decreasing grain size from sand to

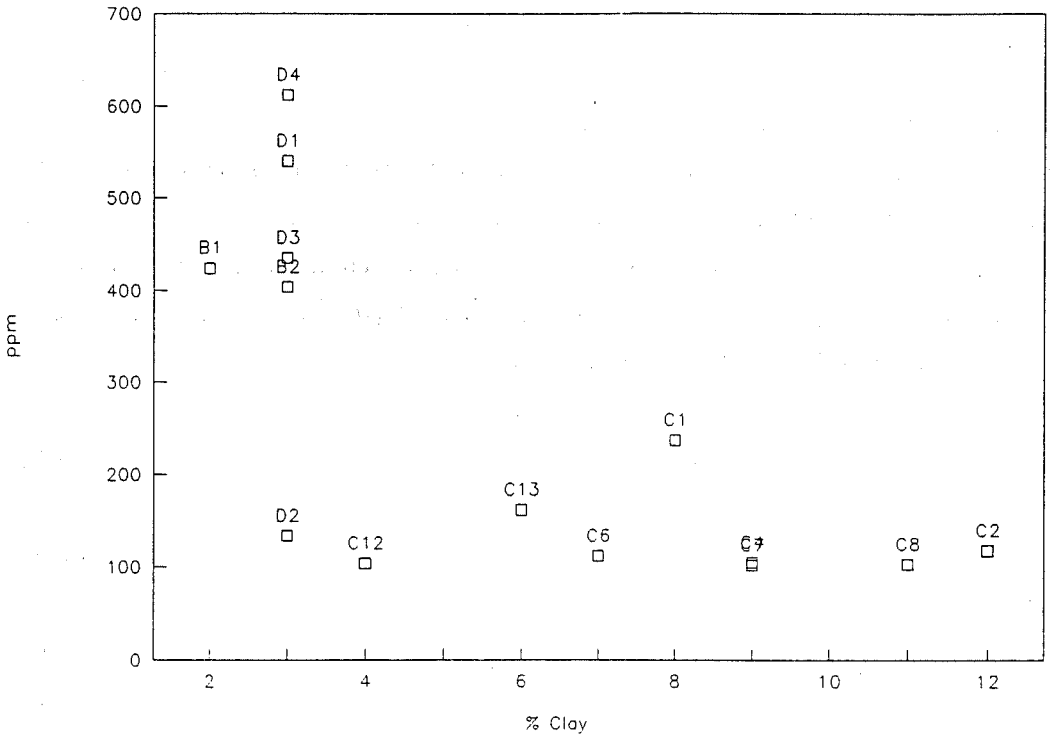

Fig. 4.5 Zinc concentration versus % clay in the clay fraction of core AHE/1a.

silt is due to an increase in surface area, and corresponding metal adsorption capacity (Horowitz, 1985). With decrease in grain size from silt to clay the mineralogy also changes. The flat platy surfaces of clays minerals exhibit high surface charges and cation exchange capacities (Chapter 1). Hence, clay minerals are excellent scavengers of organic matter and authigenic Fe and Mn compounds (such as hydroxides and sulphides), which have a greater capacity for heavy metal adsorption than the clay minerals themselves (Appendix 1).

4.3.2 Heavy Metal Concentrations Versus Proportion of Clay

In post-European Avon-Heathcote Estuary clay fractions, there appears to be a negative correlation between the concentration of clay (in the total sediment) and heavy metal concentrations. This relationship is illustrated using Zn in Fig 4.5. Unit C has the highest proportion of clay and the lowest Zn concentration. Unit D and B are much higher in Zn and lower in clay. This relationship is unlikely to be due to contamination because great care was taken in separation procedures (Chapter 6, Section 6.2). The clay mineralogy is uniform within each unit (Chapter 3, Section 3.5.1), so mineral composition is not the cause. A decrease in contaminant fluxes is unlikely to have caused the low levels in Unit C because the quantities of domestic and industrial waste entering the estuary increased steadily from 1925 to 1950 (Chapter 2). The only important variable left that could explain the anomaly is sedimentation rate. Lead-210 and pollen profiles (Chapter 3) reveal that sedimentation rates were 0.27cm/year near the top of Unit B, 6-12cm/year for Unit C, and around 0.5cm/year for Unit D. During Unit C deposition, the greater concentrations of suspended sediment in the rivers and estuary provided a considerably larger surface area for heavy metal entrainment, which diluted metal levels relative to those of units B and D. In fact Unit C

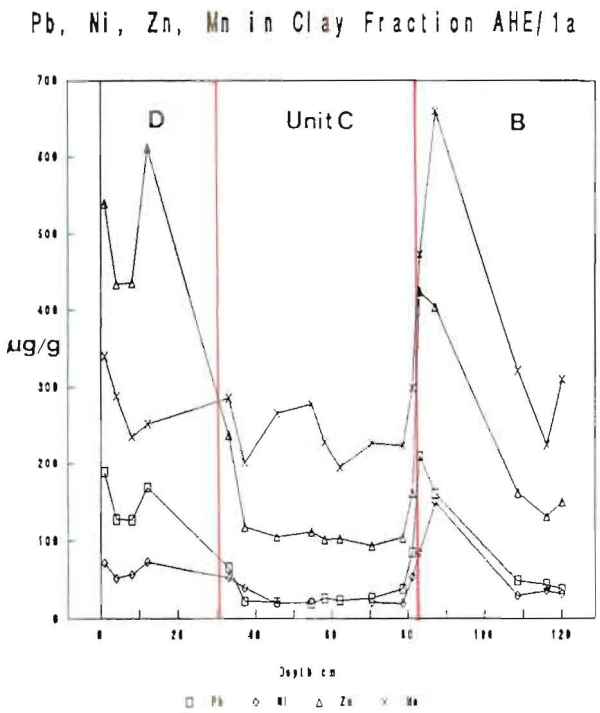

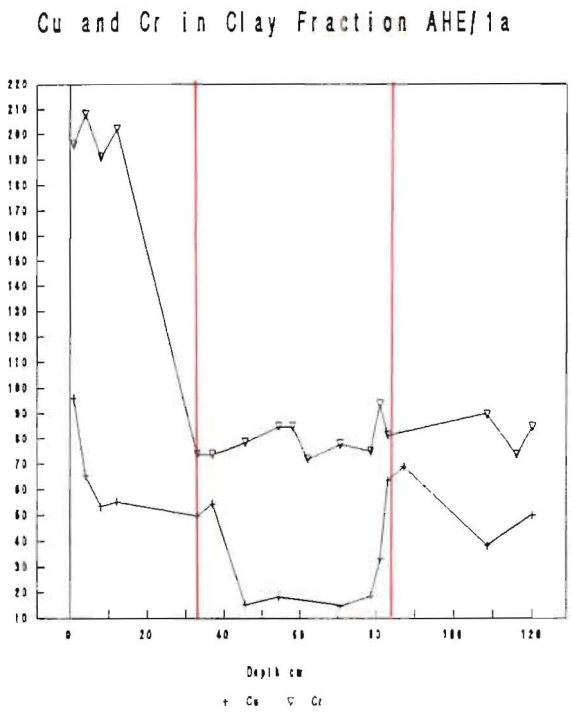

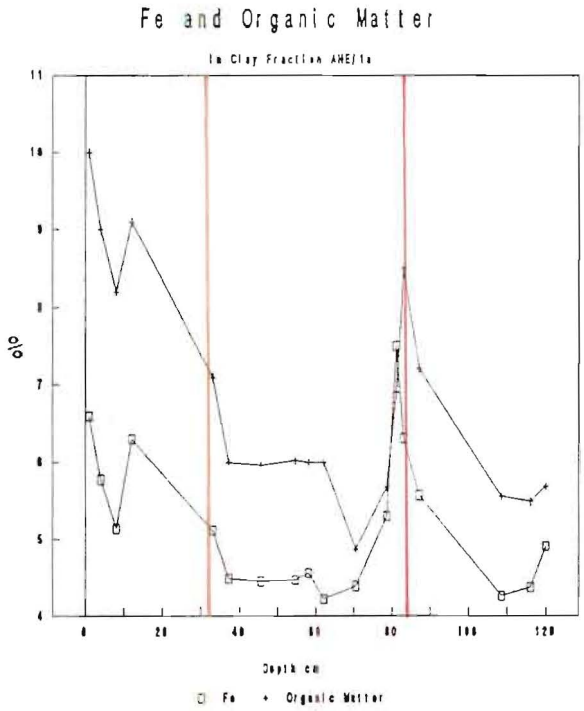

Fig. 4.6 Heavy Metal and Organic Matter Concentrations versus Depth in core AHE/1a. The red vertical lines separate the sediment units D, C, and B.

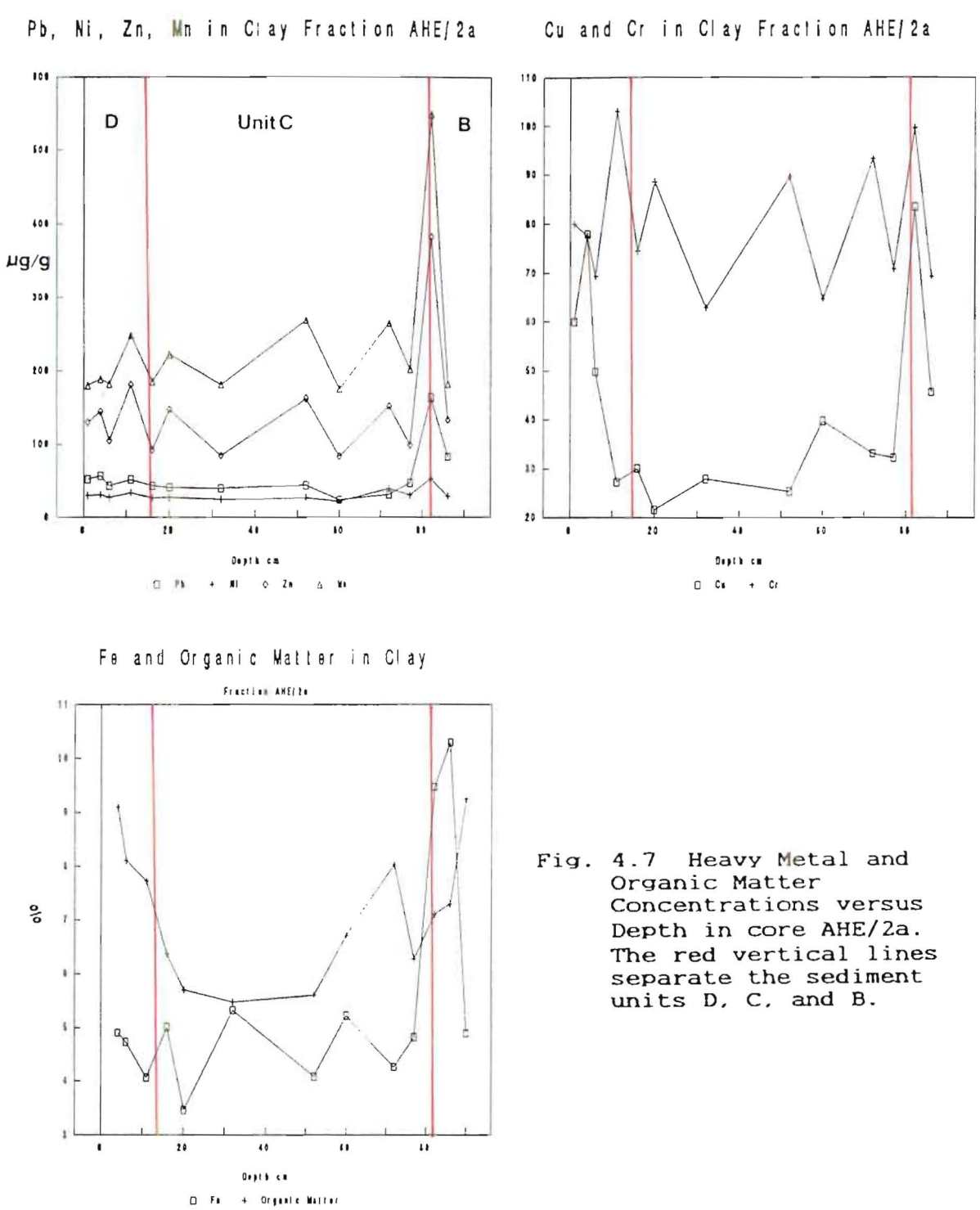

Fig. 4.7 Heavy Metal and Organic Matter Concentrations versus Depth in core AHE/2a. The red vertical lines separate the sediment units D, C, and B.

Zn concentrations (and other heavy metals) are not significantly elevated above that of the internationally accepted baseline value for the pelitic grain size presented in Table 4.1.

4.4 HEAVY METAL DISTRIBUTIONS WITH DEPTH

Because the clay fraction is the more important substrate for metal attachment (Chapter 1, Section 1.3), depth distribution discussions will refer primarily to the clay fraction profiles.

4.4.1 Metal and Organic Matter Distributions in Avon-Heathcote Estuary Clay Fractions

4.4.1.1 Vertical Trends

Figures 4.6 to 4.11 contain graphs of heavy metal distributions with depth for cores AHE/1a, 2a, 3a, 3b, 5, and 6. The positions of unit D, C, and B boundaries are shown by vertical lines.

Most cores exhibit: 1) baseline metal concentrations in the deeper levels of Unit B, 2) peak metal and organic matter concentrations near the top of Unit B, 3) baseline or near baseline metal levels in Unit C (see Table 4.1 for comparison), 4) peak metal and organic matter levels about half way up Unit D, and 6) increasing organic matter and either increasing or decreasing heavy metal concentrations above the Unit D peak. The heavy metal distributions found by Hay (1988) for core RH2 from in front of the City Outfall Drain show an identical pattern (Fig. 4.2).

In a few cores Fe shows a different pattern. Iron highs and lows are often slightly out of step with other metals, and in a few profiles Fe shows a reverse pattern of enrichment and depletion to organic matter (Fig. 4.8).

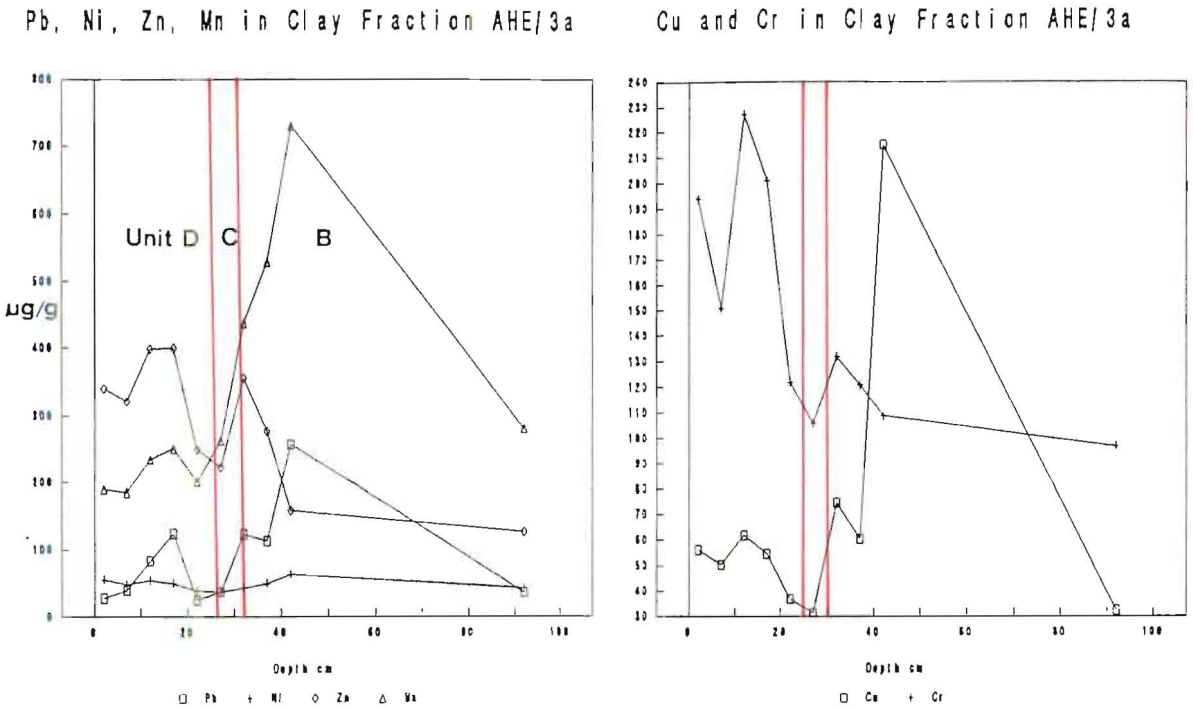

Fig. 4.8 Heavy Metal and Organic Matter Concentrations versus Depth in core AHE/3a. The red vertical lines separate the sediment units D, C, and B.

4.4.1.2 Interpretations of Metal and Organic Matter Behaviour

UNIT B

The distinctive metal and organic matter peak observed at the top of Unit B and across the contact between units C and B occurs in the black zone enriched in coke, coal, and ash particles. Pollen, ^{210}Pb, and historical data on sedimentation changes date this horizon around 1900 to 1925; at the time the Woolston and Sydenham areas were the main industrial centre of New Zealand. Widespread coal burning by industries and homes supplied high levels of carbon matter , sulphides (from sulphate) and some of the contribution of the other metals. These particles were probably washed into the estuary with stormwater. The stratified nature of the black deposit in core RH2 indicates that stormwater was a significant transport medium. However, some ash probably settled from the atmosphere during this period.

Industrial effluents were the other major source of metal and organic contamination at the time. At the peak there were many tanneries (Cr), and metal foundries (Cu, Zn, Fe, Pb, Ni, Cr) discharging directly into the Heathcote River and the City Outfall Drain (Chapter 2, Section 2.8).

Metal levels are not elevated at the base of core AHE/6 and not significantly elevated in core AHE/5 (Figs 4.10 and 4.11). The contact between units C and B is intensely bioturbated in core 6 (Appendix 2.0, Section A2.1), which suggests that the black zone has been reworked and sediment redistributed. The base of core AHE/ 5 contained stratified sand, mud and carbonaceous layers. Despite the presence of the carbonaceous streaks metal levels were not significantly elevated which suggests that the highly polluted zone was not reached in this core. Most metal concentrations are rising slightly near the base of core AHE/5.

During the early "iron working" period the level of

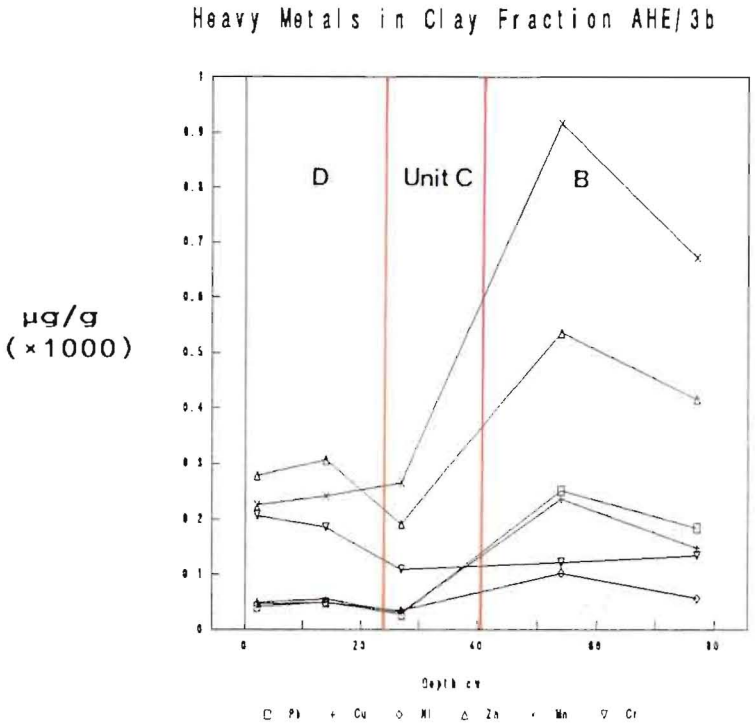

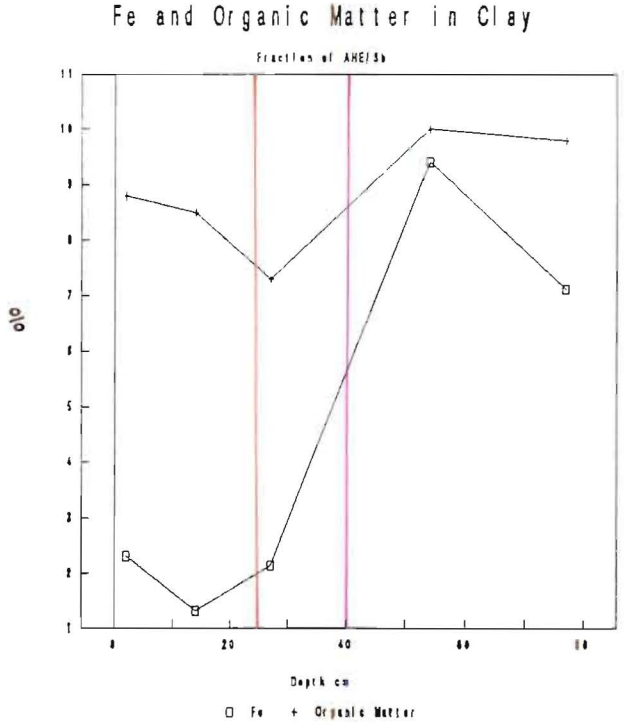

Fig. 4.9 Heavy Metal and Organic Matter Concentrations versus Depth in core AHE/3b. The red vertical lines separate the sediment units D, C, and B.

sulphate ions in the sediments probably increased dramatically due to sulphur oxide emissions from coal burning (Hem, 1989). In addition, fly ash particles are also rich in sulphur compounds. Since the 1880's partially treated and untreated wastes high in organic matter were entering the Avon-Heathcote Estuary from the Sewage farm, a soap and candle factory in Humphreys Drive, septic tanks along the southern shores of the estuary, and effluents entering the rivers and City Outfall Drain (Chapter 2, Table 2.1). Hence, it is reasonable to assume that most surface sediments near the head of the estuary were anaerobic due to decomposition of high concentrations of organic matter. Under these conditions the sulphate ions (derived from coal burning) would be reduced to sulphide ions. The increased quantities of sulphide ions probably forced chemical equilibria in favour of metal sulphide precipitation (ie displacing the sulphide precipitation zone downwards in Figs 1.2 and 1.3). Hence, Fe and Mn sulphide precipitates may contribute to the black colouration of sediment at the top of Unit B. Some Fe and Mn would have entered the estuary with industrial wastes and soot particles. However, most anthropogenic emissions of these two metals are not high enough to have had a significant impact on Fe and Mn concentrations in sediments of the estuary (Table 4.1).

Today, the low Eh values (-3.0 to -4.0V), and neutral pH (7-7.5) values of pore water measured near the top of Unit B, suggest reduced free metal ions. Normally under such conditions free metal ions and organo-metallic species would migrate upwards to oxygenated sediment and precipitate as oxides and hydroxides (Chapter 1, Section 1.6). However, the high salinity of the ground water (6 to 10ppt) would provide a continuous source of sulphide ions (via sulphate reduction), which would maintain chemical equilibria in favour of sulphide precipitates. This situation, combined with the impenetrability of Unit C has probably stabilised the chemical environment and Fe and Mn

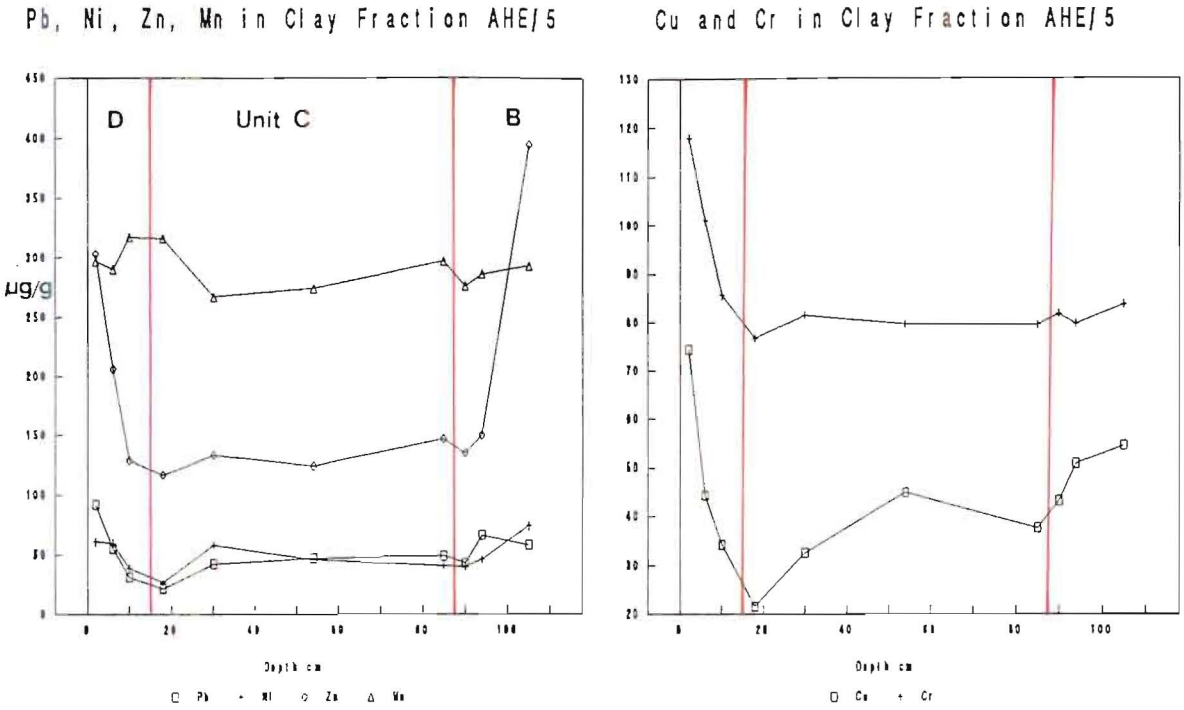

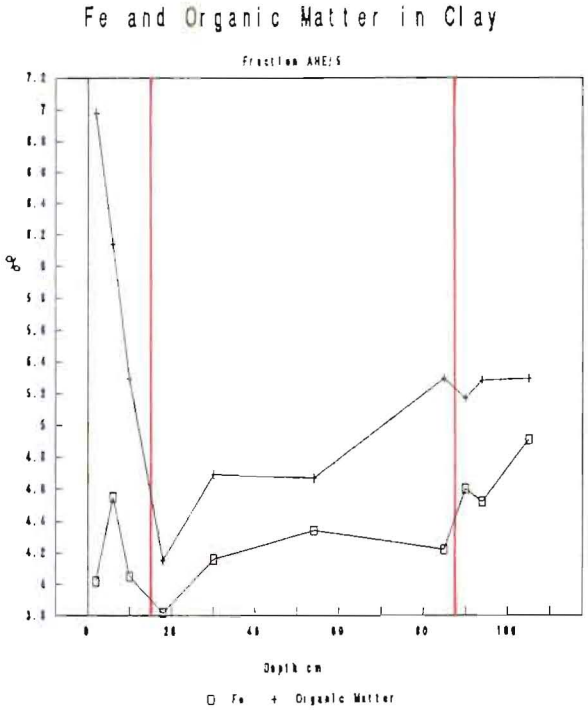

Fig. 4.10 Heavy Metal and Organic Matter Concentrations versus Depth in core AHE/5. The red vertical lines separate the sediment units D, C, and B.

sulphide compounds. In this layer other heavy metals are possibly 1) coprecipitated with Fe and Mn sulphides, 2) adsorbed onto the surfaces of the charcoal and ash particles, and 3) complexed with organic matter adsorbed on sediment surfaces.

Although some of the early industries were short-lived (Chapter 2), the industries that survived expanded and pollution was a serious problem in the Heathcote River from 1860 to 1973. In addition, coal has been a major household and industrial fuel throughout Christchurch's history. Such information suggests that heavy metal and organic matter levels should continue to rise with time in the sediments. However, results from Unit C, show that this is clearly not the case.

UNIT C

The low metal levels in Unit C suggest little or no coal burning and industrial activity in the vicinity of the estuary while this sediment accumulated. Historical records (Chapter 2), pollen data, and ^{210}Pb data (Chapter 3, Section 3.6) reveal that Unit C was deposited between 1925 and 1950-60, during a period of mechanical sweeping of the Avon and Heathcote Rivers.

The sediment originally accumulated in the rivers between 1880 and 1925 as a result of stormwater runoff from Christchurch City and market garden development in the Heathcote Valley. Even though the lower reaches of the Heathcote River were polluted during the early period, the high sedimentation rate probably prevented sediment from becoming severely contaminated. During the period that the Heathcote River was swept, it received high quantities of sediment eroded during land development on the Port Hills. Nearly all the sediment swept from above the Woolston area of the Heathcote River and the Avon River would have been relatively "clean" because 1) the sedimentation rates were high during silting, and 2) these areas have received minimal industrial runoff. Therefore, the source of Unit C

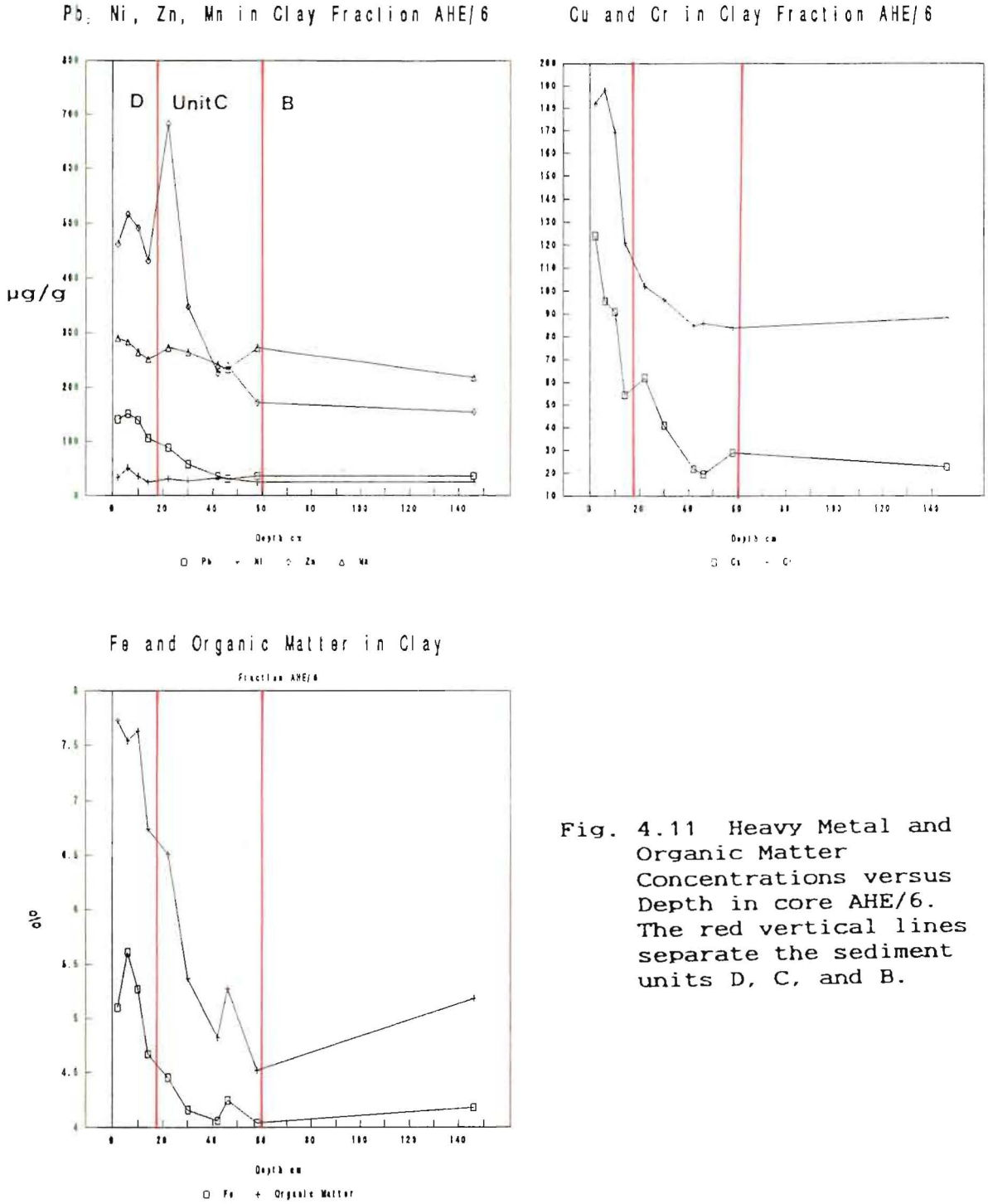

Fig. 4.11 Heavy Metal and Organic Matter Concentrations versus Depth in core AHE/6. The red vertical lines separate the sediment units D, C, and B.

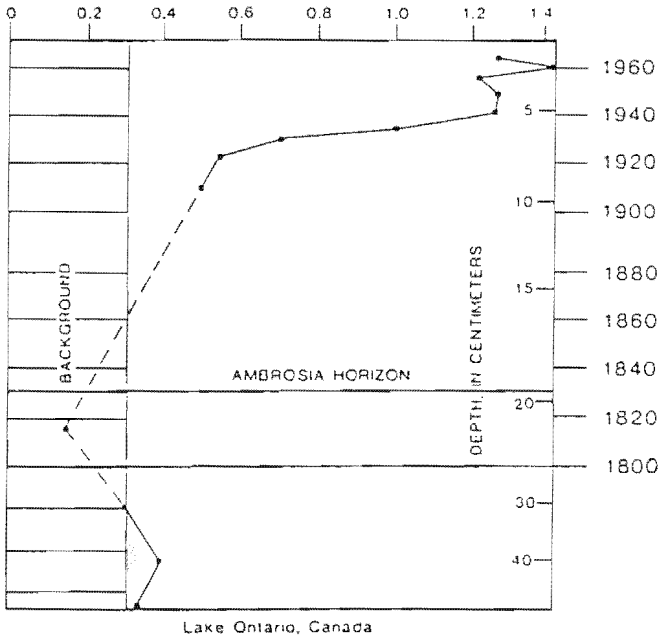

Fig. 4.12 Mercury levels in Lake Ontario Sediment (Thomas, 1972).

sediment was largely uncontaminated with heavy metals and organic matter.

The reason Unit C sediment did not accumulate significant quantities of metal during deposition, despite widespread industrial activity, was also the rapid sedimentation. As discussed in Section 4.3.2, while Unit C was accumulating, 12 to 25 times as much sediment surface was available for metal entrainment than during deposition of units B and D. In addition, Unit C is composed of more clay than units B and D (Fig. 4.5), which further increased the surface area available for metal adsorption.

Heavy metal dilution during periods of rapid sedimentation are commonly reported in the literature. For instance Fig. 4.12 contains data from Thomas (1972) on Hg levels in Lake Ontario. Mercury levels around 0.25 μg/g reflect natural background levels. At approximately 25cm below the surface, Hg concentrations reach a minimum of 0.14μg/g, which corresponds to a period of active deforestation by settlers between 1800 and 1820. While Unit C metal concentrations are not diluted below background levels (Table 4.4), they are clearly diluted relative to underlying Unit B, and levels expected considering that between 1925 and 1950 5 to 10 million litres per day of untreated industrial waste was discharged directly into the Heathcote River (Chapter 2, Section 2.3.4). (The low Mn concentrations produced in this study are partly due to methodology (see Chapter 6, Section 6.6.2).)

UNIT D

When Unit C deposition ceased, heavy metal and organic matter levels rose rapidly in Unit D sediment due to 1) high waste fluxes from industries on the Banks of the Heathcote River, 2) stormwater runoff from the City Outfall Drain, and 3) discharge from a number of domestic effluents during the 1950's and 1960's (such as septic tanks from the southern banks of the estuary, a starch factory located in the Humphreys Drive area, and treated effluent from the CDB

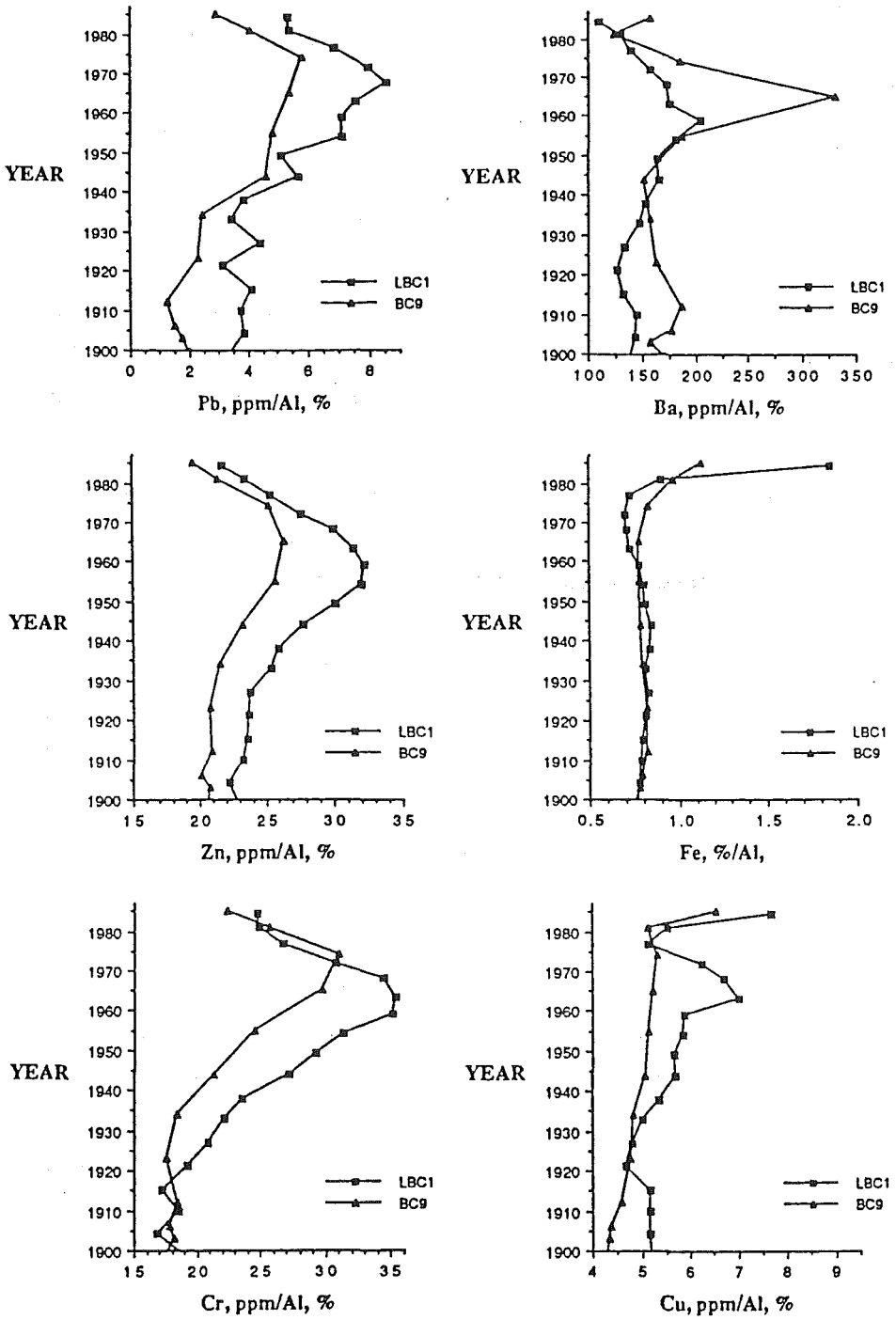

Fig. 4.13 Downcore distributions of Pb/Al, Zn/Al, Ba/Al, Cr/Al, Fe/Al, and Cu/Al since 1900 in cores from Santa Monica and Dan Pedro Basins near Southern California, offshore of Los Angeles (Finney and Huh, 1989).

Ponds). In addition, the sudden deceleration in sedimentation rate lowered the sediment surface area available for metal uptake. Therefore, individual sediment (clay) grains probably adsorbed higher concentrations of metals and organic matter than during Unit C deposition.

After 1950, the rising quantity of effluent (Table 2.3) entering the estuary from the sewage ponds increased the load of nitrogen and phosphate compounds to the estuary (Knox and Kilner, 1973). These nutrients stimulated growth of all organic life, which caused eutrophication of the estuary (Chapter 2, Section 2.7.2). The steady increase in organic matter observed in all cores from the base to surface of Unit D is probably caused by an increase in decaying biota associated with eutrophication. The evidence presented in Chapter 2 indicates that the estuary was in a state of eutrophication during Unit C deposition, which was enhanced by the high mud content. However, as with the heavy metals, the high sedimentation rate most likely diluted organic matter levels in Unit C.

The heavy metal and organic matter peak near the middle of Unit D probably corresponds with a pre-1972 high. Lead-210 data dates this peak spanning the period 1958 to 1968 (±10 years; Chapter 3, Section 3.6.2.3). Therefore, this peak probably represents the levels reached before all the domestic and industrial effluents were removed from estuary and rivers, and diverted to the Christchurch Drainage Board treatment plant.

Since the 1970's many developed countries have improved the quality of effluents discharged into local water systems. Hence, there are numerous sedimentary profiles in the literature showing a decrease in metal concentrations after 1970. One example is illustrated in Fig. 4.13 (Finney and Huh, 1989). Figure 4.13 contains heavy metal sediment profiles from Santa Monica and Dan Pedro Basins near the Southern California Borderlands, offshore of Los Angeles. Peak contamination occurred from the 1930's to the early 1970's due to industrial runoff,

atmospheric inputs and sewage effluent. Improvements in wastewater treatment in the late 1960's and 1970's is reflected in the decreasing metal concentrations after 1970.

In the present study, the sample interval of 4cm means that most Unit D samples span 9 years. A finer sample interval would have located the 1972 peak with greater accuracy, and may explain the absence of the peak in AHE/5. The peak is also insignificant in core AHE/2a (compared with Unit C concentrations). However, the absence of the 1972 peak in core AHE/2a is more likely to be due to the location of this core on the eastern slopes away from contaminant sources.

Directly above the 1972 peak, metal levels drop. Lead, Ni, Mn, and Fe levels remain low at the surface in cores AHE/2a, 3a, 3b, and 6 whereas Cu, Cr, Zn and organic matter levels continue to increase but not significantly in core 2a. In cores AHE/1a and 5 all metals and organic matter increase near the surface. In cores RH2 Pb, Zn, and organic matter continue to increase up to the surface (Fig. 4.2).

Even though in 1973, the Christchurch Drainage Board (CDB) commenced releasing effluent from the ponds only with the outgoing tide, the quantity of effluent entering the estuary has continued to rise (Table 2.3). Hence, the increase in organic matter towards the surface in all cores is most likely caused primarily by the CDB sewage effluents as discussed above. However, the drain and rivers possibly also transport some organic debris and carbon particles, particularly in the winter months when coal consumption increases.

The Zn and Pb increase after 1972, in cores near the river entrances, (AHE/5 and 6) and the stormwater drain, (RH2) reflect stormwater runoff rich in Pb from petrol emissions and Zn from roof gutters and paint pigments.

Post 1972 Cr, Cu, and Zn enrichment in cores AHE/3a, 3b, and 6 is most likely derived from the pond effluents. Christchurch domestic sewage sludge contains high levels of

Zn (2080μg/g) and Cr (4780μg/g). In fact, the Cr content of the Christchurch City sewage sludge is probably amongst the highest levels in the world because global averages range from 8 to 550μg/g (Nriagu and Pacyma, 1988).

The rising levels of all metals after 1972 in core AHE/1a reflect the influence of both the City Outfall Drain and sewage pond effluents in the estuary near Sandy Point. The predominant wind currents cause sewage effluents to flow south along the western slopes to become ponded in the Heathcote Basin (Chapter 2, Section 2.1.2).

The increasing Cu, Cr, Zn, and Pb concentrations near the surface of core AHE/5 may relate to a combination of stormwater, and occasional industrial discharges along the banks of the Heathcote River.

The high organic matter content and the anaerobic neutral to slightly alkaline pH conditions in sediments near the head of the estuary favour metal sulphide precipitation. Shortly after deposition, some heavy metals may either precipitate as sulphides or with Fe and Mn sulphides. The rapidly decreasing Eh values with depth (at constant pH, Chapter 3, Section 3.2.1.2) suggests that some surface bound metals and organic matter should be remobilised and migrate upwards. However, due to evaporation at low tide, interstitial water salinities are high (Knox and Kilner, 1973), which may stabilise sulphide compounds. Generally Fe and Mn concentrations have not risen significantly since 1972, which indicates that these metals are not affected by current day anthropogenic activity. Higher concentrations of these metals around the 1972 level may relate to higher quantities of sulphides. Sulphide precipitation may have been higher when large quantities of untreated domestic and industrial waste were discharged into the system.

The high metal levels at the top of Unit D in some cores could relate to decreasing sedimentation rates. However, decreasing sedimentation rates should preconcentrate all metals in all cores. Some metals are

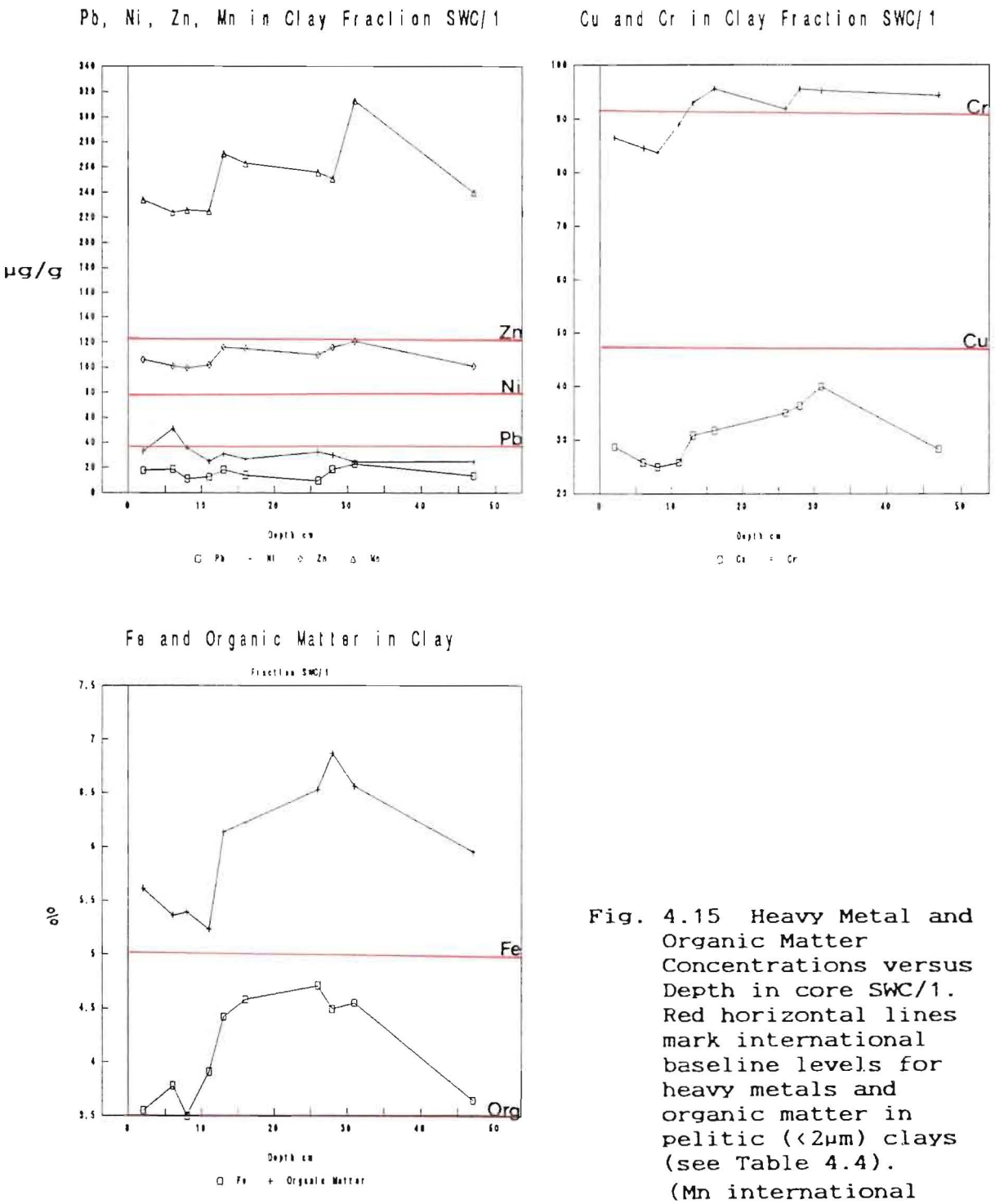

Fig. 4.15 Heavy Metal and Organic Matter Concentrations versus Depth in core SWC/1. Red horizontal lines mark international baseline levels for heavy metals and organic matter in pelitic (<2µm) clays (see Table 4.4). (Mn international baseline levels are 600-800µg/g.)

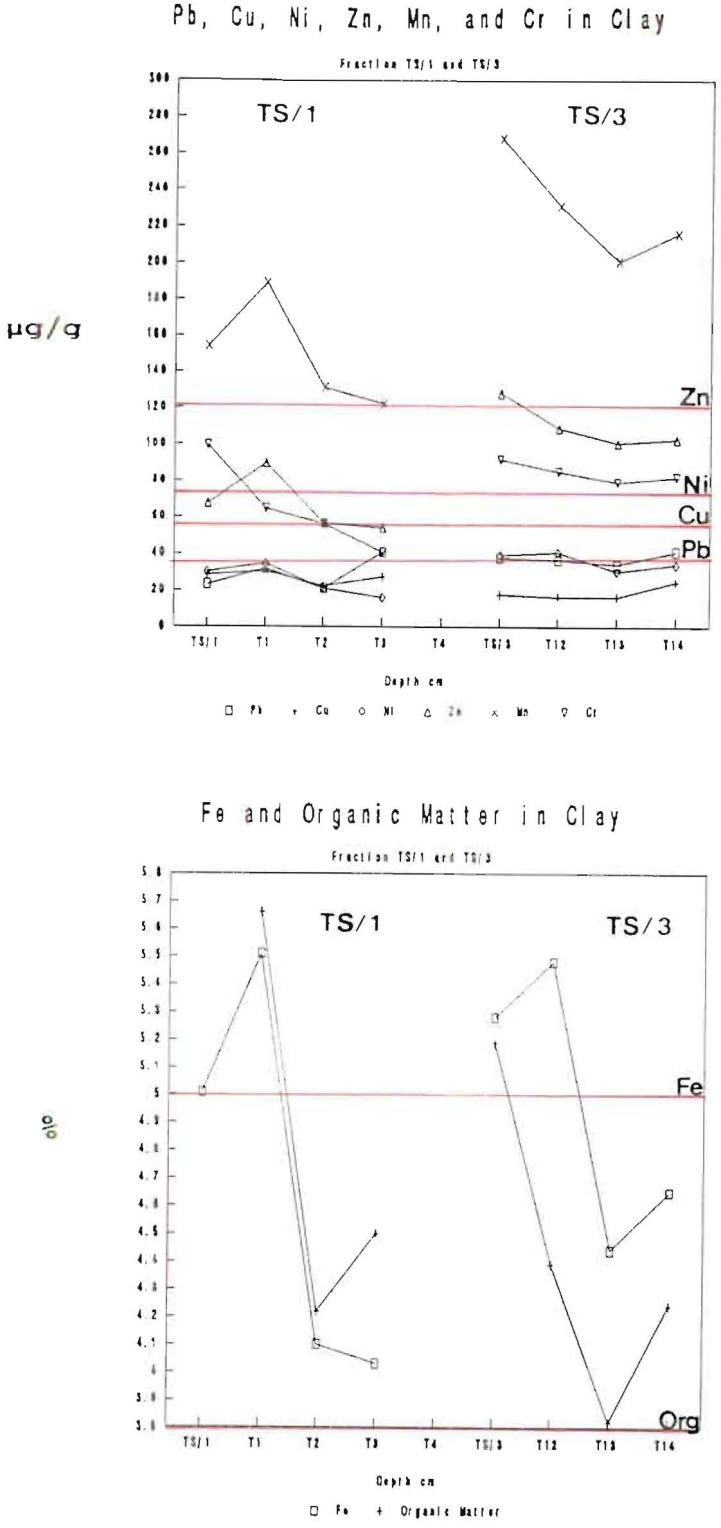

Fig. 4.16 Heavy Metal and Organic Matter Concentrations versus Depth in cores TS/1 and TS/3. Red horizontal lines mark international baseline levels for heavy metals and organic matter in pelitic (<2µm) clays (see Table 4.4).

(Mn international baseline levels are 600-800µg/g.)

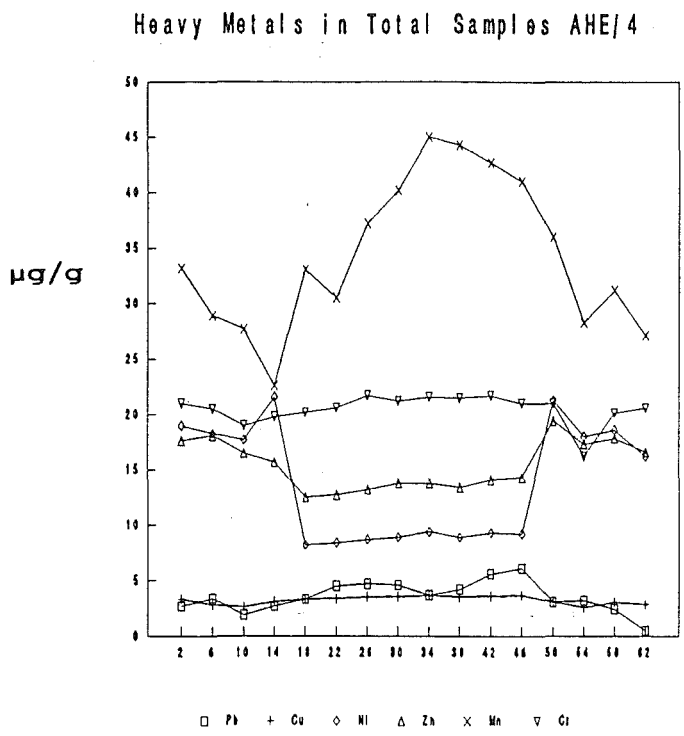

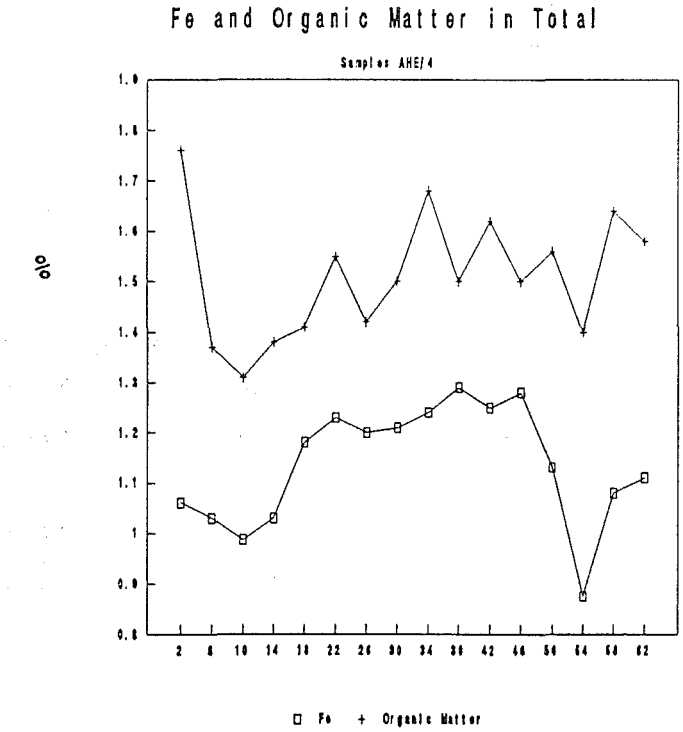

Fig. 4.14 Heavy Metal and Organic Matter Concentrations versus Depth in core AHE/4.

rising in some cores while others are not and most metals have stabilised in Unit D of core AHE/2a. Hence sedimentation rates are unlikely to be affecting metal levels at present.

The presence of the pre-1972 high in most cores suggests that sedimentation has been fairly continuous since 1950 and that little or no erosion has occurred since Unit C ceased accumulating. These findings support the ^{14}C, ^{210}Pb, and pollen data presented in Chapter 3.

4.4.2 Heavy Metal Distributions in Core AHE/4

The homogeneous fine sand in core AHE/4 was analysed as total sediment, and the results are presented in Fig. 4.14. All metals, except Ni, are either parallel or below the baseline sand values presented in Table 4.4. The high Ni concentrations near the top and base of the core mirror decreases in Fe, Mn and organic matter. Such variability is probably due to diagenetic rather anthropogenic influences.

The generally uncontaminated profiles of core AHE/4 and Unit D of AHE/2a suggest that present day stormwater, industrial, and sewage effluent discharges are only affecting muddy sediments near the head of the estuary. However, more cores should be studied on the eastern and southern shores to substantiate this conclusion.

4.4.3 Heavy Metal and Organic Matter Distributions in SWC/1, TS/1 and TS/3 Clay Fractions

The heavy metal and organic matter distributions in cores SWC/1, TS/1, and TS/3 are presented in Figs 4.15 and 4.16. All heavy metal concentrations at both sites are below internationally accepted baseline values for pelitic sediments (horizontal lines in Figures). Similar results were obtained for core SWC/2, which are summarised in Table 4.5 (and tabulated in the Appendix 3, Table A3.6, Section A3.2). The low metal levels found in background samples of

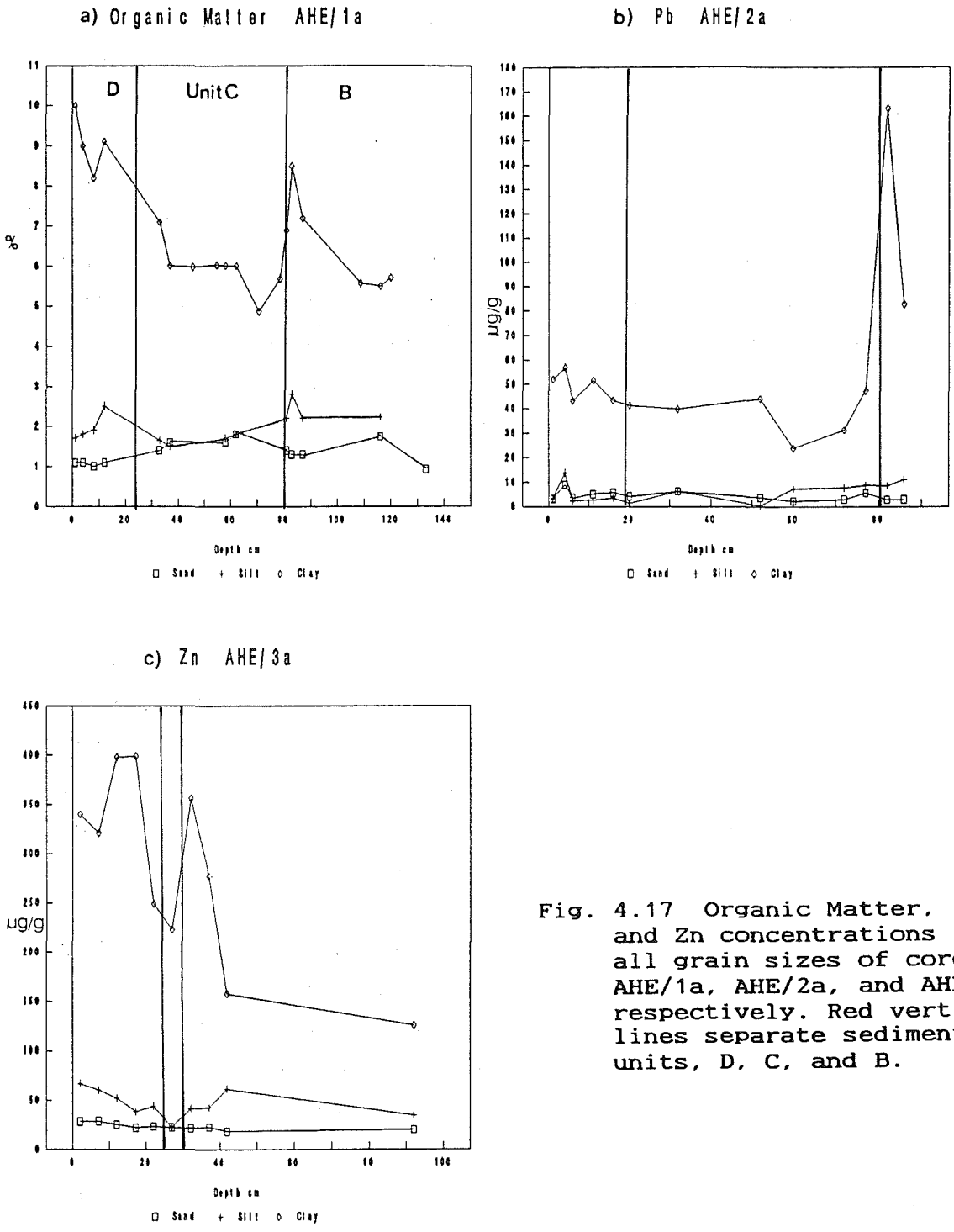

Fig. 4.17 Organic Matter, Pb, and Zn concentrations in all grain sizes of cores AHE/1a, AHE/2a, and AHE/3a respectively. Red vertical lines separate sediment units, D, C, and B.

this study relative to the international baseline most likely reflect the slightly coarser grain size (<4μm versus <2μm for the Global standard) and local mineralogy. The organic matter levels exhibited by both the Travis Swamp and Saltwater Creek Estuary sediments are 1% above the global baseline (1.8 to 3.5%), indicating that sediments in Canterbury naturally contain 4-4.5% organic matter. The increasing Fe and organic matter levels in cores TS/1 and TS/3 reflect the change from an estuarine to a swamp environment where organic matter levels are naturally higher.

4.4.4 Heavy Metal and Organic Matter Distributions in Silt and Sand Fractions

All heavy metals and organic matter exhibit similar behaviour in sand and silt fractions regardless of locality or depth. In Fig. 4.17, organic matter, Pb, and Zn from cores AHE/1a, AHE/2a, and AHE/3a, respectively illustrate the behaviour. Generally sand metal concentrations are uniform with depth, which indicates that the majority of heavy metals are lattice bound in this size fraction.

Silt depth profiles tend to mimic clay distributions, but the variability is insignificant (ie within experimental error). Such behaviour is most likely caused by the small component of clay minerals (10%, Chapter 3, Section 3.5.4) present in the silt grain size.

All heavy metals and organic matter were significantly elevated in the sand and silt fractions of the 6 to 8cm black zone in core AHE/2a (Figures 3.7a and 4.17b). In contrast, the clay fraction exhibited insignificant enrichment of most metals. Under certain conditions Fe and Mn hydroxy and sulphide compounds are formed as coarse grained precipitates (Forstner and Wittmann, 1981). The pH (7) and Eh (-0.24V) of the black horizon predicts sulphide deposits. Hence, metal and organic enrichment at 6-8cm in core AHE/2a is probably due metal co-precipitation or

adsorption onto silt and sand sized grains as Fe and Mn sulphide precipitates.

4.5 HIERARCHIAL CLUSTER ANALYSIS OF HEAVY METALS AND ORGANIC MATTER

Multiple regression and Q-mode techniques such as cluster analysis sometimes reveal correlations that are distinct or overlapping between heavy metals and each of Fe, Mn and organic matter. Often Fe and Mn form separate phases and therefore metals that exhibit a high positive correlation with Fe may exhibit a low negative correlation with Mn (Horowitz, 1985). In addition high metal-metal (e.g. Cd-Zn, Pb-Zn, Cr-Zn, Cr-Cu) correlations may reveal anthropogenic rather than lithogenic sources of metals in sediments.

In this study relationships were examined using the hierarchial clustering method of Massart and Kaufman (1983). The method involves constructing similarity matrices for heavy metals and organic matter using correlation coefficients. The similarity data is then processed either using computer programs or by hand (if the number of metals is small), and a dendogram is produced which ranks the data in such a way that small clusters are included in large ones.

In this study cluster analyses were performed on the following data sets 1) sand, 2) silt, 3) clay, 4) clay from Saltwater Creek and Travis Swamp (baseline), 5) Clay from the black zone at the top if Unit B (Unit B), 6) clay from Unit C, and 7) clay from Unit D.

All dendograms are presented in Fig. 4.18, where dashed lines represent the level of significance (α=0.05) using Pearsons distribution. The similarity matrices are presented in Appendix 3.0, section A3.3.

Discussions will be with regard to general trends rather than the behaviour of individual metals.

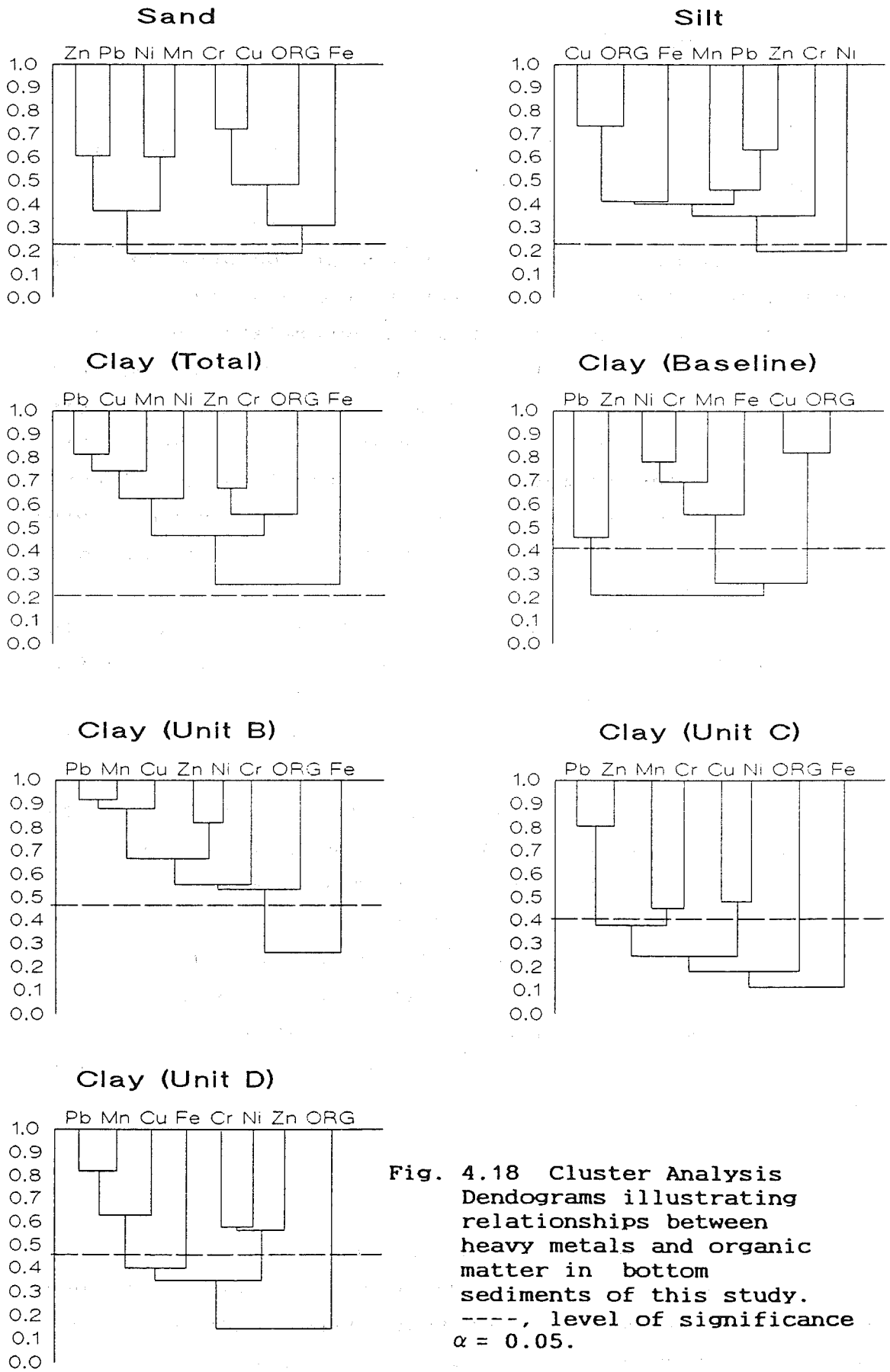

Fig. 4.18 Cluster Analysis Dendograms illustrating relationships between heavy metals and organic matter in bottom sediments of this study. ----, level of significance $\alpha = 0.05$.

4.5.1 Sand and Silt Clusters

Both the sand and silt fractions produced similar cluster groups. Two distinct clusters include Fe-Organic-Cu, and Pb-Zn with a lesser relationship to Mn. In sand Cr is more strongly associated with the Cu-Organic-Fe group than in silt. The main difference between the two dendograms is that Ni correlates with Mn in sand but not in silt, and that Cr and Cu are highly correlated in sand.

Although Fe is a natural component of most minerals, organic matter is not. Hence, the Fe-organic-Cu group probably represents the authigenic mineral phase either carried into the estuaries (Avon-Heathcote and Saltwater Creek) by the rivers and sea and/or material precipitated during estuarine mixing. These minerals are probably held in the red crusty material observed in the sand fraction under the microscope (Chapter 3, Section 3.5.2). Hence, some dissolved Fe is probably precipitated as hydroxides during estuarine mixing.

The significance of the Fe-organic-Cu cluster has probably been enhanced by the low Fe recoveries (81%, Chapter 6). Some minerals were not totally dissolved by the acid during extraction. Hence the proportion of mineral Fe relative to authigenic Fe may have been lowered.

The Pb-Zn-Mn group may relate to natural lithogenic distributions of metals within the mineral grains. The slight differences between the sand and silt dendograms may reflect the small percentage (10%) of clay minerals in the silt fraction, whereas the sand fraction contains no clay minerals.

4.5.2 Total Clay Clusters

The total clay dendogram indicates that generally all heavy metals and organic matter are correlated. Manganese and organic matter are more significantly clustered with heavy metals than Fe. This pattern suggests that in the

clay size fraction, Mn sulphides and organic matter are more important substrates for metal attachment than Fe sulphides.

4.5.3 Baseline Clay Clusters

The baseline clay dendogram (Saltwater Creek and Travis Swamp) resembles the sand and silt dendograms, but the Cu-Organic group is not clustered with Fe, and the Pb-Zn cluster is not related to Mn. The Cu-organic group probably again represents the authigenic phase, whereas the Pb-Zn group is lithogenic. The third group Fe-Mn-Cr-Ni could relate to either 1) clay mineralogy, and/or 2) surface bound Fe and Mn compounds containing adsorbed Ni and Cr.

4.5.4 Post-European Clay Clusters

The clusters of the 3 post-European clay fractions all contain distinct and insignificantly related Fe and organic matter groups. Unit C contains the Pb-Zn group characteristic of the baseline clays, sand, and silt fractions, and two weak correlations for Mn-Cr and Cu-Ni.

A new group, Pb-Mn-Cu, has emerged in Unit D and Unit B sediment of the black zone, and a Ni-Zn group which correlates with Cr in Unit D.

These correlations most likely reflect anthropogenic activity surrounding the Avon-Heathcote Estuary, since 1860. Most Fe is probably transported as hydroxy compounds and precipitated during estuarine mixing as in the sand silt, and baseline sediments. The Pb-Mn-Cu and Cr-Ni-Zn groups of both units B and D are probably derived from industrial, stormwater, and sewage effluent discharge into the estuary system. Both the City Outfall Drain and rivers transported metal and organic enriched effluents into the estuary while all 3 units accumulated. Hence, the individual sources cannot be identified by the cluster

analysis.

Hay (1988) clustered the clay fraction of City Outfall Drain sediments and found a significant Pb-Zn-Organic correlation. This correlation probably reflects a stormwater origin rich in Pb (from street dust) and Zn (from roofing and paint pigments) and organic matter (washed from the City surfaces including ash and charcoal from coal combustion).

The significant organic matter correlation with Pb-Mn-Cu-Zn-Ni-Cr in sediment near the top of Unit B supports the interpretation that the black material in this layer is derived principally from ash and soot particles emitted from industries around the turn of the century (ie metals and organic matter are from the same source). The separate grouping of Fe in this layer suggests that Fe enrichment is not related to anthropogenic activity. This result supports the conclusion of Section 4.4 that Fe has been precipitated as sulphides in the black layer. Mn may also be present in Mn sulphides. If so, then Mn sulphides and organic matter are important substrates for heavy metal attachment near the top of Unit B.

The absence of the Pb-Mn-Cu and Ni-Zn-Cr groups in Unit C is probably due to the rapid deposition of this unit. These groups may be present, but are indistinguishable from the natural component by cluster analysis. The slight differences between the Unit C dendogram and that of the baseline clays may reflect the anthropogenic influence.

The distinctly separate organic matter group in Units C and D suggests a new or additional source of organic matter to the estuary, which is unrelated to other sources of metals. The organic rich effluents discharged to the estuary through historical times and the increase in organic matter in the sediment resulting from eutrophication of the estuary are possible sources.

Table 4.4: Background Levels of Metals found in Various Sediments (μg/g)

Average Global(1) Shale and Clays(4)	Sandstone(2,3)	Fossil(3) Lake (<2μm)	Recent(3) Lakes remote areas Europe (<2μm)
Mn 850(600[4])	50[3] (390)	400-960	760
Zn 95	16	105-115	118
Cr 90 (60[4])	35	47-59	62
Ni 68 (32[4])	2	46-51	66
Cu 45 (21[4])	2[3] (15)	25-51	45
Pb 20	7	16-30	34
Fe 4.67%	major	1.8-3.2%	4.3%
Cd 0.2-0.3	.02	0.2-0.3	0.4
Org.		1.8-3.5%	16%

(1) Turekian & Wedepohl 1961
(2) Drever 1982
(3) Forstner and Wittmann 1981
(4) Salomons and Forstner 1984

4.6 DETERMINATION OF HEAVY METAL ENRICHMENT IN THE AVON-HEATHCOTE ESTUARY

Now that the geological parameters, sedimentation rate, grain size distribution, mineralogy, depositional environment, and provenance have been established in the Avon-Heathcote Estuary (Chapter 3) heavy metal enrichment can be determined with confidence.

Enrichment calculations compare sediments to 1) average shale and average sandstone (Table 4.4), 2) uncontaminated sediment of the same composition from outside the study area, and 3) similar sediment from pre-historic levels in sediment cores.

Table 4.4 contains average background reference values commonly used by many workers in determining heavy metal enrichment in sediments. Some of these values have already been introduced in earlier parts of this chapter. The average standard shale values in column 1 were first produced by Turekian and Wedepohl (1961). These values are a consensus of a large data set from studies carried out in the 1950's. The original data set has been improved in recent times due to cleaner analytical techniques (Salomons and Forstner, 1984). The importance of understanding grain size distributions is illustrated by the low sandstone background values compared with clay values in Table 4.4.

The samples used for setting up the standard background data were obtained from widely different environments, hence these reference values are not always an ideal comparison. Nevertheless, the standards do provide a quick check on heavy metal enrichment in a given area.

A more realistic assessment of contamination can be obtained if samples are compared to uncontaminated samples of the same composition. Baseline sediments are chosen from either near the study area or from deeper levels in cores. Care must be taken to account for possible diagenetic affects when using sediment from the base of cores.

Once the baseline reference data have been obtained

then a choice of calculations is available to compute the level of contamination. The most common heavy metal enrichment calculations include the Index of Geoaccumulation (Igeo), Pollution Load Index (PLI), Enrichment Factor (EF) and Contamination Factor (CF) (Araujo et al, 1988; Forstner and Salomons, 1980; Hornung et al, 1989; Nicolaidou and Nott, 1989; Premazzi et al, 1986).

The Index of geoaccumulation is calculated from

$$Igeo = \log_2 \frac{Cn}{1.5Bn},$$

where Cn is the concentration of a particular heavy metal in the clay fraction and Bn is the background value. The factor of 1.5 is introduced to include possible variations of background data which are attributable to lithogenic variations in the sediment (Glasby et al, 1988; Stoffers et al, 1986). Each step, from one class to the next higher class relates to a doubling of metal concentrations. An index of class 6 corresponds to 100 fold enrichment above background.

The simplest calculation involves the contamination factor (CF) which is defined as the ratio of a pollutant in the surficial sediment to the natural background level. The degree of contamination is a sum of contamination factors for all metals studied. Degrees of contamination <6 are considered insignificant, whereas values above 24 are considered highly significant (Premazzi et al, 1986). More elaborate calculations involving the CF have been used by Hamouda and Wilson (1989) to calculate the Pollution Load Index (PLI). This technique is useful in that it can be used to compare areas within estuaries or compare between 2 or more estuaries.

Another common method of calculating the degree of metal pollution in sediments involves the Enrichment Factor (EF), which is discussed in Appendix 3.1 in relation to grain size correction. The Enrichment Factor:

Table 4.5 Comparison of Sand Fraction Results between Cores

	Pb µg/g	Cu µg/g	Ni µg/g	Zn µg/g	Mn µg/g	Fe %	Cr µg/g	ORGANIC %
AHE/1a	7.66	4.67	12.70	25.30	54.50	1.17	20.50	1.40
2a	4.42	4.55	9.73	21.10	42.10	1.10	22.40	1.80
3a	5.39	7.30	9.03	23.80	44.20	1.53	26.90	1.40
5	3.17	6.63	9.80	22.80	47.10	1.40	26.61	1.55
6	6.41	6.66	8.17	30.90	43.20	1.07	28.50	1.80
RH2*	25.60	9.30	12.30	38.00	147.00	1.94	34.20	2.59
TS/1	2.29	2.95	12.80	20.20	33.10	.95	19.70	1.28
TS/3	2.58	5.45	5.97	19.90	37.50	1.10	18.20	1.11
SWC/1	3.05	3.87	6.04	16.90	35.60	.90	17.40	.96
SWC/2	3.38	8.53	7.82	25.70	41.30	1.28	21.70	1.44
Baseline#	7.00	2-15	2.00	16.00	50-390	-	35.00	-

Errors are within 10% of mean Values.
All data are mean values for each core; -, no data.
#, Internationally accepted Baseline values (Drever, 1982; Forstner and Wittman, 1981)
*, calculated from data of Hay (1988).

Table 4.6 Comparison of Silt Fraction Results between Cores

	Pb µg/g	Cu µg/g	Ni µg/g	Zn µg/g	Mn µg/g	Fe %	Cr µg/g	ORGANIC %
AHE/1a	15.40	12.10	13.80	46.80	75.00	1.80	48.20	2.00
2a	6.42	17.00	12.00	36.90	69.00	1.72	34.60	2.65
3a	8.62	17.30	13.20	47.20	86.70	2.28	44.90	2.24
5	6.94	10.10	10.10	46.50	72.45	1.94	32.40	1.80
6	10.80	13.30	11.00	51.60	47.90	2.20	43.80	2.35
RH2*	11.60	8.40	13.70	49.10	630.00	3.15	38.40	2.11
TS/1	UD	8.84	13.50	28.50	65.70	1.49	30.30	1.90
TS/3	UD	7.21	15.10	23.50	28.50	1.48	30.20	1.41
SWC/1	2.53	7.49	10.50	24.20	20.80	2.03	31.00	1.86
SWC/2	UD	9.64	17.50	32.40	37.90	1.48	32.40	1.59

Errors are within 10% of mean Values.
All data are mean values for each core; -, no data; UD, undetectable.
*, calculated from data of Hay (1988).

$$EF_{(M)} = \frac{[M]_s / [Al]_s}{[M]_a / [Al]_a},$$

where M_s and Al_s are the heavy metal and Al concentrations in the sediment of interest, while M_a and Al_a are their respective concentrations in a suitable baseline (Bordalo, Costa and Peneda, 1986; Hornung et al, 1989).

4.6.1 Metal Enrichment in Sand and Silt fractions

Tables 4.5, 4.6 and 4.7 contain a summary of the heavy metal data obtained from the Avon-Heathcote Estuary, Saltwater Creek Estuary, and Travis Swamp. All sediment raw data is tabulated in Appendix A3.2.

Generally in the sand and silt fractions most metals and organic matter are not significantly elevated above baseline levels. However, Organic matter, Mn, and Pb of RH2 sand, and Mn of RH2 silt show significant enrichment. These high results may be partly due to clay-organic aggregates forming during drying. Hay (1988) separated sand from mud by dry sieving. The author found that wet sieving helped disaggregate fine grained agglomerates, which were retained in the sand fraction after dry sieving.

Reference sediment Mn recoveries in this study are generally 75% of those of Hay (1988) (Chapter 6, Fig. 6.7), which is not low enough to account for the difference in Mn levels between RH2 (and the drain) and the estuary. Some Mn (and Fe) in the area of the drain is probably derived from ash particles and stormwater piping. However these sources are generally not high enough in Mn to have produced the concentrations detected by Hay (1988) in silts of the City Outfall Drain and adjacent estuary (Table 4.1). Therefore, Mn enrichment in RH2 silt may result from silt-sized precipitates of Mn sulphides.

4.6.2 Metal Enrichment in the Clay Fractions

In Table 4.7 clay heavy metal data from the Avon-

Table 4.7 Comparison of Clay Fraction Results Between Units and Baseline Samples

	Pb µg/g	Cu µg/g	Ni µg/g	Zn µg/g	Mn µg/g	Fe %	Cr µg/g	ORGANIC %
Surface (Avon-Heathcote Estuary)								
1a	189.00	96.00	72.10	540.00	340.00	6.59	196.00	10.00
2a	52.00	60.00	30.00	130.00	180.00	4.90	80.00	9.10
3a	28.50	56.10	55.70	340.00	190.00	4.54	194.00	8.70
5	92.00	74.40	61.00	303.00	297.00	4.00	118.00	7.00
6	140.00	124.00	33.20	462.00	290.00	5.10	182.00	7.70
RH2*	244.00	62.70	42.90	528.00	1120.00	7.57	202.00	8.93
Unit D								
1a	153.00	67.60	63.90	430.00	279.00	5.95	199.00	9.10
2a	50.10	63.90	28.90	126.00	186.00	4.40	73.50	7.90
3a	60.30	52.00	49.90	341.00	212.00	5.00	179.00	7.48
5	92.00	74.40	61.00	303.00	297.00	4.02	118.00	6.98
6	143.00	104.00	40.10	490.00	279.00	5.33	180.00	7.63
RH2	150.00	67.80	48.50	406.00	1345.00	8.73	189.00	7.84
Unit B (Black horizon in top 2-4cm)								
1a	186.00	66.30	117.00	414.00	566.00	4.44	81.40	7.85
2a	163.00	83.50	54.40	383.00	549.00	10.30	99.70	6.29
3a	164.00	117.00	52.60	264.00	565.00	7.92	121.00	7.39
RH2	152.00	88.10	102.00	282.00	3071.00	9.30	96.40	7.51
Unit B (Background, pre-1850 A.D)								
1a	43.50	56.10	32.40	148.00	285.00	4.51	82.70	6.25
3a	36.50	32.40	43.50	126.00	280.00	5.86	96.80	7.40
6	31.20	22.80	30.00	200.00	235.00	4.10	84.00	5.00
RH2	40.70	40.70	44.80	129.00	849.00	4.35	86.60	5.34
Unit C								
1a	30.50	35.10	31.40	105.00	238.00	4.63	77.70	6.10
2a	40.70	28.70	28.30	125.00	213.00	4.56	80.50	6.32
3a	44.30	35.50	41.50	225.00	274.00	6.54	116.00	7.17
5	40.10	34.20	42.90	130.00	289.00	4.14	79.40	4.70
6	58.10	41.00	26.90	348.00	265.00	4.16	96.10	5.87
RH2	82.20	35.50	55.60	170.00	1381.00	7.95	79.40	5.73
Background References								
TS/1	29.30	27.00	25.30	91.90	149.00	4.16	60.30	4.80
TS/3	37.50	18.90	36.20	110.00	229.00	4.96	84.70	4.41
TS (Av)	33.20	22.95	30.75	100.95	189.00	4.56	72.50	4.60
SWC/1	15.90	30.80	36.00	109.00	250.00	4.11	91.00	5.99
SWC/2	37.90	38.20	38.50	122.00	244.00	4.84	100.00	6.00
Baseline#	20-30	21-45	32-70	95-120	600-800	4-5	60-90	1.8-3.5

Errors are 10-20% of the mean values; TS (Av), average of values for TS/1 and TS/3.
All data are mean values for each unit or core. *, raw data from Hay (1988).
#, Internationally accepted Baseline values (Turekian and Wedepohl, 1961;
Salomons and Forstner, 1984; Forstner and Wittmann, 1981)

Heathcote Estuary are averaged for horizons of specific interest in each unit, and compared to mean values from the baseline cores of the Travis Swamp and Saltwater Creek Estuary.

Generally most metals and organic matter appear significantly elevated in surface samples, Unit D, and the black horizon near the top of Unit B, whereas Unit C and pre-1850 Unit B clay are not enriched in metals. Most metals are not elevated in Unit D sediments of cores AHE/2a and 3a (accept Cr and Zn in AHE/3a).

The Fe and Mn data is uniform except in the black horizon of Unit B and RH2. The results of the cluster analysis show that generally Fe distributions are not affected by the presence or absence of other metals, hence Fe may be an acceptable conservative element for enrichment calculations. However, the elevated Fe concentrations in the black zone at the top of Unit B are not related to the enrichment of the other metals in this zone (Fig. 4.18). Hence, Enrichment Factors (EF) calculated using Fe as the conservative element may suppress the real degree of metal contamination in this zone. To account for this possibility, enrichment will be determined with and without Fe as the conservative element and the results compared.

Tables 4.8 and 4.9 present heavy metal enrichment calculated using the Enrichment Factor (EF) and the Index of Geoaccumulation (Igeo) respectively. It is considered that EF values above two are significant, while the classes of Igeo are:

Class	**Igeo** (Stoffers et al. 1986)	
0	0	Uncontaminated
1	0-1	Uncontaminated to moderately contaminated
2	1-2	Moderately contaminated
3	2-3	Moderately to strongly contaminated
4	3-4	Strongly contaminated
5	4-5	Strongly to extremely contaminated
6	>5	Extremely contaminated

The Avon-Heathcote Estuary sediments are geologically and chemically more similar to sediments of the Travis

Table 4.8 Enrichment Factors (EF) for Heavy Metals and Organic Matter of Avon-Heathcote Estuary Clay Fractions

	Pb	Cu	Ni	Zn	Mn	Fe	Cr	ORGANIC
Unit D								
1a	3.51	2.26	1.59	3.26	1.13	1.00	2.10	1.51
2a	1.55	2.89	.97	1.29	1.02	1.00	1.05	1.78
3a	1.65	2.07	1.48	3.08	1.02	1.00	2.25	1.48
5	3.12	3.68	2.25	3.40	1.78	1.00	1.85	1.72
6	3.66	3.88	1.12	4.15	1.26	1.00	2.12	1.42
RH2*	2.35	1.54	.82	2.10	3.72	1.00	1.36	.89
Unit B (Black horizon in top 2-4cm)								
1a	5.72	2.97	3.91	4.21	3.08	1.00	1.15	1.75
2a	2.16	1.61	.78	1.68	1.29	1.00	.61	.60
3a	2.83	2.94	.98	1.51	1.72	1.00	.96	.92
RH2	2.23	1.88	1.63	1.37	7.97	1.00	.65	.80
Unit B (Background, pre-1850 A.D)								
1a	1.32	2.47	1.07	1.48	1.52	1.00	1.15	1.37
3a	.85	1.10	1.10	.97	1.15	1.00	1.04	1.25
6	1.04	1.10	1.09	2.20	1.38	1.00	1.29	1.21
RH2	1.28	1.86	1.53	1.34	4.71	1.00	1.25	1.22
Unit C								
1a	.90	1.51	1.01	1.02	1.24	1.00	1.06	1.30
2a	1.22	1.25	.92	1.24	1.13	1.00	1.11	1.37
3a	.92	1.08	.94	1.55	1.01	1.00	1.12	1.09
5	1.32	1.64	1.54	1.42	1.68	1.00	1.21	1.12
6	1.91	1.96	.96	3.78	1.54	1.00	1.45	1.40
RH2	1.41	.89	1.04	.97	4.19	1.00	.63	.71

EF=(Metal(sample)/Fe(sample))/(Metal(TS)/Fe(TS))
TS; Travis Swamp average from Table 4.7.
*, Hay (1988).

Swamp than those of the Saltwater Creek Estuary (Chapter 3). Hence, the average clay fraction results of both Travis Swamp cores (TS Av) are chosen as the baseline values (Table 4.7).

4.6.2.1 Enrichment Factors

Generally Unit C and pre-1850 Unit B show insignificant enrichment (EF<2) in all metals and organic matter. The significant Mn enrichment found in these zones of core RH2 is principally due to the higher Mn yield obtained by Hay (Chapter 6). The high Zn levels in core AHE/6 are due to an isolated result of 682μg/g near the top of Unit C, which may correlate with a spillage of raw sewage from the ponds in the late 1950's. This result is at the level that correlates with a death assemblage of Mactra ovata at Pleasant Point (Chapter 3, Section 3.6.1).

Generally Pb, Cu, and Zn show significant enrichment in sediments of Unit D and the top of Unit B from near the river and drain entrances (AHE/1a, 5, 6, and RH2), and less significant enrichment in cores AHE/2a and 3a, which are away from the river and drain entrances. Significant Cr and Zn enrichment occurs in Unit D sediment from cores adjacent to the Christchurch Drainage Board pond outfalls (cores AHE/1a, 3a, and 6). The black zone at the top of Unit B shows significant Pb, and Cu enrichment in most cores, and Zn, Ni, and Mn enrichment in AHE/1a. Organic matter shows minor enrichment in all units of all cores.

4.6.2.2 Index of Geoaccumulation

Generally the Indexes of Geoaccumulation agree closely to enrichment calculated using EF.

However, the Igeo values show slight to moderate organic matter enrichment in Unit D of all cores. Organic matter levels have increased about 1½ times since 1950, which is a major increase in the quantity of organic matter, considering it is naturally present in quantities around 4.5%.

Table 4.9 Calculation of Enrichment using the Index of Geoaccumulation (Igeo)

	Pb	Cu	Ni	Zn	Mn	Fe	Cr	ORGANIC
Surface (Avon-Heathcote Estuary)								
1a	1.92	1.48	.64	1.83	.26	-.05	.85	.54
2a	.06	.80	-.62	-.22	-.66	-.48	-.44	.40
3a	-.81	.70	.27	1.17	-.58	-.59	.84	.33
5	.89	1.11	.40	1.00	.07	-.77	.12	.02
6	1.49	1.85	-.47	1.61	.03	-.42	.74	.16
RH2*	2.29	.87	-.10	1.80	1.98	.15	.89	.37
Unit D								
1a	1.62	.97	.47	1.51	-.02	-.20	.87	.40
2a	.01	.89	-.67	-.27	-.61	-.64	-.57	.20
3a	.28	.60	.11	1.17	-.42	-.45	.72	.12
5	.89	1.11	.40	1.00	.07	-.77	.12	.02
6	1.52	1.60	-.20	1.69	-.02	-.36	.73	.15
RH2	1.59	.98	.07	1.42	2.25	.35	.80	.18
Unit B (Black horizon in top 2-4cm)								
1a	1.90	.95	1.34	1.45	1.00	-.62	-.42	.19
2a	1.71	1.28	.24	1.34	.95	.59	-.13	-.13
3a	1.72	1.76	.19	.80	.99	.21	.15	.10
RH2	1.61	1.36	1.14	.90	3.44	.44	-.17	.12
Unit B (Background, pre-1850 A.D)								
1a	-.20	.70	-.51	-.03	.01	-.60	-.40	-.14
3a	-.45	-.09	-.08	-.27	-.02	-.22	-.17	.10
6	-.67	-.59	-.62	.40	-.27	-.74	-.37	-.46
RH2	-.29	.24	-.04	-.23	1.58	-.65	-.33	-.37
Unit C								
1a	-.71	.03	-.55	-.53	-.25	-.56	-.49	-.18
2a	-.29	-.26	-.70	-.28	-.41	-.58	-.43	-.13
3a	-.17	.04	-.15	.57	-.05	-.06	.09	.06
5	-.31	-.01	-.10	-.22	.03	-.72	-.45	-.55
6	.22	.25	-.78	1.20	-.10	-.72	-.18	-.23
RH2	.72	.04	.27	.17	2.28	.22	-.45	-.27

Igeo = log2(Cn/1.5Bn), where Cn is metal concentration in sample, and Bn is metal concentration in baseline sample, Ts (Av), from Table 4.7.
*, calculated from data of Hay (1988).

Units C and baseline B show zero enrichment in all cores (ignoring the high metal recoveries of Hay, 1988). The black layer at the top of Unit B shows moderate Pb, Cu, Zn, and Mn enrichment in all cores, while Ni is not significantly enriched in cores AHE/2a and 3a. Unit D shows moderate Pb, Cu, and Zn Igeo values in all cores, except AHE/2a and 3a. As mentioned above, cores AHE/2a and 3a are away from most river and drain entrances, which explains their low metal contamination. However, there is some Cr and Zn enrichment in Unit D of core AHE/3a. Generally Ni, Fe , Mn and organic matter are not enriched in any unit. Organic matter and Cr show slight to moderate enrichment in Unit D, and Fe and Mn show moderate enrichment in the black horizon of Unit B. Moderate Cr enrichment occurs in cores adjacent to the outfall of the sewage ponds (cores AHE/1a, 3a, and 6).

In the Avon-Heathcote Estuary Unit D metal enrichment is comparable to that in the Manukau, Waitemata (Auckland City), and Wellington (Wellington City, Fig 1.0) harbours of the north Island. Stoffers et al. (1986) found Igeo classes from 1 to 2 for most areas of Wellington Harbour and values above 3 in small pockets adjacent to discharge points of industrial effluents and near wharfs. Most Igeo classes ranged 2 to 3 for sediments of the Manukau and Waitemata harbours of Auckland City, with values of 4 to 5 in small localised areas near industries (Glasby et al. 1988). Glasby et al. found sediment enrichment adjacent to the Manukau Sewage purification works in the 0 to 1 range for Zn, Pb, Ni and Cu, which is similar to results found here. The main contaminant sources were stormwater runoff and industrial wastes.

4.7 CONCLUSION OF SUB-SURFACE HEAVY METAL AND ORGANIC MATTER DISTRIBUTIONS

Generally heavy metal and organic matter distributions in sediment profiles from the Avon-Heathcote Estuary fit

closely to that predicted by the historical synthesis (Chapter 2). The pre-European sediments in Unit B contain similar levels of all metals and organic matter to sediments of the Travis Swamp and Saltwater Creek Estuary. Despite the differences in chemical environment between the Saltwater Creek Estuary and the Travis Swamp, most metal and organic matter concentrations are similar between the two locations.

Sediment dated 1900 to 1925 near the top of Unit B is moderately enriched in metals (including Fe) and organic matter. Peak levels are found in the black coloured zone of all cores including RH2 (Hay, 1988). Around the turn of the century, high metal fluxes originated from a combination of industrial sources (including tanneries, Cr; brass and iron works, Zn, Cu, Fe, Ni, Mn; Gasworks, fly ash Pb, and Mn), and stormwater loaded with ash, charcoal and industrial effluents. Most contaminants were transported to the estuary via the Heathcote River and the City Outfall Drain. Although Fe was probably also discharged in high quantities from factories during the "iron working" days, contamination would have been obscured by the high natural Fe levels in the sediments (4-5%).

Organic matter enrichment in the sediment at the top of Unit B was caused by organic rich effluents from 1) the sewage ponds, 2) septic tanks along the southern banks of the estuary, and 3) a soap factory in Humphreys Drive (in addition to the high flux of ash particles).

Coal combustion probably increased sulphate emissions to the estuary during the period. Hence the black colour in sediment deposited around the turn of the century may result from a combination of soot particles (ash, charcoal) and Fe and Mn sulphide precipitates. The high level of organic matter in this layer suggests that conditions were most likely anaerobic at the time, which would favour metal sulphide precipitation.

Despite the large quantities of industrial and domestic waste discharged into the Avon-Heathcote Estuary

system between 1925 and 1950, the heavy metal and organic matter concentrations in Unit C are not significantly elevated relative to baseline. Contamination was prevented by the approximately 25 times greater sediment surface area available for metal attachment during Unit C deposition than during units B and D deposition. The increase in surface area was caused by Unit C's rapid sedimentation rate and high clay content.

Heavy metal and organic matter concentrations increase rapidly from the base of Unit D until a point which probably corresponds with the early 1970's. Metal and organic matter levels drop in sediment immediately above this point. This pattern corresponds with the sudden decrease in sedimentation rates from Unit C (6 to 12 cm/year) to Unit D (around 0.5cm/year), and rising effluent fluxes. Between 1968 and 1972 the starch factory in Humphreys drive, closed down, and all the industrial and domestic effluents discharging into the estuary and Heathcote River were diverted to the Christchurch Drainage Board treatment Plant. The abrupt removal of such large quantities of untreated effluent (well over 10 million litres per day) is most likely responsible for the dramatic drop in metal levels around the 1972 point in cores from the Avon-Heathcote Estuary.

After 1972 the increase in organic matter observed in all cores is probably due to slowly rising quantities of suspended matter (algae) and nutrients discharged to the estuary from the sewage ponds.

The common wind circulation patterns in the estuary drive non-saline waters from the Avon and Heathcote Rivers, sewage ponds and City Outfall Drain into the Heathcote Basin, which has turned this depository into the **major sink** for heavy metals and organic matter in the Avon-Heathcote Estuary. The most anaerobic conditions were observed in the Heathcote Basin. Even though most of the pond effluent leaves the estuary on a tidal cycle a considerable proportion of dead algae are probably deposited in the

Heathcote Basin along with sediments from the Heathcote River. During prolonged storms turbulent water may increase the oxygen content in the surface sediments. Such conditions may remobilise heavy metals into overlying water. Hence, the Heathcote Basin may be a potential source of heavy metals to overlying water.

The uncontaminated sediments in core AHE/4 and Unit D of core AHE/2a indicate that the ponds and drains are only influencing heavy metal levels in sediment near the head of the estuary from the Avon depository across the western slopes to the Heathcote Basin. However the rising organic matter levels in Unit D of core AHE/2a indicate that eutrophication is affecting the whole estuary.

The elevated sediment metal levels observed by CDB near the old outlet of the Mt Pleasant septic tank are most likely derived from a thermal spring in the area.

The extreme Cr (10708μg/g), Zn (6215μg/g), and Pb (55000μg/g) contamination observed in the 1980's adjacent to industrial discharge points in the Woolston area suggests that some factories are still emptying effluent into the Heathcote River despite widespread removal of wastes from the river in the early 1970's.

The results of this study agree with previous studies in that Pb and Zn are the most significantly enriched metals in the Avon-Heathcote Estuary. Nickel is generally insignificantly enriched in all units except near the top of Unit B, which probably correlates with metallurgy industries in the early days. In addition, Fe and Mn concentrations are generally not elevated in sediments of the estuary except near the drain and the top of Unit B, which is probably due to their precipitation as sulphides.

The rapid drop in heavy metal and organic matter levels with depth in the Avon and Heathcote rivers, observed by Anderson (1985), Hulse (1983), and Purchase (1983), supports the historical analysis in that most near surface sediment in the rivers post-dates 1950.

Further research would be useful on Unit D sediments

of the Southern shores, McCormacks Bay, and Moncks Bay to determine the impact of urban activity on these areas of the estuary.

A BRIEF SURVEY OF HEAVY METAL CONCENTRATIONS IN SUSPENDED SEDIMENT AND WATER OF NON-SALINE WATERS ENTERING THE AVON-HEATHCOTE ESTUARY

4.8 INTRODUCTION

A limited study was undertaken to determine heavy metal concentrations in the suspended matter and to a lesser extent the dissolved phase entering the Avon-Heathcote Estuary from each major point source (Avon River, Heathcote River, City Outfall Drain, and sewage ponds 5 and 6). The principal aim was to determine whether or not any of these waterways are supplying high concentrations of heavy metals to the Avon-Heathcote Estuary at the present time.

Between 26 February 1988 and 17 July 1989 water samples were collected at low tide, every 6 weeks, from near the entrances of the Avon River (Wainoni Bridge), Heathcote River (Catherine St), City Outfall Drain (Charlesworth St), and the outlets of ponds 5 and 6 (Fig 2.2). It was necessary to go a short distance up the rivers and the drain to match their salinities with those of the ponds. Consequently some of the Woolston industrial area was missed. Hence metal concentrations will be a minimum for the Heathcote River.

4.9 PROCEDURE AND QUALITY CONTROL IN WATER ANALYSIS

All laboratory procedures (including acid washing of plastic and glassware) were carried out in a class 100 Clean Room. Samples were collected in 1 litre polypropylene bottles. Prior to use, the sample bottles and other

Table. 4.10 Detection Limits Obtained During Water Study (ng/ml).

	Graphite Furnace AAS				Flame AAS		
	Cu	Pb	Cr	Ni	Zn	Mn	Fe
n	69	79	40	60	118	122	111
X	.06	.04	.02	.03	.02	.02	.02
$Xe_{(.05)}$	.001	.001	.002	.002	.002	.002	.003

n; number of analyses of the blank.
X; detection limit (mean blank absorbence + 3s, corrected to sample volume).
$Xe_{(.05)}$; error on X at 95% Confidence.

Table. 4.11 Results of SD-N-1 Analysed During Water Study (all data μg/g, except Fe which is %).

	Graphite Furnace AAS				Flame AAS		
	Cu	Pb	Cr	Ni	Zn	Mn	Fe
n	14	14	8	14	14	13	12
X	72.5	125	128	29	445	603	3.12
μ	72.2	120	149	31	439	777	3.64
$Xe_{(.05)}$	7.33	11.8	10.4	3.67	43.5	71.8	0.45
Y (%)	100	104	86	94	101	77.6	85.7

X; mean SD-N-1 concentration.
μ; certified mean SD-N-1 concentration, recognised by IAEA (1988).
$Xe_{(.05)}$; error of X.
Y; $(X/\mu)100$, percentage yield of X.

utensils were soaked in 4M AR nitric acid for 48 hours, and rinsed several times with Millique de-ionised water (DI). Filter papers were desiccated for 12 hours and weighed prior to filtering.

Plastic disposable gloves were used when collecting the water samples. Initially the sample bottles were rinsed with river water at a point down stream of the collection site. The water samples were taken upstream of the bottle-holding hand, at a water depth of 20cm, and at a distance from the river bank of about 1m. Water temperature, pH, Eh, and salinity were measured at each site after sample collection. All meters were calibrated in the field with standard buffers (American Public health Association (AHPA), 1971).

Immediately after collection the water samples were transferred to the Clean Room. Sample volumes of 250 ml were filtered through acid washed membrane filters of pore size 0.45 μm (Millipore). The 5 filtered samples, 5 unfiltered samples (250 ml), 1 analytical blank (250 mls of filtered de-ionised water), and 1 reference sample were transferred to acid washed 500 ml round bottomed flasks, frozen, and freeze dried.

The reference sample analysed with each batch consisted of either a Chemaqua water reference (Mattingley, 1988, and pers comm.) or a diluted solution of digested sediment reference SD-N-1 (IAEA, 1988). The heavy metals in SD-N-1 were extracted by boiling 0.1g of sediment in 4M HNO_3 for 30 minutes. The extract was not filtered to include suspended sediment comparable to the total water samples.

Filter papers were retained after filtering, dried, desiccated again for 12 hours, and re-weighed to measure the quantity of suspended matter in each sample.

During freeze drying samples slowly sublimed, over 2 days, until all the water disappeared. When freeze drying was complete, the flasks were transferred to the Clean Room, where the residues were taken up in 25 mls of hot

Table. 4.12 Results of Chemaqua Water Samples (ng/ml)

(Round) Sample	Pb	Cu	Ni	Cr	Zn	Mn	Fe
	(Graphite Furnace AAS)				(Flame AAS)		
(13)							
26	8.0	6.0	UD	2.0	78.7	9.02	10.3
μ_{26}	UD	10.0	UD	<40	90	16	21
27	366	335	383	2.0	301	1.5	9.5
μ_{27}	370	330	420	<4	300	5.0	30
(14)							
28	0.7	0.1	UD	0.10	3.42	3.01	94.2
μ_{28}	0.99	1.8	<1	0.11	2.94	3.7	104
29	2.0	3.0	UD	0.05	30.1	40.3	370
μ_{29}	3.6	3.3	<3	0.87	30.1	60.1	533

μ_{26}; Interlaboratory mean for sample 26, Round 13 (Mattingley, 1988).
UD; undetectable.

(80°C) 4M Aristar nitric acid and left (for approximately 1 hour) to cool to room temperature (20 to 25°C) before being frozen prior to analysis. Suspended matter concentrations ranged from 2 to 40 mg total in each sample, hence the hot acid was considered adequate to extract the metals from the suspended sediments into the water. This was considered comparable to the SD-N-1 extraction of the reference sediment above.

The final solutions were analysed for Pb, Cu, Ni, and Cr by Graphite Furnace Atomic Absorption Spectroscopy (GFAAS), using aqueous calibration, peak area mode, and continuum source background correction. Tables 4.10, 11, and 12 present the detection limits, SD-N-1, and Chemaqua results respectively. Iron, Mn, and Zn were analysed by Flame AAS.

Rainfall data were obtained from the Christchurch meteorological office. High or low rainfall may affect the quantity of water in each system, and hence may dilute or preconcentrate heavy metals in the water systems. Consequently rainfall data is averaged for a three day period prior to sampling (including the day of sampling).

The Dissolved Phase was taken as the water that passed through the 0.45μm filter paper. The total water was the unfiltered water sample. Metal concentrations in the suspended sediment were calculated by subtracting metal concentrations in the dissolved phase from the total water and correcting to the volume of water and weight of suspended sediment in the respective sample.

Generally precision was excellent with errors of the means around 10% (Cu 10.1%, Pb 9.4%, Cr 8.1%, Ni 21.6%, Zn 9.9%, Mn 11.9%, and Fe 14.1%). The accuracy was over 94% for Cu, Pb, and Ni, whereas the accuracy was around 86% for Fe and Cr and 78% for Mn (Table 4.11). Iron, Cr, and Mn recoveries could probably be improved by using the technique of standard additions.

a) Water Temperature and pH

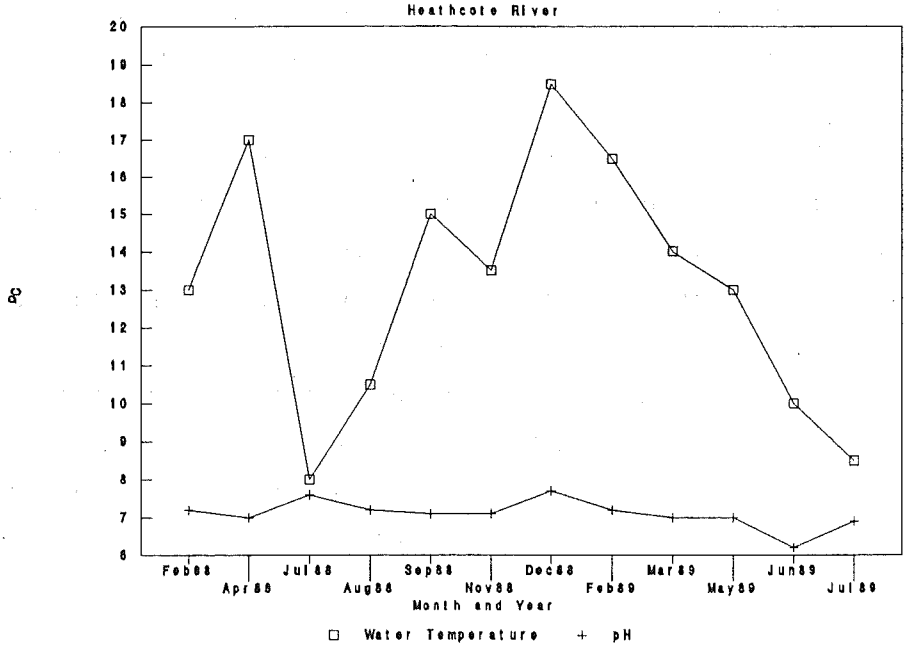

b) Water Temperature and pH

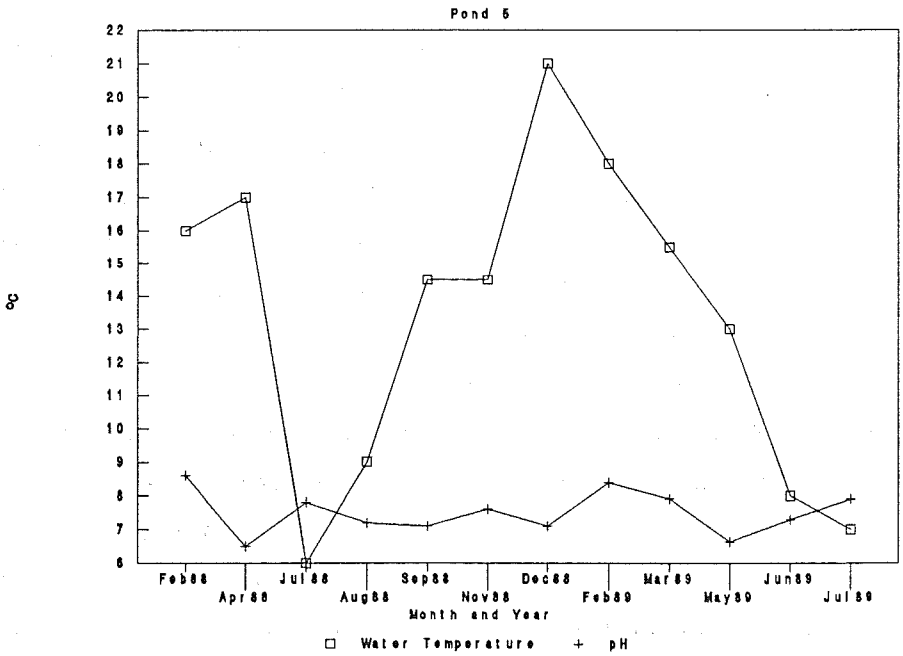

Fig. 4.19 Water temperature and pH of the Heathcote River (a) and Pond 5 (b)

4.10 SEASONAL DISTRIBUTIONS OF HEAVY METALS IN TOTAL AND DISSOLVED WATER, AND SUSPENDED SEDIMENTS

All raw data from the water study are tabulated in Appendix 3.4. The pH averaged 7-7.6 at all sites. Eh values were also fairly consistent (0.12-0.16V), but increased slightly from September to February 1989 at most sites (Table A3.10 to A3.14). As expected water temperature is higher in summer (November to February) than winter (June to August). There appears to be no relationship between the environmental measurements (Eh, and pH) and rain fall around the time of sampling (compare Fig. 4.19a and b with 4.20a).

4.10.1 Heavy Metal Distributions in the Dissolved Phase

Representative data for all metals in the dissolved phase at all sites are presented in Fig. 4.20b and 4.21 a and b (Raw data are tabulated in Appendix 3.4, Tables A3.15 to A3.19.) In ponds 5 and 6 most metal concentrations were highest in winter (June to September) and were lowest in the summer months (November to March, Fig. 4.21b). The same distributions were observed to a lesser extent in the rivers and drain. Metal distributions in the rivers (Fig. 4.20b, and 4.21a) and drain also parallel the rain fall curve in Fig 4.20a. Kim (1990) studied Pb, Cd, and Zn in the dissolved phase of the Avon and Heathcote Rivers over the period July 1987 to June 1988, and found a high correlation between Zn and rainfall.

The rise in dissolved metal concentrations during periods of high rainfall probably relates to surface runoff rich in metals from petrol emissions (Pb, Cu, Ni, Cr), galvanised roofs (Zn), house paint (Zn), and stormwater piping (Cu, and Fe). The ponds would be less affected by such runoff because stormwater is channelled to the rivers and the City Outfall Drain. The most significant increases were observed for Pb and Zn in the City Outfall Drain

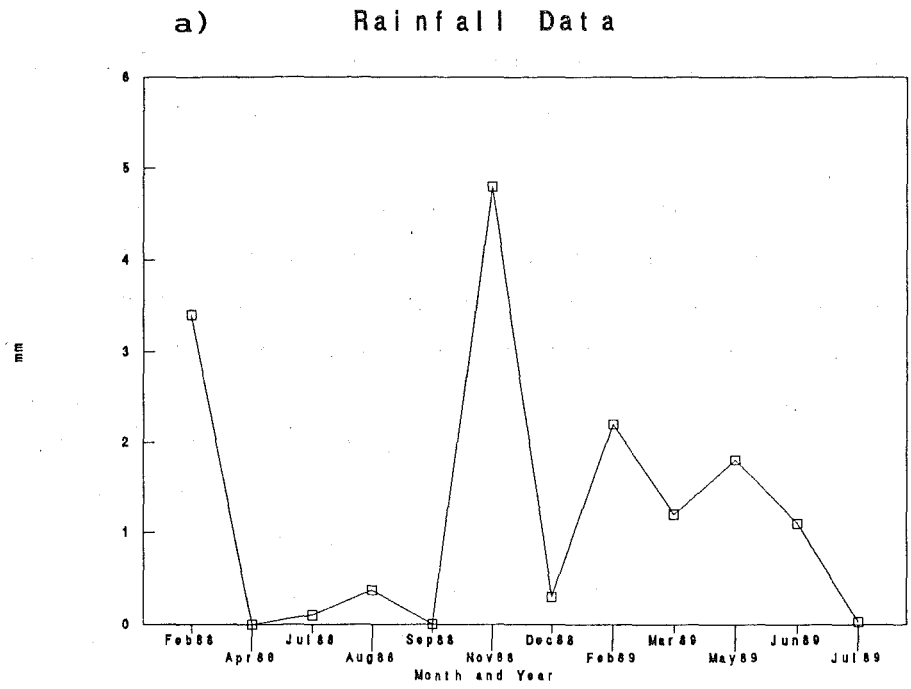

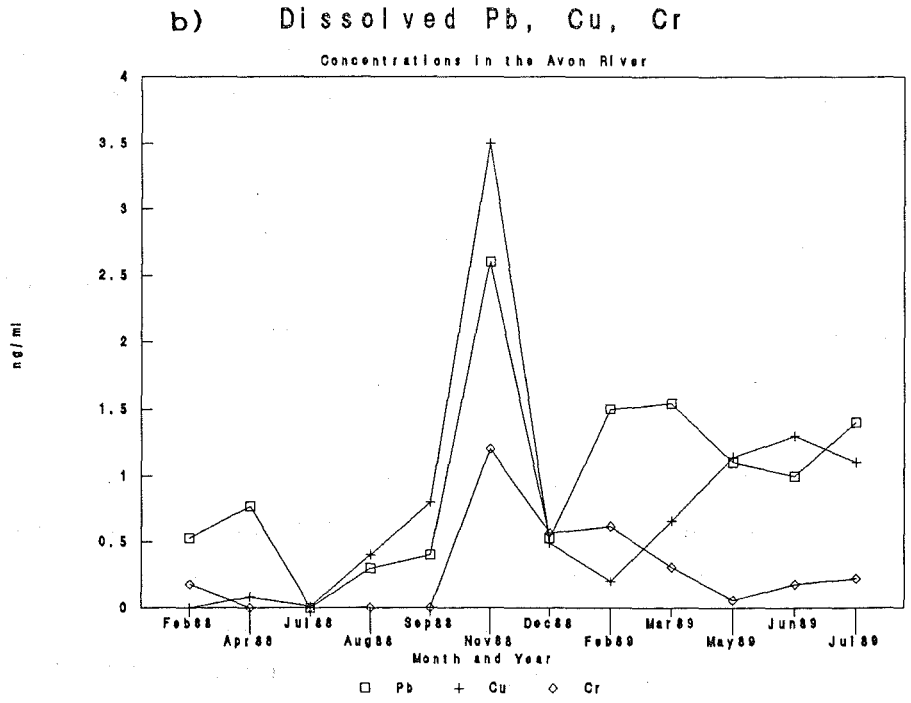

Fig. 4.20 Rainfall data (a) and dissolved Pb, Cu, and Cr concentrations in the Avon River (b).

during the high rainfall of February 1988 (3.4ng/ml Pb, and 65ng/ml Zn) and November 1988 (7.20ng/ml Pb and 108ng/ml Zn; Appendix 3.4, Table A3.17).

The pattern of high dissolved metal concentrations in winter and low in summer may reflect an increase in atmospheric emissions in Christchurch during winter. In winter, conditions are commonly less windy than summer. During periods of calm weather a smoggy haze may cover the Christchurch area. The smog is caused principally by 1) the high proportion of wood and coal-burning fires, 2) generally stable air, and 3) the low inversion layer. Because Christchurch is flat a large number of residents cycle to work in the summer months. However, during the smoggy winter months many more residents travel in motor vehicles. Hence, the concentrations of all heavy metals emitted to the atmosphere rises in winter due to an increase in coal, wood, and petrol combustion. In addition, surface runoff should increase in winter because rainfall is higher than summer. However, this pattern was obscured by the considerable length of time between sampling (6 weeks).

4.10.2 Heavy Metal and Suspended Matter Distributions in Total Water

Figures 4.22 and 4.23 contain representative curves of total heavy metal and suspended matter concentrations observed in the water courses over the sampling period. Generally, the graphs indicate that the total heavy metal content in each water system is governed by the concentration of suspended matter present. The suspended matter in the ponds is green (due to algae), whereas that in the rivers and drain is brown (due to sediment and possibly Fe hydroxides). Figures 4.22a and b show that total metal and suspended sediment concentrations are higher in the ponds in summer than winter, which reflects the high algae content of the ponds in summer. In fact

a) Dissolved Zn, Mn, and Fe

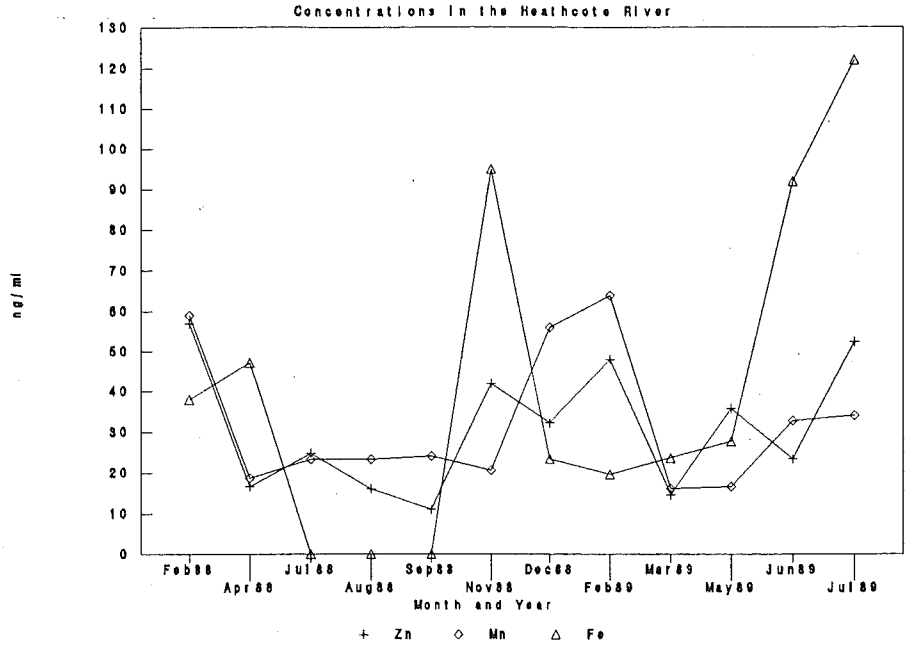

b) Dissolved Ni, Cu, Cr, and Mn

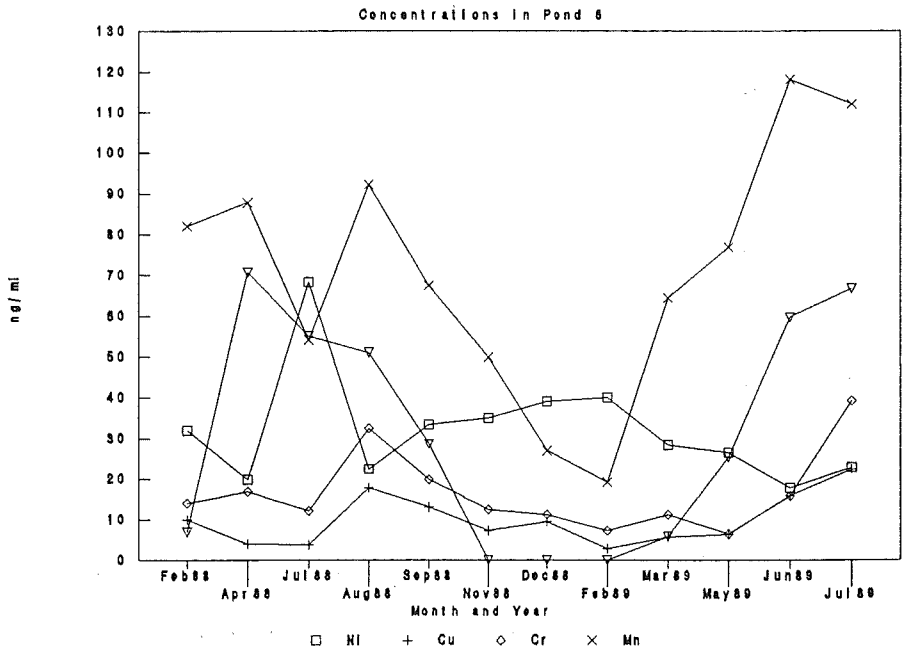

Fig. 4.21 Dissolved heavy metal concentrations in the Heathcote River (a) and Pond 6 (b).

a) Total Mn and Suspended Matter

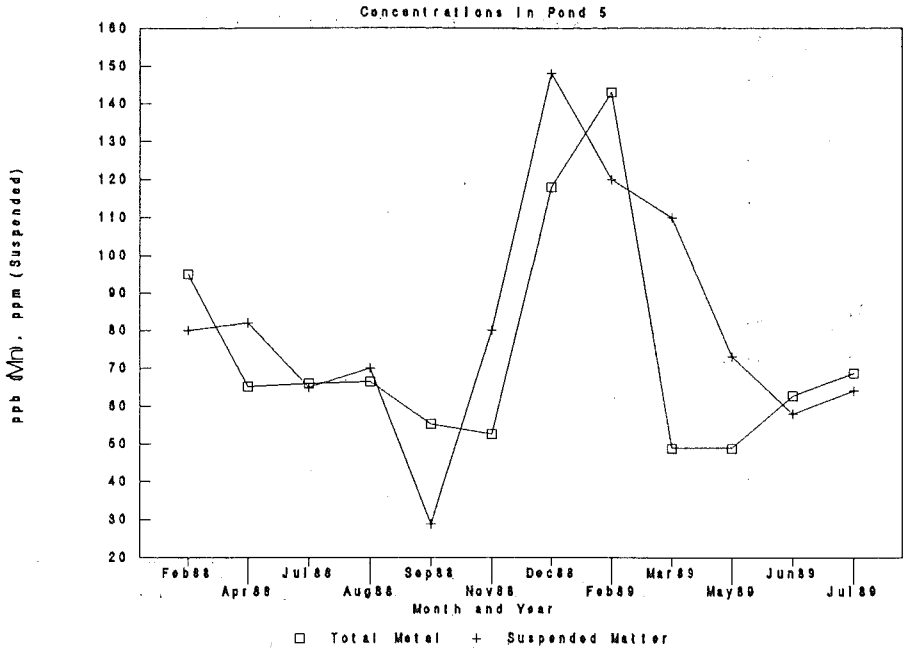

b) Total Zn and Suspended Matter

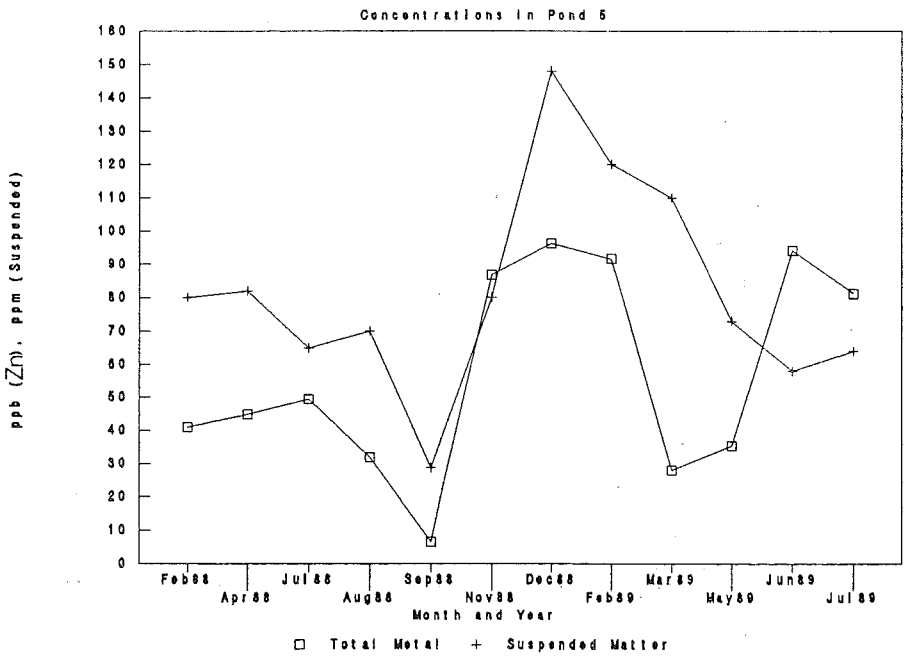

Fig. 4.22 Total Mn (a), Zn (b), and suspended matter (a,b) in Pond 5.

a) Total Zn and Suspended Matter

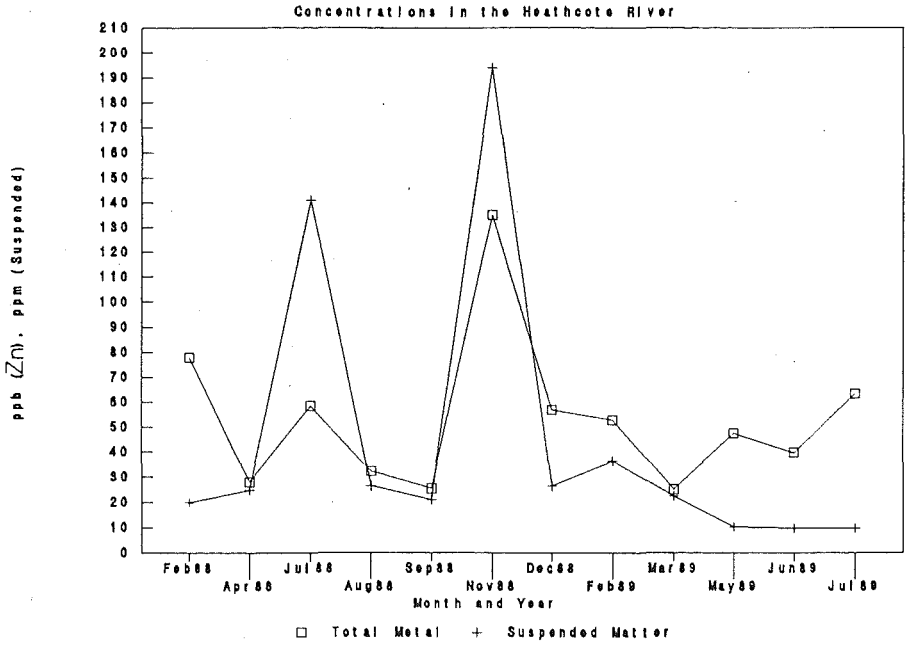

b) Total Mn and Suspended Matter

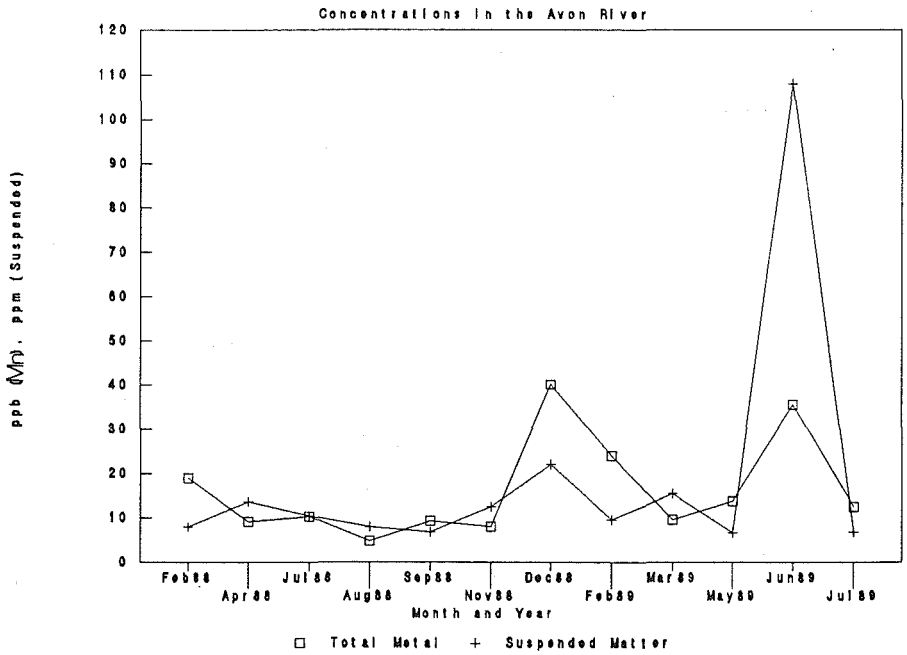

Fig. 4.23 Total Zn and suspended matter in the Heathcote River (a), and total Mn and suspended matter in the Avon River (b).

almost all of the suspended matter in the ponds is living algae (Dr. J.Robb, Biologist, Christchurch Drainage, pers comm.).

The total metal distributions in the Heathcote River, and City Outfall Drain closely parallel the changes in rainfall (Fig. 4.23a). Figure 4.23b illustrates the high correlation between total Mn and suspended matter in the Avon River, which is highest in June 1989.

4.10.3 Heavy Metal Distributions in Suspended Sediment

Typically all suspended matter heavy metal concentrations (except Mn) peak in mid winter (June-July) 1988, and 1989 (Figures 4.24 to 4.27). The high Pb levels at all sites in November 1988 most likely reflect greater stormwater runoff rich in street dust. The higher Fe concentration in the City Outfall Drain in September 1988 (Fig. 4.27b) may be caused by rust inside the upper reaches of the drain or an increase in Fe hydroxides precipitates. During the warmer spring and summer conditions, an increase in aquatic plant life probably causes an increase in dissolved oxygen concentrations in most water systems. Such conditions may enhance Fe and Mn hydroxide/oxide precipitation. The slight increase in Eh of most water systems (especially the ponds) from September to February supports such a conclusion.

Manganese suspended matter concentrations are highest in summer for all sites including the City Outfall Drain (Fig. 4.27a). This pattern suggests that as water temperatures increases dissolved Mn is precipitated as Mn hydroxy compounds. As mentioned above this pattern may relate to an increase in oxygen content of the water systems associated with an increase in aquatic plants. The trough in the dissolved Mn curve of Pond 6 (Fig. 4.21b) supports such behaviour. However dissolved Mn levels increase in the drain and Heathcote River during the summer, which may reflect metal preconcentration in the

a) Cu Concentration in Suspended Sediment

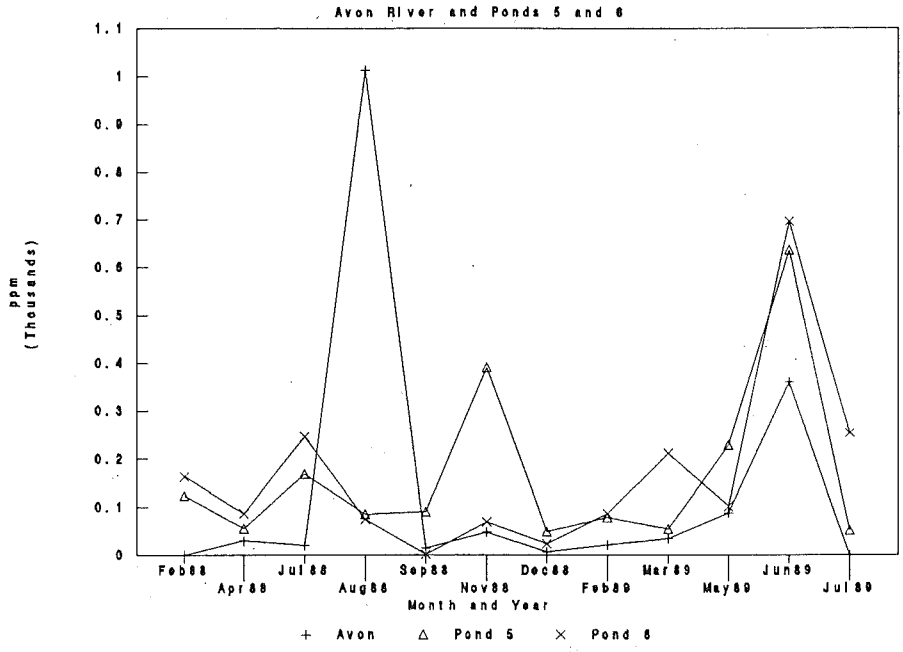

b) Cu Concentration in Suspended Sediment

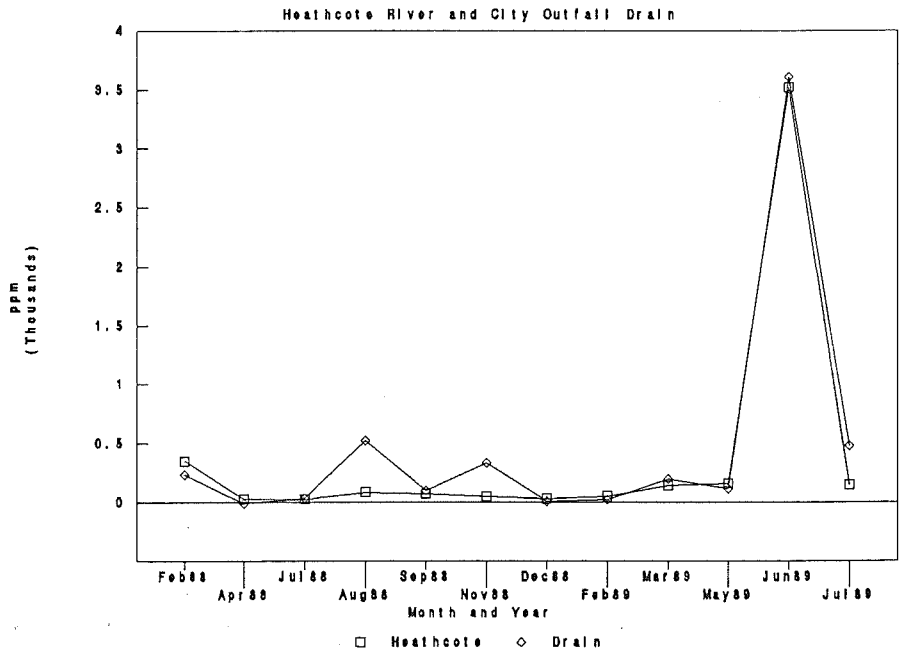

Fig. 4.24 Copper concentration in suspended sediment of non-saline water systems entering the Avon-Heathcote Estuary.

a) Pb Concentration in Suspended Sediment

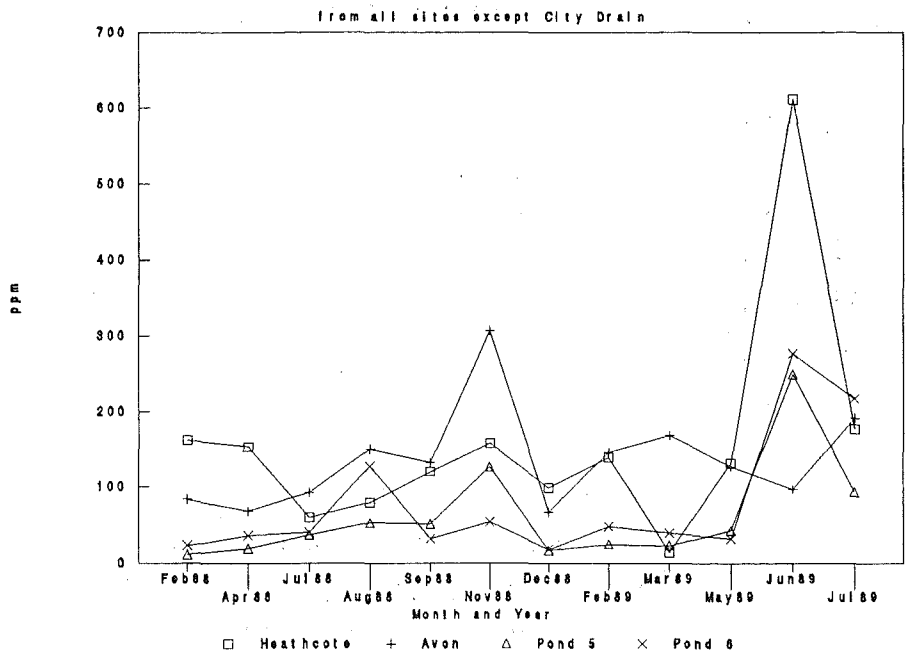

b) Pb Concentration in Suspended Sediment

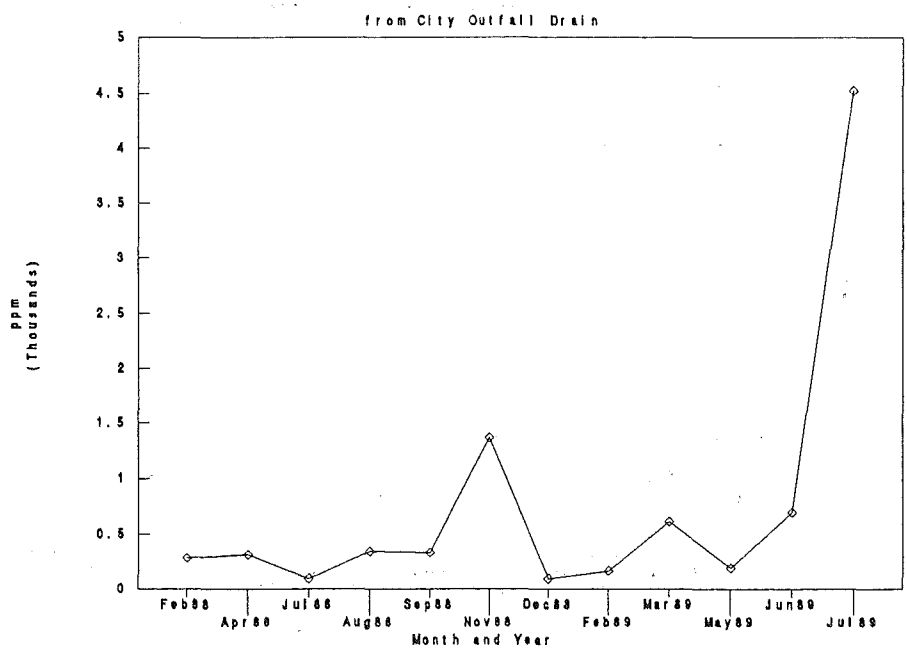

Fig. 4.25 Lead concentration in suspended sediment of non-saline water systems entering the Avon-Heathcote Estuary.

a) Cr Concentration in Suspended Sediment

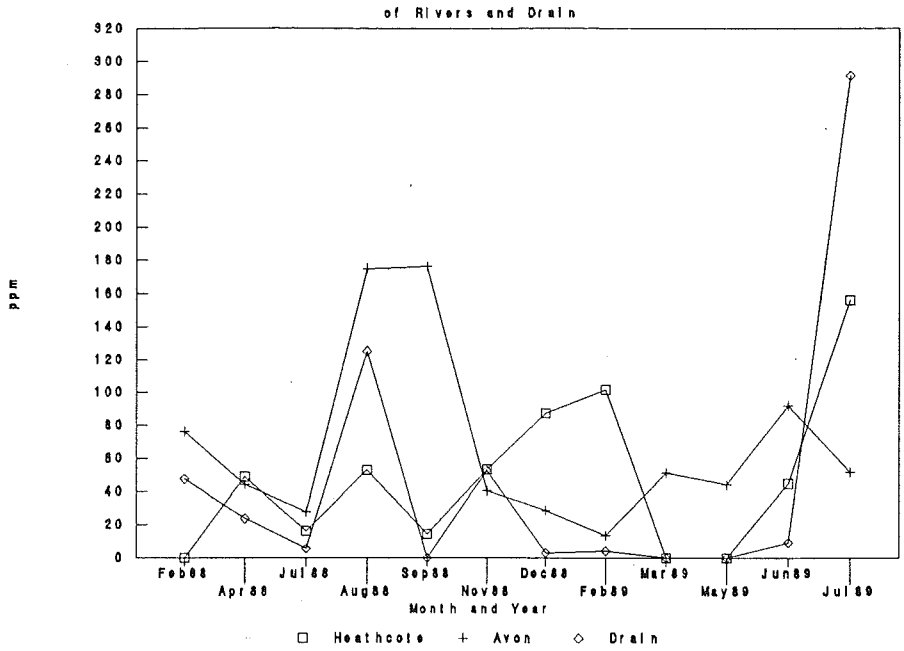

b) Cr Concentration in Suspended Sediment

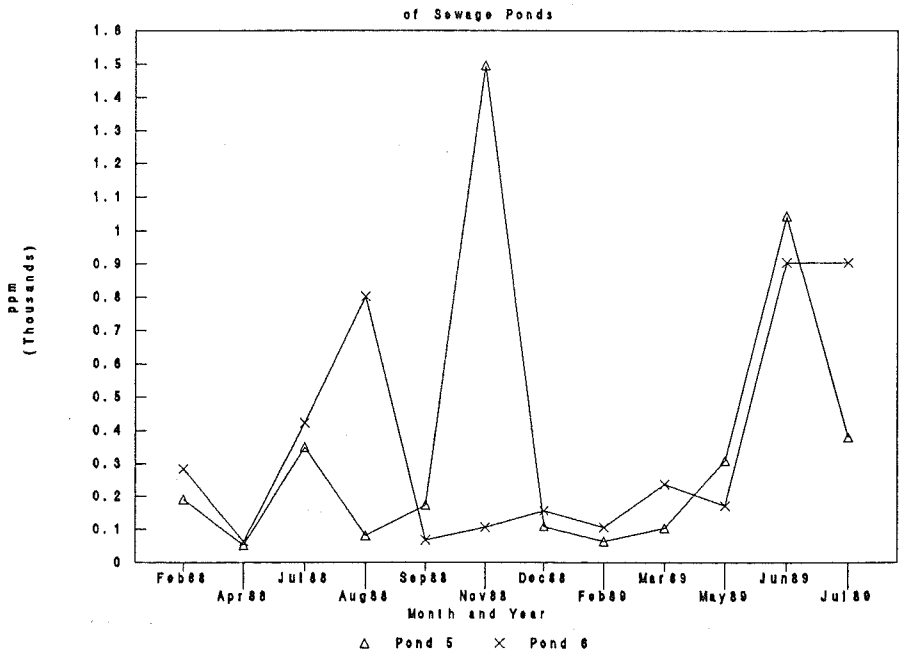

Fig. 4.26 Chromium concentration in suspended sediment of non-saline water systems entering the Avon-Heathcote Estuary.

generally lower summer water levels.

The elevated Cr suspended matter concentrations in Pond 5 during November 1988 (Fig 4.26b) suggests some sludge was collected in the sample. Bad weather conditions at the time may have stirred up the sludge in the bottom of the pond suspending it with the algae.

4.11 HIERARCHIAL CLUSTER ANALYSIS OF HEAVY METALS IN THE SUSPENDED SEDIMENT

Heavy metal relationships were examined in the suspended matter of all the water systems using the hierarchial clustering method of Massart and Kaufman (1983), which is outlined in Section 4.5. The results are presented in Fig. 4.28 (Similarity Matrices are tabulated in Appendix 3.4, Table A3.30).

Generally the rivers, drain and ponds are similar in that Fe and Mn form one cluster, and Pb and Zn form another group with or without Cu or Cr depending on the water system. Iron and Mn are not significantly correlated with the Pb-Zn group at any of the sites (α=0.05). None of the clusters except Pb-Cr is significant at the 5% level in the City Outfall Drain, which reflects the small sample size (n=12).

In the bottom sediments Fe and Mn cluster separately (Fig 4.18), whereas in the suspended sediment they cluster together. This pattern probably relates to the differing chemical environments of the aerated surface waters versus the anaerobic bed of the estuary. Referring to Figs 1.3 and 4.29 the environmental conditions (Eh 0.12 to 0.16V, and pH 7 to 7.6) and dissolved Fe and Mn concentrations (20 to 500 μg/l, Fe; 10 to 100 μg/l, Mn; Tables A3.15 to A3.19) of all water systems favour Fe and Mn precipitation as hydroxy compounds. In addition, dissolved oxygen measurements at all sites are around 8 to 10ppm, which indicates aerated water conditions (Deely, 1987). The cluster groups observed suggest that these two metals have precipitated as

a) Mn Concentration in Suspended Sediment

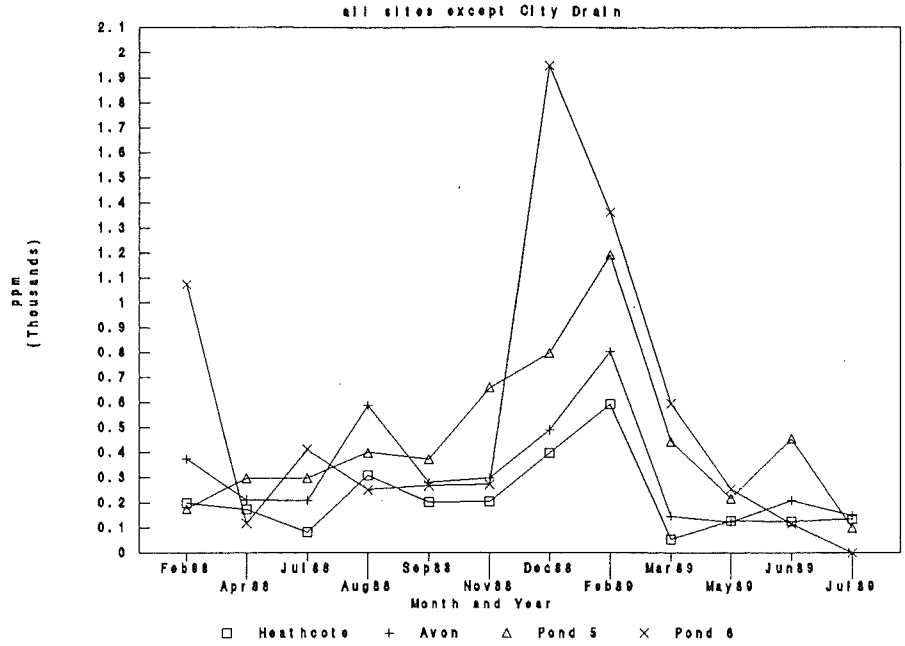

b) Fe Concentration in Suspended Sediment

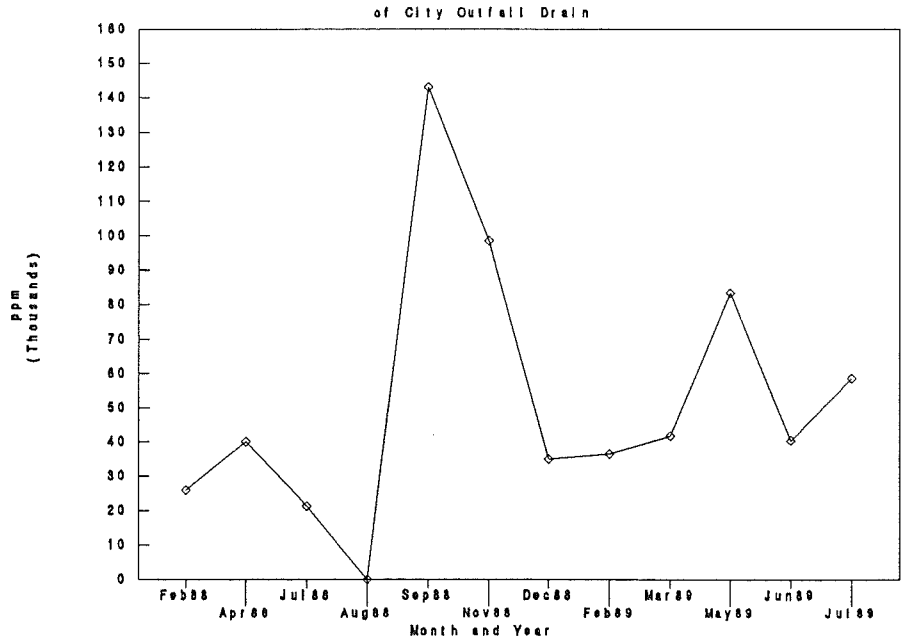

Fig. 4.27 Manganese and Fe concentrations in suspended sediments of non-saline water systems entering the Avon-Heathcote Estuary.

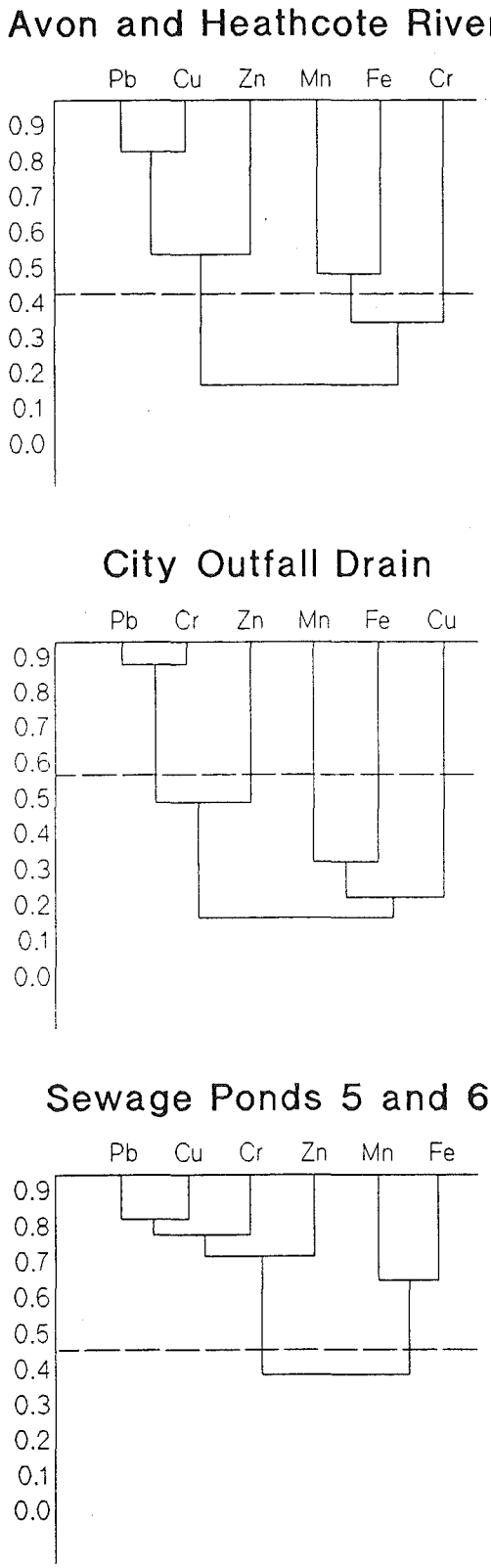

Fig. 4.28 Cluster Analysis Dendograms illustrating relationships between heavy metals in the suspended matter of non-saline water systems entering the Avon-Heathcote Estuary. -----, level of significance $\alpha = 0.05$.

hydroxides on suspended matter and are perhaps incorporated into the algal tests during growth.

The Eh and pH diagrams do not take into account the influence of ionic strength, solid and dissolved organic matter, and other inorganic phases. However, normally metal solubilities are controlled by adsorption-desorption equilibria and are below that predicted by Eh-ph diagrams (Davis, 1990; Drever, 1982). Hence, the high Mn and Fe concentrations in the dissolved phases of all the waterways would shift the carbonate and hydroxide zones of the Eh-pH diagrams (Fig 4.29) to the left favouring precipitation as hydroxy compounds. This interpretation is also supported by significant Fe-Mn correlations found in the bottom sediments of the rivers and the drain by Anderson, 1985; Hay, 1988; and Hulse, 1983. In addition, these workers also found the Pb-Zn-(Cu) cluster, which was observed in the suspended and bottom sediments of this study. Although these metals are common pollutants, this cluster probably reflects a natural chemical relationship between Zn, Pb, and Cu because it was also observed in the baseline sediments of this study (Fig 4.18).

4.12 AN ESTIMATION OF HEAVY METAL AND SUSPENDED MATTER FLUXES TO THE AVON-HEATHCOTE ESTUARY

4.12.1 Suspended Matter Fluxes

The suspended sediment fluxes have been estimated for each water system using the following flow rates: Heathcote River 97,804m^3/day; Avon River 280,800m^3/day; Pond 5 (1/3)136,575m^3/day; and Pond 6 (2/3)136,575m^3/day (Christchurch Drainage Board, 1988; Knox and Kilner, 1973; Dr J. Robb, Christchurch Drainage, pers comm.) and the mean suspended matter concentrations found in this study (Table 4.13). No data were available for the City Outfall Drain. It is assumed that the suspended load from the drain is an insignificant source of bottom sediment to the Avon-

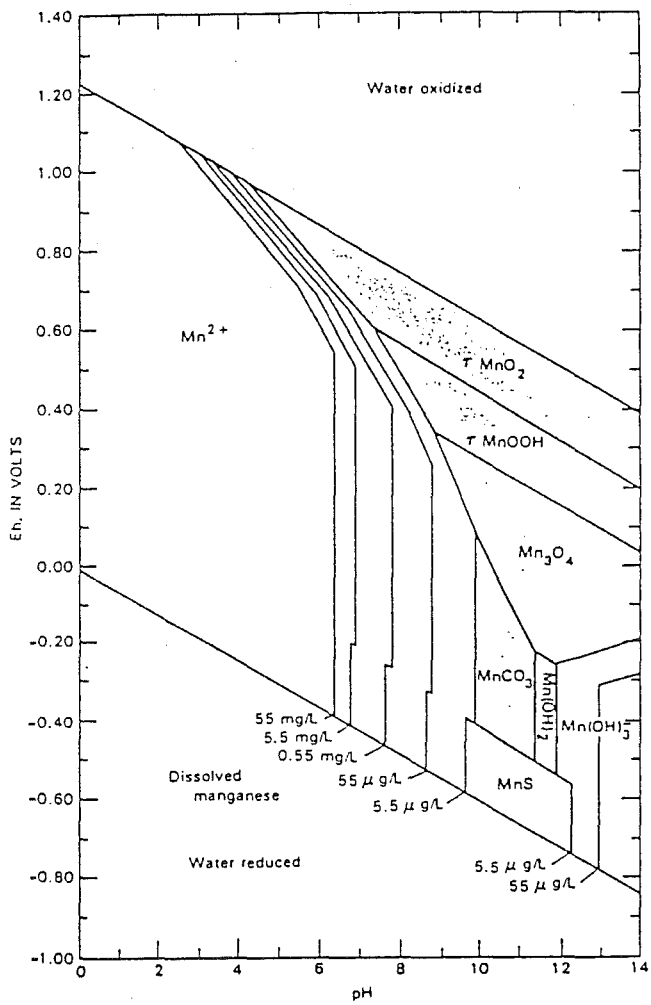

Fig. 4.29 Eh-pH stability fields of Mn at 25°C, 1 atmosphere pressure, 96mg/l SO_4^{2-}, and 61mg/l HCO_3^- (Hem, 1989).

Heathcote Estuary.

Table 4.13 Mean Suspended Matter Concentrations and Fluxes to the Avon-Heathcote Estuary

	Concentration (μg/g)	Flux (g/day)	Flux (kg/year)
Heathcote Rr	61.2±23	5,985,666	2,184,768
Avon Rr	11.4±3	3,201,120	1,168,409
Pond 5	84.2±24	3,794,873	1,385,129
Pond 6	67.6±7	6,039,347	2,204,362

The results of the present study (Table 4.13) indicate that half the Avon-Heathcote Estuary's present sediment budget from terrestrial water sources is derived from the treated effluents of the Christchurch City Council sewage ponds, whereas the other half is derived from the combined Avon and Heathcote Rivers. Analyses supplied to the author from the Drainage Board contain suspended matter concentrations ranging from 31 to 109 μg/g in Pond 5, and 32 to 62 μg/g in Pond 6 (during 1988 and 1989), which is similar to the mean concentrations presented in Table 4.13.

The majority of the suspended matter in the treatment ponds is living algae, with species varying depending on time of year and water temperatures (Dr. J. Robb, biologist, Christchurch Drainage). When the ponds discharge into the estuary many algae probably die due to the increased salinity. Even if during perfect weather conditions 80 to 90% of the effluent leaves the estuary during the outgoing tide, 10 to 20% of the effluent will be retained during two tidal cycles per day, which would cause a significant increase in the amount of organic matter deposited in the sediments.

During east and southwest winds the effluent flows south along the western flats and is ponded in the Heathcote Basin (Fig. 2.3, Section 2.1.2, Chapter). During such conditions the amount of effluent leaving the estuary would be reduced considerably. Hence, the dead algae (and other suspended sediment) probably settle and enrich the

Table 4.14 Average Heavy Metal Concentrations in Suspended Matter

	Pb µg/g	Cu µg/g	Ni µg/g	Zn µg/g	Mn µg/g	Fe %	Cr µg/g
Heathcote	159.00	103.00	3.00	752.00	217.00	2.27	48.00
Avon	136.00	136.00	12.00	622.00	323.00	2.70	69.00
Drain	753.00	470.00	7.00	1888.00	825.00	5.20	47.00
Pond 5	63.00	168.00	65.00	531.00	450.00	.34	362.00
Pond 6	79.00	168.00	13.00	462.00	555.00	.29	352.00
TS (Av)	33.20	22.95	30.75	100.95	189.00	4.56	72.50

Errors; 20 to 50 %, α=0.05, TS (Av) average values for TS/1 and TS/3

Table 4.15 Heavy Metal Concentrations in the Clay Fraction of Unit D Sediments

	Pb µg/g	Cu µg/g	Ni µg/g	Zn µg/g	Mn µg/g	Fe %	Cr µg/g
Surface							
1a	189.00	96.00	72.10	540.00	340.00	6.59	196.00
2a	52.00	60.00	30.00	130.00	180.00	4.90	80.00
3a	28.50	56.10	55.70	340.00	190.00	4.54	194.00
5	92.00	74.40	61.00	303.00	297.00	4.00	118.00
6	140.00	124.00	33.20	462.00	290.00	5.10	182.00
RH2*	244.00	62.70	42.90	528.00	1120.00	7.57	202.00
Average values for whole depth of Unit D							
1a	153.00	67.60	63.90	430.00	279.00	5.95	199.00
2a	50.10	63.90	28.90	126.00	186.00	4.40	73.50
3a	60.30	52.00	49.90	341.00	212.00	5.00	179.00
5	92.00	74.40	61.00	303.00	297.00	4.02	118.00
6	143.00	104.00	40.10	490.00	279.00	5.33	180.00
RH2	150.00	67.80	48.50	406.00	1345.00	8.73	189.00

*, Data from Hay (1988); errors are 10-20% of the mean values

organic detritus in the Heathcote Basin.

The results of this study suggest that the treatment ponds are supplying high concentrations of organic matter in the form of dead algae to the estuary. Such high levels of organic matter (combined with N and P compounds in the effluents) are most likely largely responsible for the anaerobic conditions which predominate in most areas of the estuary. These results support the findings of previous studies such as Knox and Kilner (1973), which show that the estuary is in a state of eutrophication brought about by the pond effluents.

4.12.2 Mean Heavy Metal Concentrations in suspended Sediment

Table 4.14 presents the mean heavy metal concentrations in the suspended sediment of the different water systems and the background values estimated from the clay fraction of Travis Swamp. For comparison the heavy metal concentrations in Unit D clay are given in Table 4.15. It is assumed that the suspended sediment is in the grain size range $<4\mu m$ and that the proportion of metal extracted from the suspended sediment is similar to that extracted from the bottom sediments (based on the excellent SD-N-1 metal recoveries from both studies). Due to the high errors (caused by seasonal variation) enrichment calculations were not undertaken.

Despite the high errors, a few useful trends are apparent. Firstly the City Outfall Drain is significantly elevated in Pb, Cu, Zn, Mn, and Fe relative to the other water systems. Secondly the suspended matter of the sewage ponds is enriched in Cr, and low in Pb, and Fe relative to the drain and rivers. None of the waterways is enriched in Ni.

All systems are enriched in Cu and Zn relative to the Travis Swamp (TS (Av)). Lead is predictably high in the drain and rivers, whereas Cr does not appear to be enriched

Table 4.16 Average Heavy Metal Concentrations in the Dissolved Phase

	Pb ng/ml	Cu ng/ml	Ni ng/ml	Zn ng/ml	Mn ng/ml	Fe ng/ml	Cr ng/ml
Heathcote	.18	1.33	1.88	31.20	32.40	40.70	1.38
Avon	.97	.81	0.00	8.95	11.03	185.00	.28
Drain	1.07	.88	.18	33.00	71.00	181.00	.52
Pond 5	.61	6.50	29.80	15.70	31.90	120.00	10.10
Pond 6	1.15	9.87	32.12	26.50	30.80	199.00	16.60

Errors; 20 to 50 %, α=0.05

Table 4.17 Baseline Dissolved Heavy Metal Data from New Zealand Rivers and New Zealand Water Quality Criteria

BASELINE WATER (NZ)	Pb ng/ml	Cu ng/ml	Ni ng/ml	Zn ng/ml	Mn ng/ml	Fe ng/ml	Cr ng/ml
Waitekauri Valley (1)	<.09	.25	.22	.90	-	-	.21
Coromandal Streams (2)	.50	.50	-	1.00	92-240	-	-
Manuherikia Valley (3)	.03	.15	.10	.15	-	-	-
WATER QUALITY CRITERIA (4)							
Drinking Water (NZ)	50.00	50.00	13.40	5000.00	-	-	50.00
Fish & Shellfish	2-50	30.00	100.00	40-170	-	-	50.00
Ecosystem Protection	25.00	4.00	7.10	58.00	-	-	18.00

(1) Kennedy et al., 1987; (2) Tunnicliff and Beaumont, 1986;
(3) Ahlers and Hunter, 1989; (4) Smith, 1982 and 1986; Williams, 1985
(based on US EPA standards, 1985; & NZ Board of Health standards, 1984)
-, no data

in these water courses. The Fe content of the suspended sediments is about half that in the bottom sediments of the Avon-Heathcote Estuary. The increase in Fe going from the non-saline water systems to the estuary suggests that this metal is precipitated as hydroxy compounds during estuarine mixing. This conclusion is supported by low Fe concentrations in most Christchurch street dust (2.39%) and soil (2.0%).

The higher concentrations of Pb, Zn, and Mn found in the suspended sediment of the drain and rivers is paralleled in Unit D clay of cores AHE/1a, 6, and RH2 from the associated depositories. The Cr content (352 to 362μg/g) in the suspended matter of the ponds is higher than in Unit D sediments of core AHE/3a (194μg/g); this discrepancy could be due to dilution by the low Cr sediments of the estuary.

The low Pb levels in the ponds are also found in Unit D sediment of core AHE/3a. Hence, the predominant water currents flowing south from the ponds into the Heathcote Basin prevent stormwater from the drain affecting sediments on the western slopes.

4.12.3 Mean Heavy Metal Concentrations in the Dissolved Phases of Each water System

Generally the dissolved metal concentrations are 1000 to 100,000 lower than in the suspended matter (Table 4.16 versus 4.14). As for the suspended sediment data, errors are high as a result of seasonal variability. In the dissolved phase Cu, Ni, and Cr are significantly elevated in the ponds compared with other water systems.

A comparison of the dissolved metal results of this study with the sparse baseline data available from New Zealand back country springs and rivers (Table 4.17) suggests that Zn levels are significantly enriched in all water systems. The high Cr, Cu, and Ni values in the ponds are also significant.

Elevated metal concentrations in ponds 5 and 6 are most likely influenced by the sewage sludge on the floor of the ponds (Table 4.1).

The high Zn levels in the rivers and drain most likely reflect stormwater runoff containing Zn from roofing and paint pigments. The generally lower dissolved heavy metal content of the Avon River probably reflects the higher flow (and water volume) in this river relative to the other systems (Section 4.12.1).

The low Pb levels in water of the rivers and drain (in contrast to high Pb concentrations in the corresponding suspended sediment) supports the conclusion that most anthropogenic Pb in the estuary and associated water systems is derived from street dust.

Local baseline data on Fe and Mn levels in water was not obtained. Hem (1989) states that typical Fe and Mn concentrations in aerated river waters at normal pH ranges are around 10ng/ml and 1000ng/ml respectively. However, these concentrations vary considerably because many Fe and Mn inorganic and organic colloids pass through 0.45μm filters. The high Fe levels in water of this study indicate that some colloidal Fe species are present.

The dissolved concentrations of most metals are below New Zealand's requirements for safe human consumption of water and shellfish (compare Tables 4.16 and 4.17). However Cu, Ni, and Cr levels in the ponds and Zn levels in all the waterways are fairly close to the maximum levels recommended to protect natural ecosystems.

4.13 CONCLUSION: HEAVY METALS IN SUSPENDED MATTER AND WATER OF THE NON-SALINE WATER COURSES ENTERING THE AVON-HEATHCOTE ESTUARY

The suspended matter and water (dissolved phase) of the sewage ponds are high in Cr, Zn, and Cu. These metals are most likely derived from the sewage sludge. In addition the dissolved phase of the ponds is also high in Ni, which

is not affecting sediments in the estuary. The combination of slowly increasing effluent discharge and high metal and suspended matter concentrations suggests that the ponds are the source of the rising Cr, Cu and Zn concentrations in Unit D sediments of Cores AHE/1a, 3a (and b), and 6, as well as organic matter in Unit D of all cores.

The very high Pb, Cu, Zn, Mn, and Fe, in the suspended sediment of the City Outfall Drain indicates that this drain is a source of these metals to the sediments in the Heathcote Basin. This conclusion is supported by the rising metal levels from the base of Unit D towards the surface in cores RH2 and AHE/1a. Iron and Manganese are probably preconcentrated in the drain sediments as authigenic oxyhydrates.

The high Zn levels in the dissolved phase of all water systems are probably due to stormwater containing Zn washed from galvanised roofs, house paint (rivers and drain) and sewage sludge (ponds). The very high Zn levels in the bottom sediments of the City Outfall Drain (2080μg/g) relative to Christchurch Street Dust and soils (135 to 850μg/g) suggests that dissolved Zn is rapidly adsorbed onto sediments as it enters the drain.

The low Pb levels in the pond suspended matter and Unit D sediment of cores AHE/3a and b indicate that the influence of the drain is localised to the Heathcote Basin and provides further evidence that wind induced water circulation patterns in the estuary are causing localised enrichment in the Heathcote Basin.

The increase in dissolved and suspended matter metal concentrations in the ponds during winter probably reflect the drop in algae and increase in atmospheric emissions of most metals associated with cold weather.

The parallel behaviour of heavy metals and rainfall in both the suspended and dissolved phases of the rivers and drain suggests that the principal present day source of metals to these water courses is stormwater runoff. The general metal increase in the waters during winter also

supports a stormwater origin for most metals. Generally in winter, coal and petrol combustion increases in Christchurch. Hence, stormwater will be richer in most metals over the winter period. Other supporting evidence comes from the high metal levels in the Christchurch street dust (such as 10700μg/g of Pb at Riccarton Road) and present day bottom sediments of the City Outfall Drain (3296μg/g Pb) and both the Avon and Heathcote Rivers. The high Pb levels in Christchurch Street dust and some soils suggests that petrol combustion is having a significant affect on **most** sediments in the Christchurch metropolitan area including the estuary. The Pb concentrations in river and drain suspended matter are probably also influenced by occasional industrial contamination.

The cluster analyses of the suspended and bottom sediments suggests that Fe and Mn are transported as hydroxy compounds in most water systems, with minor association with the other heavy metals. The Pb-Zn cluster is found in all bottom sediment grain sizes and all suspended sediments, which indicates a strong relationship between these two metals regardless of source (anthropogenic or lithogenic).

Although organic matter was not studied in the water systems, it seems probable that most of the anthropogenically-derived heavy metals are transported attached to organic matter (colloidal and solid) in the water systems. Solid organic matter is probably attached to the suspended sediment.

The non grouping between Fe, Mn, and organic matter in the bottom sediments (Fig. 4.18) suggests chemical transformations occurring during estuarine mixing include 1) coagulation of organic matter with metal desorption, and 2) Fe hydroxy precipitation with little or no metal adsorption. Other data that suggest Fe hydroxide precipitation during estuarine mixing include 1) the higher Fe concentrations in the clay fractions of the bottom sediments compared with suspended sediment and Christchurch

soils and street dust (Tables 4.1, 4.14 and 4.15), 2) the presence of red crusty goethite type matter in the sand fractions, and 3) observations by Millward (1975) of high Fe oxide levels in the muddiest areas of the estuary (possibly near the turbidity maxima).

Manganese levels are not significantly different between the suspended and bottom sediments. However, the bottom sediments show more significant Mn-heavy metal correlations than the sediments of the non-saline water systems (suspended and bottom). This result suggests that somewhere in the estuarine mixing and sediment deposition process Mn oxides/sulphides have adsorbed heavy metals. Bottom sediments are strongly anaerobic, hence Fe and Mn phases are more likely to be sulphides than oxides. Manganese oxides precipitated during estuarine mixing may adsorb metals released from organic matter during coagulation and flocculation. Alternatively, heavy metals may be adsorbed on Mn compounds after deposition. Soon after mixing sediments are deposited on the bed of the estuary where they enter a reducing environment. Under these conditions oxides and hydroxides are dissolved and sulphide compounds are formed. Hence, metals may be adsorbed onto Mn phases after deposition.

CHAPTER 5

A SYNTHESIS OF CHANGES IN SEDIMENT AND HEAVY METALS THROUGHOUT THE HISTORY OF THE AVON-HEATHCOTE ESTUARY

The following chapter synthesises conclusions from the historical, geological and heavy metal investigations presented in Chapters 2, 3, and 4 of this thesis.

The discussion of the Avon-Heathcote Estuary is divided into five main historical periods: 1) pre-1850 A.D., 2) 1850 to 1925, 3) 1925 to around 1950, 4) 1950 to 1972, and 5) 1972 until 1990.

5.1 PRE-1850

About 2000 years ago the east coast was 1-2km inland of its present position. A shallow protected bay (containing Unit T4 as the bottom sediment) existed at the position of the Travis Swamp. At the time the Avon River discharged from the north into the bay. As the bay prograded southeastwards an estuary formed near the head of the bay. Sediment units, B', T2, and T3 were laid down inside the estuary, whereas Unit A' accumulated inside the inlet and along the coast. At about the same time, the Heathcote River discharged into the sea south west of the Heathcote Basin (Fig 3.11). The area of the Avon-Heathcote Estuary was probably occupied by shallow coastal waters, where Unit A formed the bottom sediment.

Polynesian activity which caused large scale burning and deforestation of the Canterbury plains, between 500-700 years B.P., may have started the major Ohuan dune-building phase around 500 years B.P. Erosion resulted in large quantities of sediment entering the major rivers (including the Ashley, and Waimakariri). The east coast prograded as the sediment accumulated. Swamps replaced estuaries (Travis

Swamp), and estuaries migrated seaward replacing shallow coastal waters (Avon-Heathcote and Saltwater Creek Estuaries).

The Avon-Heathcote Estuary probably formed as sediment supplied to the coast by the Waimakariri River drifted southward with long-shore currents. Growth of the South Brighton spit would have gradually swamped the Avon River forming the Travis Swamp (Unit T1). When the spit reached Banks Peninsula growth would have ceased, ponding the Avon and Heathcote Rivers together in the Avon-Heathcote Estuary. The sharp contact between units A and B and the uniform character of Unit B sediment suggests that this transition was fairly rapid and that the estuary was stable from 450 years B.P. until the arrival of the European settlers in 1850 A.D.

During the pre-European period heavy metal levels were a natural baseline unaffected by Polynesian activity.

5.2 1850 TO 1925

5.2.1 Changes in Sedimentation

When the European settlers arrived in 1850 AD the bed of the Avon-Heathcote Estuary consisted of Unit B muddy sand, which was accumulating at a slow rate around 0.15cm per year. The Christchurch area consisted largely of swampy terrain interspersed with sand dunes. Both the Avon and Heathcote rivers meandered across the swampy areas. The river channels were 7 to 10 metres deep in most places, and formed wide meanders with several large loops as they traversed the estuary.

The laying of 7 stormwater drains, 3 to each river and 1 to the estuary between 1875 and 1880 lowered the Christchurch water table and caused a major silting period in the Avon and Heathcote rivers. Siltation was enhanced by the low water gradients, combined with prolific growth of introduced plants, such as willows and watercress in the

river beds. Silting also affected the City Outfall Drain. The silt washed into the drain and rivers consisted of Late Pleistocene loess, which flanks the north west side of Banks Peninsula, and forms most of the dunes and swamps of Christchurch (such as the Travis Swamp).

Some silt may have reached the estuary during this period. However, the early period of settlement from 1850 to 1925 had little affect on sedimentation in the Avon-heathcote Estuary which is evident from the uniform grain size distributions and low sedimentation rates (0.27cm per year) of Unit B sediment.

The construction of the Tram Causeway across McCormacks Bay in 1907 resulted in the erosion of Skylark Island and changes in the positions of the channels in Moncks Bay. The increased supply of sediment to the mouth of the estuary caused changes in the inlet and spit configuration around 1920.

5.2.2 Changes in Heavy Metals

Many industries developed in the Woolston area between 1860 and 1880. Widespread coal burning by domestic and industrial users created a smoggy atmosphere, particularly in Woolston and Sydenham. Because early urban activities in Christchurch caused only a minor increase in sedimentation rates in the Avon-Heathcote Estuary (0.15 to 0.27cm/year) this period can be identified by a black sooty layer rich in coal, coke, and ash particles. Coal burning debris entered the estuary via the rivers and City Outfall Drain.

The Heathcote River was rapidly silting at the same time that it was being contaminated with industrial wastes. Runoff from market gardens, developed in the Heathcote Valley between 1912-14, intensified silting and possibly diluted some of the pollutants deposited in the river during this period. While the heavier sediment accumulated in the rivers the lighter coal and ash particles were carried into the estuary. Ash particles would also have

reached the estuary through airborne emissions.

During the major "iron working" period between 1880 and 1925 high concentrations of heavy metals and organic matter accumulated in sediment near the top of Unit B. Most metals (Pb, Cu, Ni, Zn, and Cr) were derived from industries along the Heathcote River and stormwater runoff (from the rivers and the City Outfall Drain).

The high Fe and Mn concentrations in sediments of the early period may relate to Fe and Mn sulphide precipitation. These deposits may also contribute to the black colour of the sediment. The high organic matter levels probably caused the anaerobic conditions necessary for sulphide precipitation. (Coal combustion and Fe industries were also a source of Fe and Mn, but emissions were probably not high enough to account for the level of enrichment observed in the sediments.)

5.3 1925 TO 1950-60

5.3.1 Changes in Sedimentation

Most of the silt deposited in the Avon and Heathcote Rivers from 1880 to 1925 was swept into the estuary by a mechanical river sweeper, between 1925 and 1950. During this period the silt supply to the rivers increased as a result of large scale stormwater drain laying to the outer suburbs of Christchurch City. Hence, it was necessary to continuously clear the rivers on and off for 30 years, until most of Christchurch's surface was paved.

As Unit C accumulated, the estuary bed changed from predominately sand and sandy mud to almost entirely mud. The rapid deposition of Unit C (6-12cm per year) caused the disappearance of the eelgrass Zostera and possibly other flora and fauna. Contemporaneously, the estuary received a continuous release of untreated wastes from 5 septic tanks along the southern shores of the estuary, a starch factory

in the Humphreys Drive area, and industries along the banks of the Heathcote River, as well as the partially treated wastes of the CDB treatment plant. The combined affect of rapidly accumulating fine grained substrate, and widespread discharge of organic and nutrient rich effluents lead to pockets of organically polluted sediment adjacent to the outfalls. These areas included 1) the Heathcote and Avon depositories, 2) areas adjacent to the Ferrymead, St Andrews Hill, Mt Pleasant, and Redcliffs septic tank outfalls, and 3) the western slopes. Euglena, and sewage fungus numbers were high in these areas and shellfish virtually disappeared. The increase in nutrients and organic matter, and fine grained sediment deposited during this period caused eutrophication of the estuary. Hence, new forms of organic life flourished in areas away from the contaminated zones and bioturbation was intense. In addition, due to an increase in organic detritus the sediment was anaerobic in many parts of the estuary.

It is unclear from the historical and geological evidence presented, exactly when Unit C deposition ceased, but it was sometime between the late 1940's and early 1960's and may have varied from area to area. There is no evidence of widespread erosion over a long period. However, one would expect considerable re-working and redistribution of sediment as a result of the intense bioturbation. The evidence suggests that erosion was principally confined to the perimeter of the estuary and the edges of the river channels, where no Zostera plants were present to bind the sediment together. The ever increasing tidal compartment, caused by runoff from the CDB treatment plant and upgrading of stormwater facilities in Christchurch, is responsible for the erosion around the perimeter of the estuary.

5.3.2 Changes in Heavy Metals

During this period many early industries died out, but the pollution of the Heathcote River remained severe.

Despite the large quantities of industrial and domestic waste discharged into the estuary system between 1925 and 1950, the heavy metal and organic matter concentrations in Unit C are not significantly elevated relative to baseline concentrations. A combination of rapid sedimentation rate and higher clay and silt content diluted the effects of contamination.

5.4 1950 TO 1972

5.4.1 Changes in Sedimentation

The combination of 1) the stabilisation of the spit, 2) recolonisation of the Zostera plants along the edges of channels, and 3) reduced sedimentation rates (around 0.5cm per year) indicates that the estuary stabilised between 1950 and 1972. Muddy sand similar to Unit B (Unit D) accumulated.

5.4.2 Changes in Heavy Metals

The sudden decrease in sedimentation rate resulted in heavy metal and organic matter concentrations increasing rapidly from the base of Unit D until a point which corresponds with the early 1970's. Christchurch had an unexpected population growth between 1950 and 1960, which resulted in the number of sewer connections tripling. Hence, the quantity of effluent discharged from the CDB Treatment Plant grew, which contributed to the increase in organic matter levels in the sediment. However, most effluents have not had much effect on the eastern shores since 1950.

5.5 1972 UNTIL 1990

5.5.1 Changes in Sedimentation

Today Unit D is slowly accumulating (around 0.5cm/year) in most areas of the estuary. The anaerobic conditions of the estuary bed are being maintained by 1) the large quantity of effluent discharged from the treatment plant, 2) organic matter decay in the sediments, and 3) remobilisation of nutrients from sediments deposited before 1972.

5.5.2 Changes in Heavy Metals

Between 1968 and 1972 the starch factory in Humphreys Drive closed down and all the industrial and domestic effluents discharging into the estuary and Heathcote River were diverted to the Christchurch Drainage Board Treatment Plant. The sudden removal of over 10 million litres per day of untreated wastes resulted in a dramatic drop in metal concentrations in sediments deposited in the estuary shortly after 1972.

Even though, in 1973, the treatment plant ceased discharging effluent into the estuary during the incoming tide, the quantity of effluent and suspended sediment (predominately algae) discharged from the ponds has slowly increased. Consequently, sediment organic matter levels have continued to rise throughout the estuary.

The Cr, Cu, and Zn concentrations in sediments on the western slopes and the Avon depository are slowly rising due to the treatment plant effluent.

The Heathcote Basin is the major sink for heavy metals and organic matter in the Avon-Heathcote Estuary. Stormwater high in Pb, and Zn entering the estuary via the Heathcote River and City Outfall Drain is ponded in the Heathcote Basin during most incoming tides. In addition, the predominant tidal currents push the Avon River south

across the western shores forcing the effluents from the ponds and the Avon River water into the Heathcote Basin to be ponded with waters from the City Outfall Drain and Heathcote River. Such conditions are enriching sediments in the Heathcote Basin in all metals and organic matter. Consequently, the Heathcote Basin could be a potential source of heavy metals to overlying waters during stormy periods. In contrast the eastern shores are not receiving significant quantities of metals from any source. However, eutrophication is affecting organic matter levels throughout the estuary.

Elevated metal levels in front of the old Mt Pleasant drain may be due to a thermal spring in the area.

Zinc and Pb are the most significantly enriched metals in sediments at the head of the estuary. Street dust containing Pb from petrol emissions is the predominant source of Pb to the estuary. Zinc is derived from 1) stormwater runoff containing Zn from galvanised roofing and zinc oxide house paints, and 2) the sewage effluents.

As tetraethyl leaded petrol is slowly replaced by unleaded petrol in the next few years the lead levels should dramatically drop in sediment of the Avon-Heathcote Estuary. Zinc and organic matter levels will probably not decrease because galvanised Fe is still a major building material and the quantity of effluent discharged from the treatment ponds seems to be slowly rising.

Generally Ni, Fe and Mn are not significantly enriched in sediments currently being deposited in the estuary except near the City Outfall Drain. High Fe and Mn concentrations in this area are most likely caused by precipitation and concentration of these metals in sulphides.

Further research would be useful to establish any heavy metal contamination in the Moncks and McCormacks Bay areas and to monitor changes in metal and organic matter levels in the estuary bed over the next 10 years.

5.6 POSSIBLE METAL PHASE RELATIONSHIPS IN THE AVON-HEATHCOTE ESTUARY

Most Fe and Mn probably enter the estuary as hydroxy compounds in the aerated water from the rivers, drain and ponds. Other heavy metals most likely enter the estuary primarily associated with clay mineral phases, organic matter, and adsorbed onto Fe/Mn hydroxy compounds.

During estuarine mixing the rising pH and salinity cause dissolved Fe to precipitate as hydroxides in turbidity maxima regions near the head of the estuary. Flocculation and coagulation of organic colloids and solids may result in some metal desorption from these species. Manganese oxides may adsorb some metals desorbed from the organic matter.

Once sediments are deposited they enter a reducing environment where organic matter decays depleting sediments, even at the surface in oxygen. Near the head of the estuary Fe and Mn sulphides, organic matter, and clay minerals are the main substrates available for metal attachment in the sediment. In the Avon-Heathcote Estuary, most metals are probably adsorbed or coprecipitated onto Mn sulphides, which themselves coat mineral (predominantly clay) surfaces. In Unit B organic matter is also an important heavy metal substrate. In more recent sediments organic matter and Fe phases are less important than Mn phases for heavy metal attachment in the bottom sediments of the Avon-Heathcote Estuary. However, since 1950, Fe-heavy-metal associations are more significant than earlier, which suggests that Fe phases are increasing in importance as heavy metal substrates. Such a change may be brought about by an increase in Fe sulphide precipitation in the sediments. The cause may be a combination of slow sedimentation rate, anaerobic conditions, and high levels of sulphide ions.

CHAPTER 6

METHODS AND QUALITY CONTROL IN ANALYSIS OF SEDIMENT CORES

6.1 INTRODUCTION

6.1.1 Objectives of Analytical Work

Heavy metals are analysed in sediments by measuring instrument signals relative to their concentrations in prepared solids and solutions. All signals possess background noise, which limits the lowest concentration that can be detected. The type of background noise depends on both the sensitivity and the instrument employed. All instruments have both natural and instrumental background component (Potts, 1987). The precision of signals depends on the following; counting statistics, signal to background ratio, instrumental noise, drift, and sensitivity. The closer the signal is to the background noise the poorer the precision (Gellender, 1982). The degree of accuracy obtainable hinges on interference effects which vary depending on instrumentation, and the chemical make-up of the sample. Before the heavy metals of interest are studied the accuracy and precision must be proven by analysing international reference materials, instrumental and analytical blanks, and checking day to day consistency.

6.1.2 Accuracy and Precision

There are two main categories of errors 1) determinate (systematic) and 2) indeterminate (random). Determinate errors are related to precision and arise from methodic, operative, and instrumental sources. Analysts are subject to systematic bias, such as reading a scale. To guard against such bias, analysts should carefully monitor

technique performance by analysing as many reference materials as possible.

Indeterminate errors are related to accuracy and are an inherent part of sample preparation and instrumentation and cannot be eliminated. In instruments, sources include electronic noise, random emission of X-rays, and flame flicker. An estimate of these errors can be made by repetitive measurement of the same sample.

Errors related to precision are expressed in terms of standard deviations, average deviations, coefficient of variations, and ranges. These parameters disclose the amount of agreement amongst a group of results but implies nothing about their relationship to the true value. Accuracy is quantified using international reference materials and is expressed by absolute and relative errors, and percentage yields.

6.1.3 Contamination

Contamination is a serious problem in trace analysis, particulary at analyte concentrations below 1 part per million (ppm). Trace metal results reported prior to 1980 were consistently a factor of 10 to 100 higher than reported in recent years, due to poor contamination control (Gellender,1982). The wide circulation of certified reference materials in the last decade has revealed the earlier contamination problems. Analysts now assess contamination routinely by analysing blank solutions and reference materials with every batch of samples.

The main sources of contamination in trace analysis include 1) equipment (sampling and analytical), 2) laboratory environment, and 3) analytical reagents. Examples of these three categories include sieving and grinding equipment, metal sample implements, leachates from container walls, dust, sweat, flaking paint, and exhaust fumes. If the total mass of element being analysed is less than 10-100 μg, dust fallout from the laboratory

environment is a serious problem (Potts, 1987). In such circumstances the blank is the limiting factor to successful analysis.

Consideration should also be given to the possibility that trace elements may be lost at any stage of the analytical procedure. If trace metals solutions are not stored in an acid environment then metals may be adsorbed by the container walls in less than 12 hours. Container adsorption is particulary serious when dealing with solutions containing concentrations below 1 ppm.

6.1.4 Detection Limits

The detection limit is related to the confidence that may be placed on distinguishing a signal from the background measurement (Potts, 1987). Irrespective of technique, quantitative data cannot be obtained within 3 standard deviations of the analytical blank. Therefore it is imperative that analysts estimate detection limits prior to assessing the precision.

6.1.5 Reference Materials

Reference materials are analysed by many laboratories using a wide variety of methods. Consequently the true value is often a consensus estimate from quite separate data. The uncertainty quoted for the true value should almost always exceed the precision obtainable by an individual technique. Therefore to be sure of obtaining good accuracy analysts should measure as many reference materials as possible (Ellis and Steel, 1982, Potts, 1987).

The main function of the primary reference material is to determine accuracy. The primary reference sediments chosen should be as close as possible to the real sample in 1) the nature of the matrix and 2) the concentration of the metals. Frequently, such reference materials are limited in quantity and not always an ideal match to the samples under

investigation. Therefore, it is often necessary for analysts to prepare their own secondary references, in addition to the primary certified reference material.

Secondary references consist of one or two of the analyst's own samples which are analysed as unknowns with each batch of samples. Study of secondary references allows analysts to identify calibration drift from batch to batch throughout the entire span of a project and hence calculate realistic analytical precision.

6.1.6 Instrumentation

Despite the many important advances in trace element analysis there is still no readily available technique superior to all others for determining the majority of elements (Florence, 1988).

Techniques tend to fall in two categories 1) automated multi-element techniques with high precision that are expensive and complicated, and 2) inexpensive simple easy to use techniques with single element analysis that are not so easily automated. X-ray Fluorescence Spectrometry (XRF) and Flame Atomic Absorption Spectroscopy (FAAS), from categories 1) and 2) respectively, are amongst the most widely used techniques for analysis of the major and trace elements as a group (Govindaraju, 1984). Both methods were available for this study. The majority of heavy metal sediment analyses were carried out using FAAS because 1) the detection limits are lower than XRF (Table 6.1), and 2) small sample weights are required. Many samples, particulary in the clay grain size weighed less than 1g, which is too small for accurate detection by XRF.

Table 6.1 Detection Limits for XRF and FAAS

	Cr µg/g	Cu µg/g	Fe µg/g	Mn µg/g	Ni µg/g	Pb µg/g	Zn µg/g
XRF	10	6	10	13	6	6	9
FAAS	6	1	3	1.2	3	1	8

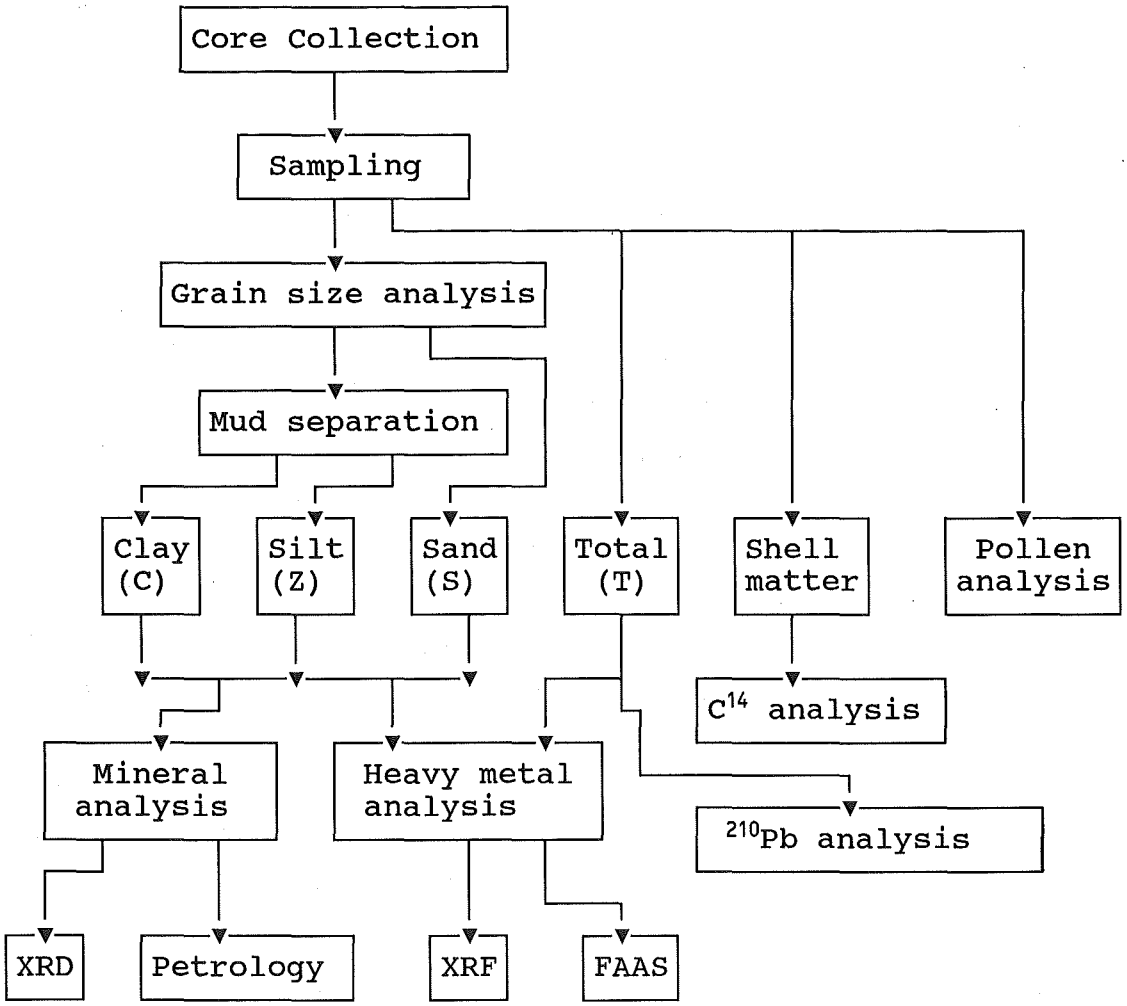

Fig. 6.1 Stages of bottom sediment sample handling.

X-Ray Fluorescence Spectroscopy was used as a cross check on the accuracy of FAAS.

6.2 CONTAMINATION CONTROL DURING SAMPLE HANDLING

The flow diagram in Fig. 6.1 shows the stages of sample handling. All equipment used in core collection, subsampling, and analysis was cleaned prior to use by the method outlined in Fig. 6.2. No metal objects were employed at any stage of sample handling. All equipment was stored in plastic lined cupboards. Hence, contamination from equipment was kept to a minimum. Although laboratory surfaces were covered with plastic, which was cleaned daily, some minimal contamination from dust would have been unavoidable. Slight contamination by reagents is also unavoidable but is limited to the levels governed by AnalaR (AR) grade chemicals and is insignificant as far as the study of bottom sediments is concerned.

6.2.1 Experiments Monitoring Contamination During Grain Size Separation

Grain size separation involves 1) sieving samples through 63μm nylon sieves to separate sand and mud and 2) separating mud into silt (4-63μm) and clay (<4μm) fractions by settling in columns. Refer to Chapter 3 (Fig. 3.16) for details of the technique.

The separation of the sand and mud by sieving required about 20 minutes of time and all sieving materials had been pre-washed by the method outlined in Fig 6.2. Thompson and Bankton (1970) examined contamination using sieving apparatus and found insignificant contamination after sieving samples through nylon mesh.

Column separations of mud fractions consumed over 6 litres of double distilled water and 500ml of saturated NaCl solution per sample. A batch of 10 samples required 4 to 6 weeks to separate. The risk of contamination was

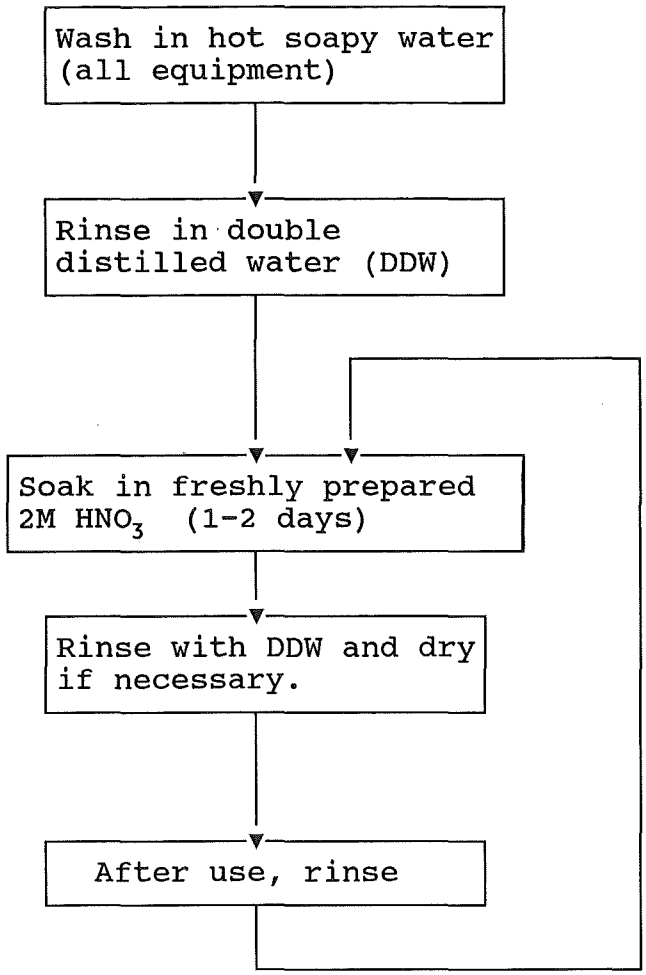

Fig. 6.2 Procedure used to clean equipment in this study.

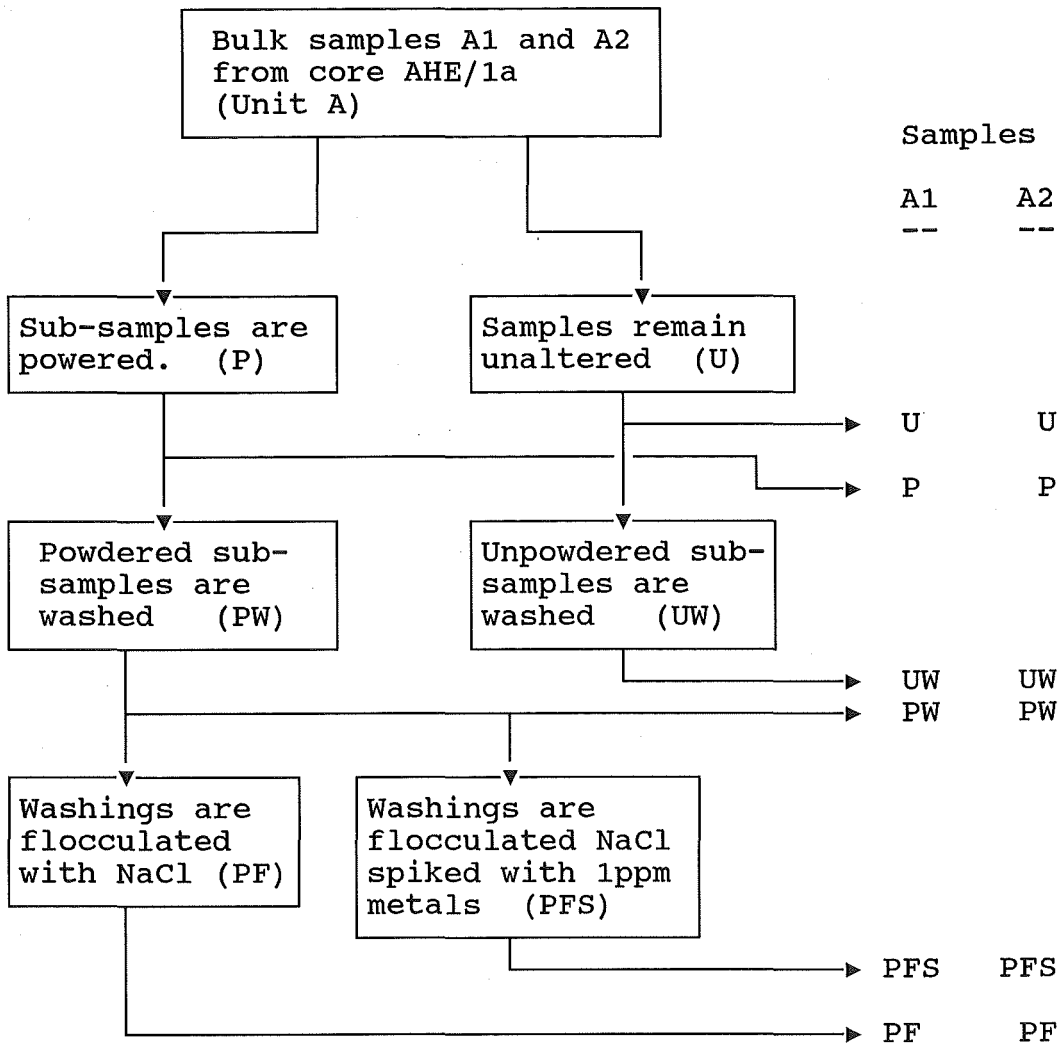

Fig. 6.3 Procedure of Grain Size Separation Contamination Test 1.

considered high during this period. Hence, it was necessary to undertake experiments to see where potential metal gain and loss lies in this process. Two separate tests were designed. Test 1 involved an attempt to contaminate sediment under controlled conditions. Test 2 involved repeat separations of clay and silt samples to see if there is any difference in the heavy metal content between mud separations.

6.2.1.1 Test 1

Figure 6.3 helps to explain the procedure of Test 1. Two sand sample fractions (A1 and A2) from Unit A of core AHE/1a were each split into two subsamples. One subsample from each pair was subsequently powdered. The four subsamples were added to 1 litre columns and made up to the mark with double distilled water. Duplicate columns were set up for the powdered fractions. Each column contained about 20g of sediment. The six columns were stirred and left to stand for 4 hours after which the top 20cm containing the clay fraction, were siphoned off and poured into large beakers. Twenty mls of saturated NaCl solution were poured into each beaker and the solutions were left to flocculate. The salt solution added to 2 of the powdered separates was spiked with 1ppm Zn, Ni, Pb, Cu, and Fe. All the columns were siphoned 10 times to completely separate the coarser grains (silt) from finer grains (clay). No flocculates were collected from the columns containing uncrushed fractions. The final flocculated solutions were centrifuged with repeated washings of distilled water to remove the salt. Once dry, all samples were 1) analysed for organic matter by weight loss on ignition, 2) digested in HF/HNO_3, and 3) analysed for Pb, Ni, Cu, Zn, Fe by FAAS. The final samples analysed were labelled U (uncrushed), UW (uncrushed and washed), P (powdered), PW (powdered and washed), PF (powdered, washed and flocculated), PFS (powdered, washed and flocculated with spiked NaCl solution).

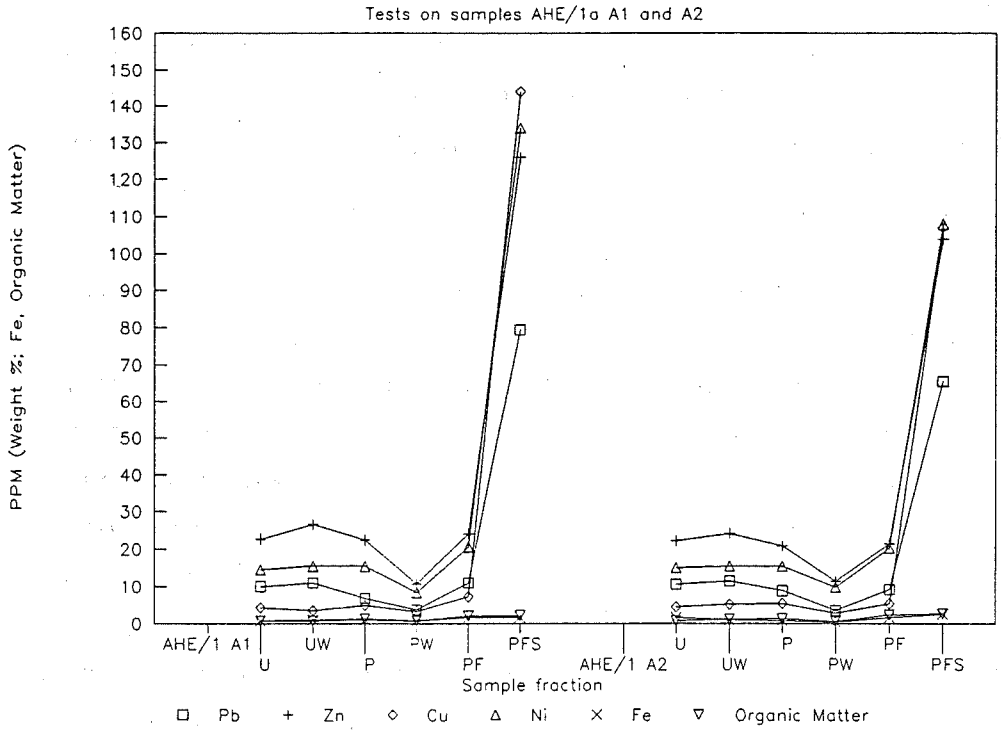

Fig. 6.4 Results of Column Separation Test 1.

Sand samples were chosen because there were no clay and silt samples available large enough for the experiment. Samples were powdered in order to create broken bonds and hence chemically active surfaces analogous to clays. Most silt particles are silt sized sand grains, hence uncrushed sand is considered to behave similarly to silt in the column.

The results of all treatments are graphed in Fig.6.4. As expected the levels of metals are more or less equal for U, UW, and P fractions of both samples A1 and A2. The grain surfaces of the uncrushed sand will be in equilibrium with respect to trace metals at neutral pH. Hence washing these samples in distilled water should not alter the heavy metal content. Powdering samples should not change the heavy metal content as long as the mill is clean. However, the powdered washed fractions (PW) show that metals can be lost in the washing process. The final flocculated powders (PF) yield similar metal concentrations to the untreated powders. These results indicate that any metals lost in the washing process are replaced during flocculation. In other words there was metal loss during the washing process and metal contamination during flocculation, but these two cancel each other.

Figure 6.4 and Table 6.2 show that PFS samples were seriously contaminated with all heavy metals, except Fe, despite exhaustive washing of final flocculates. Another important result was the elevated organic matter content of flocculated samples (PF, PFS). The greater weight loss on ignition is probably due to an increase in sediment water content rather than higher organic matter levels. An increase in water content could arise by a hydrolysis reaction at the surface of the freshly cleaved sediment. When minerals cleave broken bonds attract OH^- groups from water to balance the charge, hence water is dissociated (Davis, 1989). The resulting slight acidity of the water explains why metals were lost during the washing of the

Table 6.2 Results of Column Tests of Powdered Samples A1 and A2.

	Pb µg/g	Zn µg/g	Cu µg/g	Ni µg/g	Fe %	ORGANIC %
A1P	6.8	22.4	4.9	15.5	1.1	1.4
A1PF	11.0	24.1	7.2	20.6	1.7	2.1
A1PFS	79.4	126.0	144.0	134.0	1.7	2.1
A2P	8.8	20.9	5.4	15.4	1.0	1.4
A2PF	9.2	21.4	5.4	20.3	1.6	2.4
A2PFS	65.5	104.0	107.0	108.0	1.6	2.7

P; powdered sample.
PF; powdered sample, separated and flocculated with NaCl.
PFS; powdered sample, separated and flocculated with NaCl, spiked with 1ppm Pb, Zn, Cu, Ni, Fe.

powdered samples. Such ion exchange behaviour may be exhibited by clay minerals.

It can be concluded from the results of the uncrushed (U) and uncrushed and washed (UW) samples that column separation has little or no affect on the silt fraction. However, the results of the powdered samples (P, PF, PFS) suggest that there is a potential for 1) heavy metal loss from clay minerals in the columns, and 2) metal contamination of clays during flocculation with saturated NaCl solution. In addition, the powdered samples reveal that there is a two fold increased weight loss on ignition (usually taken as organic matter) from the columns (PW) to the beakers (PFS) (Table, 6.2). This result indicates that the separation technique may bias towards higher levels of organic matter in clay fractions compared with silt and sand.

Freshly milled sand samples are not an ideal model for clays and may be more or less reactive. Presumably marine clay minerals are in equilibrium with respect to heavy metals at neutral pH. If so, then the repeated mud separations of Test 2 should yield identical heavy metal concentrations for the silt and clay fractions.

6.2.1.2 Test 2

Because the results from Test 1 suggest that the clay fraction may become contaminated during grain size separation it was considered worthwhile to perform a further separation on existing clay and silt fractions.

The fractions ZT3 (silt) and CT3 (clay), from Unit T3 in the Travis Swamp, were derived from the same mud sample by column separation. Five grams of each fraction were added a second time to different 1 litre columns of water. The separation and analysis methods were the same as described in Test 1. However, only 4 separations were possible because of the small sample size. A shorter settling time, 1 hour (instead of 4), was required for silt ZT3 because no clay was present in the sample.

Table 6.3 Results of Column Separations of Silt TS/1 3 (ZT3), and Clay TS/1 3 (CT3).

Sample	Pb µg/g	Cu µg/g	Ni µg/g	Zn µg/g	Fe %	Mn µg/g	Cr µg/g	ORGANIC %
ZT3	8.9	46.3	8.3	34.6	1.5	43.0	24.1	1.5
FZT3	13.6	54.7	11.1	43.7	1.9	56.5	31.3	1.8
CT3	29.8	40.7	19.7	107.0	4.3	163.0	64.3	4.1
FCT3	30.4	50.1	19.2	109.0	4.2	163.0	59.0	4.0

ZT3; ZT3 from first column separation
FZT3; ZT3 from second column separation.

Table 6.4 Total Heavy Metal Content in Sediments before (T) and after (Tf) Grain Size Separation

Sample	Pb µg/g	Cu µg/g	Ni µg/g	Zn µg/g	Fe %	Mn µg/g	Cr µg/g	ORGANIC %
AHE 3aC1 (FAAS)								
T	8.87	7.57	10.87	43.80	1.46	55.80	34.66	3.10
Tf=S+Z+C	8.34	7.84	10.12	41.42	1.63	82.60	35.09	2.28
AHE 1C8 (FAAS)								
T	22.34	7.46	15.82	29.10	2.14	84.35	56.00	2.85
Tf=S+Z+C	19.19	8.05	15.11	32.68	2.07	88.37	63.26	2.36
SD-N-1 (FAAS)								
T	105.00	83.00	25.20	479.00	3.01	427.00	128.00	11.30
Tf=S+Z+C	108.64	101.14	27.80	438.13	2.99	419.21	135.49	8.89
AHE 5B2 (XRF)								
T	22.00		20.00	55.00	2.46	240.00	37.00	
Tf=S+Z+C	21.19		17.47	58.90	2.50	297.08	40.82	
AHE 6C-B1 (XRF)								
T	18.00		11.00	47.00	2.06	379.50	32.00	
Tf=S+Z+C	16.24		10.22	47.48	2.05	405.61	26.68	

S, sand concentration; Z, silt concentration; C, clay concentration.

The results of this test are shown in Table 6.3. There is no significant difference in heavy metal content between CT3 (first separation) and FCT3 (second separation) indicating that careful work will not contaminate clays. Heavy metal levels of FZT3 (second separation) are slightly higher than ZT3 (first separation). The higher heavy metal levels of ZT3 are most likely due to 1) further grain size segregation favouring removal of silt sized clay minerals, and/or 2) contamination during flocculation with saturated NaCl. (Clay minerals are higher than silt minerals in heavy metals (see chapter 1 and 4). In addition, most silt studied here contains a small proportion of silt sized clay minerals (Chapter 3).)

The results of the Tests 1 and 2 indicate the following 1) there is a potential for metal loss from the columns by repeated washing with distilled water, 2) clay fractions are at risk of heavy metal contamination when flocculated with large quantities of saturated NaCl solution, and 3) there is possible water adsorption by clay minerals during separation. Hence, when performing a grain size separation the following must be performed 1) cover all beakers and columns with fresh plastic wrap, 2) the columns must be properly rinsed after acid washing to prevent slight acidity of the water during separation, 3) use AnalaR grade, or better, NaCl to make up the saturated solution.

All column separations were carried out under the above conditions and contamination was negligible, which is demonstrated by Table 6.4. Table 6.4 compares the metal content of total sediment samples (T, unseparated) with the total metal (Tf) from sand, silt, and clay fractions added together in their proportions. For most metals the difference between T and Tf is insignificant.

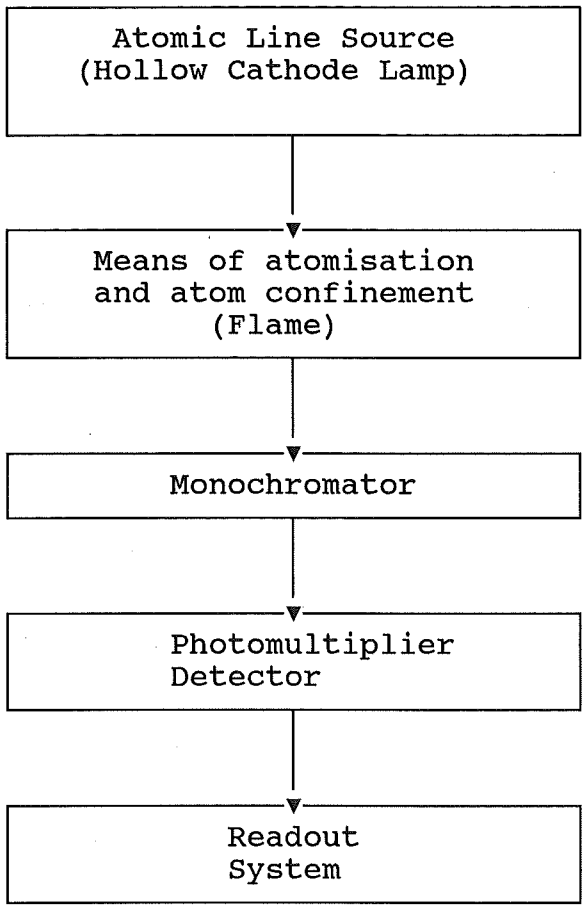

Fig. 6.5 Instrumentation of Flame Atomic Absorption Spectrometer (FAAS).

6.3 FLAME ATOMIC ABSORPTION SPECTROSCOPY

6.3.1 Introduction

Flame Atomic Absorption Spectroscopy (FAAS) was first proposed by Walsh in 1955 and is now the most popular trace element analytical technique in the world (Ewing, 1985; Florence, 1988). It is a simple and inexpensive technique that is applicable to a wide variety of major and trace elements. The main advantages are high sensitivity, less than 3μg/g for most elements (see Table 6.2 for detection limits), which can be improved on 20 to 50 times by pre-concentration techniques such as chelation and solvent extraction. Short term precision is excellent 1-3% (Coefficient of Variation). Longer term precision is 3-5% for major elements and 10-15% for trace elements (Buckley and Cranston, 1971). The main disadvantages are 1) single element analysis, and 2) samples need to be taken into solution which is time consuming and requires analysis of analytical and instrumental blank solutions.

6.3.2 Instrumentation

Figure 6.5 summarises the instrumentation used in FAAS. The atomic line source is either a hollow cathode lamp or an electrodeless discharge lamp. The flame is both the means of atomising the sample and the means of maintaining a cell of atomic vapour within the light path of the instrument. The cathode in the source lamp contains the metal of interest. Atomic spectra of the element are excited in the lamp. Samples are atomized by nebulisation by which the sample aerosol is premixed with flame gases. Radiation from the hollow cathode lamp passes through the flame and the degree of atomic absorption is detected using a monochromater tuned to the wavelength of the emission line.

Most lamps require a short warm up time and are stable

over very long periods. The noisiest component in the measurement chain is short term drift in the hollow cathode lamp output, which can be reduced by using the double beam instrument mode. When the double beam mode is employed the source lamp beam is split, one beam passing through the flame and the other by-passing the flame before recombining with the first beam before detection by the monochromater and readout system. The atomic absorption signal is then measured relative to the reference beam. Since drift in output affects both beams this sort of error can be eliminated.

The exact mechanism of atomisation depends on 1) chemical reactivity of the element, 2) the matrix present, and 3) flame temperature and composition (Potts, 1987). The rate of atomisation depends on the initial particle size and distribution. For optimum absorption particles need to be small and uniform.

Flame flicker is another major source of noise. The two common flames used are mixtures of air-acetylene and nitrous oxide acetylene. Both flames consist of primary (inner) and secondary (outer) reaction zones where gases are combusted and samples atomised. The secondary reaction zone in the air-acetylene flame produces strong background emission signals which contribute to the noise. The higher velocity and temperature of the nitrous oxide acetylene flame reduces such background emission.

6.3.3 Interferences of FAAS

The interferences of FAAS are well known and documented (Potts, 1987; Ewing, 1985; Hosking et al 1977). There are three main interference categories: 1) chemical, 2) instrumental, and 3) spectral. Chemical interferences arise from both ionisation, and refractory (stable) compound formation in the flame. A typical refractory compound is $Ca_3(PO_4)_2$ which significantly decreases the Ca signal in a phosphate medium (Hosking et al., 1977). The main methods

of suppressing chemical interferences include 1) adding ionisation suppressor or releasing agents, 2) matrix matching of standards and samples, and 3) using the hotter nitrous oxide flame.

Instrumental interferences arise from 1) uneven nebuliser flow rate, 2) viscosity differences between sample and standards, 3) different depth of capillary immersion in sample, 4) length of capillary, and 5) affect of sample matrix on flame temperature. These interferences can be overcome by careful work, such as cleaning the capillary tube, and using the method of standard additions when solutions are very viscous.

Spectral interferences arise from 1) atomic spectral line overlap of 2 or more elements, and 2) non-specific absorbance due to either molecular species in the flame or scatter of hollow cathode lamp radiation from particles in the flame. The most effective way of removing spectral interferences is by utilising Zeeman correction where spectral lines are split by a magnetic field (Rothery, 1986). However, the instrument (Varian Techtron AA 1475 spectrophotometer) used for this study employed continuum-source background correction which assumes that the background absorption is continuous over the spectral bandwidth of the monochromater. A deuterium lamp produces a continuous broadband spectrum. Total absorption is made with the hollow cathode lamp, while measurement with the deuterium lamp gives background absorption only. As the atomic line is very narrow it makes virtually no contribution to background absorption. The analyte signal can only be obtained by electronic subtraction of the deuterium lamp signal from the hollow cathode lamp signal. It is important to use background correction when metals are present in very small concentrations.

Potts (1987) reviews major elemental interferences and correction methods using the air-acetylene flame. Copper, and Zn usually exhibit no interference, and background correction is not usually required. Iron is also free from

Table 6.5 Flame AAS Instrumental Conditions

Element	Wavelength (nm)	Slit Width (nm)	Lamp current (mA)	Background correction	Attenuation	Flame
Cr	357.9	0.2	7	off	out	NA
Cu	324.8	0.5	3	off	out	AA
Fe	248.3	0.2	6	off	out	AA
Mn	279.5	0.2	5	off	out	AA
Ni	232.0	0.2	4	on	in	AA
Pb	217.0	1.0	4	on	in	AA
Zn	213.9	1.0	5	on	in	AA

NA; nitrous oxide acetylene
AA; air acetylene

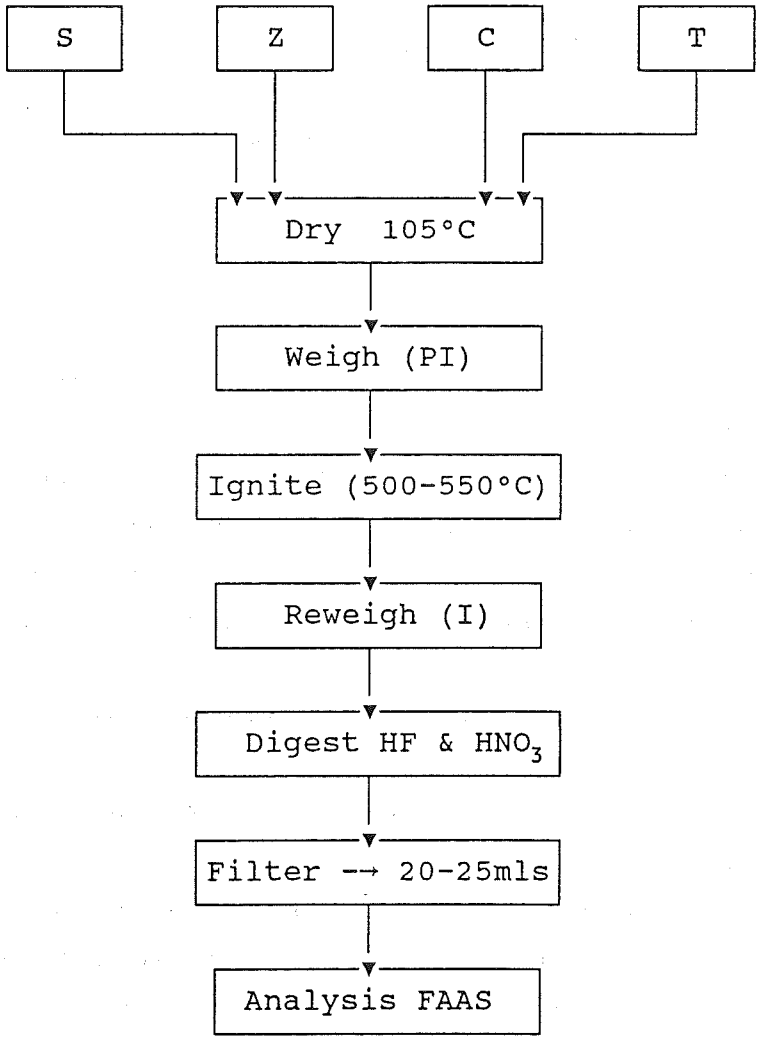

Fig. 6.6 Procedure used to analyse heavy metals and organic matter in bottom sediments (S, sand; Z, silt; C, clay; T, total).

interference but more reliable results are obtained using the nitrous oxide acetylene flame. Lead and Ni are subject to non-specific absorption and hence background correction is required. Interferences commonly occur for Cr because Cr^{4+} and Cr^{3+} have different absorption lines, and Cr_2O_3 is a very stable compound. Chromium interference is counteracted in the presence of Fe or by employing the hotter nitrous oxide acetylene flame. Mn is subject to matrix effects which can be overcome by using the standard additions technique. The instrumental conditions used in this study for analysis of Pb, Cu, Ni, Zn, Fe, Mn, and Cr are presented in Table 6.5.

HEAVY METAL ANALYSIS OF SEDIMENTS BY FAAS

6.4 Analytical Procedures

Figure 6.6 summarises the procedure involved in analysing sand (S), silt (Z), clay (C), and total sediment (T) samples by FAAS. Samples were analysed in batches of 12, including the analytical blank, the primary reference SD-N-1 ,and where possible a secondary reference. Each batch usually contained samples from the same grain size and the same core, which minimised within core and within grain size errors.

Two digestion procedures were initially tried. The first procedure follows that of Hulse (1983) with slight modifications. Initially samples were roughly weighed in 10 ml beakers and oven dried at 105°C overnight to remove any water. Subsequently, the samples were desiccated for 2 hours and weighed accurately to 4 decimal places before ashing in a furnace at 550°C for 8 hours to remove organic matter. After cooling the samples were again desiccated for 2 hours prior to reweighing. The ignited reweighed samples were transferred to polypropylene beakers, dampened with double distilled water (DDW), and placed over a water bath. Next, concentrated HF and HNO_3 (HF/HNO_3) were added to the

Table 6.6 Sediment Digestion Summary

Sample	Weight g	Digestion Mixture
Total	1-1.5	6ml conc. HNO_3 & 12ml 40% HF (x2)
Sand	1-1.5	6ml conc. HNO_3 & 12ml 40% HF (x2)
Silt	1.0	6ml conc. HNO_3 & 12ml 40% HF (x2)
Clay	0.2-0.3	3ml conc. HNO_3 & 6ml 40% HF (x2)

(all acids AR grade)

samples, in quantities shown in Table 6.6. The acid sediment solutions were evaporated to dryness over the water bath, and the above acid digestion repeated. The final residues were taken up in 6 mls of 4M HNO_3 and filtered using 5 ml aliquots of DDW into 20 or 25 ml volumetric flasks and analysed by FAAS under the conditions outlined in Table 6.5.

The second method was basically the same as procedure 1 except samples were boiled once in 20 mls of 4M HNO_3 for 30 minutes and filtered into 25 ml flasks. The accuracy and precision of method 1 was better than method 2 (see section 6.6), so HF/HNO_3 digestion was adopted for the course of this study. Filter residues from HF/HNO_3 digestion were retained and later analysed by XRD and XRF to determine the mineral and heavy metal content.

6.5 CONTAMINATION CONTROL IN ANALYTICAL PROCEDURES

Risk of contamination occurred during analyses at the following stages: 1) sediment digestion (from acids HF/HNO_3 and dust), 2) filtering (filter paper), and 3) FAAS instrument (nebuliser capillary). The influence of laboratory dust was kept to a minimum by keeping fume cupboards clean and closed, and by shutting laboratory doors to avoid traffic. Contamination from AR grade reagents was considered negligible in terms of the specifications and amounts used.

Analytical blanks, instrumental blanks, and repeat filter washings were analysed throughout the duration of the study to keep track of contamination, and detection limits.

6.5.1 Filtering

Contamination was kept to a minimum during filtering by 1) covering filter funnels with plastic wrap, and 2) prewashing filter papers in 4M HNO_3 followed by rinsing

with DDW.

The filtering step had the potential for metal loss because the final metal solutions were small in volume (20 to 25 mls). Larger volumes would have reduced this problem but produced more dilute analyte solutions, possibly below FAAS detection. Hence, to ensure the maximum metal yield, less than 5 ml aliquots of water were added at a time to filters, and allowed to drain completely before washing with more water. Filter residues were chosen randomly and rewashed into 5ml volumetric flasks to check the efficiency of the filtering step. For all metals analysed by FAAS the efficiency of filtering was between 97 and 100%. Gain of metal ions is also possible from the filter paper. Pre-washing the papers with 4M HNO_3 removed this problem, which was confirmed by analytical blanks.

6.5.2 Blank Solutions

Both instrumental and analytical blanks were run with each batch of samples. The instrumental blank consisted of 5mls of 4 M HNO_3 in 100ml volumetric flask made up to the mark with DDW. These proportions were the same as used to make up the standard solutions. The instrumental blank was used to zero the instrument. The analytical blank was carried through the same procedure as the samples except without sample. Metal levels in the analytical blanks ranged from undetectable to 0.15μg/g (ppm), and were subtracted from all sample results, in each batch.

6.5.3 Detection Limits

The detection limit (DTL) of each batch of analyses was calculated using the instrumental blank. There are many methods available for measuring the detection limit and these are discussed fully by Potts (1987). Generally there are two main types of DTLs 1) the "absolute" which is the smallest amount detectable but not accurately (ie

Table 6.7 Detection Limits for Total Sediment, Sand, Silt, and Clay analysed by Fame AAS.

	Pb µg/g	Cu µg/g	Ni µg/g	Zn µg/g	Fe %	Mn µg/g	Cr µg/g
Total	4.0	.1	.9	<.50	1.3	1.3	4.1
Sand	2.7	.2	.7	.53	2.9	.3	1.2
Silt	1.6	.2	.2	<.50	1.5	2.7	5.7
Clay	6.3	.8	2.8	<.50	7.2	2.7	8.7
Potts (1987)	1.0	1.0	3.0	.80	3.0	1.2	3.0

qualitative) and the "relative" which can be expressed accurately with a known error. The relative DTL is usually expressed as either the Lower Limit of Detection X_{LLD} (which is 3 standard deviations (3s) above the average blank mean (Xb) or the Limit of Determination X_{LOD} (which is 6s above Xb) (Potts, 1987).

Potts recommends that for quantitative work analysts should make 10 determinations of the blank and calculate X_{LOD}. In this study over a period of several years more than 1300 blank determinations were made for each element. Hence, a very reliable estimate of the standard deviation of Xb was obtained and the Lower Limit of Detection was considered a satisfactory estimate of the DTL.

Before the detection limits could be calculated, the instrumental blank signals were converted to concentration values applicable to the average sediment weight analysed in each batch.

All batches analysed contained samples of the same composition (matrix) and grain size, which included 1) total sediment, 2) sand, 3) silt, and 4) clay. The quantities analysed are given in Table 6.6. Each batch of samples varied with respect to matrix and sample weight. Hence, it was necessary to calculate detection limits for each of the four different grain size groups.

The average values of all the batch detection limits, for each grain size, are given in Table 6.7, together with the data of Potts (1987). (The errors on the detection limits are approximately 10%). Generally speaking the detection limits of the total, sand, and silt fractions are below the limits published by Potts (1987). The higher detection limits exhibited by the clay fraction are probably due to contamination. Contamination would be more noticeable in the clay size fraction than the other fractions due to the small sample weight analysed (Table 6.6). The main contaminants are Pb, Cr, and Fe, which are probably derived from laboratory dust.

Table 6.8 SD-N-1 Statistics (HF/HNO3 Method of Digestion; FAAS)

Statistic	Pb µg/g	Cu µg/g	Ni µg/g	Zn µg/g	Mn SA µg/g	Mn Aq µg/g	Fe SA %	Fe Aq %	Cr µg/g	ORG %
n	34	34	32	33	32	24	32	24	31	32
M	99.3	74.7	26.5	433	582	520	2.96	2.96	141	10.5
X	99.7	73.8	27.2	439	561	519	2.87	2.96	139	10.4
s	10.3	4.38	3.4	47	70.7	44.9	.595	.414	9.55	1.18
CV	10.3	5.86	12.5	10.7	12.6	8.66	20.8	14	6.88	11.4
Y	83.1	102	87.7	100	72.2	66.8	78.9	81.3	93.3	
Xe	3.6	1.53	1.23	16.7	25.5	18.7	.215	.172	3.5	.426
Xe (%)	3.6	2.1	4.5	3.8	4.5	3.6	7.5	5.8	2.5	4.1
μ	120	72.2	31	439	777	777	3.64	3.64	149	
CI of μ	112-132	68.1-75.2	27-34	423-452	728-801	728-801	3.53-3.78	3.53-3.78	125-161	
CI of σ	8.63-14.4	3.67-6.14	2.76-4.62	38.8-64.9	57.4-96.1	34.9-63	.483-.809	.322-.581	7.63-12.8	.959-1.6

n, number of analyses; M, median; X, mean sample set; s, standard deviation of sample set; CV, coefficient of variation, Y, percentage yield; Xe, error of the mean; μ, certified mean (IAEA); CI, 95% confidence interval; σ, certified standard deviation.

6.6 ACCURACY AND PRECISION OF FLAME ATOMIC ABSORPTION SPECTROSCOPY

To obtain the best accuracy contamination levels should be at the minimum, which cannot be improved upon and parallels the work carried out in other laboratories. Therefore, once detection limits are known the best way to assess accuracy and precision is analysing primary and secondary reference materials.

The primary reference material used in this study is a marine sediment, SD-N-1/2, from the North Sea. Several comprehensive reports exist containing intercomparison studies of this reference material. The most recent report is International Atomic Energy Agency (IAEA) report G4.12, 1988.

6.6.1 Accuracy and Precision of SD-N-1 analysis by FAAS

Tables 6.8 and 6.9 contain final error statistics of SD-N-1 by the HF/HNO_3 and HNO_3 digestion methods respectively. The trimmed raw data can be found in Tables A4.1 and A4.2 of Appendix 4.

The method of data trimming involved eliminating any results more than 3 standard deviations (3s) either side of the mean X. (Assuming that the data is normally distributed then 99.7% of the results will lie within X±3s (Anderson, 1987; Lister, 1982).) There were no more than 2 outliers per metal and some had no outliers. The mean, X, of the trimmed data was then compared to the median (M), to check that the data were normally distributed. For almost all metals X and M agreed to within 1% so no further data trimming was necessary.

The following error statistics were computed for each metal: 1) the standard deviation (s), 2) coefficient of variation CV ((s/X)100, standard deviation expressed as percentage of the mean), 3) percentage yield Y ((X/μ)100,

Table 6.9 SD-N-1 Statistics (HNO3 Method of Digestion; FAAS)

Statistics	Pb μg/g	Cu μg/g	Ni μg/g	Zn μg/g	Mn Aq μg/g	Fe Aq %	Cr μg/g
n	20	19	17	19	14	11	14
M	99.9	74.6	21.6	402	509	2.6	78.8
X	98.7	73.6	22	374	514	2.66	77.6
s	9.55	3.86	1.66	51.8	40.6	.342	16.1
CV	9.67	5.25	7.51	13.9	7.9	12.9	20.8
Y	82.3	102	71	85.2	66.2	73.1	52.1
Xe	4.47	1.86	.854	25	23.4	.23	9.29
Xe (%)	4.53	2.53	3.88	6.68	4.56	8.64	12
μ	120	72.2	31	439	777	3.64	149
CI of μ	112-132	68.1-75.	27-34	423-452	728-801	3.53-3.78	125-161
CI of σ	7.26-14	2.92-5.7	1.24-2.5	39.1-76.6	29.4-65.4	.239-.6	11.7-25.9

(see Table 6.8 for definitions of the statistical symbols)

where μ is the certified mean supplied by IAEA), 4) error of the mean Xe ($\pm t_{(.05)}$ $s/\sqrt{n}$, where $t_{(.05)}$ is the students t statistic at 95% confidence with n-1 degrees of freedom), and 5) percentage error of the mean Xe (%) ((Xe/X)100, error of mean expressed as a percentage).

A comparison of SD-N-1 percentage error (Xe (%)) and yield (Y) values in Tables 6.8 and 6.9 shows that the HF/HNO_3 method of digestion produced better precision and accuracy than the HNO_3 method. Hence, the HF/HNO_3 method was adopted. The precision obtained by the HF/HNO_3 is excellent with errors (Xe (%)) less than 5% for most metals. The method of standard additions (SA) was employed to try and improve the accuracy of Fe and Mn. Table 6.8 shows that the standard additions technique produced slightly better yields (Y) than aqueous calibration (Aq), but at the expense of the precision (CV, Xe, Xe (%)). Precision is considered more important than accuracy in this study, because the ultimate goal is to compare batches of samples. Therefore aqueous calibration was adopted for Fe and Mn analyses.

Errors (Xe (%)) of less than 10% and within the confidence interval of the certified means (μ) are considered acceptable. Under these conditions FAAS analysis of SD-N-1 produced accurate results for Cu, Ni, Zn, and Cr. Despite the low percentage yields (Y) of Pb (83%), Mn (67%), and Fe (81%) the precision of these metals is excellent (Xe (%) Pb=3.6%, Fe=5.8%, Mn=3.6%). Hence, the proportion of Pb, Fe, and Mn recovered is accurately characterised. The reason for the low recoveries of Pb, Fe, and Mn will be discussed in the next two sections.

6.6.2 Comparison of SD-N-1 Accuracy with other analysts using HF/HNO_3 Digestion.

Figure 6.7 A-G compares mean SD-N-1 metal values obtained by different analysts working in the Chemistry Department of Canterbury University over the last 7 years.

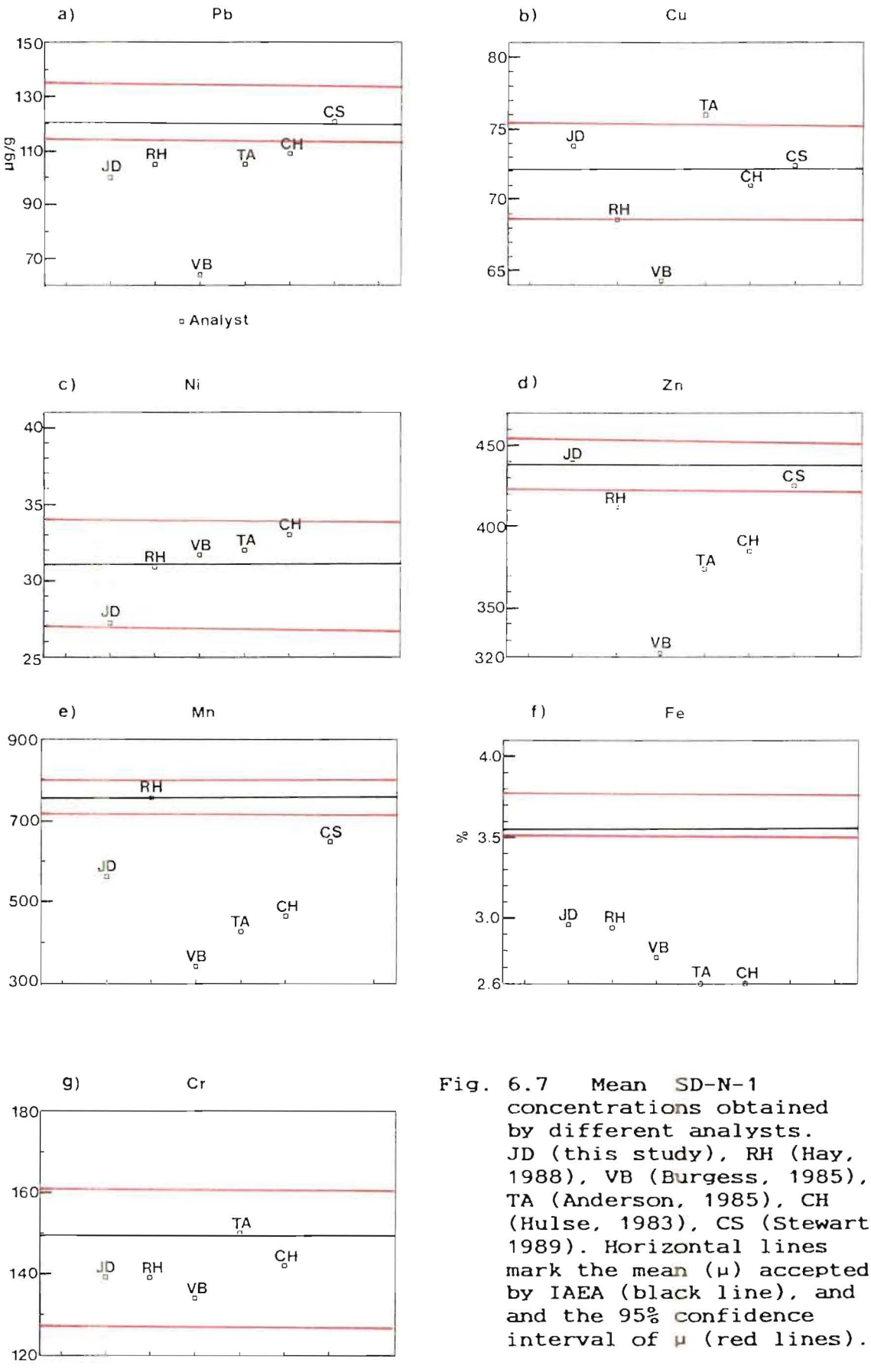

Fig. 6.7 Mean SD-N-1 concentrations obtained by different analysts. JD (this study), RH (Hay, 1988), VB (Burgess, 1985), TA (Anderson, 1985), CH (Hulse, 1983), CS (Stewart, 1989). Horizontal lines mark the mean (µ) accepted by IAEA (black line), and and the 95% confidence interval of µ (red lines).

All analysts were post-graduate students analysing SD-N-1 by essentially the same technique as outlined in section 6.4. The main variations were 1) Hay (1988) analysed Fe, and Mn using the method of standard additions, and 2) Stewart (1989) ashed samples in platinum crucibles directly over a bunsen burner. Stewart, also, used a higher proportion of HF to HNO_3 than other analysts, and evaporated samples over a low temperature sand bath in platinum crucibles. Stewart's method did not produce a digestion residue. Consequently Stewart's samples were taken up directly in acid without filtering.

Almost all analysts obtained good accuracy for Cu, Ni, and Cr and low results for Pb, Fe, Mn, and Zn. However, Stewart produced excellent accuracy for Pb, and Zn. Stewart did not analyse Fe, Ni, and Cr, and her Mn result was the best recovery by aqueous calibration. The excellent Mn recovery obtained by Hay was accomplished using the method of standard additions.

There is a general bias towards low Pb, Fe, Zn, and Mn results for all analysts except Stewart. The main difference between Stewart's technique and the other analysts is in the filtering step. Stewart did not filter her samples. All other analysts filtered into 20 or 25ml volumes, except Burgess (1985) who filtered some samples into 10 ml volumetric flasks. The evidence suggests that some metals are trapped in the digestion residues and not removed by filtering.

The higher concentrations of HF relative to HNO_3, employed by Stewart, combined with slow fuming of these acids over a sand bath resulted in more efficient digestion with a minimum final residue enabling samples to be taken up directly without filtering. The water bath technique used by the other analysts involved a lower proportion of HF to HNO_3, and solutions evaporated more quickly, hence digestion was less efficient. Consequently, a white residue remained weighing approximately 10% of the initial sample weight. It was necessary to filter samples because the

residue tended to clog the nebuliser capillary. Despite the disadvantages of the water bath technique it was possible to analyse 12 to 20 samples at a time, compared to 3 using the platinum crucibles. Hence, the water bath technique is more economical when large studies are undertaken. In future the water bath technique could be improved by lowering the bath temperature and increasing the quantity of HF used.

6.6.3 XRF and XRD analysis of HF/HNO_3 Residues

The decomposition of sediments is affected by the reaction of hydrofluoric acid with silica, which forms gaseous silicon tetrafluoride (Forstner and Wittmann (1981). A possible reaction is $MSiO_3 + 6HF \rightarrow SiF_4 + 3H_2O + MF_2$. Aluminium fluorides are also produced when large quantities of HF had been added to clay samples. A number of HF acid digestion precipitates have been identified in the literature. These include CaF_2, $MgAlF_5.xH_2O$, $NaAlF_4.xH_2O$, $Fe(II)(Al,Fe(III))F_5.xH_2O$ (Langmyhr and Kringstad, 1966), and K_2SiF_6 (Fahey, 1971).

Complete decomposition of sediments by HF is a "time-honoured" procedure that may require several weeks of repeated treatment (Maxwell, 1968). Even when severe methods have been used some minerals (particularly heavy minerals) remain resistant (Maxwell, 1968; Neuerberg, 1961). Minerals containing elements, such as Pb and Mg, which from insoluble fluorides dissolve slowly because the precipitated fluoride shields the sample from further attack by the acid.

In this study it was noticed that smaller sample weights produced better metal recovery. Clay samples weighing approximately 0.4g yielded half as much metal as samples weighing around 0.095g if the same quantity of acid was used. Naturally, some of the increased metal yield will be due to contamination. However, intermediate weights produced intermediate yields, which suggests that smaller

sample sizes allow more efficient HF attack of the sediment. As a result of this finding all sample weights were kept within 5-10% of one another.

After samples were digested in concentrated HF and HNO_3 white residues remained bearing similar grain size to the original sediment. The low metal yields obtained here and by the other analysts suggests that some heavy metals are trapped in the digestion residues, even after filtering. A small number of residues were retained and analysed by X-Ray Fluorescence (XRF) and X-Ray Diffraction (XRD). Because the quantity of residue remaining was small it was necessary to analyse composite samples. Digestion residues from all units of core AHE/6 were combined for each grain size.

The final samples RS/6 (sand), RZ/6 (silt), RC/6 (clay) were analysed by X-ray Diffraction Analysis (XRD). The results of the XRD analysis were search matched with data stored in the μPDSM Search Match software (Geology Department, University of Canterbury) to obtain an estimate of the chemistry of the residues.

Clay residue RC/6 produced an 85% match with the synthetic aluminium fluorides $NaMgAlF_6.H_2O$ (ralstonite) and K_2NaAlF_6 (elpasolite) and lesser matches with minerals, $NaAlSi_3O_8$ (albite), and $KAl_2(Si_3Al)O_{10}(OH,F)_2$ (muscovite). The silt residues favoured various synthetic fluorosilicates (such as $NaCa_2Si_4O_{10}F$), hydroxides, synthetic lead silicate ($PbSiO_3$), and minerals albite, and illite. Sand residues contained lead silicate, fluorosilicates, albite, and pumpellyite. There were no aluminium fluorides in the sand and silt residues.

These results show incomplete dissolution of some minerals by HF. Albite is abundant in all grain sizes studied (Chapter 3). Pumpellyite is a common mineral in the heavy mineral suite of the sand fraction, whereas illite is abundant (44%) in the clay fractions and less common in the silt fractions (7%). The muscovite present in the clay residue may have been produced by alteration of illite,

because illite is the common phyllosilicate in the clay fractions. The aluminium fluorides in the clay residues and the fluorosilicates, and lead silicates in the sand and silt residues are precipitation products of reactions between HF and minerals during sediment decomposition.

The incomplete dissolution of some minerals and precipitation of others (especially lead silicate) suggests that heavy metals are not completely removed from the residues after digestion. X-Ray Fluorescence (XRF) analysis of SD-N-1 and a composite total sediment residue (AHE/6) revealed that the digestion residues do contain some heavy metals.

Approximately 30% of the major element assemblage could not be accounted for by XRF, so it was assumed that the presence of fluoride accounted for this anomaly. (The XRF instrument (Geology Department, University of Canterbury) is not calibrated for the analysis of major quantities of fluorides.) Hence, all the results were recalculated to account for 30% fluoride. The results are tabulated in Table 6.10 along with the relative errors of SD-N-1 analysed by FAAS. (The values of the digestion residues are corrected to the average weight of the original size fraction analysed.)

Table: 6.10 Heavy Metal Concentrations in Acid Digestion Residues and Relative Errors (RE) for SD-N-1 analyses by FAAS

	SD-N-1 (RE) µg/g	SD-N-1 Residue µg/g	Composite Residues AHE/6 µg/g
Pb	20.0	13	8.0
Ni	3.0	undetectable	undetectable
Zn	0.0	8	14.0
Mn	258	180*	92.0
Fe	0.7%	.5%	0.48%
Cr	10.0	undetectable	undetectable

* detection limit of Mn is 190ppm
RE; μ-X, where μ is the certified mean (IAEA) and X is the mean obtained in this study.

Table 6.10 shows that the Pb, and Fe contents of the acid digestion residue of SD-N-1 are similar to the relative errors found for FAAS analysis of SD-N-1. The evidence proves that bias in the FAAS technique is due metal retainment in digestion residues. Metals are probably firmly bound into the digestion residue compounds, which are of low solubility in the acid mixture. The results of repeat filtering show that over 97% of all metals passed through the filter paper into the volumetric flasks, hence metals were not retained in the residues as a result of poor filtering technique. The Zn content of the residues suggests that some Zn is also retained, but the value is within experimental error.

6.6.4 Calculation of Precision using Secondary References

It was not considered practical to duplicate analyses because 1) sand, silt, and clay fractions obtained by column separation were generally small and 2) material was required from each fraction for XRF and mineralogy studies. Therefore, it was necessary to incorporate reference material in every analysis.

The primary reference, SD-N-1, is a fine grained sediment from the Scheldt Estuary of the North Sea. The approximate mineral composition is 60% quartz, 20% calcite, 10% clay minerals, 6% feldspars, 3% NaCl, and 1-2% pyrite. In contrast, the sediment samples from the Avon-Heathcote Estuary, Saltwater Creek Estuary, and Travis Swamp are composed mainly of quartz, feldspar, rock fragments, and clay minerals. The concentrations of these minerals vary between grain sizes but are uniform within each grain size (for all localities; see Chapter 3). These samples differ from SD-N-1 in 1) the proportions of quartz and feldspar, and 2) the absence of calcite, pyrite, and NaCl. Hence, it was decided that as far as precision was concerned it would be better to use internal references with similar composition to each grain size. The emphasis in this study

Table 6.11 Secondary Reference Statistics on Heavy Metals analysed by FAAS

Statistic	Pb µg/g	Cu µg/g	Ni µg/g	Zn µg/g	Fe SA %	Fe Aq %	Mn SA µg/g	Mn Aq µg/g	Cr µg/g	ORG %
SA1B9										
n	4	5	5	5	3	4	3	5	6	4
M	3.73	5.86	10.2	19.7	1.3	1.39	53.9	39.8	28.1	1.4
X	3.76	5.88	10.5	20.1	1.39	1.39	52.3	44.6	28	1.41
s	.102	.246	.859	.934	.27	.093	6.91	10.9	1.89	.25
CV	2.72	4.19	8.16	4.65	19.3	6.69	13.2	24.4	6.8	17.8
Xe	.162	.305	1.07	1.16	.671	.148	17.2	13.5	1.98	.4
Xe (%)	4.31	5.19	10.2	5.77	48.3	10.7	32.8	30.3	7.1	28.2
ZT3										
n	4	7	7	6	5	7	5	5	8	7
M	4.06	5.84	8.72	26.9	1.92	1.72	67.1	51	30.2	1.65
X	4.15	6.2	8.85	28	1.94	1.65	67.9	47.5	30.7	1.7
s	1.14	.994	.489	4.49	.136	.121	7.36	5.5	3.83	.204
CV	2.72	16	5.53	16	6.99	7.3	10.8	11.6	12.5	12
Xe	1.81	.919	.452	4.71	.169	.112	9.14	6.83	3.2	.189
Xe (%)	43.7	14.8	5.11	16.8	8.7	6.78	13.5	14.1	10.4	11.1
CT3										
n	8	5	7	6	5	6	6	5	7	7
M	37.8	20.7	26.3	125	4.26	4.25	319	221	71.5	4.22
X	36.5	21.2	27.8	136	4.46	4.24	316	234	75.7	4.38
s	4.63	1.9	4.64	30.4	.654	.499	39	21.8	9.81	.717
CV	12.7	9	16.7	22.4	14.6	11.8	12.3	9.33	13	16.4
Xe	3.87	2.36	4.29	31.9	.812	.524	40.9	27.1	9.07	.663
Xe (%)	10.6	11.1	15.5	23.5	18.2	12.4	12.9	11.6	12	15.1

n, number of analyses, M, median; X, mean sample set; s, standard deviation of sample set;
CV, coefficient of variation; Y, percentage yield; Xe, error of the mean.

is on relationships within individual grain sizes (sand, silt, clay). Therefore, secondary references were chosen one from each grain size; the primary reference SD-N-1/2 was considered adequate for the total sediment. The references ZT3 (silt from TS/1 T3), CT3 (clay from TS/1 T3), and SA1B9 (baseline sand from Unit B of core AHE/1a) were selected as secondary references. These samples were chosen for two reasons. Firstly, they were the most plentiful samples present in each grain size. Secondly, they were from pre-historic horizons, hence contained baseline levels of heavy metals closer to the detection limits. Consequently, maximum errors would be obtained.

All data were trimmed and statistics computed by the method outlined section 6.6.1. The statistics are reported in Table 6.11 (raw data Appendix 4, Table A4.3).

Unfortunately, the total sample available of each reference was small. Consequently the number of analyses was small. Values of n ranged from 4 to 8 which was not considered large enough to determine long term precision for a 3 year study of heavy metals. So it was necessary to find a statistical technique that would incorporate the excellent precision obtained with SD-N-1 with the precision obtained by each of the secondary references to find realistic errors for each sediment group.

The method of Lindley (1965) involving Bayesian statistical estimates for normal variance was chosen. The statistics produced an estimate of true variance σ^2 for each reference material by undertaking numerous calculations involving an initial estimate of the variance (Θ^2) and the variance s^2 obtained from the data set in Table 6.11.

The method is briefly explained as follows. Initially a "prior" estimate of the sample variance (Θ^2) for each secondary reference (SR) is chosen. This estimate is based on all the prior knowledge available, and is an estimate of the variance expected. The chi squared distribution was chosen to represent the prior distribution of Θ^2. In this

study the estimate of Θ^2 was made using the variance of SD-N-1 (SD-N-1 showed excellent precision and had a large data set so was considered to yield the best possible estimate of the variance). The coefficient of variation (CV, (s/X)100) of SD-N-1 was used to calculate the estimate of Θ^2 for metals of each SR as follows. From Table 6.8 the CV of Pb is 10.3% for SD-N-1, and from Table 6.11 the mean (X) of Pb is 36.5 for CT3. Therefore, the prior estimate of the standard deviation (Θ) for Pb CT3 is:

$$10.3/100 \times 36.5 = 3.76 \quad (CV_{SD\text{-}N\text{-}1}/100(X_{CT3}))$$

and the prior estimate of Θ^2 is $(3.76)^2 = 14.1$. An arbitrary 50% was added to the estimates of Θ^2 for Pb in SA1B9 and ZT3 because the mean values (X, Table 6.11) are close to the detection limits (Table 6.7) for sands and silts.

From Lindley (1965) the prior distribution of the variance Θ^2 is chi squared with Vo degrees of freedom and is approximately normal for large Vo. Equations:

$$\Theta^2 = \sigma o^2 Vo/Vo-2 \qquad 1)$$

and

$$Var\Theta^2 = 2\sigma o4Vo^2/(Vo-2)^2(Vo-4) \qquad 2)$$

from Lindley are the equations that describe the prior estimate of the variance (Θ^2) and the variance of that estimate ($var\Theta^2$). In order to compute the final statistics these equations require solving for the statistical parameters Vo and σo^2. These calculations were performed by Professor J.J Deely, Department Mathematics, University of Canterbury (see Appendix 4, section A4.3 for workings). The final equations were:

$$Vo = 4+(2\Theta^2/var(\Theta^2)) \quad (var(\Theta^2) = (\Theta^2/4)^2 \qquad 3)$$

and

$$\sigma o^2 = \Theta^2(1-2/Vo) \qquad 4)$$

Table 6.12 Bayesian Statistical Data for Secondary References Sand AHE/1B9 (SA1B9), Silt TS/1 3 (ZT3), and Clay TS/1 3 (CT3)

Sample	Pb µg/g	Cu µg/g	Ni µg/g	Zn µg/g	Fe %	Mn µg/g	Cr µg/g	ORGANIC %
SA1B9								
X	3.8	5.9	10.5	20.1	1.4	44.6	28.0	1.4
σ^2	.2	.1	1.6	4.2	.0	28.3	3.7	.0
Xe	.4	.3	1.1	1.8	.2	4.7	1.5	.2
Xe (%)	12.0	5.0	11.0	9.0	13.0	11.0	6.0	12.0
CV (%)	12.0	5.6	12.0	10.2	14.4	11.9	6.9	12.3
ZT3								
X	4.2	6.2	8.8	28.0	1.6	47.5	30.7	1.7
σ^2	.4	.3	1.1	10.7	.0	18.6	6.4	.0
Xe	.6	.4	.8	2.6	.2	3.8	1.8	.1
Xe (%)	15.0	6.0	9.0	9.0	10.0	8.0	6.0	9.0
CV (%)	15.0	8.4	11.6	11.7	13.6	9.1	8.2	11.8
CT3								
X	36.5	21.2	27.8	136.0	4.2	234.0	75.7	4.4
σ^2	15.5	1.8	13.7	319.0	.3	419.0	38.9	.3
Xe	2.7	1.2	2.7	14.2	.5	17.9	4.6	.4
Xe (%)	8.0	6.0	10.0	11.0	11.0	8.0	6.0	9.0
CV (%)	10.8	6.3	13.3	13.1	13.8	8.8	8.2	12.5

X; Mean heavy metal or organic matter (ORGANIC) concentration (from Table 6.11)
σ^2; Variance calculated by method of Lindley (1965).
Xe; Error of the mean (95% Confidence).
Xe (%); Error expressed as a percentage of the mean.
CV; Coefficient of Variation.

Equations 3) and 4) are only valid if Vo > 4 otherwise the variance is undefined. When Vo is large then Lindley states that σ^2 is known precisely and the distribution is approximately normal. Vo was around 35 for all elements of all SR (Table A4.4, Appendix 4), hence all prior estimates of Θ^2 fit closely to the normal distribution.

The next step is to calculate the final estimate of the true variance σ^2 using Vo, σo^2 (from equations 3 and 4), and S^2 ($s^2 n$ from the data in Table 6.11). The final computation of Lindley is the 95% confidence estimate of the true variance (σ^2), and is calculated from the "posterior" distribution using:

$$\sigma^2 = Vo\sigma o^2 + S^2 / Vo + n - 2 \qquad 5)$$

where n is the number of analyses of each reference material (SA1B9, ZT3, CT3) for a particular element. Table 6.12 contains the final estimates of σ^2 for each metal of each SR. In addition the 95% confidence errors of the mean (Xe and Xe (%)) and the coefficient of variation (CV) are tabulated. The errors were calculated using the σ^2 estimates instead of the s^2 values from the data. All values of Θ^2, Vo, σo^2, S^2, and σ^2 are tabulated in Table A4.4 of Appendix 4.

The relative errors of the means (Xe (%)) are tabulated separately in Table 6.13 with the errors calculated using conventional statistics. These results show that using the technique of Lindley (1965) realistic errors have been computed for sand, silt, and clay data. In most cases the final errors values lie between the values of SD-N-1 and the respective secondary reference. The Pb error value of 12% for SA1B9 (calculated by Bayesian Statistics) is a more realistic than 4.31% (calculated by conventional statistics), because the mean Pb concentration is close to the detection limit. Hence, the error is expected to be higher than 4.31%. All errors (CV, Table 6.12) are within the acceptable long term precision range (10-15%) quoted by

Table 6.13 Comparison of Secondary Reference Errors* derived by 1) Conventional Statistics (Co) and 2) Bayesian Statistics (By), for all grain sizes.

	Pb	Cu	Ni	Zn	Fe	Mn	Cr	ORGANIC
Total (SD-N-1)								
Co	4.0	2.0	5.0	4.0	6.0	4.0	3.0	4.0
Sand (AHE/1 B9)								
By	12.0	5.0	11.0	9.0	13.0	11.0	6.0	12.0
Co	4.3	5.2	10.2	5.8	48.3	30.3	7.1	28.2
Silt (TS/1 3)								
By	15.0	6.0	9.0	9.0	10.0	8.0	6.0	9.0
Co	43.7	14.8	16.8	6.8	14.1	14.1	10.4	11.1
Clay (TS/1 3)								
By	8.0	6.0	10.0	11.0	11.0	8.0	6.0	9.0
Co	10.6	11.1	18.2	18.2	12.9	11.6	12.0	15.1

*; Errors are expressed as percentages of the Mean X

Potts (1987).

It is concluded that good precision has been obtained using HF/HNO_3 digestion and FAAS analysis of sediments. All clay error values are less than 11%. Most silt and sand errors values are less than 12%. The highest error value is 15% for Pb in silt which accounts for the proximity of the original mean (X) of ZT3 to the detection limit.

The error values (By) tabulated in Table 6.13 are taken as the percentage errors applicable to all data (FAAS) of the respective grain size throughout this study. The analysis of total sediment was of lesser importance than individual grain sizes, hence the error values (Co) of SD-N-1 are considered adequate to represent the total sediment data.

6.7 X-RAY FLUORESCENCE ANALYSIS OF SEDIMENTS

The majority of heavy metal analyses were carried out using the FAAS technique. A small number of samples (approximately 140) from all grain sizes were also analysed using XRF. The XRF study was carried out to provide a further check on bias of the FAAS technique used in this study.

6.7.1 Instrumentation, Precision, and Accuracy of XRF Analysis

In simple terms the XRF instrumentation is as follows. A X-ray tube operated at a potential between 10-100KV generates primary X-rays which bombard a sample (which has been prepared as a compressed powder pellet or fused glass disc). During irradiation inner electrons are excited from atoms of elements in the sample. Outer electrons then fall back into the inner orbital vacancies and fluorescent X-rays of wavelengths characteristic of that element are emitted. The emission intensity of the characteristic radiation is measured and compared with that from a

standard sample.

X-ray counts are not directly proportional to atomic concentration but must first be corrected for absorption-enhancement effects caused by the influence of other elements in the sample. Norrish and Hutton (1969), Harvey et al (1973), and Norrish and Chappell (1977) describe standard iterative correction procedures based on calculation of matrix attenuation for glass discs and powder pellets.

Analytical accuracy of XRF studies depend on both the reliability of the matrix correction program and procedures used for calibration and sample preparation. Calibrations are carried out relative to known element compositions in reference materials. Therefore accuracy is critically affected by both the selection of samples to be included in the calibration set, and the confidence that may be placed on compiled compositions of reference materials. Maximum accuracy is achieved by calibrating samples against as many international rock standards as possible.

Precision of the XRF technique is excellent and is governed by Poisson statistics of X-rays counts. The instrumental precision is usually better than quoted for international data which is a combination of results from widely different laboratories and techniques. Normally precision is obtained at the 0.2% level for major elements and 1-2% for trace elements (Potts, 1987).

6.7.2 Analytical Procedures and Operating Conditions of this Study

1) Operating Conditions

All samples were analysed on an automated Philips PW 1400 X-Ray Spectrometer (located in the Geology Department of the University of Canterbury). The Spectrometer was calibrated and operated by Stephen Brown. Mass absorption corrections were made using Compton and Rayleigh tube

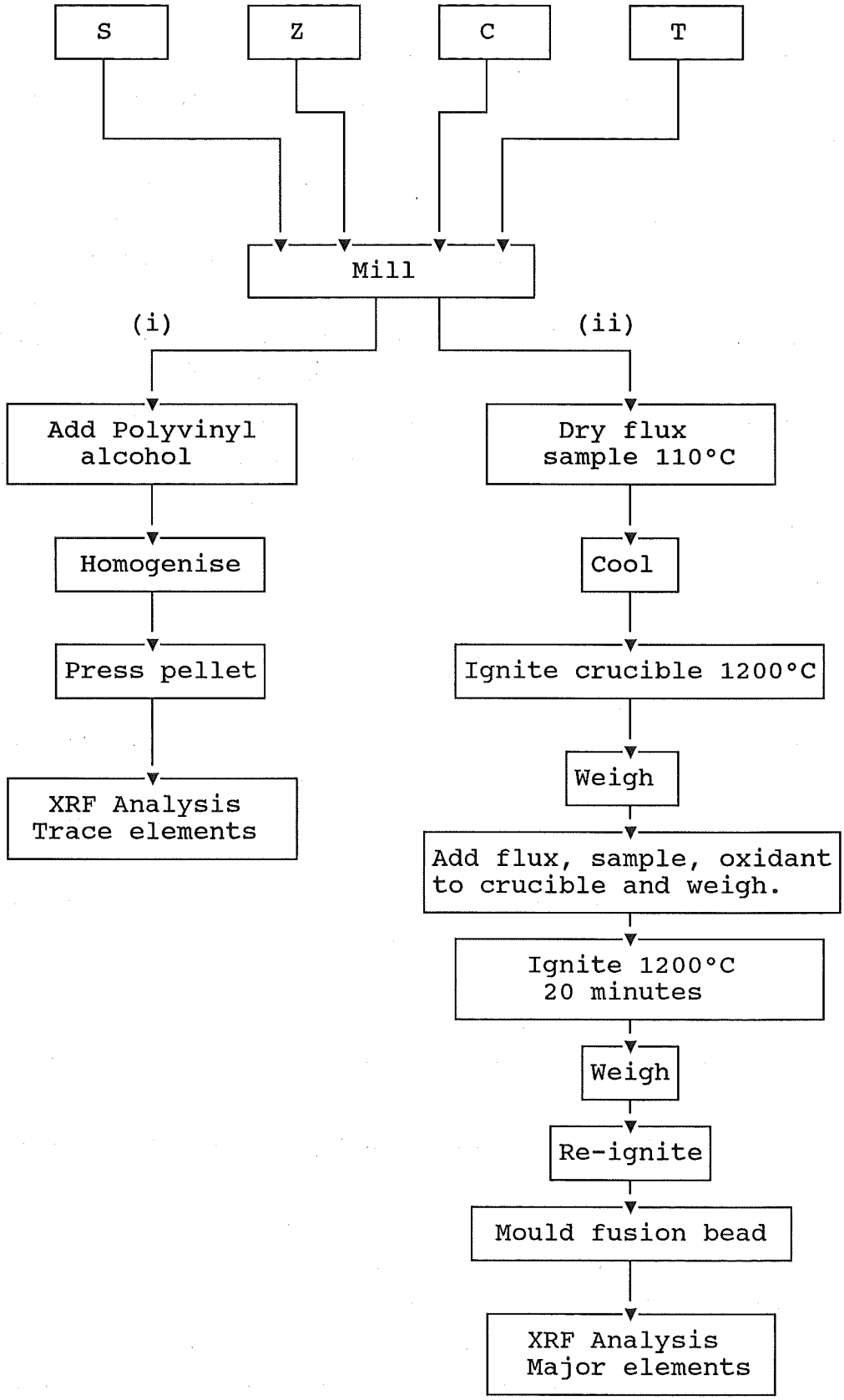

Fig. 6.8 Procedure used in XRF analysis of sediments.

lines. The software comprised the program "Base" written by R.Lee (1980, Department of Geology, University of Western Australia) and modified by Stephen Brown and Arther Alloway to improve mass absorption co-efficients and consequently analytical sensitivity and precision. Major elements (Si, Ti, Al, Fe, Mn, Mg, Ca, Na, K, P) were determined as weight % of the element oxide using fusion beads and Cr-radiation. Trace element analyses were carried out using pressed powder pellets; some analysed by Mo-radiation (Rb, Sr, Pb, Th, Ga) and others by Au-radiation (Ba, Zr, Nb, Y, La, Nd, Ce, V, Cr, Ni, Zn). The instrument was not calibrated for Cu analysis. See Table 6.1 for detection limits of this technique.

2) Sample Preparation

Sample preparation follows the procedure outlined in Fig. 6.8. Approximately 30g of each sample was ground in a tungsten carbide ring mill which had been pre-cleaned with silica sand and washed with double distilled water and dried, then milled with some of the sample (which was discarded) and washed and dried again. Samples less than 15g were milled in a tungsten carbide ring mill. Between samples, mills were scrubbed, flushed with DDW and dried.

i) Powder Pellets

Pressed powder pellets were made by mixing 5g of powdered sample with 5 drops of 7% Polyvinyl alcohol (brand Mowiol) which formed the binding agent. The homogenised mixture was then placed in a cylindrical steel mould; a steel piston was inserted and the mixture compacted with a 5 tonne hydraulic press to form a pellet 32mm in diameter and 4mm thick. The pellets were then placed in an oven at 70°C for 12 hours to dry. In the case of some clay and silt samples there was often less than 2g of sample available. These samples were added to boric acid in ratio 1 to 5 and pressed without the addition of the binding agent. Duplicate totals and sands were prepared using boric acid

Table 6.14 Comparison of Heavy Metal Analysis of Primary References by Flame AAS and XRFS.

Reference Material	Parent Rock	Pb			Cu			Ni			Zn			Fe			Mn			Cr		
		μ	AAS	XRF	μ	AAS	XRF	μ	AAS	XRF	μ	AAS	XRF	μ	AAS	XRF	μ	AAS	XRF	μ	AAS	XRF
SD-N-1	Sediment	120.0	98.8	117.0	72.2	68.2	-	31.0	23.0	29.0	439.0	499.0	448.0	36400.0	30700.0	43000.0	777.0	542.0	812.0	149.0	134.0	162.0
SY3	Syenite	133.0	117.0	111.0	17.0	14.6	-	11.0	2.4	14.0	244.0	251.0	246.0	45400.0	35300.0	-	2480.0	1690.0	-	11.0	6.3	12.0
MRG-1	Gabbro	10.0	<10.0	9.0	134.0	133.0	-	193.0	192.0	194.0	191.0	180.0	202.0	125300.0	82500.0	124600.0	1318.0	872.0	1160.0	430.0	282.0	485.0
NIMG	Granite	40.0	20.5	41.0	12.0	9.6	-	8.0	<2.0	6.0	50.0	32.4	53.0	13500.0	5610.0	13400.0	162.0	23.9	<100.00	12.0	5.5	13.0
NIML	Lujarite	43.0	41.9	42.0	13.0	13.0	-	11.0	<2.0	7.0	400.0	374.0	383.0	66600.0	58300.0	69800.0	5968.0	2989.0	6120.0	10.0	8.4	14.0
NIMS	Syenite	5.0	<10.0	4.0	19.0	18.6	-	7.0	2.3	11.0	10.0	5.0	13.0	9360.0	4320.0	10100.0	77.5	23.0	<100.00	12.0	8.5	11.0
MAG-1	Mud	24.0	10.5	-	30.0	28.3	-	53.0	38.0	-	130.0	107.0	-	47500.0	40300.0	-	760.0	310.0	-	97.0	102.0	-
SCO-L	Shale	31.0	30.2	-	28.7	28.2	-	27.0	17.8	-	103.0	119.0	-	35900.0	29200.0	-	410.0	250.0	-	68.0	69.6	-
RE*	CI 95%			±1.1						±.739			±3.16			±400			±190			±.54

μ; certified mean value quoted in the literature (Govindaraju, 1989; IAEA, 1988)
All results are μg/g.
* RE; relative errors calculated for NIM-G, and SY-3 (Weaver, et al, 1990)
-; no data

to check reproducibility relative to pure sample pellets. Four pure boric acid pellets were run as analytical blanks.

ii) Fusion beads

Fusion beads were prepared following the methods described by Norrish and Hutton (1969), Harvey et al (1973), and Schroeder (1980). The method is summarised as sequence ii) in Fig. 6.8. Pre-weighed 0.3g samples and flux (blended lithium tetraborate, lithium carbonate and lanthanum oxide) were oven dried at 110°C for 12 hours prior to bead preparation. Batches of 3 samples and a flux were prepared at a time (30-40 minutes). Each sample was mixed with 1.61g of flux and a few grains of oxidant (NH_4NO_3) in a platinum crucible. Crucibles were heated at approximately 1200°C for 20 minutes, then cooled to room temperature and reweighed to determine any weight loss. The crucibles and contents were then reheated for a further 20 minutes. Each melt was subsequently poured into a pre-heated (250°C) aluminium mould and then compressed to make a bead. The beads were cooled slowly by successive 1 hour periods on high temperature and low temperature hot plates. All beads were stored in plastic bags and desiccated until analysed. The weight loss on ignition was determined for each sample using the flux and sample weight changes. A flux blank was analysed to check for contamination.

6.7.3 Accuracy and Precision of the XRF Method

Table 6.14 contains results of Pb, Cu, Ni, Zn, Fe, Mn, and Cr analyses of standard reference materials by FAAS and XRF compared with the certified values of Govindaraju (1989) and IAEA (1988). Generally the XRF results are slightly higher and more accurate than the results by FAAS. There was not enough sediment to duplicate pellets. Hence, error statistics were not computed because only one analysis was performed for each reference. However, Table 6.14 presents standard deviations reported by Weaver et al (1990) for XRF results of NIM-G and SY-3, which illustrate

Table 6.15 Results of Intercomparison of FAAS and XRF

Metal & Sample	X(XRF)	X(FAAS)	X(D)	S(D)	X(D)e	CI of X(D)	X(FAAS)/ X(XRF)100 %
Fe							
Total	1.9	1.3	.5	.2	±.08	0.4-.42	71.0
Sand	1.8	1.1	.8	.4	±.24	0.52-1.0	63.0
Silt	2.5	2.3	.2	.4	±.20	0.02-.42	92.0
Clay	5.9	4.4	1.4	.8	±.43	0.97-1.83	75.0
Mn							
Total	241.0	74.3	170.0	64.0	±28.4	142-198	31.0
Sand	221.0	82.1	149.0	127.0	±97.6	51.4-247	37.0
Silt	295.0	148.0	195.0	115.0	±73.1	122-268	50.0
Clay	649.0	432.0	269.0	178.0	±127	142-396	66.0
Pb							
Total	17.3	8.5	8.8	4.7	±1.83	7.0-10.7	49.0
Sand	17.8	4.0	13.8	3.2	±2.28	11.5-16.1	22.0
Silt	30.9	20.9	10.0	8.5	±7.14	2.82-17.1	68.0
Clay	70.8	33.8	37.0	15.3	±7.87	29.1-44.9	48.0
Cr							
Total	30.6	28.8	1.8	4.4	±1.6	0.2-3.4	94.0
Sand	32.6	29.6	5.3	10.5	±6.35	-1.02-11.7	91.0
Silt	43.4	37.2	6.2	10.8	±5.06	1.11-11.2	86.0
Clay	77.8	79.9	-2.1	16.5	±8.48	-9.05-6.42	103.0
Ni							
Total	10.7	12.3	-1.6	3.6	±1.32	-2.91- -0.27	115.00
Sand	10.9	8.9	2.0	2.6	±1.85	0.18-3.88	81.0
Silt	12.2	11.1	1.1	4.1	±2.29	-1.15-3.43	91.0
Clay							
Zn							
Total	45.3	25.5	19.9	8.1	±2.97	16.9-22.9	56.0
Sand	48.7	25.2	23.5	13.5	±8.16	15.3-31.7	52.0
Silt	63.2	37.0	26.2	20.7	±9.69	16.5-35.9	59.0
Clay	196.0	167.0	28.7	92.3	±47.5	-18.8-76.2	85.0

X(XRF), mean of XRF Data; X(FAAS), mean of FAAS Data;
X(D), X(XRF)-X(FAAS); S(D), standard deviation of X(D);
X(D)e, error of X(D) at 95% Confidence; CI of X(D), 95% confidence interval of X(D). All results in μg/g except Fe (%).

the excellent precision of the Geology Department instrument. The results in Table 6.14 show excellent accuracy for Pb, Ni, Zn, Fe, and Cr. Manganese results are slightly more variable.

6.7.4 Intercomparison of XRF and FAAS

A large number of samples, from each grain size, were analysed by both techniques. The average difference, X(D), between the two techniques for individual samples (within each grain size) is presented in Table 6.15. The standard deviation S(D) and the 95% confidence interval of the mean X(D) are also given. If the confidence interval contained zero or lay within errors either side of zero then the difference between the two techniques was considered insignificant.

Flame Atomic Absorption Spectroscopy yielded lower Fe results than XRF. The Mn results produced by XRF are just on the detection limit of the technique, so X(D) values are below the error values. (However Mn results are also lower for FAAS.) Lead results tend to be 5-15ppm lower by FAAS than those by XRF. These values are similar to the relative error obtained for SD-N-1 and the concentrations found in the digestion residues (Table 6.10). Chromium and Ni results are not significantly different. Zinc FAAS values are approximately 20-30 ppm below respective XRF values.

All metal results are higher, except Cr and Ni, using XRF than FAAS. The results of 1) other analysts (FAAS), 2) XRD and XRF analyses of HF/HNO_3 digestion residues and 3) the intercomparison between XRF and FAAS show that the digestion residues clearly contain some Pb, Fe, Zn, and Mn. Hay (1988) compared Cr, and Ni results between the two techniques and also obtained good agreement for both metals.

REFERENCES

ABBEY, S. 1983: Studies in "Standard Samples" of Silicate Rocks and Minerals 1969-1982. Geol. Surv. Canada, Paper 83: 15p.

ACKERMANN, F. 1980: A Procedure for Correcting the Grain Size Effect in Heavy Metal Analysis of Estuarine and Coastal Sediments. Environ. Tech. Letters 1: 518-527.

ACKERMANN, F.; BERGMANN, H.; SCHLIECHERT, U. 1983: Monitoring of Heavy Metals in Coastal and Estuarine Sediments - A Question of Grain Size: <20μm versus <60μm. Environ. Tech. Letters 4: 317-328

AGGETT, J.; SIMPSON, J.D. 1986: Copper Chromium and Lead in Manukau Harbour Sediments. New Zealand Journal of Marine and Freshwater Research 20: 661-663.

AHLERS, W.W.; HUNTER, K.A. 1989: Mass Transport and Natural Distributions of some Trace Metals in the Manuherikia River, Central Otago. In McLaren, R.G.; Haynes, R.J; Savage, G.P. (Editors). Trace Elements in New Zealand: Proc. N.Z. Trace Element Group Conference November 1988, Lincoln College Canterbury: 37-46.

AHLF, W.; CALMANO, W.; FORSTNER, U. 1986: The Effects of Sediment-Bound Heavy Metals on Algae and Importance of Salinity. In Sly, P.G. (Editor). Sediments and Water Interactions. Springer-Verlag N.Y.: 320-324.

ALLEN, G.P. 1971: Relationship Between Grain Size Parameter Distributions and Current Patterns in the Gironde Estuary (France). J. Sediment. Petrology. 41(1): 74-88

AMERICAN PUBLIC HEALTH ASSOCIATION (APHA), 1971: Standard Methods for Examination of Water and Wastewater (13th ed.). American Public Health Association, American Waterworks Association and Water Pollution Control Federation, Washington D.C.: 874p.

ANDERSON, J.C. 1949: Old Christchurch in Picture and Story. Simpson and Williams Ltd, Christchurch, New Zealand: 500p.

ANDERSON, R.L. 1987: Practical Statistics for Analytical Chemists. Van Nonstrand Reinhold Company Inc.: 316p.

ANDERSON, T. 1985: Geochemistry of Christchurch River Sediments: The Avon River. BSc Hons Thesis, Chemistry Department University of Canterbury: 10p.

ANGELIDIS, M.; GRIMANIS A.P., 1989: Geochemical Partitioning of Co, Cr, Fe, Se, Zn, in Polluted and Non-polluted Marine Sediments. Environmental Pollution 62: 31-46.

APPLEBY, P.G.; OLDFIELD, F. 1978: The calculation of Lead-210 Dates assuming a Constant Rate of Supply of Unsupported ^{210}Pb to the sediment. Catena Vol 5: 1-8.

ARAUJO, M.F.D.; BERNARD, P.C.; VAN GRIEKEN, R.E. 1988: Heavy Metal Contamination in Sediments from the Belgian Coast and Scheldt Estuary: Marine Pollution Bulletin 19(6): 269-273.

ASTON, S.R,; CHESTER, R. 1976: Estuarine Sedimentary Processes. In BURTON, J.D.; LISS, P.S. "Estuarine Chemistry. Academic (Press) London Ltd: 37-52.

BALLS, P.W. 1989: Trend Monitoring of Dissolved Trace Metals in Coastal Sea Water - A Waste of Effort. Marine Poll. Bulletin 20: 546-548.

BARNETT, B.; FORBES, S.; ASHBROFT, C. 1989: Heavy Metals on the South Bank of the Humber Estuary. Marine Pollution Bulletin 20(1): 17-21.

BARR, D. (Personal Communication.) 81 Main Road, Redcliffs, Christchurch, New Zealand.

BENNINGTON, S.L. 1979: Some Aspects of the Biology and Distribution of Amphibola crenata (Gastropoda: Pulmonata) with Special Reference to Possible Effects of Pollution from Sewage Outfalls. Unpublished PhD Thesis, University of Canterbury, Department of Zoology. Christchurch, New Zealand.

BIGGS, L.R. 1947: The Formation Control and Utilisation of the Coastal Sand Dunes between the Waimakariri River and the Sumner Estuary. M.A. Honours, Geography Department, University of Canterbury.

BISCAYE, P.E. 1964: Distinction between Kaolinite and Chlorite in Recent Sediments by X-ray Diffraction. The American Mineral. 49: 1281-1289.

BLAKE, G.J. 1964: Coastal Progradation in Pegasus Bay. MSc Thesis, Geography Department, University of Canterbury: 188p.

BLATT, H.; MIDDLETON, G.; MURRAY, R. 1980: Origin of Sedimentary Rocks. 2nd Edition. Prentice-Hall, Inc., New Jersey: 782p.

BLOOM, H. 1975: Heavy Metals in the Derwent Estuary. Chemistry Department, University of Tasmania: 121p.

BORDALO COSTA, M.M.; PENEDA, M.C. 1989: Heavy Metal Detection in the Sediment-Water Components of the Sado Estuary by Multielement Analysis. Environmental Technology Letters. 10: 697-705.

BRADY, J.E.; HUMISTON, G.E. 1980: General Chemistry Principles and Structure. John Wiley and Sons, Inc. Canada: 779p.

BRINDLEY, A.W.; BROWN, G. 1980: Crystal Structures of Clay Minerals and their X-ray Identification. Mineralogical Society Monograph No. 5: 495p.

BROWN, L.J. 1986: Thermal and Mineral Spring Sampling Banks Peninsula. New Zealand Geological Survey Field Report. M36/466: 2p.

BROWN, L.J.; WILSON, D.D. 1988: Stratigraphy of the Late Quaternary Deposits of the Northern Canterbury Plains, New Zealand. New Zealand Journal, Geology Geophysics 31: 305-335.

BROWN, L.J.; WEBER, J.H. in press: Geology of Christchurch Urban Area. (1:25,000) N.Z. Geol. Surv. Misc. Series. Map (1 Sheet) notes.

BROWN, L.J.; WEBER, J.H. in prep: Thermal and Mineral Water at the Margin of Banks Peninsula and Canterbury Plains.

BRUCE, A. 1952: Report on a Biological and Chemical Investigation of the Waters in the Estuary of the Avon and Heathcote Rivers. Unpublished Christchurch Drainage Board Report: 40p.

BRUCE, A. 1953: Biological and Chemical Investigation of the Waters of the Avon and Heathcote Rivers. Unpublished Christchurch Drainage Board Report: 22p.

BRULAND, K.W. 1983: Trace Elements in Sea-Water. Chapter 45, In Riley, J.P.; Chester, R. (editors) Chemical Oceanography. Vol 8: 157-229

BRUUN, P. 1978: Stability of Tidal Inlets -Theory and Engineering. Developments in Geotechnical Engineering. Vol. 23. Amsterdam, Elsevier: 506p.

BRUUN, P.; GERRITSEN, F. 1960: Stability of Coastal Inlets. Amsterdam, North Holland: 123p.

BUCKLEY, A. 1989: An Electron Microprobe Investigation of the Chemistry of Ferromanganese Coatings on Freshwater Sediments. Geochem. Cosmochim. Acta 53: 115-124.

BUCKLEY, D.E.; CRANSTON, R.E. 1971: Atomic Absorption Analyses of 18 Elements from a Single Decomposition of Aluminosilicate. Chem. Geol. 7: 273-284

BURGESS, V. 1985: Analysis of Christchurch Estuary Sediments. Unpublished B.Sc Hons Thesis, Chemistry Department, University of Canterbury, Christchurch, New Zealand: 20p.

BURTON, J.D. 1976: Basic Properties and Processes in Estuarine Chemistry. In Burton, J.D.; Liss, P.S. (editors) Estuarine Chemistry. Academic (Press) London Ltd: 1-36.

BURTON, J.D. 1977: Chemical Processes in Estuarine and Coastal Waters: Environmental and Analytical Aspects. Publication of Scientific Section meeting in London on 17 March 1977.

BURTON, J.D. 1978: Behaviour of some Trace Chemical Constituents in Estuarine Waters. Pure and Applied Chemistry 50: 385-393.

BURTON, J.D.; LISS, P.S. 1976: Estuarine Chemistry. Academic Press Inc. (London) Ltd: 229p.

CALMANO, W.; FORSTNER, U. 1983: Chemical Extraction of Heavy Metals in Polluted River Sediments in Central Europe. Sci. Tot. Envir. 28: 77-90.

CALMANO, W.; AHLF, W.; FORSTNER, U. 1988: Study of Metal Sorption/Desorption Processes on Competing Sediment Components with a Multichamber Device. Environmental Geological Water Science 11(1): 77-84.

CAMERON, J. 1970: Biological Aspects of Pollution in the Heathcote River, Christchurch, New Zealand. New Zealand Journal Marine Freshwater Res. 4(4): 431-444.

CARSON, M.A. 1986: Migration of the Ashley River Mouth, 1980-1986: Historical Precedents Possible Causes, and Options Open to the Board. Unpublished Summary Report, North Canterbury Catchment Board: 10p.

CAUWET, G. 1987: Influence of Sedimentological Features on the Distribution of Trace Metals in Marine Sediments. Marine Chemistry 22: 221-234.

CHANTON, J.P.; MARTENS, C.S.; KIPPHUT, G.W. 1983: Lead-210 Sediment Geochronology in a Changing Coastal Environment. Geochim. et Cosmochim. Acta. 47: 1791-1804.

CHAU, Y.K. 1986: Occurrence and Speciation of Organo-metallic Compounds in Freshwater Systems. Sci. Tot. Envir. 49: 305-323.

CHRISTCHURCH DRAINAGE BOARD (CDB) 1988: Heavy Metals in the Rivers and Estuaries of Metropolitan Christchurch and Outlying Areas. Unpublished Report of Christchurch Drainage Board: 221p.

CHURCHMAN, G.J. 1980: Clay Minerals Formed from Micas and Chlorites in some New Zealand Soils. Minerals 15: 59-76.

CRONAN, D.S. 1972: Skewness and Kurtosis in Polymodal Sediments from the Irish Sea. Journal of Sedimentary Petrology 42(1): 102-106.

DAHAB, O.A. 1989: Chromium Biogeochemical Cycle in Abu Kir Bay, East of Alexandria, Egypt. Est. Coast. Shelf Sci. 29: 327-340.

DARBY, D.A.; ADAMS, D.D.; NIVENS, W.T. 1986: Early Sediment Changes and Element Mobilization in a Man-made Estuarine Marsh. In Sly P.G. (Editor) Sediments and Water Interactions. Springer-Verlag N.Y.: 343-351.

DAVIS, J.A. 1990: Control of Trace Metal Concentrations by Sorption Process. In the Programme and Abstracts of the 2nd International Conference of Trace Metals in the Aquatic Environment, Sydney Australia, July 8-14, 1990: 63.

DAVIS, J.C. 1973: Statistics and Data Analysis in Geology. John Wiley and Sons, Inc.: 550p.

DEAN, R.B.; DIXON, W.J. 1951: Analytical Chemistry 23: 636p.

DEELY, J.M. 1987: Heavy Metal Distributions in the Avon-Heathcote Estuary. Unpublished M.Sc report, Geology Department, University of Canterbury, Christchurch, New Zealand: 39p.

DEELY, J.M. 1989: Trace Metal Distributions in Sediments of the Avon-Heathcote and Saltwater Creek Estuaries, Christchurch. In Trace Elements in New Zealand Environmental Human and Animal. Proc. New Zealand Trace Elements Group Conference, 30 November-2 December 1988. Lincoln College, Canterbury: 47-56.

de FOREST, A.; PETTIS R.W.; FABIS, G. 1978: Analytical Acceptability of Trace Metal Levels found in Ocean Waters around Australia. Australian Journal Marine Freshwater Res. 29: 193-204.

de GROOT, A.J.; SALOMONS, W.; ALLERSIMA, E. 1976: Processes Affecting Heavy Metals in Estuarine Sediments. In Burton, J.D.; Liss, P.S. (editors) Estuarine Chemistry. Academic (Press) London Ltd: 131-157.

DEHAIRS, F.; BAEYENS, W.; VAN GANSBOEKE, D. 1989: Tight Coupling Between Enrichment of Iron and Manganese in North Sea, Suspended Matter and Sedimentary Redox Processes: Evidence for Seasonal Variability. Estuarine, Coastal and Shelf Science 29: 457-471.

DELAUNE, R.D.; CAMBRELL, R.P.; KNOX, R.S. 1989: Accumulation of Heavy Metals and PCB'S in an Urban Lake. Environmental Technology Letters 10: 753-762.

de SAZUA, C.M.M.; PESTANA, M.H.D.; LACERDA ,L.D. 1986: Geochemical Partitioning of Heavy Metals in Sediments of Three Estuaries Along the Coast of Rio De Janeiro (Brazil). The science of the Total Environment 58: 63-72.

de THEIR, W. 1976: Sumner to Ferrymead. Pegasus Press, New Zealand: 216p.

DICKSON, R.J.; HUNTER, K.A. 1981: Copper and Nickel in Surface Waters of Otago Harbour. New Zealand Journal, Marine Freshwater Research 15: 475-480.

DILLON P.J.; SCHOLER, P.J.; EVANS, H.E. 1986: ^{210}Pb Fluxes in Acidified Lakes. In Sly P.J. (editor) Sediments and Water Interactions. Springer-Verlag N.Y. Berlin, Heidelberg, London, Paris, Tokyo: 491-499.

DISSANAYAKE, C.B. 1984: Geochemistry of the Muthurajawela Peat Deposits of Sri Lanka. Fuel 63: 1949-1960.

DOBSON, A.D. 1930: Reminiscence of Arthur Dudley Dobson: Engineer. Whitcomb and Tombs, Christchurch, New Zealand: 219p.

DONAZZOLO, R.; MERLIN. O.H.; MITTURIJAND M.L.; PAVONI, B. 1984: Heavy Metal Content and Lithological Properties of Recent Sediments in the Northern Adriatic. Marine Pollution Bulletin 15(3): 93-101.

DREVER, J.I. 1982: The Geochemistry of Natural Waters. Prentice-Hall, Inc. Englewood Cliffs, N.J. 7632: 388p.

DYER, K.R. 1973: Estuaries: A Physical Introduction. John Wiley & Sons: 140p.

EAKINS, J.D.; MORRISON, R.T. 1978: A New Procedure for the Determination of Lead-210 in Lake and Marine Sediments. Inter. Jour. Appli. Radiation and Isotopes 29: 531-536.

EDGERLEY, W.; TUNNICLIFF, C. 1989: Determination of Heavy Metals at Ultra-trace Levels in Natural Waters. In McLaren, R.G.; Haynes, R.J.; Savage, G.P; (Editors) Trace Elements in New Zealand Environmental, Human and Animal. Proc. New Zealand Trace Elements Group Conference November 1988: 271-274.

EDGINGTON, D.N.; ROBBINS, J.A. 1976: Records of Lead Deposition in Lake Michigan Sediments since 1800. Environmental Science and Technology 10(3): 266-273.

EL GHOBARY, H.; LATOUCHE, C. 1986: A Comparative Study of the Partitioning of Certain Metals in Sediments from Four Near Shore Environments of the Aquitaine Coast (Southwest France). In Sly P.G. (Editor) Sediments and Water Interactions. Springer-Verlag N.Y.: 105-124.

ELLIS, J.B.; REVITT, D.M. 1982: Incidence of Heavy Metal in Street Surface Sediments. Solubility and Grain Size Studies. Water, Air and Soil Pollution 17: 87-100.

ELLIS, P.J.; STEELE, T.W. 1982: Five Robust Indicators of Central Value. Geostandards Newsletter 6(2): 207-216.

ERIKSON, E. 1985: Principles and Applications of Hydrochemistry. Chapman and Hall: 192p.

EVANS, R.D.; CORNETT, R.J.; McCULLOCH, V.A. 1986: The Use of Sediments as Indicators of Point and Diffuse Source of Pollution. In Sly P.G. (Editor) Sediments and Water Interactions. Springer-Verlag N.Y.: 123-132.

EWING, G.W. 1985: Instrumental Methods of Chemical Analysis. McGraw-Hall, New York.

FAHEY, J.J. 1971: The Removal of Potassium Silicofluoride Formed in the Determination of Coesite and Stishovite. The American Mineralogist 56: 2145-2146.

FARMER, J.G. 1978: The Determination of Sedimentation Rates in Lake Ontario Using the ^{210}Pb Dating Method. Canadian Journal Earth Science 15: 431-437.

FARMER, J.G.; LOVELL, M.A. 1984: Massive Diagenetic Enhancement of Manganese in Loch Lomand Sediments. Environmental Technical Letters 5: 257-262.

FARRAH, H.; PICKERING, W.F. 1976: The Sorption of Zinc Species by Clay Minerals. Australian Journal Chemistry 29: 1649-56.

FERGUSSON, J.E.; Ryan, D.E. 1984: The Elemental Composition of Street Dust from Large and Small Urban Areas Related to the City Type, Source and Particle Size. Sci. Tot. Envir. 34: 101-116.

FERGUSSON, J.E.; FORBES, E.A.; SCHROEDER, R.J.; RYAN, D.E. 1986: The Elemental Composition and Sources of House Dust and Street Dust. Sci. of Tot. Envir. 50: 217-221.

FERNEX, F.E.; SPAN, D.; FLATAU, G.N.; RENARD, D. 1986: Behaviour of Some Metals in Surficial Sediments of the Northwest Mediterranean Continental Shelf: In Sly P.G. (editor) Sediments and Water Interactions. Springer-Verlag N.Y.: 354-370.

FINDLAY, R.H. 1981: The Mouth of the Avon-Heathcote Estuary: A Review of the Historical Development of the Mouth of the Estuary of the Avon and Heathcote Rivers. Christchurch City Council, September 1984: 22p.

FINDLAY, R.H.; KIRK, R.M. 1988: Post 1847 Changes in the Avon-Heathcote Estuary, Christchurch: A Study of the Effect of Urban Development Around a Tidal Estuary. New Zealand Journal Marine Freshwater Res. 22: 101-127.

FINNEY B.; HUH, C. 1989: High Resolution Sedimentary Records of Heavy Metals from the Santa Monica and San Pedro Basins, California. Marine Pollution Bulletin 20(4): 181-187.

FLEET, M.E. 1984: Environmental Geochemistry: Short Course Handbook of the Mineralogical Association of Canada 10: 306p.

FLEGAL, A.R. 1986: Lead in Tropical Marine Systems: A Review. Sci. Tot. Envir. 58: 1-8.

FLORENCE, T.M. 1982: The Speciation of Trace Elements in Waters. Talanta 29: 345-364.

FLORENCE, M. 1988a: Lecture Notes: Comparison of Trace Element Analysis Techniques. CSIRO, Division of Energy Chemistry. Lucas Heights Research Laboratories Private Mail Bag 7, Sutherland, NSW 2232.

FLORENCE, T.M. 1988b: Lecture Notes. Comparison of Nuclear and Non-nuclear Techniques of Trace Analysis.

FLORENCE, T.M. 1990: Determination of the Toxic Fractions of Some Heavy Metals in Natural and Polluted Waters. In the Programme and Abstracts of the 2nd International Conference of Trace Metals in the Aquatic Environment, Sydney, Australia, July 8-14 1990: 90.

FLORENCE, T.M.; BATLEY, G.E. 1977: Talanta Mini Review: Determination of the Chemical Forms of Trace Metals in Natural Waters, with Special Reference to Copper, Lead, Cadmium and Zinc. Talanta 24: 151-158.

FOLK, R.L.; WARD, W.C. 1957: Brazos River Bar: A Study in the Significance of Grain Size Parameters. J. Sed. Petrol.27: 3-26.

FORSTNER, U. 1989: Contaminated Sediments: Lectures on Environmental Aspects of Particle-Associated Chemicals in Aquatic Systems. Springer-Verlag Berlin, Heidelberg, New York: 157p.

FORSTNER U.; AHLF,W.; CALMANO, W.; KERSTEN, M.; SALOMONS, W. 1986: Mobility and Heavy Metals in Dredged Harbour Sediment. In Sly P.G. (Editor) Sediments and Water Interactions. Springer-Verlag N.Y.: 371-380.

FORSTNER, U.; SALOMONS, W. 1980: Trace Metal Analysis on Polluted Sediments, Part 1: Assessment of Sources and Intensities. Environment Technical Letters: 494-505.

FORSTNER, U.; WITTMAN, G.T.W. 1981: Metal Pollution in the Aquatic Environment. 2nd Edition. Spring-Verlag, Berlin, Heidelberg, New York: 486p.

FYFE, W.S. 1984: The Geochemical Cycle. In Fleet M.E.: Environmental Geochemistry. MAC Short Course Handbook 10: 1-11.

GARDNER, L.R.; SHARMA, P.; MOORE W.S. 1987: A Regeneration Model for the Effect of Bioturbation by Fiddler Crabs on ^{210}Pb Profiles in Salt Marsh Sediments. Journal Environmental Radioactivity 5: 25-36.

GAWNE, K. 1986: Special Problems Associated with the Analysis of Heavy Metals at the Ultra Trace Level. In Baker, M.J. (Editor) Trace Elements in the Eighties. Proceedings of the conference of the New Zealand Trace Element Group, August 1984: 60-64.

GELLENDER, M. 1982: The Problems of Utilizing Trace Analysi in Regulatory Analytical Chemistry. Chemistry International 4: 8-9.

GIBB, E.S. 1981: Some Aspects of Ecology and Morphology of the Zostera Muelleri on the Avon-Heathcote Estuary, Christchurch. Unpublished B.Sc Hons Thesis. Plant and Microbiology Department, University of Canterbury,Christchurch, New Zealand.

GIBB, J.G. 1986: A New Zealand Regional Holocene Eustatic Sea-level Curve and its Application to Determination of Vertical Tectonic Movements. Royal Society of New Zealand Bulletin 24: 377-395.

GIBBS, R.J. 1977: Transport Phases of Transition Metals in the Amazon and Yukon. Geological Society American Bulletin. Vol. 88: 829-843.

GIBBS, R.J.; ANGELIDIS, M. 1989: Effect of Sludge Digestion on Metal Segregation During Ocean Dumping. Marine Pollution Bulletin 20 (1): 503-508.

GLASBY, G.P.; STROFFERS, P.; WALTER, P.; DAVIS K.R.; RENNER, R.M. 1988: Heavy Metal Pollution in Manukau and Waitemata Harbours, New Zealand. New Zealand Journal of Marine and Freshwater Research 22: 595-611.

GLASSEY, P.J. 1986: Geotechnical Properties of Lime Stabilised Loess, Port Hills, Canterbury. MSc Thesis Geology Department, University of Canterbury, Christchurch, New Zealand.

GLEGG, G.A.; TITLEY, J.G.; MILLWORD, G.E.; GLASSON, D.R.; MORRIS, A.W. 1988: Sorption Behaviour of Waste Generated Trace Metals in Estuarine Waters. Water Science Technology 20(6-7): 113-121.

GOLTERMAN, H.L.; GLYMO, R.S.; OHNSTAD, M.A.M. 1978: Methods of Chemical Analysis of Fresh Waters. Oxford, Blackwell 172p.

GONZALEZ, M.; LERA, L.; TORRESS, I. 1985: Heavy Metals Distribution in Surface Sediments and Core Samples from Havana Bay, Cuba. In Lekkas T.D. (editor) Heavy Metals in the Environment: International Conference, Athens, September 1985.

GOVINDARAJU, K. 1989: 1989 Compilation of Working Values and Sample Description for 272 Geostandards. Special Issue of Geostandards Newsletter 8: 113p.

GOVINDARAJU, K 1984: 1984 Compilation of Working Values and Sample Descriptions for 170 International Reference Samples of Mainly Silicate Rocks and Minerals. Geostandard Newsletter Special Issue 8.

GREENAWAY, R.L.N. 1976: Research Notes New Brighton Area. Heldby Dr. J. Robb, Christchurch City Council (Drainage) Laboratory, Pages Road, Bexley.

GREENE-KELLY, R 1953: The Identification of Montmorillonoids in Clays. Journal of Soil Science 4(2): 233-237.

GRIFFIN, R.A.; SHIMP, N.F. 1976: Effect of pH on Exchange Adsorption or Precipitation of Lead from Landfill Leachates by Clay Minerals. Environmental Science and Technology 10(13): 1256-1260.

GRIFFIN, R.A.; SHRIMP N.F.; STEELE, J.D.; RODNEY R.R.; WHITE A.W.; HUGHES G.M. 1976: Attenuation of Pollutants in Municiple Landfill Leachate by Passage through Clay. Environmental Science and Technology 10(13): 1262-1268.

GRIFFITHS, E. 1973: Loess of Banks Peninsula. New Zealand Journal of Geol. Geophys. 16(3): 657-75.

GRIFFITHS, G.A. 1979: Recent Sedimentation History of the Waimakariri River, New Zealand. New Zealand Journal of Hydrology 18: 6-28.

GRIMANIS, A.P.; KALOGEROPOULOS, N.; ZAFIROPOULOS, D.; VASSILAKI-GRIMANI, M. 1985: Chromium in the Water Column and Sediment Cores from Saronikos Gulf. In T.D Lekkas (Editor) Heavy Metals in the Environment. International Conference, Athens September 1985.

GUNSON, D. 1983: Collins Guide to the New Zealand Sea Shore. William Collins Ltd Auckland: 240p.

GUY, R.D.; CHAKRABARTI, C.L.; McBAIN, D.C. 1978: An Evaluation of Extraction Techniques for the Fractionation of Copper and Lead in Model Sediment Systems. Water Research 12: 21-24.

HAMILTON, E.I. 1989: Some Heavy Metals in Sediments from Darwin Harbour, Australia. Marine Pollution Bulletin 20(2): 91-92.

HAMOUDA, M.S.; WILSON, J.G. 1989: Levels of Heavy Metals along the Libyan Coastline. Marine Pollution Bulletin 2(12): 621-624.

HARBISON, P. 1986: Mangrove Muds -A Sink and Source of Trace Metals. Marine Pollution Bulletin 17(6): 246-250.

HARRISON, S.P.A. 1976: Holocene Stratigraphy of the Avon-Heathcote Estuary. Unpublished BSc Hons Report, Geology Department, University of Canterbury, Christchurch, New Zealand: 49p.

HARVEY, P.K.; TAYLOR, D.M.; HENDRY, R.D.; BANCROFT, F. 1973: An Accurate Fusion Method for Analysis of Rocks and Chemically Related Materials by X-ray Fluorescence Spectrometry. X-Ray Spectrum 2: 33-44.

HART, B.T. 1982: Trace Metals in Natural Waters 1 Speciation. Chemistry In Australia 49(7): 260-265.

HART, B.T.; DAVIES S.H.R. 1978: A Study of the Physico-chemical Forms of Trace elements in Natural Waters and Wastewaters. Department of National Development Australian Water Resources Council Res Project No. 74/60. Technical Paper 35.

HART, B.T.; DAVIES S.H.R. 1977: A Batch Method for the Determination of Ion-exchangeable Trace Metals in Natural Waters. Australian Journal Marine Freshwater Research 28: 397-402.

HAWKINS, D.N. 1957: Beyond the Waimakariri: A Regional History. Whitcombe and Tombs Ltd, Christchurch, New Zealand: 465p.

HAY, R.L. 1988: Studies on Heavy Metals in the Sediments of a Storm Water Drain and the Avon-Heathcote Estuary. Unpublished MSc Thesis Chemistry Department, University of Canterbury, New Zealand: 133p.

HEATH, R.A. 1975: Stability of Some New Zealand Coastal Inlets. New Zealand Journal Marine Freshwater Res. 9(4): 449-457.

HELIOS-RYBICKA, E.; FORSTNER, U. 1986: Effect of Oxyhydrate Coatings on the Binding Energy of Metals by Clay Minerals. In Sly P.G. (Editor) Sediments and Water Interactions. Springer-Verlag N.Y.: 381-385.

HEM, J.D. 1976: Geochemical Controls on Lead Concentrations in Stream Water and Sediments. Geochemical et Cosmochimica Acta 40: 599-609.

HEM, J.D. 1989: Study and Interpretation of the Chemical Characteristics of Natural Water. U.S. Geological Survey Water Supply Paper 2254: 263p.

HENDY, C.H. 1988: The Release of Heavy Metals from Sulphide Bearing Mine Wastes. New Zealand Geochemical Group Newsletter 81: 32.

HERCUS, A.I. 1948: A City Built on a Swamp: The Story of the Drainage of Christchurch 1850-1903.

HOBEN, E.D. 1914: Christchurch, Fair Tree Set City of the Plains. Christchurch Press Co. Ltd, New Zealand: 96p.

HODKINSON R.; CRONAN D.S.; GLASBY G.P.; MOORBY, S.A. 1986: Geochemistry of Marine Sediments from the Lau Basin, Havre Trough, and Tonga-Kermadec Ridge. New Zealand Journal Geol.Geophys. 29: 335-344.

HORNUNG, H.; KRAM M.D.; COHEN Y. 1989: Trace Metal Distributions on Sediments and Benthic Fauna of Haifa Bay, Israel. Estuarine, Coastal and Shelf Sciences 29: 43-56.

HOROWITZ, A.J. 1985: A Primer on Trace Element-Sediment Chemistry. U.S. Geological Survey. Water Supply Paper 2277: 67p.

HOSKING J.W.; SNELL, N.B.; STURMAN B.T. 1977: An Atomic Absorption Interferences Experiment. Journal of Chemical Education 54 (12): 128-130.

HOUNSELL, W.K. 1935: Hydrographical Observations in Auckland Harbour. Trans. Royal Society of New Zealand 64 (3): 257-271.

HOYLE W.C.; ATKINSON, A. 1979: Retardation of Surface Adsorption of Trace Metals by Competitive Complexation. Applied Spectroscopy 33 (1): 37-40.

HULSE, C.A. 1983: Geochemistry of Christchurch River Sediment: Unpublished BSc Hons project, Chemistry Department, University of Canterbury, New Zealand: 15p.

HUME, T.M.; NELSON, C.S. 1982: X-Ray Diffraction Analytical Procedures and Some Mineralogical Characteristics for South Auckland Region Sediments and Sedimentary Rocks with Special Reference to their Clay Fraction. University of Waikato, Occasional Report 10: 33p.

HUME, T.M.; McGLONE, M.S. 1986: Sedimentation Patterns and Catchment use Change Recorded in the Sediments of a Shallow Tidal Creek, Lucas Creek, Upper Waitemata Harbour, New Zealand. New Zealand Journal Marine Freshwater Res. 20: 677-687.

HUME, T.M.; GIBB, J.G. 1987: The "Wooden-Floor" Marker Bed: A New Method of Determining Sedimentation Rates in Some New Zealand Estuaries. Journal Royal Society of New Zealand 17(1): 1-7.

HUME, T.M.; FOX M.E.; WILCOCK, R.J. 1989: Use of Organochlorine Contaminants to Measure Sedimentation Rates in Estuaries: A Case Study from the Manukau Harbour. Journal Royal Society of New Zealand Vol. 19(3): 305-317.

HUNTER, K.A.; HO, F.W.T. 1980: Copper Nickel and Cadmium in Ocean Waters. In Baker M.J (Editor) Trace Elements in the Eighties. Proceedings of the Conference of the New Zealand Trace Element Group August 1984: 35-43.

INTERNATIONAL ATOMIC ENERGY AGENCY (IAEA) 1988: AQCS Intercomparison Runs Reference Materials 1988. Analytical Quality Control Services I.A.E.A Report G4.12. (.P.O. Box 100, A 1400, Vienna, Austria.)

ITTEKKOT, V.; SAFIULLAH, S.; ARAIN, R. 1986: Nature of Organic Matter in Rivers with Deep Sea Connections: The Ganges-Brahmaputra and Indus: Sci. Tot. Envir. 58: 93-107.

IVES, D. 1973: Nature and Distribution of Loess in Canterbury, New Zealand. New Zealand Journal Geol. Geophys. 16(3): 587-610.

IVANOVICH, M.; HARMON, R.S. 1982: Uranium Series Disequilibrium. Applications to Environmental Problems. Clarendon Press Oxford: 563p.

JACKSON, M.L. 1956: Soil Chemical Analysis -Advanced Course. Published by Author, Department of Soil Science, University of Wisconsin, Madison. 986p.

JOHNS, W.D.; GRIM, R.E.; BRADLEY, W.F. 1954: Quantitative Estimations of Clay Minerals by Diffraction Methods. Journal Sediment Petrology 24(2): 242-257.

JOHNSTONE, A.H. 1956: Canterbury Books 1847-1955: A Bibliography. Whitcombe and Tombs Ltd: 195p

JONES, M.B. 1979: Some Methods for Assessing the Toxicity of Pollutants to Aquatic Animals in Water and Soil. Technical Publication 18: 35-40.

JONES, S.H. 1978: Investigation into Christchurch Treatment Works Pipeline From Pond No. 6 to Estuary Low Flow Channel. Unpublished Christchurch Drainage Board Report: 15p.

JORDAO, C.P.; NICKLES, G. 1989: Chemical Associations of Zn, Cd, Pb, and Cu in Soils and Sediments Determined by Sequential Extraction Techniques. Environment Technology Letters 10: 743-752.

KATEMA, G.; PIJPERS, F.W.; 1981: Quality Control in Analytical Chemistry. John Wiley and Son Inc: 276p.

KEITH, L.H. 1983: Principles of Environmental Analysis. Analytical Chemistry 55: 2210-2218.

KENNEDY, P.; TUNNICLIFFE, C.; EDGERLEY W.; LENNIE, A. 1987: Causes of Variability in Trace Element Concentrations in Waters from the Waitekauri Valley. Abstract New Zealand Geochemical Group Conference Nelson, September 1987.

KHEBOIAN, C.L.; BAUER, C.F. 1987: Accuracy of Selective Extraction Procedures for Metal Speciation in Model Aquatic Sediments: Analytical Chemistry 59: 1417-1423.

KIM, N.D. 1990: Studies in the Concentrations and Chemistry of Cadmium in the Environment. Unpublished PhD Thesis, University of Canterbury,Christchurch, New Zealand: 394p.

KIRK, R.M. 1979: Dynamics and Management of Sand Beaches in Southern Pegasus Bay: Unpublished Report, Christchurch City Engineers Department, Christchurch City Council, Christchurch, New Zealand: 173p.

KNOX, G.A. 1974: Report on an Investigation of Blaketown Lagoon, Greymouth. Estuarine Research Unit Department of Zoology, University of Canterbury, New Zealand.

KNOX, G.A.; BOLTON L.A.; SAGAR, P. 1976: The Ecology of Westshore Lagoon, Ahuriri Estuary, Hawkes Bay. Estuarine Research Unit, 125: 89p.

KNOX, G.A.; BOLTON, L.A.; HACKWELL, K. 1978: The Ecology of the Benthic Macroflora and Fauna of Brooklands Lagoon, Waimakariri River Estuary. Estuarine Research Unit 16.

KNOX, G.A.; KILNER A.R. 1973: The Ecology of the Avon-Heathcote Estuary. Unpublished report of Christchurch Drainage Board, Christchurch, New Zealand: 358p.

KNOX, G.A.; MILLHOUSE, D.G.; FENWICK, G.D.; AGAR P. 1976: Report on a Preliminary Investigation of Okanto Lagoon, Westland. Estuarine Research Unit, Department of Zoology, University of Canterbury, Christchurch, New Zealand.

KREGEI-GRAF, K. 1975: Geochemical Facies in Sediments. Soil Science 118(1): 21-23.

KRUMGALZ, B.S. 1989: Unusual Grain Size Effect on Trace Metals and Organic Matter in Contaminated Sediments. Marine Pollution Bulletin 20(2): 608-611.

LAGERWERFF, J.V.; BROWER, D.L. 1973: Division S-2-Soil Chemistry: Exchange Absorption or Precipitation of Lead in Soils Treated with Chlorides of Aluminum, Calcium and Sodium. Soil Science Society of American Proc. 37: 11-13.

LALOU, C. 1982: Sediments and Sedimentation Processes. Chapter 16. In Ivanovich M.; Harmon R.S.; Uranium Series Disequilibrium: Applications to Environmental Problems. Clarendon Press Oxford: 431-458.

LAMB, R.C. 1963: Early Christchurch. Canterbury Public Library, Christchurch, New Zealand: 102p.

LAMB, R.C. 1981: From the Banks of the Avon the Story of a River. A.M. and A.W. Reed Ltd, Wellington, New Zealand: 184p.

LANGMYHR, F.J.; KRINGSTAD, K. 1966: An Investigation of the Composition of the Precipitates Formed by the Decomposition of Silicate Rocks in 38-40% Hydrofluoric Acid: Anal. Chim. Acta 35: 131-135.

LAXEN, D.P.M.; HARRISON, R.M. 1977: Review Paper: The Highway as a Source of Water Pollution: An Appraisal with Heavy Metal Lead. Water Research 11: 1-11.

LEDFORD-HOFFMAN, P.A.; De MASTER, D.J.; NITTROUER, G.A. 1986: Biogenic-silica Accumulation in the Ross Sea and the Importance of Antarctic Continental-Shelf Deposits on the Marine Silica Budget. Geochim. et Cosmochim. Acta 50: 2099-2110.

LEENAERS, H.P. SCHOUTEN, C.J.; RANG, M.C. 1988: Variability of the Metal Content of Flood Deposits: Environ. Geol. Water Science 11(1): 95-106.

LERMAN, A. 1979: Geochemical Processes: Water and Sediment Environments: 481p.

LEWIS, D.W. 1982: Practical Sedimentology. An Apteryx Book: 255p.

LINDLEY, D.V. 1965: Introduction to Probability and Statistics from a Bayesian Viewpoint: Part 2 Inference. Cambridge University Press London, N.W.1: 291p.

LINGERAK, W.A.; WENSVEEN-LOUTER, A.M.; SLANINA, J. 1985: The Determination of Zinc, Cadmium, Lead, and Copper in Precipitation by Computerized Differential Pulse Voltammetry. International Journal Envir. Anal. Chem. 19: 85-98.

LINDZEY, J.T. 1944: A Short Study of the Hydrography of the Avon and Heathcote Rivers. Trans Proc Royal Soc. of New Zealand 73: 365-376.

LISTER, B. 1982: Evaluation of Analytical Data: A Practical Guide for Geoanalysts: Geostandards Newsletter 6(2): 175-205.

LIVINGSTONE, D.A. 1963: Chemical Composition of Rivers and Lakes. In Data of Geochemistry 6th Edition. U.S. Geol. Surv. Prof. Paper 440-G: 64p.

LUSH, D.L. 1984: Regional Geochemical Surveys. In M.E. Fleet (Editor) Environmental Geochemistry. MAC Short Course Handbook 10: 197-216.

McFADGEN, B.G. 1989: Late Holocene Depositional Episodes in Coastal New Zealand. New Zealand Journal of Ecology 12 (Supplement): 145-149.

McGLONE, M.S. 1989: The Polynesian Settlement of New Zealand in Relation to Environmental and Biotic Changes. New Zealand Journal of Ecology (12) Supplement): 115-129.

McLAREN R.G. 1989: Forms of Manganese in Some Soils of Different Drainage Status in Greywacke Alluvium. In McLaren R.G; Haynes R.J.; Savage G.P. (Editors) Trace Elements in New Zealand: Environmental Human and Animals Proc. New Zealand Trace Elements Group Conference November 1988, Lincoln College, Canterbury, New Zealand: 95-102.

MacKENZIE, D. (Personal communication.) Wellington Street. Ashley.

McMANUS, J.; DUCK, R.W.; ALRASOUL, A.M.A.; THOMAS, J.D. 1985: Effects of Storage Before Analyzing Suspended Sediment Samples from Lakes, Rivers and Estuaries. Jour. Sed. Petrol. 55: 613-4.

MACPHERSON, J.M. 1978: Environmental Geology of the Avon-Heathcote Estuary. Unpublished PhD Thesis, Geology Department, University of Canterbury, Christchurch, New Zealand: 222p.

MACPHERSON, J.M. 1979: Response to Urbanisation of the Avon-Heathcote Estuary, Christchurch, New Zealand. Environmental Geology. 2: 23-27.

McSAVENY, M.J.; WHITEHOUSE, I.E. 1989: Anthropic Erosion of Mountain Land in Canterbury. New Zealand Journal of Ecology 12 (Supplement): 151-163.

McWILLIAM, P.J. (Personal Communication). 22 Golf Links Road, Shirley, Christchurch, New Zealand.

MALM, O.; PFEIFFER, W.C.; FISZMANN, M.; AZCUE, J.M.P. 1989: Heavy Metal Concentrations and Availability in the Bottom Sediments of the Paraiba Do Su-Guandu River System, Brazil. Environment Technology Letters 10: 675-680.

MANCE, G. 1987: Pollution Threat of Heavy Metals in Aquatic Environments: Elsevier Applied Science Publishers Ltd, Essex England: 372p.

MARGER, L.J.; MILNE. J. 1951: The Eelgrass Catastrophe: Scientific American 184: 52-55.

MARTENS, C.S.; GOLDHABER, M.B. 1978: Early Diagenesis in Transitional Sedimentary Environments of the White Oak River Estuary, North Carolina: Limmnol. and Ocean. 23(3): 428-441.

MARTINCIC, D.; KWOKAL Z.; STOEPPLER, M.L.; BRANICA, M. 1989: Trace Metals in Sediments from the Adriatic Sea: Sci. Tot. Envir. 84: 135-147.

MASSART, D.L.; DIJKSTRA, A.; KAUFMAN, L. 1978: Evaluation and Optimization of Laboratory Methods and Analytical Procedures. Elesvier Scientific Publishing Company, Amsterdam, the Netherlands: 596p.

MASSART, D.L.; KAUFMAN, L.; 1983: The Interpretation of Analytical Chemical Data by the Use of Cluster Analysis. Elesvier Scientific Publishing Company, Amsterdam, the Netherlands: 490p.

MATTHEWS, K.M.; POTIPIN, J.K. 1985: Extraction of Fallout ^{210}Pb from Soils and its Distribution in Soil Profiles. Journal Environmental Radioactivity 2: 319-331.

MATTINGLEY, B.I. 1989: The Chemaqua Inter-Laboratory Comparison Programme: In McLaren R.G: Haynes, R.J.; Savage, G.P. (Editors) Trace elements in New Zealand Environmental, Human and Animal. Proc. New Zealand Trace Elements Group Conference November 1988, Lincoln College, Canterbury, New Zealand: 275-286.

MAXWELL, J.A. 1968: Rock and Mineral Analysis. John Wiley and Son Inc: 584p.

MITCHEL, P.A. 1989: Geology Hydrothermal Alteration and Geochemistry of the Iamalele (D'Entrecasteaux Islands, Papua New Guinea) and Wairakei (North Island, New Zealand) Geothermal area. PhD Thesis Geology Department, University of Canterbury, Christchurch, New Zealand.

MEADE, R.H. 1972: Transport and Deposition of Sediment in Estuaries. Geological Society America Inc. Memoir 133: 91-120.

MILLHOUSE, D. 1975: The Trace Metal Content of Animals from McCormacks Bay, Avon-Heathcote Estuary, Christchurch. Estuarine Research Unit, Report 4: 10p.

MILLHOUSE, D. 1977: Trace Metals in the Avon-Heathcote Estuary, Christchurch, New Zealand. Department of Zoology, University of Canterbury. Estuarine Research Unit Report 8: 8p.

MILLWARD, W.A.M. 1975: Physical Characteristics of an Estuarine Environment. Unpublished MSc Thesis, Geography Department, University of Canterbury, New Zealand: 121p.

MILNER, H.B. 1962a: Sedimentary Petrography: Volume 1, Methods in Sedimentary Petrography. George Allen and Unwin Ltd: 643p.

MILNER, H.B. 1962b: Sedimentary Petrography Vol 2, Principles and Applications. George Allen and Unwin Ltd. London: 715p.

MONITORING AND ASSESSMENT CENTRE UNIVERSITY OF LONDON 1986: Historical Monitoring. Marc. Report 31: 320p.

MOORE, H.E.; POET S.E. 1976: ^{210}Pb Fluxes Determined from ^{210}Pb and ^{226}Ra Soil Profiles. Journal Geophys. Res. 81(6): 1056-1058.

MORRIS, A.W. 1986: Removal of Trace Elements in the Very Low Salinity Region of the Tamar Estuary, England. Sci. Tot. Envir. 49: 297-304.

MORRISON, J.P. 1948: The Evolution of a City. The Story of Growth of the City and Suburbs of Christchurch the Capital of Canterbury in Years from 1850 to 1903. Christchurch City Council: 197p.

MULLER, G. 1979: Schwermetalle in den Sedimenten des Rheins-Veranderungen Seit 1971. Umschau 79: 778-783.

NEUERBURG, G.J. 1961: A Method of Mineral Separation Using Hydro-fluoric Acid: The American Mineralogist Vol 46: 1498-1501.

NICHOLSON, M.D. 1989: Analytical Results: How Accurate are They? How Accurate Should They be? Marine Pollution Bulletin 20: 33-40.

NICOLAIDOU, A.; NOTT J.A. 1989: Heavy Metal Pollution Induced by a Ferro-nickel Smelting Plant. Sci. Tot. Envir. 84: 113-117.

NICOLAIDOU, A.; DANCUCCI, M.A.; ZENETOS, A. 1989: The Impact of Dumping Coarse Metalliferous Waste on the Benthos in Evoikos Gulf, Greece. Marine Pollution Bulletin 20: 28-33.

NIEBOER, E.; SANFORD, W.E. 1984: Essential, Toxic and Therapeutic Functions of Metals. In Fleet M.E. (Editor) Environmental Geochemistry. Mac Short Course Handbook 10: 149-168.

NIMMO, M.; VAN DEN BERG, C.M.G.; BROWN, J. 1989: The Chemical Speciation of Dissolved Ni, Cu, V, Fe in Liverpool Bay, Irish Sea. Estuarine Coastal and Shelf Science 29: 57-74.

NORRISH, K.L.; CHAPPELL, B.W. 1977: X-ray Fluorescence Spectrometry. In Zussman J. (Editor) Physical Methods in Determinative Mineralogy. Academic Press Inc. (London) Ltd: 201-272.

NORRISH, K.; HUTTON J.T. 1969: An Accurate X-ray Spectrographic Method for the Analysis of a Wide Range of Geological Sample. Geochim, Cosmochim. Acta 33: 431-454.

NORTH CANTERBURY CATCHMENT BOARD 1986: Ashley River Mouth Stability and Options. Unpublished Report, North Canterbury Catchment Board and Regional Water Board: 5p.

NRIAGU, J.O. (ed) 1978: The Biogeochemistry of Lead in the Environment. Part A, Ecological Cycles. Elsevier/North Holland Biomedical Press, Amsterdam.

NRIAGU, J.O. 1986a: Chemistry of the River Niger. (1): Major Ions. Sci. Tot. Envir. 58: 81-88.

NRIAGU, J.O. 1986b: Chemistry of the River Niger (2): Trace Elements. Sci. Tot. Envir. 58: 89-92

NRIAGA, J.O. 1990: Trace Metal Pollution of Lakes: A Global Perspective. In the Programme and Abstracts of the 2nd International Conference of Trace Metals in the Aquatic Environment, Sydney, Australia, July 8-14 1990: 18.

NRIAGU, J.O.; PACYNA, J.M. 1988: Quantitative Assessment of Worldwide Contamination of Air, Water and Soils by Trace Metals. Nature 333: 134-139.

NURNBERG, H.W.; MART, L. 1985: Distribution and Fate of Heavy Metals in the Oceans. In Lekkas T.D. (Editor) Heavy Metals in the Environment. Proceedings of an International Conference, Athens, September 1985: 340-342.

OGILVIE, G. 1978: The Port Hills of Christchurch. A.H. and A.W. Reed Ltd, Wellington N.Z. 246p.

PAGE, H. (Personal Communication): 173 Idris Road, Bryndwar, Christchurch, New Zealand.

PATRICK, M. 1985: Trace Metals in the Aquatic Environment: The Example of Taranaki. Journal Royal Society of New Zealand 15(4): 385-388.

PAULSON, A.J.; CURL, H.C.; FEELY, R.A. 1989: Estimates of Trace Metal Inputs from Non-Point Sources Discharged in to Estuaries. Marine Pollution Bulletin 20 (11): 549-555.

PAULSON, A.J.; FEELY, R.A.; CURL, H.C; CRECELIUS, E.A; GEISELMAN, T. 1988: The Impact of Scavenging on Trace Metal Budgets in Puget Sound. Geochim. Cosmochim. Acta 52: 1765-1779.

PELLENBORG, R.E.; CHURCH, T.M. 1978: Storage and Processing of Estuarine Water Samples for Trace Metal Analysis by Atomic Absorption Spectrometry. Analytica Chimica Acta 97: 81-86.

PENNEY, S.E. 1982: The Estuary of Christchurch: A History of the Avon-Heathcote Estuary, its Communities, Clubs, Controversies and Contributions. Penney Ash Publications, Christchurch: 269p.

PFEIFFER, W.C.; FISZMAN, M.; MALM, O.; MAURICIO, AZCUE. 1986: Heavy Metal Pollution in the Paraiba Po Sul River, Brazil. Sci. Tot. Envir. 58: 73-79.

PHILLIPS, D.J.H. 1989: Trace Metals and Organocholrines in the Coastal Waters of Hong Kong. Marine Pollution Bulletin 20(7): 319-327.

PHILLIPS, D.J.H.; MACDONALD, MOTT.; 1990: Trace Elements in Tropical Marine Environments. In the Programme and Abstracts of the 2nd International Conference of Trace Metals in the Aquatic Environment, Sydney Australia, July 8-14 1990: 37.

PICKERING, W.F. 1978: Analytical Aspects of Lead, Sorption by Solids. Talanta 25: 727-729.

POTTS, P.J. 1987: A Handbook of Silicate Rock Analysis. Blackie in USA, Chapman and Hall.

PREMAZZI, G.; PROVINI, A.; GAGGINO, G.F.; PARISE, G. 1986: Geochemical Trends in Sediments from 13 Italian Subalpine Lakes. In Sly P.G. (Editor) Sediments and Water Interactions. Springer-Verlag N.Y.: 157-165.

PROVINI, A.; GAGGINO, G.F. 1986: Depth Profiles of Cu, Cr and Zn in Lake Orta Sediments (Northern Italy). In Sly P.G. (editor) Sediments and Water Interactions. Springer-Verlag N.Y.: 167-174.

PURCHASE, N.G. 1983: A Study of the Factors which Affect the Use of Biological indicators as Monitors of Lead. Unpublished PhD Thesis, Department of Chemistry, University of Canterbury, Christchurch, New Zealand: 351p.

PURCHASE, N.G.; FERGUSSON, J.E. 1986a: Chione (Austrovensus) stutchburyi, a New Zealand Cockle as a Bio-indicator for Lead Pollution. Environment Pollution (Series B) 11: 137-151.

PURCHASE, N.G.; FERGUSSON, J.E. 1986b: The Distribution and Geochemistry of Lead in River Rediments, Christchurch, New Zealand. Environmental Pollution (Series B) 12: 203-216.

RABILTI, S.; BOLDRIN, A.; MENEGAZZO, J.; VITTURI, L. 1983: Relationship Between Surface Area and Grain Size in Bottom Sediments. Journal Sediment Petrology 53: 665-667.

RAESIDE, J.D. 1964: Loess Deposits of the South Island, New Zealand, and Soils Formed on Them. New Zealand Journal Geol. Geophys. 7: 811-835.

RAWLENCE, D.J.; WHITTON, J.S. 1977: Elements in Aquatic Macrophytes, Water, Plankton, and Sediments Surveyed in Three North Island Lakes. New Zealand Journal of Marine and Freshwater Research 11(1): 73-93.

REED, J.J. 1951: Marine Sediments Near Sumner, Canterbury, New Zealand. New Zealand Journal of Science and Technology. September 1951: 129-137.

REEVES, R.D.; BROOKS R.R. 1978: Trace Element Analysis of Geological Materials. John Wiley & Sons Inc. Canada: 421p.

RENDELL, P.S.; BATLEY G.E.; CAMERON A.J. 1980: Absorption as a Control of Metal Concentrations in Sediment Extracts. Environmental Science Technology 14: 315-318.

RIFFALDI, R.; LEVI-MINZI, R.; FRANCOSOLDATINI, G. 1976: Lead Absorption by Soils. Water, Air, and Soil Pollution 6: 111-128.

RICE, D.L.; WHITLOW, S.I. 1985: Diagenesis of Transition Metals in Bioadvectic Marine Sediments. In LEKKAS T.D (Editor). Heavy Metals in the Environment International Conference Athens , September 1985.

RITCHIE, J. (personal communication): 75 Soleares Ave, McCormacks Bay.

ROBBINS, J.A.; EDGINGTON D.N. 1975: Determination of Recent Sedimentation Rates in Lake Michigan Using ^{210}Pb and ^{137}Cs. Geochim. et Cosmochim. Acta 39: 285-304.

RODRIGO, A.G. 1985: The Avon-Heathcote Estuary: An Analysis of the Distribution of Sediments and Their Associated Heavy Metals with Special Reference to its Effects on the Distribution of the Mudflat snail. Amphibola crenata (Martyn). Unpublished BSc Hons Thesis, Zoology Department, University of Canterbury, Christchurch, New Zealand.

RODRIGO, A.G.1989: Surficial Sediment Heavy Metal Associations in the Avon-Heathcote Estuary, New Zealand. New Zealand Journal Marine and Freshwater Research 23: 255-262.

ROTHERY, E. 1986: Analytical Methods for Zeeman Graphite Tube Atomizers. Varian Techtron Pty Ltd, Mulgrave, Victoria, Australia: 193p.

SALOMONS, W.; FORSTNER, U. 1980: Trace Metal Analysis on Polluted Sediments. Part 2: Evaluation of Environmental Impact. Environmental Technological Letters. 1: 506-517.

SALOMONS, W.; FORSTNER, U. 1984: Metals in the Hydrocycle. Springer-Verlag. Berlin Heidelberg, H.Y. Tokyo: 349p.

SCHNEIDER, B.; WEILER, K. 1984: A Quick Grain Size Correction Procedure for trace Metal Contents of Sediments. Environmental Technological Letters 5: 245-256.

SCHROEDER, B.; THOMPSON, G.; SULANOWSKA, M.; LUDDEN, J.N. 1980: Analysis of Geological Materials Using an Automated X-ray Fluorescence System. X-Ray Spectrum 9: 198-205.

SCHUBEL, R.J.; MEADE, R.H. 1977: Mans Impact on Estuarine Sedimentation. Estuarine Pollution Control and Assessment. Proceeding of a Conference 1, US Environment Protection Agency of Water Planning and Standers, Washington DC: 193-209.

SCOTT, E.F. 1963: Christchurch Data. Notes and Comments on the Christchurch Drainage and Sewerage Systems. Unpublished Report, Christchurch Drainage Board, Christchurch, New Zealand.

SCRUDATO, R.J.; ESTES, E.L. 1975: Clay-Lead Sorption Relations. Environmental Geology Vol: 167-170.

SCRUDATO, R.J.; LONG, D.; WEINBLOOM, R. 1987: Mercury Contribution to an Adirondack Lake. Environmental Geology and Water Sciences 9(3): 131-138.

SHARMA, P.; GARDNER, L.R.; MOORE, W.S.; BOLLINGER, M.S. 1987: Sedimentation and Bioturbation in a Salt Marsh as Revealed by ^{210}Pb, ^{137}Cs, ^{7}Be Studies. Limonl. Oceanogr. 32(2): 313-326.

SHELLEY, D. 1985: Optical Mineralogy. (second edition) Elsevier Science Publishing Co., Inc 52, Vanderbilt Ave, N.Y. 10017: 321p.

SIKORA, L.J.; KEENEY, D.R. 1983: Further Aspects of Soil Chemistry Under Anaerobic Conditions. Chapter 6 in A.J.P. Gore (Editor) Ecosystems of the World: Mires, Swamp, bog, fen, and moore. Elseiver Scientific Publications Company: 247-256.

SMALE, D. 1987: Heavy Minerals in Cretaceous Cenozoic Sandstones in Canterbury. New Zealand Geological Survey Report SL17: 61p.

SMALE, D. 1988: Detrital Pumpellyite and Epidote Group Minerals in Cretaceous and Tertiary Sandstones in the South Island, New Zealand. Journal Sedimentary Petrology 58(6): 985-991.

SMILLIE, R.H.; HUNTER, K.; LOUTIT, M. 1981: Reduction of Chromium (V1) by Bacterially Produced Hydrogen Sulphide in a Marine Environment. Water Research 15: 1351-1354.

SMILLIE, R.H.; LOUTIT, M.W. 1982: Removal of Metals from Sewage in an Oxidation Pond System. New Zealand Journal of Science 25: 371- 376.

SMITH, D.G. 1982: The United States Environmental Protection Agency's 1980 Ambient Water Quality Criteria: A Compilation for Use in New Zealand. Water and Soil Misc. Publication 33: 72p.

SMITH, D.G. 1985: Sources of Heavy Metal Input to the New Zealand Aquatic Environment. Journal of the Royal Society of New Zealand 15(4): 371-384.

SMITH, D.G. 1986: Heavy Metals in the New Zealand Aquatic Environment: A review. Water and Soil Publication No. 100: 188p.

SPERLING, K.R.F. 1978: Determination of Heavy Metals in Seawater and in Marine Organisms by Flameless Atomic Absorption Spectroscopy. Fresenius 2 Anal. Chem. 292: 113-119.

STEPHENSON, R.L. 1981: Aspects of the Energetics of the cockle. Chione Austrovenus Stutchburyi in the Avon-Heathcote Estuary, Christchurch, New Zealand. Unpublished PhD Thesis, Department of Zoology, University of Canterbury, Christchurch, New Zealand.

STEVENSON, C.D. 1985: Analytical Advances and Change Perceptions of Environmental Heavy Metals. Journal Royal Society of New Zealand 15 (4): 355-362.

STEWART, C. 1989: Spatial and Temporal Trends in Trace Metal Deposition in Canterbury, New Zealand. Unpublished PhD Thesis, Chemistry Department, Canterbury University, Christchurch, New Zealand.

STILLER, M.; IMBODEN, D.M. 1986: ^{210}Pb in Lake Kinneret Waters and Sediments: Residence Times and Fluxes. In Sly P.J. (Editor) Sediments and Water Interactions Springer-Verlag, N.Y.: 501-511.

STOFFERS, P.; GLASBY, G.P.; PLUGER, W.L.; WALTER, P. 1983: Reconnaissance Survey of the Mineralogy and Geochemistry of Some New Zealand Lake and Nearshore Sediments. New Zealand Journal of Marine and Freshwater Research 17: 461-480.

STOFFERS, P.; GLASBY, G.P.; WILSON C.J.; DAVIS, K.R.; WATTER, P. 1986: Heavy Metal Pollution in Wellington Harbour. New Zealand Journal of Marine and Freshwater Research 20: 495-512.

STUMM, W.; MORGAN, J.J. 1981: Aquatic Chemistry. An Introduction Emphasizing Chemical Equilibria in Natural Waters. John Wiley & Sons. Inc : 780p.

SUBRAMANIAN, V.; VAN GRIEKEN, R.; VANIT DACK, L. 1987: Heavy Metals Distributions in the Sediments of Ganges and Brahmaphutra Rivers. Environmental Geology Water Sciences. 9(2): 93-104.

SUGGATE, R.P. 1958: Late Quaternary Deposits of the Christchurch Metropolitan Area: New Zealand Journal Geo. Geophysics 1: 103-122.

SUGGATE, R.P. 1968: Post Glacial Sea-level rise in the Christchurch Metropolitan area, New Zealand. Geologic En Mijnbouw 47(4): 291-297.

TANAKA, N.; TAKEDA, Y.; TSUNOGAI, S. 1983: Biological Effect on Removal of Th-234, Po-210 and Pb-210 from Surface Water in Funka Bay, Japan. Geochim. Cosmochim. Acta. 47: 1783-1790.

TAYLOR, D. 1986: Changes in the Distribution Patterns of Trace Metals in Sediments of the Mersey Estuary in the Last Decade (1974-1983). Sci. Tot. Envir. 49: 257-295.

TESSIER, A.; CHAMPBELL, P.G.C.; BISSON, M. 1979: Sequential Extraction Procedure for the Speciation of Particulate Trace Metals. Analytical Chemistry 51(7): 844-850.

TRESSIER, A.; CARIGNAN, R.; DUBREUIL B.; RAPIN F.; 1989: Partitioning of Zinc Between the Water column and the Oxic Sediments in Lakes. Geochim. Cosmochim. Acta 53: 1511-1522.

THOMAS, R. 1972: The Distribution of Mercury in the Sediment of Lake Ontario. Canadian Jour. Earth Sci. 9: 636-651.

THOMPSON, E.F. 1930: An Introduction to the Natural History of the Heathcote Estuary and Brighton Beach, Canterbury, New Zealand. A Study of Littoral Ecology. Unpublished MSc Thesis in Biology, Canterbury College, New Zealand.

THOMPSON, G.; BANKSTON, D.C. 1970: Sample Contamination for Grinding and Sieving Determined by Emission Spectrometry. Appl. Spectr. 24: 210-219.

TIMPERLEY, M.H. 1979: Metals in the Water of the Waikato River, New Zealand. New Zealand Journal of Science 22: 273-9.

TIPPING, E.; HETHERINGTON, N.B.; HILTON, J.; THOMPSON, D.W.; BOWLES, E ; HAMILTON-TYLER, A. 1985: Artifacts in the Use of Selective Chemical Extraction to Determine Distributions of Metals Between Oxides of Manganese and Iron. Anal. Chem 57: 1944-1946.

TOPPING, G. 1986: Quality of Data: With Special Reference to the Measurement of Trace Metals in Marine Samples. Sci. Tot. Envir. 49: 9-25.

TOWN, R.M.; POWELL, H.K.J. 1989: Interaction of Humic Acid with Hydrophobic Metal Complexes. In McLaren R.G.; Haynes, R.J.; Savage G.P. (Editors) Trace Elements in New Zealand: Environmental, Human and animal. Proceedings New Zealand Trace Elements Group Conference, November 1988. Lincoln College, Canterbury: 79-84.

TUNNICLIFF, C.; BEAUMONT, H.; 1986: Trace Metal Levels in Coromandel Streams. In Baker M.J. (Editor) Trace Elements in the Eighties. Proceedings of the Conference at the New Zealand Trace Element Group, August 1984: 24-30.

TUREKIAN, K.K.; WEDEPOHL, D.H. 1961: Distribution of the Elements in Some Major Units of the Earths Crust. Bulletin Geological Society Amer. 72: 175-192.

VALENTA, P.; DUURSMA, E.K.; MERKS, A.G.A.; RUTZEL, H.; NURNBERG, H.W. 1986: Distribution of Cd, Pb, Cu Between the Dissolved and Particulate Phase in the Eastern Scheldt and Western Scheldt Estuary. Sci. Tot. Envir. 53: 41-76.

VAN DEN BERG, C.M.A. 1986: Organic-Copper Interactions in Guanabara Bay, Brazil. An Electrochemical Study of Copper Complexation by Dissolved Organic Material in a Tropical Bay. Sci. Tot. Envir. 58: 37-45.

VELBEL, M.A. 1984: Weathering Processes of Rock Forming Minerals. In Fleet, M.E. (Editor) Environmental Geochemistry MAC Short Course Handbook 10: 67-111.

VETTER R.C. 1974: Oceanography the Last Frontier Voice of America. Forani Series: 430p.

VISHER, G.S. 1969: Grain Size Distributions and Depositional Processes. Journal Sedimentary Petrology 39(3): 1074-1106.

VOUTSINOU-TALIADOURI, F.; VARNAVAS, S.P. 1985: Distribution of Cr, Zn, Cu, Pb and Organic Carbon in the Surface Sediments of Northern Euboicos Bay, Greece. In T.D. Lekkas (Editor) Heavy Metals i n the Environment. International Conference Athens September 1985: 356-358.

WEAVER, C.E. 1958: Geologic Interpretation of Argillaceous Sediments. Part 1, Origin and Significance of Clay Minerals in Sedimentary Rocks. Bulletin American Association Petroleum Geologists 42: 254-271.

WEAVER, C.E. 1961: Clay Minerals of the Ouachita Structural Belt and Adjacent Foreland. In Ouachita Systems, Austin, University of Texas Pub. 6120: 401p.

WEAVER, S.D.; GIBSON, I.L.; HOUGHTON, B.F.; WILSON C.J.N. 1990: Mobility of Rare Earth and Other Elememts During Crystallization of Peralkaline Silicic Lavas. Jour. Volc. Geother. Res. 43: 57-70.

WEBB, B.F. 1965: Report on a Biological Investigation of the Estuary of the Avon and Heathcote Rivers. Report, Christchurch Drainage Board, New Zealand.

WIGRAM, H.F. 1916: The Story of Christchurch, New Zealand. The Lyttelton Times Co. Ltd: 269p.

WILLIAMS, B.L. 1985: Ocean Outfall Handbook. A Manual for the Planning, Investigation, Design and Monitoring of Ocean Outfalls to Comply with the Water Quality Management Objectives. Water and Soil Miscellaneous Publication 76: 218p.

WILSON, D.D. 1976: Hydrogeology of Metropolitan Christchurch. Journal of Hydrology Vol. 15(2): 101-120.

WILSON, D.D. 1986: Erosional and Depositional Trends in Rivers of the Canterbury Plains, New Zealand. Journal of Hydrology 24(1): 32-44.

WILSON, J. 1989: Christchurch Swamp to City: A Short History of the Christchurch Drainage Board 1875-1989. Te Waihora Press, Lincoln, New Zealand: 96p.

WILSON, M.J. 1987: A Handbook of Determinative Methods in Clay Mineralogy. Chapman and Hall, New York: 308p.

WINDOM, H.; SMITH, R.; RAWLINSON, C.; HUNGSREUGS, M.; DHARMVANIJ, S.; WATTAYAKORN, G. 1988: Trace Metal Transport in a Tropical Estuary. Marine Chemistry 24: 293-305.

WHITTEN, D.G.A.; BROOKS, J.R.V. 1972: A Dictionary of Geology. Penguin-Books: 495p.

WHITTON, J.S.; CHURMAN, G.J. 1987: Standard Methods of Mineral Analysis of Soil Survey Samples for Characterisation and Classification in New Zealand Soil Bureau. New Zealand Soil Bureau Report 79: 27p.

WRIGHT, F.F. 1974: Estuarine Oceanography. McGraw-Hill: 76p.

WRIGHT, M.S.; DEELY, J.M.; COYLE, S. SEWELL, R.J. 1989: Sheet QM 380 Canterbury. Geological Resource Map of New Zealand 1:250,000. N.Z. Geol. Surv. Report M175.

YUDUAN, W.U.; CHANGYI, LU.; HUANG JIANDONG, LIN YULING 1988: Removal of Heavy Metals from Sediments by Mangroves in Jiulong Estuary, Xiamen Harbour, China. Water Science Technology 20 (6/7): 49-54.

YETTON, M.D. 1986: Investigation and Remedial Methods for Subsurface Erosion Control in Banks Peninsula Loess. MSc Thesis, University of Canterbury, Christchurch, New Zealand.

ZAFIROPOULOS, D. 1985: Heavy Metals in Mediterranean Waters and Sediments. In Lekkas, T.D. (Editor) Heavy Metals in the Environment. International Conference in Athens, September 1985: 366-368.

ZIEGLER, C.K.; LICK, W. 1988: The Transport of Fine Grained Sediment in Shallow Waters. Environmental Geol. Water Science 11(1): 123-132.

APPENDIX 1.0 (Appendix to Chapter 1)

A1.1 PHASE RELATIONSHIPS BETWEEN SEDIMENT AND HEAVY METALS

A1.1.1 The Problem of Phase Analysis in Sediments

Information on chemical partitioning in sediments is useful in distinguishing anthropogenic from natural sources of heavy metals, and for making predictions on (1) bioavailability, (2) transport modelling and (3) potential metal remobilisation (Horowitz, 1985).

The most common method used to study heavy metal phases is partial chemical extraction. This method involves selective chemical extraction of some or all of the following phases (1) ion exchangeable, (2) carbonate, (3) reducible (normally Fe and Mn hydroxy compounds), (4) oxidisable (usually organic matter or sulphides), and (5) residual (lattice bound). A number of sequential extraction methods are available. The most common ones are discussed in detail by Forstner (1989), Horowitz (1985) and Salomons and Forstner (1984). The three step extraction technique proposed by Salomons and Forstner (1980) is probably one of the most useful chemical techniques for determining phase association in sediments (especially surface bound versus lattice bound metals). All surface bound metals are removed using an initial extraction in acidified hydroxylamine hydroxide at pH 2, followed by re-extraction of the readsorbed metals with ammonium acetate. Finally the residual bound metals are removed using concentrated $HF/HClO_4$ acid. This type of extraction is said to avoid metal redistribution problems, which are associated with the more rigorous methods.

A1.1.2 Heavy Metal Phase Relationships

Sediment metal collectors include clay minerals, organic matter, Fe and Mn hydroxides, and Fe and Mn

sulphides. The ability of substrates to accumulate heavy metals in descending order is MnO_2 > humic acids > Fe oxides > sulphides > clays (Forstner, 1989; Horowitz, 1985). The order will vary however, depending on the physico-chemical character of the sediment environment (such as Eh, pH, solute concentration, and solute form).

The partitioning of heavy metals in these substrates seems to be a dynamic process in which substrates compete for different metals or metal complexes. Heavy metal partitioning is influenced by 1) the absolute and relative concentrations of the metals themselves, and 2) the relative concentrations of the various substrates.

Bonding processes in sediments include (1) adsorptive bonding, (2) co-precipitation with hydrous Fe and Mn oxides, (3) complexation with organic molecules, and (4) incorporation into crystalline minerals (Forstner and Wittmann, 1981). The particular metal sediment phase found generally relates to the prevailing redox and acidity conditions of the associated water, as shown by Figs 1.2, 1.3, and Table 1.3 in Chapter 1.0.

Results of sequential extraction studies show the following, (1) generally the reducible fraction (Fe/Mn hydroxy compounds) is the more important phase for metal attachment in oxidising sediment environments, (2) the oxidisable fraction (organic matter and sulphides) is more important in sediments from a reducing environment (such as near a sewage outlet), and (3) the lithogenic (residual) fraction decreases in relative importance when sediments are heavily contaminated (Angelidis and Grimanis, 1989; De Souza et al, 1986; Drever, 1982; Gibbs and Angelidis, 1989; Jordao and Nickless, 1989; Paulson et al., 1988; and Stoffers et al, 1986).

A1.1.3 Heavy Metal Bonding in Sediments

Over 90% of heavy metals are carried into estuaries attached to particulate matter (Salomons and Forstner,

1984). The order decreases Al>Fe>Mn>Co>Zn>Ni>Cu>Cd. The fine grained substrates that accumulate heavy metals all possess the hydroxyl group OH^-. The entities that are often involved in metal entrainment are therefore (1) Si-OH, Al-OH_2, Al-OH (clays), (2) Fe-OH, Mn-OH (Fe and Mn hydroxide) and (3) OOC-OH, phenol-OH (organic matter). In strongly acidic environments these groups will accept a proton and become $-OH_2^+$ and in strongly alkali environments they will lose a proton and become $-O^-$. Therefore, the net charge on the surface of substrates will depend strongly on pH. Consequently in acid environments the cation exchange capacity of substrates is low, due to competition with protons (while anion exchange is high), and in alkaline conditions the cation exchange capacity is high, due to the negative oxide surfaces. The uptake of heavy metals will increase from near zero to almost 100% through a pH range of 1-2 units for most substrates. The pH at which surface charges are zero (called the zero point charge) depends on the type of substrate and the prevailing environmental conditions. At pH below 3 SiO_2, MnO_2, kaolinite, and montmorillonite will exhibit negative surface charges, whereas Fe oxides and Al oxides surfaces become negative well above pH 7 (Drever, 1982; Forstner and Wittmann, 1981; Salomons and Forstner, 1984). Therefore, in most natural aquatic conditions Mn oxides, silica, and clay minerals exhibit a greater affinity for heavy metals than $Fe(OH)_2$ and Al_2O_3.

With increasing pH, metal adsorption increases in the order Ag<Cd<Zn<Cu<Pb. Therefore, Pb and Cu are more strongly bonded to surfaces at low pH than Cd and Zn.

All the processes of heavy metal entrainment in sediments, except inert lattice bonding, are reversible under changing chemical conditions. However, some studies show that with duration of time heavy metals become more strongly attached to sediments and are less easily desorbed (Salomons and Forstner, 1984).

A1.1.3.1 Heavy Metal-Detrital Phase Relationship

Heavy metal bonding in detrital minerals is determined by crystal chemistry of the source rocks, which includes properties such as ionic radii and electron configuration (Forstner, 1989). Zinc is incorporated in distinct lattice positions of biotites and amphiboles where it replaces Fe^{2+} and Mn^{2+}. Potassium in silicate structures of muscovite and alkali feldspar may be replaced by Pb during mineral formation. Heavy minerals often contain significantly high metal concentrations and frequently exhibit a close relationship to source rocks on a regional scale.

A1.1.3.2 Heavy Metal-Clay Phase Relationship

Clay minerals are fine grained, crystalline, hydrous silicates with structures of the layer lattice type. Because of their structure clay minerals are effective ion exchangers. Generally clay minerals are found in the grain sizes below 2-4 μm.

The composition of clays usually consists of closely packed tetrahedral silicate layers between octahedral brucite ($Mg(OH)_2$) and gibbsite ($Al(OH)_3$) layers (Blatt et al, 1980; Drever, 1982). Individual sheets are normally held together by van der Waal forces, whereas covalent bonds hold the Al^{3+}, Mg^{2+}, OH^-, Si^{4+}, and O^{2-} ions together within the layers. Clay minerals consist of different combinations of these layers with considerable substitution of Al^{3+} for Si^{4+}, Mg^{2+}, and Fe^{2+}, while Fe^{2+} and Al^{3+} may substitute for Mg^{2+}. When a clay particle, such as a smectite, is suspended in water some of the interlayer cations pass into solution resulting in a negative charged framework surrounded by a diffuse cloud of cations in a double layer. Generally the double layer consists of one layer of ions, more or less, attached to the solid surface and an outside more diffuse layer in which ions are free to move. Cations in the diffuse layer exchange rapidly whereas

those in the fixed layer exchange slowly, if at all (Drever, 1982).

In addition to pH, the clay mineral cation exchange capacity is dependent on charge imbalances caused by (1) broken bonds around the edges of Si-Al units, (2) Al^{3+} substitution for Si^{4+} in the tetrahedral layers, and 3) divalent ion substitution for Al^{3+} in the octahedral layers (Forstner and Wittmann, 1981). Consequently there may be trace metal substitution within the silicate framework as well as on the surface. The cation exchange capacity of clays increases in the order kaolinite < chlorite < illite < vermiculite < montmorillonite, which corresponds to decreasing particle size and increasing surface area (Forstner and Wittmann, 1981).

The open structure of three layer type clays (montmorillonite, illite, and smectite/illite) also offers diffusion type sorption sites where metals may become semi-irreversibly incorporated into the lattices during diagenesis (Helios-Rybicka and Forstner, 1986). This behaviour may explain why clay minerals exhibit stronger metal bonding over time.

The principal role of clay minerals in metal attachment is to act as mechanical substrates for the precipitation and flocculation of organic matter and Fe and Mn hydroxy compounds, which are more effective scavengers of heavy metals (Horowitz, 1985).

A1.1.3.3 Organic Matter - Heavy Metal Phase Relationships

Chemically humic acids appear to be high molecular weight polymers with a large number of carboxylic and phenolic functional groups (Drever, 1982). Organic matter surfaces available for metal uptake can arise in three possible ways: (1) from bacteria and algae, (2) from breakdown of plant and animal matter, and (3) from lower molecular weight organics sorbed on clay surfaces (Calmano and Forstner, 1983; Martens and Goldhaber, 1978; Salomons

and Forstner, 1984).

Organic matter can adsorb 1 to 10% dry weight of Co, Cu, Fe, Pb, Mn, Mo, Ni, Ag, V, and Zn due to the negative charged surfaces of the colloids. The mechanism of entrainment involves metal exchange with hydrogen of the OH groups which was discussed earlier. Humic acids show a high degree of selectivity for divalent ions as opposed to monovalent. Organic matter affinity for heavy metals generally decreases in the order Pb>Cu>Ni>Co>Zn>Fe >Mn>Ba>Ca>Mg>NH_4>K>Na (Forstner and Wittmann, 1981; Horowitz, 1985). Organic matter interacts strongly with metals in solution probably through formation of chelate type complexes which may increase the solubility of metals at higher pH and Eh conditions. Copper-organic complexes are particularly common in sediment interstitial waters (Aggett and Simpson, 1986).

A1.1.3.4 Heavy Metal Partitioning with Fe and Mn Hydroxy Compounds

Iron and Mn hydrous oxides and hydroxides are ubiquitous in estuarine waters and sediments. Freshly precipitated unstable (active) forms are amorphous or microcrystalline in nature and arise in air saturated environments such as turbidity maxima where rivers enter estuaries (Calmano and Forstner, 1983). The oxidation of Fe(II) is rapid at neutral pH ranges. The subsequent hydrolysis $Fe^{3+} + 3H_2O \rightarrow Fe(OH)_3 + 3H^+$ is also rapid. In addition, Fe may form complexes with phosphate and organic matter. In contrast, the oxidation of Mn(II) to Mn(IV) by oxygen ($Mn(II) + O_2 \rightarrow MnO_2$) is slow and requires more alkaline conditions than are needed for Fe oxidation. Oxidation to Mn (III) is more rapid. Occasionally some phosphate species inhibit the oxidation of Mn while others catalyse it.

Iron and Mn hydroxide precipitates slowly convert to stable (inactive) forms with time. What are usually

referred to as hydrous ferric oxides or ferric hydroxides are most likely poorly crystalline goethite (FeOOH). These orange-brown Fe oxides are more commonly attached to mineral surfaces than Mn oxides. The black Mn oxides more often occur as discrete particles of poorly crystallised birnessite or todorokite (both are varieties of manganite) which may form silt or sand-sized grains (Drever, 1982; Forstner and Wittmann, 1981). Frequently there is substitution of Mn for Fe in goethite, and Fe substitution for Mn in Mn oxides (McLaren, 1989).

Both Mn and Fe hydrous oxides have very large surface areas ranging from 200-300 m^2/g, hence they are efficient scavengers of heavy metals. Concretions of Mn and Fe oxides, commonly found near the sediment water interface, may contain up to 0.5% Cu, Ni, and Co adsorbed or co-precipitated from overlying water. Heavy metals may be sorbed on to Mn and Fe hydroxides by exchange with H^+ ions, which increases with increase in pH. The degree of metal adsorption will depend on metal concentration, hydroxide concentration, and heavy metal speciation (Horowitz, 1985). Birnessite and todorokite contain slightly less than two oxygen atoms per manganese, hence are capable of co-precipitating at least 10 times as many heavy metals as Fe oxides. In some environments metal complexation with Cl^- ions and organic ligands may inhibit their adsorption by Fe and Mn hydrous oxides.

APPENDIX 2.0 (Appendix to Chapter 3)

A2.1 DESCRIPTIONS OF CORES COLLECTED FROM THE AVON-HEATHCOTE ESTUARY, TRAVIS SWAMP, AND SALTWATER CREEK ESTUARY.

KEY

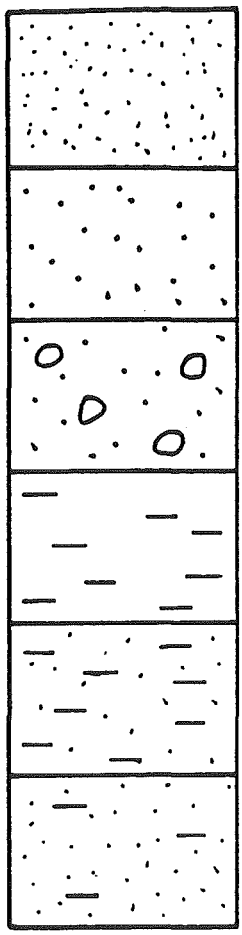

Fine Sand

Medium Coarse Sand

Coarse Sandy Gravel

Mud

Sandy Mud

Muddy Sand

Bioturbated Contact

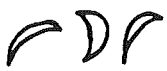

Whole Shellfish (living or dead)

Broken Shells

Black Carbonaceous Streak (coal and charcoal dust)

Fragment of Charcoal

Wood Fragment

Decaying Plant Matter

<u>Zostera nana</u> (eelgrass) Leaves

AHE/1a

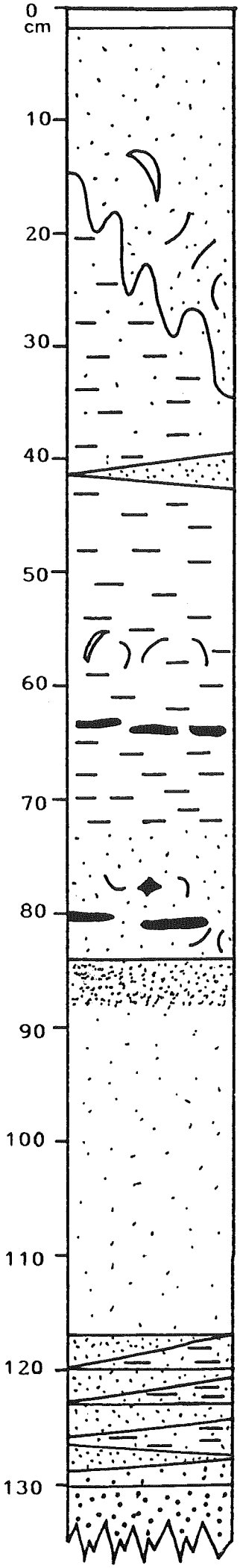

Active Layer- olive grey muddy fine sand

UNIT D- black, greyish black fine sand containing whole and broken shells

bioturbated contact

UNIT C- olive grey fine sandy mud containg black streaks of carbonaceous matter, pieces of wood, lumps of charcoal (coal), sandy laminations, and muddy zones. The sand content increases with depth below 72cm.

gradational contact (sharp colour change)

UNIT B- 84-87cm, black slightly muddy fine sand. 87-117cm, massive dark grey fine sand. 117-130cm, alternating laminations of mud, muddy fine sand, and fine sandy mud. Laminations grade upwards and downwards.

gradational contact

UNIT A- grey clear medium sand.

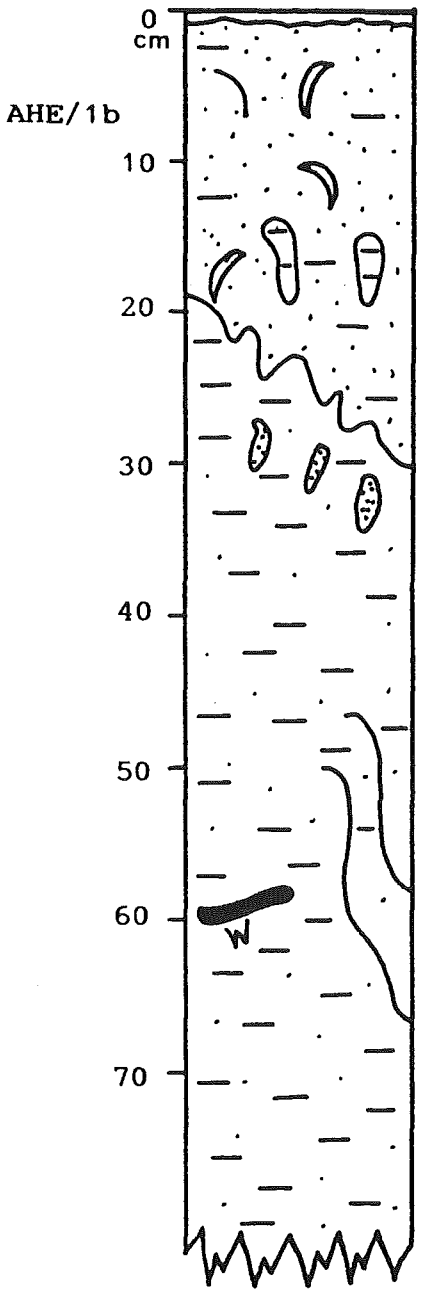

Active Layer

UNIT D- black slightly muddy fine sand containing whole and broken shells, and pods of mud similar in texture to Unit C.

——————— bioturbated contact

UNIT C- olive grey slightly sandy mud containing pods of sand similar in texture to Unit D, a wood fragment, and 10cm long leaves of Zostera nana.

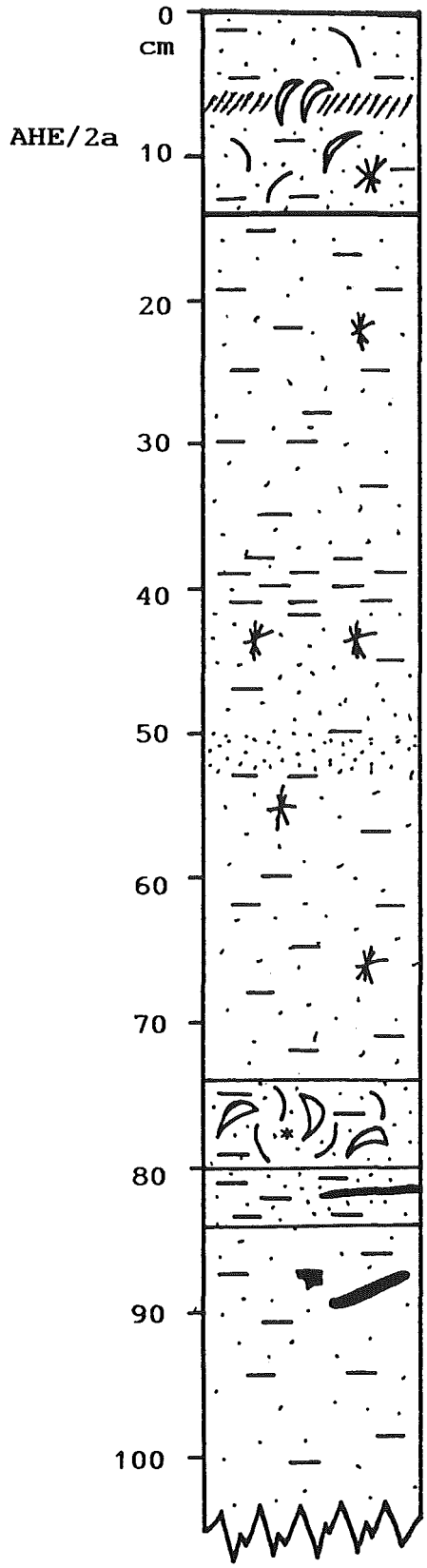

UNIT D- grey slightly muddy sand containing live and dead bivalve shellfish. A black horizon occurs at 6-8cm.

——————— sharp contact

UNIT C- olive grey muddy sand grading to sandy mud with with depth. Numerous clumps of rooting plant debris (Zostera) are present. There are also laminations of fine sand.

(* ^{14}C sample)

——————— gradational contact

UNIT B- dark grey homogeneous fine sand with occasional streaks of carbonaceous matter and lumps charcoal (above 90cm).

AHE/3a

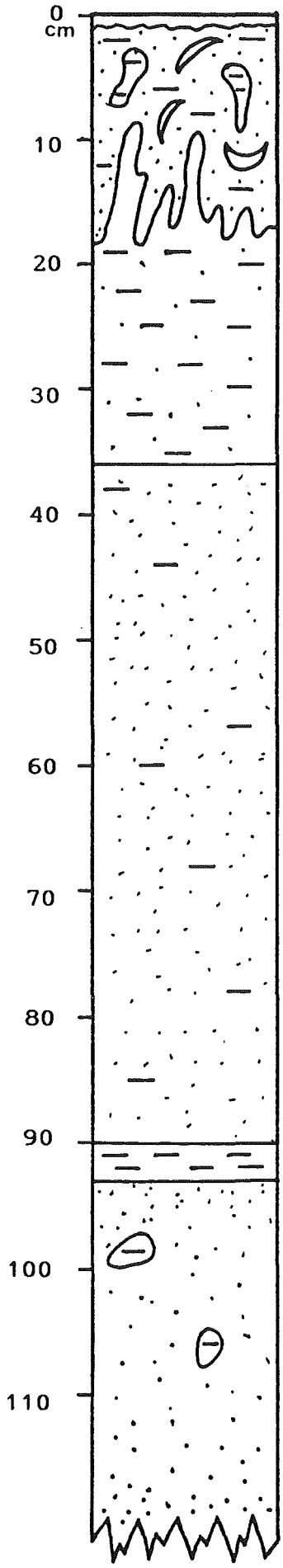

Active Layer

UNIT D- dark grey slightly greenish bioturbated muddy fine sand containing numerous live and dead Chione.

——————— bioturbated contact

UNIT C- olive grey slightly sandy mud.

——————— gradational contact

UNIT B- olive grey massive slightly muddy very fine sand. 90-93cm, olive grey mud.

——————— sharp contact

UNIT A- dark grey clean, massive medium coarse sand with occasional pods of mud. The sand coarsens with depth.

AHE/3b

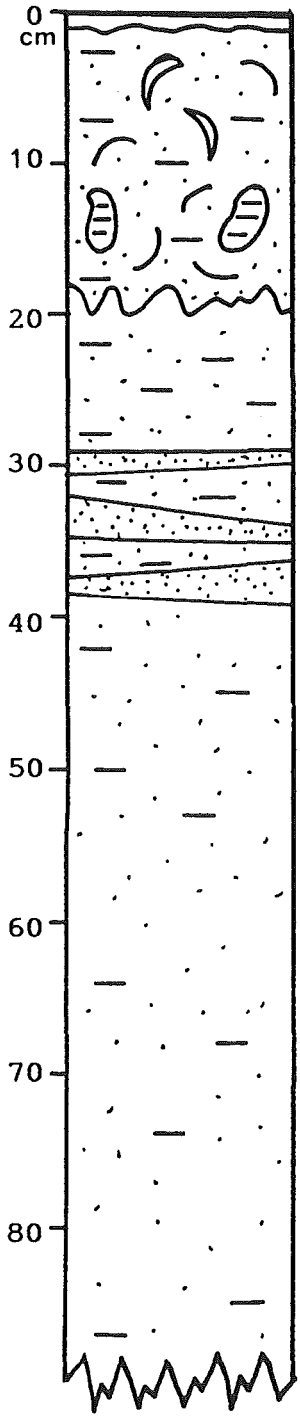

Active Layer

UNIT D- dark grey muddy bioturbated sand containing live Chione, broken shells, and pods of mud similar to Unit C.

——————bioturbated contact

UNIT C- olive grey slightly muddy sand.

——————gradational contact

UNIT B- massive olive grey muddy sand; laminated and muddier near the contact with Unit C; sandier near the base of the core.

AHE/4

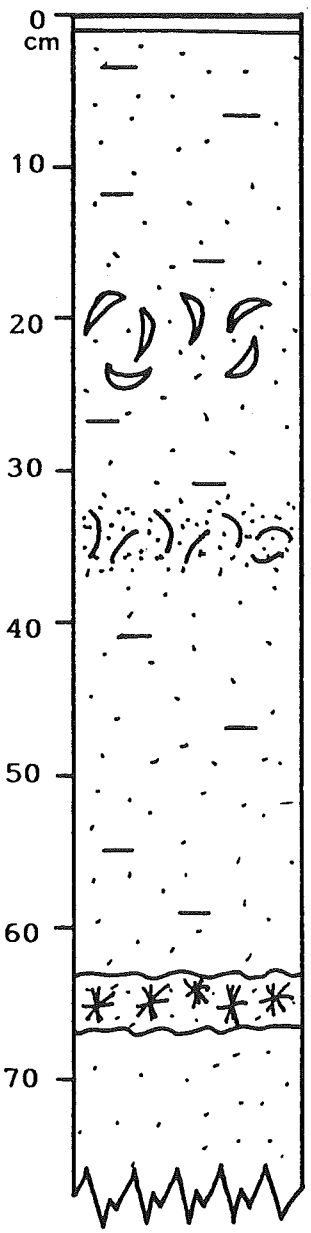

Active Layer

Homogeneous slightly muddy fine sand similar in texture to Unit B of other cores. A living assemblage of Mactra ovata occurs at 20cm. A black layer containing numerous broken shells occurs between 32 and 36cm. A layer of brown decaying plant matter occurs at 64 to 68cm. The sediment is darker in colour below 35cm and greener towards the surface.

AHE/5

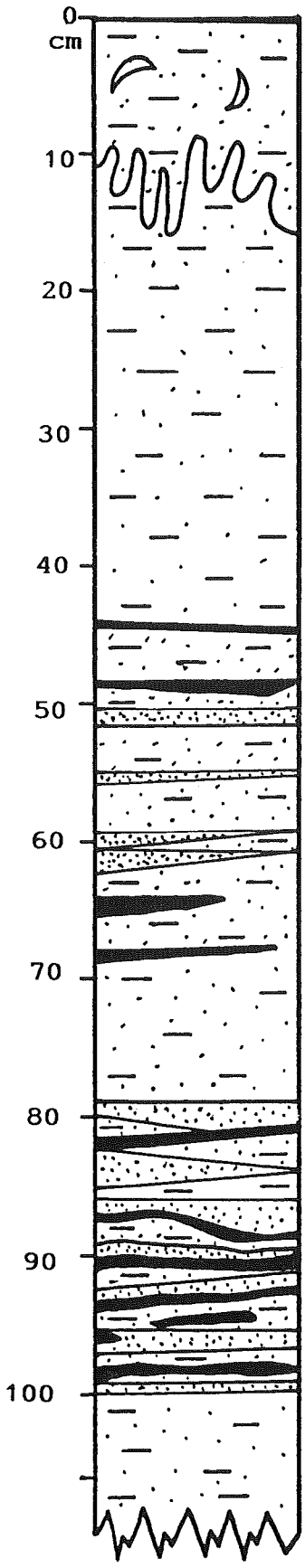

UNIT D- dark grey black medium fine sand containing live shellfish and fragments of shells.

——————— bioturbated contact

UNIT C- massive grey blue slightly sandy mud containing sandy laminations and black carbonaceous streaks.

——————— gradational contact

UNIT B- 87-100cm, laminated fine and medium fine sand containing streaky black layers (coal dust). 100-106cm, slightly laminated mud.

AHE/6

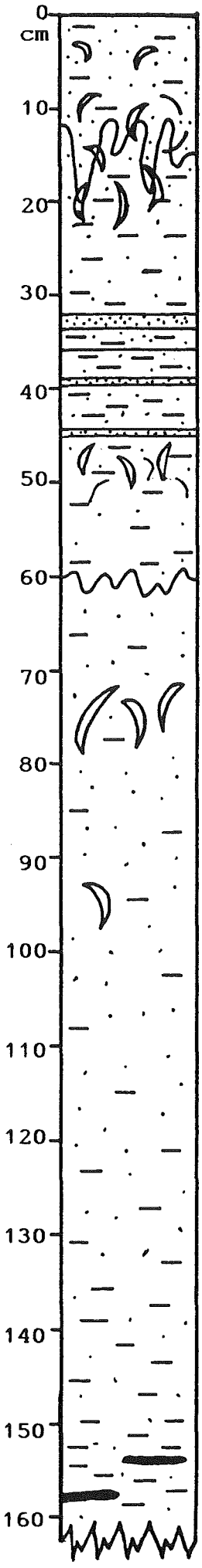

UNIT D- black slightly muddy bioturbated fine sand.

———— bioturbated contact (layer of live Mactra ovata 12 to 16cm)

UNIT C- olive grey fine sandy mud containing laminations of fine sand or mud.

Death assemblage of Mactra ovata.

———— bioturbated contact

UNIT B- slightly mottled muddy fine sand containing muddy patches throughout and occasional Mactra ovata shells. Unit B sediment is bioturbated from the base of the core to the contact with Unit C. Below 132cm muddiness increases and there are occasional streaky dark layers.

TS/1

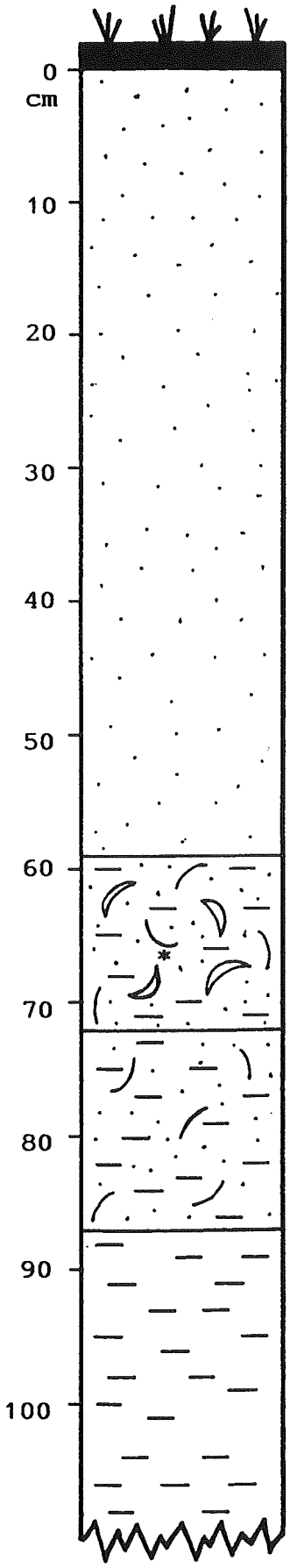

Peat

UNIT T1- massive light brownish grey mottled, weathered, slightly indurated, fine to very fine sand. Brown streaky rootlet structures extend through the sediment.

gradational contact

UNIT T2- light brown slightly indurated silty sand containing articulated and single Chione.

(* ^{14}C sample)

gradational contact

UNIT T3- light brown grey mottled weathered very fine silty sand with occasional Chione shells.

gradational contact

UNIT T4- light blue grey soft puggy mud.

TS/3

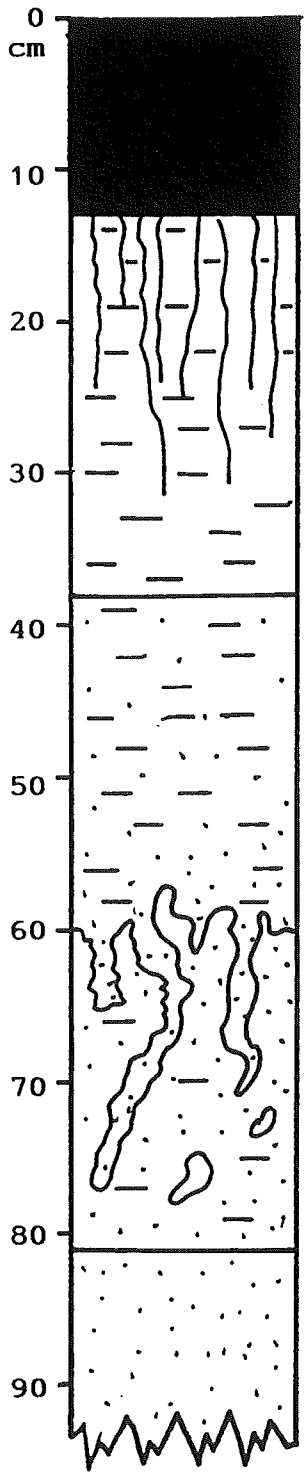

Dark brown Peat.

sharp contact

Olive grey brown soft mud with rootlets.

sharp contact

Olive grey sandy mud. The sand content increases with depth.

bioturbated contact

UNIT B'- dark grey slightly muddy fine sand containing pods of bioturbated mud.

sharp contact

UNIT A'- dark grey medium fine sand.

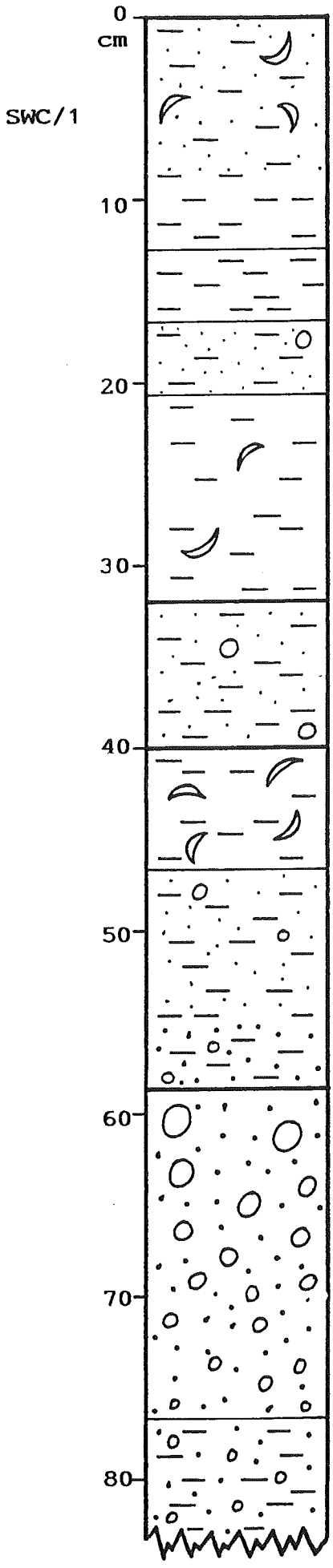

Olive grey sandy mud with cockle shells.

Olive grey mud.

Olive grey and grey black bioturbated mud.

Grey black sandy mud with occasional granules.

Dark grey black mud with occasional shells.

sharp contact

Grey black muddy medium coarse sand with occasional granules.

sharp contact

Olive grey mud with shells.

Olive grey sandy mud.

Olive grey coarse sandy mud.

sharp contact

Gravel sequence: fining upwards containing very coarse sand and a little mud. The grains are a poorly sorted mixture of of angular and rounded granules.

Coarse muddy sand with granules.

SWC/2

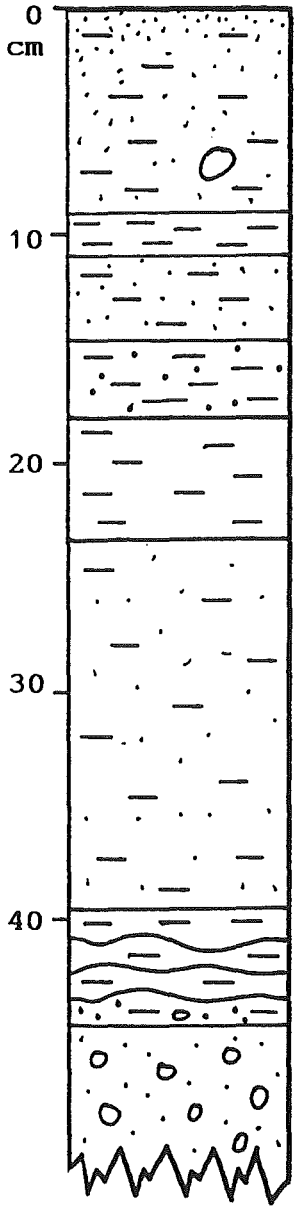

Olive grey sandy mud.

Olive grey slightly weathered mud.

Muddy medium sand.

Orange brown very weathered muddy coarse sand.

sharp contact

Olive grey homogeneous mud.

sharp contact

Orange brown very weathered muddy fine sand.

Brown less weathered fine sand.

gradational contact

Laminated medium grey black and light grey mud.
Coarse sand with granules.

Coarse sandy gravel.

A2.2 TESTS FOR QUANTIFYING QUARTZ AND ALBITE IN THE CLAY FRACTIONS

The first test involved standard additions of quartz standard to 4 subsamples of AHE/1C3 as follows: 0%, 5%, 10%, 20%. A calibration curve was constructed using concentration versus peak Height (4.25Å), and the concentration in the 0% sample was obtained by extrapolating the curve to zero on the x-axis.

The second test involved 1 standard addition of quartz to several repeats of AHE/1C3 and noting the reproducibility of traces. The concentration value was obtained by extrapolation as in 1) above.

The third test involved direct comparison of pure quartz peaks (100%) with AHE/1C3 quartz peaks.
The results are presented in Table A2.1.

Table A2.1 Tests Determining Quartz Concentration in AHE/1C3

Standard Additions	1 Addition	Direct Comparison
12.8	12.8	12
9.15	7.49	10.8
8.79	10.4	9.5
17.5	9.2	10.8
Mean 12.0±4	9.0±2	10.8±1

The direct comparison test produced the best precision. Normally standard additions would be expected to produce better results. However, because only small samples were available (<0.5g) it was difficult to obtain consistent mixing of the quartz standard in each sample, hence the poor precision. The direct comparison method was adopted for both quartz and albite analyses.

A2.3 Lead-210 Dating Method Development

Test 1

The first trial involved comparison of ^{210}Po extraction in concentrated HNO_3/HCl (Robbins and Edginton (1975) with extraction in dilute (2M) HCl, and total digestion in concentrated HF/HNO_3.

1) Concentrated Acid Extraction

Five gram samples of sediment were placed in 800ml beakers with 1ml of 7.7dpm/ml (decays per minute/ml) ^{208}Po tracer. Twenty five mls of concentrated HNO_3 and 20ml of concentrated HCl were added to each beaker and evaporated to dryness twice. To each residue 10 ml of 2M HCl was added and filtered and then re-evaporated to near dryness. The final residues were taken up in 400 mls of 0.5M HCl. Ascorbic acid (0.1g) was added to the solutions to complex Fe. The solutions were heated to 80-95°C and a polished silver disc added with a magnetic stirrer. The ^{210}Po and ^{208}Po were subsequently self plated onto the silver discs over 4 hours. (The silver discs were prepared by boiling in concentrated HCl, then polished with a metal polisher and cleaned in detergent, rinsed in hot water, followed by acetone). The radioactivity of ^{208}Po and ^{210}Po were determined by alpha-spectroscopy and counts per minute (cpm) determined by peak area (^{208}Po, 5.1MeV; ^{210}Po, 5.3MeV).

2) Dilute Acid Extraction

Five grams of sediment and 1ml of ^{208}Po tracer were boiled for 2 hours in 100ml of 2M HCl with stirring, then filtered and plated onto a silver disc as described above. The activities of ^{208}Po and ^{210}Po were determined by alpha -spectroscopy. The combined recovery and counting efficiency (E) of ^{208}Po (^{208}Po cpm/^{208}Po dpm) was approximately 5%.

3) Total Sediment Extraction

The total ^{210}Pb content in the sediment samples used in 1) and 2) above was extracted by digestion in concentrated HF and HNO_3. Five gram samples and tracers were evaporated 5 times in concentrated HF and 6M HNO_3, followed by evaporation in 100ml of concentrated HCl. The final residues were dissolved in 50ml of 3M HCl and diluted to 0.5M HCl and plated as in 1) above. Nuclide activity was measured by alpha spectroscopy.

The results of trials 1), 2), 3) are presented in Table A2.2.

Table A2.2 ^{210}Pb Method Development- Results of Test 1

Sample	Method	^{210}Pb activity (dpm/g)
AHE/1D2	Conc. HCl/HNO_3	0.453
1D2	2M HCl	0.411
1D2*	2M HCl	0.041
AHE/2C7	Conc. HCl/HNO_3	0.883
2C7	2M HCl	0.942
AHE/1D3	2M HCl	0.520
1D2	Total HF/HNO_3	1.323
1D2	Total HF/HNO_3	1.384

Conc.; concentrated.
*; second extraction of sample 1D2.

The results show insignificant differences in the ^{210}Po activity yielded by digestion in concentrated HCl/HNO_3 compared with extraction in 2M HCl. Hence, it is concluded that repeated evaporations in concentrated acid are unnecessary when 2M HCl will extract that same quantity of Polonium. The 2M HCl extraction method was preferred for this study. The total extractions of sample 1D2 reveal mineral ^{210}Po activity of (1.353-0.432) 0.922dpm/g. Hence, the extractable ^{210}Pb activity for sample 1D2 is 32% of the total ^{210}Po activity.

Re-analysis of the residue of sample 1D2 (second Po extraction in 2M HCl) yielded 0.041dpm/g ^{210}Po indicating that initial recovery of ^{210}Pb is 90%.

Test 2

Clay particles tend to form sand sized aggregates, particularly in muddy samples, which may not disaggregate in solution. The second trial involved testing the effect of HCl acid (0.1-8M) on milled and unmilled samples. The reason this test was carried out was to determine whether or not milling samples would reduce or enhance polonium extraction.

Unmilled and milled fractions of sample AHE/1C8 were extracted with ^{208}Po for 2 hours in, 0.1 to 8M, HCl and plated in 0.5M HCl as described in 1) above. The results presented in Table A2.3 show that neither milling nor length of extraction (above 1 hour) affects ^{210}Po recovery at acid strengths below 4M HCl. Above 4M HCl ^{210}Pb activities increased rapidly as mineral ^{210}Pb was extracted from the sediment.

Table A2.3 HCl Extraction of Milled and Unmilled Fractions of Sample AHE/1C8

Milled (M) Unmilled (U)	Acid Strength	Extraction Time	^{210}Pb Activity dpm/g
M	0.1Molar	1 hour	0.894
M	0.1	2	0.744
U	0.1	2	0.845
M	1.0	1	0.913
U	1.0	1	1.309
U	1.0	1	0.561
U	2.0	1	0.844
U	4.0	1	1.131
U	8.0	1	1.632
M	8.0	1	1.477

Manipulative errors were 5-10% for both tests.

On the basis of tests 1 and 2 it was decided to adopt the following method 1) Analyse 5g samples (milled), 2) add 1ml of 7.7 dpm/ml ^{208}Po tracer to each sample before adding 100ml of 1M HCl and heat for 1 hour at near boiling point, with stirring, 3) after extraction filter samples and dilute to 0.5M HCl, 4) add 0.1g of ascorbic acid to the 0.5M solution to complex Fe, 5) plate the extracted ^{208}Po

and ^{210}Po on pre-cleaned silver discs (see 1) above) for 4 hours in the 0.5M solution, 6) determine radioactivity by alpha-spectroscopy (NRL). The assumptions involved in this method are that ^{210}Po activity is in equilibrium with ^{210}Pb activity.

APPENDIX 3 (Appendix to Chapter 4)

A3.1 TECHNIQUES OF CORRECTING SEDIMENT DATA FOR GRAIN SIZE AFFECTS

The following discussion will be limited to the most commonly employed grain size correction techniques: A) grain size separation, B) treatment with dilute acid, C) inert mineral correction and D) conservative element correction. (Table 4.2, Chapter 4.0).

A3.1.1. Grain Size Separation

The ideal method of dealing with the grain size distribution problem is to separate out the sand (>63 μm), silt (4-63 μm (2 μm)), and clay (<4 μm (2 μm)) fractions and analyse the individual heavy metal contributions from each grain size. The main advantage of separating these grain size groups is that it requires only a few samples. However, separation of all 3 fractions is time-consuming, so most workers have chosen to study just one of the following fractions; (1) <63 μm (mud or silt/clay), (2) <20 μm, and (3) <4 or <2 μm (pelitic or clay). (The division between silt and clay is preferred to be <4 μm by most geologists and <2 μm by soils scientists (Lewis, 1982).

Analysis of the <63 μm fraction is rapid because this fraction can be separated by sieving, hence it is favoured by many researchers. In addition, Araujo et (1988), Forstner and Wittmann (1981) and Taylor (1986) argue for the use of the <63 μm fraction because of its recommendation by the World Health Organisation (WHO) for the following reasons. "1) Trace metals have been found to be present in the clay/silt fraction, 2) this fraction is most nearly equivalent to the material carried in suspension and hence likely to be contaminated, 3) sieving does not alter the metal concentration, and 4) numerous studies have already been performed on the <63 μm fraction

allowing better comparison of results."

However, Ackermann et al. (1983) and Nicolaidou and Nott (1989) point out that analysis of the <63 μm fraction alone does not account for variation of clay mineral content between sediment types or localities. Ackermann and co-workers found that Zn concentrations in the 20-60 μm fractions were only 9% of that determined in the <20 μm fraction. These authors favour analysing the <20 μm fraction because it contains a higher percentage of clay and is also easily separated by sieving.

Ideally one should examine the pelitic fraction (<4 μm) because it contains the largest concentration of heavy metals and almost the entire contribution from anthropogenic sources (Fig. 1.1, Chapter 1). However, this method is extremely time-consuming involving weeks of settling in tubes and has the risk of metal remobilisation if pH changes occur during the separation. Because of the effort involved this method is not as commonly employed as separation of the <63 μm, or <20 μm fractions.

A3.1.2. Treatment with Dilute Acid

Leaching of bulk sediment samples with cold 0.1-.05 M HCl is reported to remove only the mobile heavy metals bound to substances on the surface of the sediments. Data obtained this way typically compares well with data obtained by clay fraction separation. Generally, this method provides a rapid inexpensive way of establishing the gross degree to which sediments have been contaminated.

A3.1.3. Inert Mineral Correction

There is normally a direct correlation between mean grain size and quartz, feldspar and carbonate content (Forstner, 1989; Horowitz, 1985). As grain size decreases the concentration of these minerals decreases, with only minor concentrations present in the pelitic fraction.

Inert mineral corrections (IMC) are normally carried out for one of the above three minerals using the following formula: IMC = Total metal concentration x 100/(100-% inert mineral). This correction technique usually provides a reasonable assessment of the metal concentration in the fine particles. In sediments that contain high proportions of quartz, feldspar, and carbonate all three should be included in the correction calculation. Most techniques for quantifying these minerals (X-ray Diffraction and Petrography) are semi-quantitative and only provide rough corrections for accurately determined heavy metal data. Consequently, calculations of percentage inert minerals are often not comparable between different analysts and different localities.

A3.1.4. Conservative Element Correction

Conservative elements (including Al, Fe, Cs, Sc, Rb, Sm, Th, and Ti) are assumed to have a uniform flux to sediment, which is not affected by anthropogenic influences. Hence, a ratio of conservative element to contaminant (such as Cu, Zn, Pb, Ni, Cr, Cd) is a useful way of determining heavy metal enrichment. The most common conservative elements, used in studies, are Al, Fe, and Ti. The enrichment factors (EF) are calculated from the following formula:

$$EF_M = (M_s/Al_s)/(M_a/Al_a)$$

where M_s and Al_s are the trace metal and Al concentrations in the sediment of interest, while M_a and Al_a are their respective concentrations in a suitable baseline sample.

Conservative element correction has the advantage that only a few samples are required.

A3.2 RAW DATA FROM HEAVY METAL ANALYSES OF CORES

Table A3.1 Heavy Metal and Organic Matter Concentrations in Sand Fractions of cores AHE/1a 2a, 3a and 3b

AHE/1a sample	Depth cm	Pb µg/g	Cu µg/g	Ni µg/g	Zn µg/g	Mn µg/g	Fe %	Cr µg/g	ORG %
1D1	1.00	7.23	3.99	11.90	28.80	51.80	1.09	18.80	1.10
1D2	4.00	7.23	3.99	11.90	28.80	51.80	1.09	18.80	1.10
1D3	8.00	7.83	4.79	11.90	29.10	51.70	1.09	19.50	1.00
1D4	12.00	9.23	4.32	12.50	58.10	55.40	1.06	17.30	1.10
1C1	33.00	8.83	4.10	11.80	19.10	54.00	1.02	17.20	1.40
1C2	37.00	7.53	4.62	11.80	20.20	50.30	1.11	19.70	1.60
1C7	58.00	7.13	3.99	12.40	18.20	53.30	1.13	20.10	1.60
1C8	62.00	8.03	5.22	13.80	21.50	58.40	1.34	21.10	1.80
1C13	81.00	6.93	3.72	13.20	20.30	63.00	1.28	21.90	1.40
1B1	83.00	10.13	3.53	14.30	23.10	74.10	1.18	20.50	1.30
1B2	87.00	8.43	5.17	15.30	23.90	59.50	1.36	24.20	1.30
1B9	116.00	4.13	6.12	11.60	21.40	35.70	1.28	24.80	1.74
1A1	133.00	6.53	6.48	13.10	20.00	47.20	1.11	20.90	.93
AHE/2a									
2D1	2.00	3.23	3.69	8.30	18.90	30.60	1.06	20.90	1.73
2D2	6.00	9.03	5.33	11.30	25.90	50.80	.52	22.50	.93
2D3	11.00	3.53	3.69	8.10	19.50	30.20	1.04	18.50	2.02
2C1	16.00	5.13	5.93	11.10	16.60	44.90	1.56	27.40	3.84
2C2	20.00	5.73	6.16	12.40	28.10	49.90	1.21	26.20	2.06
2C5	32.00	4.33	5.66	10.40	14.50	47.90	1.44	26.30	2.44
2C10	52.00	6.23	5.58	11.60	30.10	50.80	1.08	23.60	.83
2C12	60.00	3.63	4.67	10.10	14.00	50.50	1.19	24.50	1.91
2C15	72.00	2.23	3.49	8.30	27.50	32.80	.98	18.70	1.60
2C16	77.00	2.95	3.43	7.46	18.70	39.80	1.14	21.70	1.27
2C17	82.00	5.63	4.99	11.10	22.50	47.90	.89	21.70	.68
2B1	86.00	2.90	3.29	7.76	18.10	37.60	1.20	21.90	1.06
2B2	90.00	2.93	3.21	8.60	19.20	33.20	.92	17.60	1.39
AHE/3a and b									
3aD1	2.00	7.44	16.00	9.95	28.80	56.20	1.37	32.00	1.57
3aD2	7.00	8.60	14.40	9.92	29.00	53.50	1.40	30.20	1.51
3aD3	12.00	4.76	8.40	8.77	25.50	32.20	1.17	26.40	1.22
3aD4	17.00	2.69	6.74	7.86	22.40	31.20	1.15	25.20	1.21
3aD5	22.00	7.38	6.64	8.36	23.60	55.50	1.50	25.80	1.66
3aC1	27.00	3.44	4.59	8.48	22.50	34.50	1.18	24.70	1.55
3aB1	32.00	4.01	4.00	8.06	21.90	10.30	1.70	25.70	.98
3aB2	37.00	4.87	5.60	9.50	22.90	54.40	1.44	27.10	1.31
3B3	42.00	2.34	3.63	8.12	18.70	32.30	1.21	24.00	1.09
3aB13	92.00	3.28	5.29	11.45	20.30	63.30	1.64	29.10	1.54
3bD4	14.00	8.77	9.82	9.79	27.30	44.00	1.32	26.90	1.38
3bC1	27.00	4.72	3.97	8.11	21.20	51.30	1.35	24.20	1.34

Table A3.2 Heavy Metal and Organic Matter Concentrations in Sand Fractions of cores AHE/5 and 6, TS/1 and 3, and SWC/1 and 2

AHE/5 Sample	Depth cm	Pb µg/g	Cu µg/g	Ni µg/g	Zn µg/g	Mn µg/g	Fe %	Cr µg/g	ORG %
5D1	2.00	6.68	4.18	7.97	27.00	33.90	1.08	23.20	.86
5D-C1	6.00	1.87	3.87	7.19	20.80	46.90	1.13	22.10	.87
5D-C2	10.00	1.89	3.67	6.64	17.50	40.50	.96	19.80	.99
5C1	18.00	3.35	3.70	6.56	15.60	31.10	.95	18.60	1.01
5C4	30.00	2.76	8.43	13.60	27.80	54.30	1.33	27.10	1.71
5C10	54.00	3.11	10.20	12.90	24.60	53.80	1.78	32.10	2.30
5C18	85.00	3.35	10.20	11.10	29.20	71.10	1.83	31.20	2.28
5B1	90.00	.31	6.68	9.91	20.20	40.40	1.57	30.00	1.78
5B2	94.00	.95	6.19	9.84	20.40	44.20	1.45	28.90	1.48
5B5	105.00	2.25	9.22	12.30	24.90	55.00	1.86	33.10	2.20
AHE/6									
6D1	2.00	8.16	12.00	9.94	40.20	45.90	1.26	35.40	1.39
6D2	6.00	8.69	13.00	9.82	42.80	40.60	1.29	36.30	7.64
6D3	10.00	10.00	9.45	9.44	45.00	46.40	1.19	34.80	1.32
6D-C1	14.00	12.80	9.95	9.41	49.40	43.50	1.27	33.90	1.66
6C1	22.00	6.84	5.60	6.81	34.20	52.30	.72	26.80	1.23
6C3	30.00	5.06	4.50	7.73	22.00	39.00	1.09	26.00	1.00
6C-B1	42.00	4.13	3.29	7.33	18.20	46.90	.98	23.10	.96
6C-B2	46.00	4.44	2.82	7.03	18.40	34.00	1.02	22.20	.96
6C-B5	58.00	4.72	2.95	6.70	20.70	45.00	1.03	21.80	.97
6B22	146.00	1.91	2.99	7.46	18.30	37.70	.87	24.50	1.31
TS/1									
T1	30.00	1.55	2.87	11.60	21.20	27.10	.83	19.20	1.20
T2	65.00	3.03	3.00	14.00	19.20	39.00	1.06	20.10	1.35
TS/3									
T12	47.00	2.41	4.95	5.34	18.50	43.40	.90	16.50	1.28
T13	53.00	2.57	5.72	6.15	22.30	32.40	1.36	17.10	1.03
T14	57.00	2.70	5.49	6.27	19.60	36.40	1.07	18.40	1.08
T15	63.00	2.62	5.62	6.10	19.30	37.80	1.06	20.60	1.06
SWC/1									
S1/1	2.00	3.11	3.08	5.55	15.00	33.50	.81	15.80	.91
S1/2	6.00	3.66	2.87	4.66	15.90	49.20	.82	14.70	.73
S1/3	8.00	3.45	3.37	4.92	15.10	29.80	.75	14.70	.75
S1/4	11.00	3.74	3.87	5.70	16.00	34.00	.75	15.10	.81
S1/5	13.00	3.64	4.55	5.90	16.00	34.70	.81	15.10	.96
S1/6	16.00	3.48	3.40	5.52	14.60	33.30	.74	15.30	.80
S1/10	26.00	1.58	4.85	8.21	17.90	37.80	1.32	22.80	1.34
S1/11	28.00	2.81	4.37	7.18	21.40	33.00	.96	19.10	1.08
S1/12	31.00	3.14	4.31	5.86	18.70	32.90	1.05	19.60	1.09
S1/17-18	47.00	1.89	4.02	6.93	18.50	38.00	1.00	22.10	1.09
SWC/2									
S2/2	2.00	3.75	6.25	6.66	25.60	38.70	1.05	19.10	1.05
S2/5	5.00	3.75	6.94	7.05	26.20	45.10	1.48	19.40	1.11
S2/8	13.00	3.42	7.62	8.38	25.70	45.20	1.40	21.20	1.20
S2/13	21.00	3.15	7.62	7.71	23.90	43.00	1.14	21.80	1.27
S2/25	41.00	2.85	14.20	9.32	27.20	34.50	1.34	27.10	2.55

Table A3.3 Heavy Metal and Organic Matter Concentrations in Silt Fractions of cores AHE/1a, 2a, 3a, and 3b

AHE/1a Sample	Depth cm	Pb µg/g	Cu µg/g	Ni µg/g	Zn µg/g	Mn µg/g	Fe %	Cr µg/g	ORG %
1D1	1.00	17.80	10.90	12.50	53.50	53.50	1.20	36.00	1.70
1D2	4.00	12.00	8.32	12.90	50.30	65.00	1.56	39.20	1.80
1D3	8.00	18.60	8.54	15.50	101.30	88.60	1.67	46.20	1.90
1D4	12.00	24.90	10.50	17.20	83.20	63.80	1.75	48.30	2.50
1C1	33.00	16.40	8.24	9.80	16.60	61.00	1.46	49.50	1.65
1C2	37.00	8.40	10.70	9.70	17.60	60.90	1.43		1.50
1C7	58.00	5.30	7.90	10.40	16.80	59.20	1.70		1.70
1C8	62.00	14.60		12.10	24.80	75.90	1.85		1.80
1C13	81.00	12.90	7.33	14.50	36.80	80.60	2.19	34.50	2.20
1B1	83.00	17.60	11.10	19.60	43.70	100.00	2.39	41.40	2.80
1B2	87.00	27.50	24.10	20.10	50.10	115.00	2.88	38.50	2.20
1B9	116.00	8.70	15.90	11.40	66.90	76.80	1.55	30.20	2.23
AHE/2a									
2D1	2.00	3.20	47.50	12.60	35.70	56.80	1.79	36.30	4.47
2D2	6.00	13.90	14.00	14.40	39.50	86.50	1.85	36.30	2.75
2D3	11.00	2.60	32.00	11.00	30.70	54.80	1.04	32.40	3.34
2C1	16.00	2.68	7.54	9.10	28.40	50.60	1.39	29.70	1.68
2C2	20.00	3.60	10.30	10.70	28.90	66.70	1.06	32.40	1.96
2C5	32.00	1.52	7.36	11.60	31.00	52.40	1.64	32.70	2.15
2C10	52.00	6.30	12.20	11.80	42.80	77.30	2.00	34.90	2.43
2C12	60.00	.34	6.22	8.88	23.20	54.90	1.37	31.30	1.90
2C15	72.00	7.20	18.20	12.50	59.40	84.70	1.99	36.20	4.26
2C16	77.00	7.71	9.40	10.70	32.90	73.00	1.84	34.10	2.33
2C17	82.00	8.80	14.70	14.30	37.40	83.80	2.04	38.80	1.46
2B1	86.00	8.57	15.90	15.60	47.90	93.80	2.61	40.30	2.36
2B2	90.00	11.00	25.30	12.00	42.30	61.70	1.68	34.70	3.43
AHE/3a and b									
3aD1	2.00	8.94	17.80	16.80	67.10	82.00	2.43	58.20	2.94
3aD2	7.00	9.62	16.70	15.80	60.70	82.40	2.09	58.10	2.71
3aD3	12.00	9.95	15.20	13.40	52.00	57.50	1.75	52.80	2.21
3aD4	17.00	4.45	8.92	9.61	38.60	62.80	1.49	35.90	1.64
3aD5	22.00	5.67	10.10	12.20	44.20	91.40	2.21	39.10	2.58
3aC1	27.00	2.75	6.30	7.62	23.20	48.80	1.44	28.80	1.46
3aB1	32.00	5.41	23.20	13.10	41.80	81.60	2.34	36.40	1.78
3aB2	37.00	14.50	21.90	15.10	42.60	106.00	2.83	38.40	2.14
3aB3	42.00	20.60	57.60	17.60	62.00	145.00	4.53	44.80	2.53
3aB13	92.00	4.50	13.40	15.50	35.00	115.00	2.40	41.70	2.42
3bD4	14.00	11.70	18.90	15.20	67.70	84.20	2.48	69.30	2.64
3bC1	27.00	5.00	7.14	10.50	33.90	71.10	1.67	41.60	1.90

Table A3.4 Heavy Metal and Organic Matter Concentrations in Silt Fractions of cores AHE/5 and 6, TS/1 and 3, and SWC/1 and 2

AHE/5 Sample	Depth cm	Pb µg/g	Cu µg/g	Ni µg/g	Zn µg/g	Mn µg/g	Fe %	Cr µg/g	ORG %
5D1	2.00	10.60	16.80	12.40	73.10	79.40	2.10	43.40	2.32
5D-C1	6.00	8.14	11.50	7.80	101.00	57.30	1.74	29.60	1.70
5D-C2	10.00	5.22	5.80	6.20	65.20	54.60	1.50	25.70	1.36
5C1	18.00	3.85	5.42	7.30	12.30	59.70	1.69	25.30	1.43
5C4	30.00	2.40	7.31	11.50	27.80	61.00	1.73	29.70	1.60
5C10	54.00	3.34	8.49	10.00	31.20	60.80	1.86	32.20	1.65
5C18	85.00	3.98	11.70	12.20	34.70	70.70	2.16	35.20	2.14
5B1	90.00	20.20	12.10	18.40	51.70	150.00	2.34	34.40	
5B2	94.00	8.74	11.50	11.90	34.70	63.20	2.13	34.30	1.98
5B5	105.00	2.95	10.80	11.90	33.30	67.80	2.13	34.30	1.89
AHE/6									
6D1	2.00	20.80	29.50	11.60	72.50	45.60	2.18	61.70	2.97
6D2	6.00	16.60	30.20	12.80	74.10	49.20	2.46	66.60	3.10
6D3	10.00	22.30	26.80	11.40	73.20	43.00	2.18	57.30	2.97
6D-C1	14.00	14.10	18.60	9.90	64.50	46.20	2.26	42.60	2.62
6C1	22.00	6.40	8.42	9.13	41.90	39.50	1.70	31.70	1.86
6C3	30.00	4.63	5.80	9.22	33.40	41.70	1.64	31.20	1.69
6C-B1	42.00	4.82	6.20	11.30	37.40	55.40	2.07	35.40	1.96
6C-B2	46.00	4.74	7.02	12.10	38.70	50.90	2.30	36.40	2.01
6C-B5	58.00	5.19	8.98	11.10	40.70	59.00	2.56	37.50	2.05
6B22	146.00	7.95	8.14	11.30	39.40	48.50	2.65	37.30	2.23
TS/1									
T1	53.00	UD	4.46	10.50	14.80	40.40	1.34	27.60	1.70
T2	70.00	UD	4.79	11.40	18.80	45.90	1.38	26.90	1.81
T3	83.00	UD	7.69	16.00	18.80	48.80	1.48	25.10	2.04
T4	100.00	11.00	8.48	16.00	43.40	72.50	1.85	36.10	2.00
T4	100.00	UD	18.80	32.30	46.80	121.00	1.38	35.90	1.95
TS/3									
T12	47.00	UD	6.59	15.10	24.00	34.50	1.46	29.10	1.40
T13	53.00	UD	6.34	13.90	20.50	25.60	1.44	28.50	1.31
T14	57.00	UD	7.73	15.30	24.20	24.00	1.50	30.30	1.42
T15	63.00	UD	8.17	16.20	25.20	29.70	1.52	32.90	1.49
SWC/1									
S1/1	2.00	2.05	6.26	8.58	24.00	20.50	1.59	25.50	1.53
S1/2	6.00	2.36	6.29	9.39	26.60	27.60	1.72	28.20	1.68
S1/3	8.00	2.31	6.57	9.72	21.70	18.30	1.74	29.80	1.65
S1/4	11.00	2.72	7.28	10.70	28.80	26.50	2.19	33.00	1.84
S1/5	13.00	UD	7.55	11.00	26.50	15.80	2.08	32.30	1.90
S1/6	16.00	UD	9.22	12.00	27.90	14.90	2.47	36.40	2.22
S1/10	26.00	3.20	7.20	10.70	25.40	17.60	2.22	31.80	1.80
S1/11	28.00	UD	8.03	11.10	29.20	26.10	2.29	22.50	1.98
S1/12	31.00	UD	8.78	11.80	26.40	17.30	2.42	34.10	2.01
S1/17-18	47.00	UD	7.80	9.75	25.60	43.00	1.57	36.50	1.99
SWC/2									
S2/2	2.00	UD	8.99	15.80	32.50	46.20	1.40	28.20	1.27
S2/5	5.00	UD	9.13	17.10	33.50	40.60	1.53	31.10	1.46
S2/8	13.00	UD	8.59	16.50	33.00	40.40	1.44	28.60	1.45
S2/13	21.00	UD	10.70	19.10	31.30	26.10	1.59	37.50	1.92
S2/25	41.00		10.80	18.80	31.60	36.10	1.46	36.70	1.86

UD; undetectable

Table A3.5 Heavy Metal and Organic Matter Concentrations in Clay Fractions of cores AHE/1a, 2a, 3a, and 3b

AHE/1a Sample	Depth cm	Pb µg/g	Cu µg/g	Ni µg/g	Zn µg/g	Mn µg/g	Fe %	Cr µg/g	ORG %
1D1	1.00	189.00	96.00	72.10	540.00	340.00	6.59	196.00	10.00
1D2	4.00	128.00	65.60	52.10	434.00	288.00	5.78	208.00	9.00
1D3	8.00	127.00	53.40	56.70	435.00	235.00	5.14	191.00	8.20
1D4	12.00	169.00	55.20	72.90	612.00	252.00	6.30	202.00	9.10
1C1	33.00	65.90	49.80	52.60	237.00	286.00	5.12	73.90	7.10
1C2	37.00	22.50	54.60	39.50	118.00	201.00	4.49	73.90	6.00
1C4	45.50	21.40	15.20	19.10	105.00	266.00	4.45	78.50	5.97
1C6	54.50	19.10	18.30	22.40	112.00	278.00	4.47	84.90	6.02
1C7	58.00	26.10			102.00	227.00	4.56	84.90	6.00
1C8	62.00	23.80			103.00	195.00	4.22	72.00	6.00
1C10	70.50	26.40	14.90	20.60	94.00	226.00	4.39	77.90	4.87
1C12	78.50	38.30	18.70	19.40	104.00	223.00	5.30	75.20	5.68
1C13	81.00	84.60	33.10	53.20	162.00	299.00	7.50	93.80	6.90
1B1	83.00	210.00	63.60	84.80	424.00	473.00	6.31	81.40	8.50
1B2	87.00	161.00	69.00	150.00	404.00	659.00	5.57		7.20
1B7	108.50	49.00	38.30	29.50	162.00	321.00	4.26	89.70	5.56
1B9	116.00	43.70		35.80	131.00	224.00	4.37	73.70	5.49
1B10	120.00	37.70	50.00	31.80	150.00	310.00	4.91	84.60	5.69
AHE/2a									
2D1	2.00	52.00	60.00	30.00	130.00	180.00	4.90	80.00	9.10
2D2	6.00	56.90	77.90	30.80	144.00	189.00	4.73	77.50	8.11
2D3	11.00	43.30	49.80	27.00	105.00	182.00	4.06	69.40	7.72
2C1	16.00	51.60	27.30	33.30	181.00	248.00	5.01	103.00	6.37
2C2	20.00	43.40	30.10	26.40	92.60	185.00	3.46	74.50	5.70
2C5	32.00	41.20	21.60	26.90	147.00	222.00	5.32	88.60	5.47
2C10	52.00	39.80	27.90	24.60	84.30	181.00	4.08	63.00	5.60
2C12	60.00	44.00	25.40	26.60	162.00	269.00	5.22	89.60	6.71
2C15	72.00	23.90	39.80	21.90	83.80	175.00	4.26	64.80	8.04
2C16	77.00	31.20	33.20	39.50	152.00	265.00	4.82	93.30	6.27
2C17	82.00	47.30	32.30	30.40	98.60	202.00	9.48	70.90	7.10
2B1	86.00	163.00	83.50	53.40	382.00	549.00	10.30	99.70	7.29
2B2	90.00	82.80	45.70	28.60	133.00	182.00	4.89	69.40	9.26
AHE/3a									
3aD1	2.00	28.50	56.10	55.70	340.00	190.00	4.54	194.00	8.70
3aD2	7.00	40.10	50.30	49.20	321.00	185.00	4.55	151.00	8.00
3aD3	12.00	83.90	61.80	54.80	398.00	235.00	5.35	227.00	6.54
3aD4	17.00	124.00	54.70	50.60	399.00	251.00	5.28	201.00	6.87
3aD5	22.00	25.10	36.90	39.30	249.00	201.00	5.30	122.00	7.30
3aC1	27.00	38.00	31.40	37.20	223.00	263.00	4.37	106.00	6.74
3aB1	32.00	123.00	74.60	44.20	356.00	437.00	6.20	132.00	6.96
3aB2	37.00	113.00	60.40	50.00	277.00	529.00	5.57	121.00	8.10
3aB3	42.00	257.00	215.00	63.60	158.00	730.00	9.63	109.00	7.11
3aB13	92.00	36.50	32.40	43.50	126.00	280.00	5.86	96.80	7.40
AHE/3b									
3bD1	2.00	41.80	49.20	47.00	278.00	225.00	2.31	206.00	8.80
3bD4	14.00	49.60	55.70	48.70	306.00	242.00	1.32	185.00	8.50
3bC1	27.00	27.50	31.60	34.70	191.00	266.00	2.14	109.00	7.30
3bB7	54.00	251.00	236.00	102.00	535.00	916.00	9.41	122.00	10.00
3bB13	77.00	184.00	148.00	56.20	416.00	671.00	7.11	134.00	9.80

Table A3.6 Heavy Metal and Organic Matter Concentrations in Clay Fractions of cores AHE/5 and 6, TS/1 and 3, and SWC/1 and 2

AHE/5 Sample	Depth cm	Pb µg/g	Cu µg/g	Ni µg/g	Zn µg/g	Mn µg/g	Fe %	Cr µg/g	ORG %
5D1	2.00	92.00	74.40	61.00	303.00	297.00	4.02	118.00	6.98
5D-C1	6.00	55.40	44.30	59.80	206.00	290.00	4.55	101.00	6.14
5D-C2	10.00	31.20	34.20	38.90	129.00	317.00	4.05	85.60	5.29
5C1	18.00	21.50	21.60	27.00	117.00	316.00	3.82	76.70	4.15
5C4	30.00	42.40	32.60	57.80	133.00	267.00	4.16	81.40	4.69
5C10	54.00	47.20	44.90	45.60	124.00	274.00	4.34	79.70	4.67
5C18	85.00	49.20	37.70	41.00	147.00	297.00	4.22	79.60	5.29
5B1	90.00	43.40	43.20	40.40	135.00	276.00	4.60	81.80	5.17
5B2	94.00	66.40	50.90	46.50	150.00	286.00	4.52	79.80	5.28
5B5	105.00	58.10	54.60	74.20	395.00	293.00	4.91	83.80	5.29
AHE/6									
6D1	2.00	140.00	124.00	33.20	462.00	290.00	5.10	182.00	7.73
6D2	6.00	151.00	95.60	51.20	516.00	283.00	5.61	188.00	7.54
6D3	10.00	139.00	90.90	35.80	491.00	265.00	5.27	169.00	7.63
6D-C1	14.00	106.00	54.40	25.20	431.00	252.00	4.67	121.00	6.74
6C1	22.00	88.70	62.00	31.00	682.00	273.00	4.45	102.00	6.51
6C3	30.00	58.10	41.00	26.90	348.00	265.00	4.16	96.10	5.37
6C-B1	42.00	36.30	21.80	32.60	226.00	242.00	4.06	84.60	4.82
6C-B2	46.00	31.20	19.60	30.00	239.00	233.00	4.25	85.90	5.27
6C-B5	58.00	36.20	28.90	24.70	171.00	273.00	4.04	83.90	4.52
6B22	146.00	36.50	22.80	24.90	154.00	218.00	4.18	88.30	5.18
TS/1									
T1	53.00	23.20	28.10	29.80	67.40	154.00	5.01	99.50	
T2	70.00	31.90	30.50	34.60	89.60	189.00	5.51	64.50	5.66
T3	83.00	21.10	22.20	20.80	56.60	131.00	4.10	56.20	4.22
T4	100.00	40.80	27.10	15.90	54.00	122.00	4.03	40.90	4.50
TS/3									
T12	47.00	37.80	17.70	39.50	128.00	268.00	5.28	91.80	5.19
T13	53.00	36.60	16.40	40.90	109.00	231.00	5.48	85.30	4.39
T14	57.00	34.30	16.60	30.30	101.00	201.00	4.44	79.30	3.82
T15	63.00	41.30	24.70	34.00	103.00	216.00	4.65	82.20	4.24
SWC/1									
S1/1	2.00	17.80	28.70	33.20	106.00	234.00	3.55	86.50	5.61
S1/2	6.00	18.80	25.70	34.50	101.00	224.00	3.78	84.50	5.36
S1/3	8.00	11.30	24.90	31.00	99.50	226.00	3.50	83.70	5.39
S1/4	11.00	12.70	25.80	31.80	102.00	225.00	3.91	89.00	5.23
S1/5	13.00	18.40	30.90	32.20	116.00	271.00	4.42	93.00	6.14
S1/6	16.00	14.10	31.80	42.70	115.00	263.00	4.58	95.60	6.23
S1/10	26.00	9.68	35.10	37.50	110.00	256.00	4.71	91.90	6.53
S1/11	28.00	18.90	36.40	43.70	116.00	251.00	4.49	95.60	6.87
S1/12	31.00	22.90	40.00	43.30	121.00	313.00	4.55	95.30	6.56
S1/17-18	47.00	13.50	28.30	29.80	101.00	240.00	3.64	94.40	5.95
SWC/2									
S2/2	2.00	30.20	25.70	27.70	113.00	254.00	4.21	85.60	5.21
S2/5	5.00	36.10	31.00	41.50	121.00	301.00	5.43	97.30	5.36
S2/8	13.00	53.50	38.70	42.60	140.00	316.00	5.70	109.00	5.93
S2/13	21.00	43.00	40.10	33.00	124.00	200.00	5.20	99.60	6.69
S2/25	41.00	31.50	47.90	40.70	116.00	176.00	4.18	103.00	6.71
S2/26	43.00	33.00	45.90	45.20	119.00	216.00	4.32	99.40	6.14

Table A3.7 Heavy Metal and Organic Matter Concentrations in Total Sediment Samples from cores of this Study

AHE/1a	Depth cm	Pb µg/g	Cu µg/g	Ni µg/g	Zn µg/g	Mn µg/g	Fe %	Cr µg/g	ORG %
1D2	4	17.2	4.81	13.7	28.7	47.8	1.17	28.5	1.5
1D3	8	20.5	4.73	14.4	31.9	70.3	1.26	26.5	1.4
1D4	12	18.2	4.96	12.4	26.1	43.2	1.06	27.6	1.4
1D-C1	17	8.75	3.19	8.43	39.6	52	1.42	27.7	2.44
1C1	33	16.8	5.34	14.5	19.1	54.2	1.53	36.2	2.1
1C1	33	21.3	8	15.3	35.8	133	1.57		2.6
1C2	37	22.7	6.69	17.8	26.7	78.2	1.91	46.1	2.6
1C2	37	6.62	4.67	8.39	31.3	65.4	1.74	30.1	2.48
1C2	37	12.3	9.63	15.5	39.9	196	1.69		3.1
1C3	42	15.2	11.2	15.4	35.5	135	1.66		2.6
1C4	46	43.4	10.7	14.6	46.3	137	1.56		2.7
1C7	58	19.6	6.79	16.8	22.7	60.9	1.91	50.7	2.7
1C8	62	22	7.6	20.1	28.3	83.6	2.12	57.7	2.9
1C13	81	7.3	6.41	14.8	26.9	62.6	1.73	27.7	2.1
1B1	83	7.13	5.21	15.2	25.1	74.2	1.57	25.3	1.8
1B2	87	7.23	6.72	15	24.5	69.2	1.67	27.2	1.5
1A1	133	7.73	4.32	12.8	20.9	50.9	1.17	19.2	1
TS/1									
T1	30	4.83	5.16	16.4	26.1	48.4	1.43	30	2.14
T2	65	4.03	5.43	17.3	32	49.4	1.44	29.7	2.33
AHE/4									
4/1	2	2.73	3.34	19	17.6	33.2	1.06	21	1.76
4/2	6	3.43	2.83	18.3	18.1	28.9	1.03	20.5	1.37
4/3	10	1.93	2.68	17.7	16.5	27.7	.987	19	1.31
4/4	14	2.73	3.15	21.6	15.7	22.6	1.03	19.8	1.38
4/5	18	3.33	3.33	8.2	12.5	33.1	1.18	20.2	1.41
4/6	22	4.53	3.4	8.4	12.7	30.5	1.23	20.6	1.55
4/7	26	4.73	3.53	8.7	13.2	37.2	1.2	21.7	1.42
4/8	30	4.63	3.56	8.9	13.8	40.2	1.21	21.2	1.5
4/9	34	3.73	3.72	9.4	13.8	45	1.24	21.6	1.68
4/10	38	4.23	3.56	8.9	13.4	44.3	1.29	21.5	1.5
4/11	42	5.63	3.63	9.3	14.1	42.7	1.25	21.7	1.62
4/12	46	6.13	3.7	9.2	14.3	41	1.28	21	1.5
4/13	50	3.13	3.11	21.3	19.4	36	1.13	21	1.56
4/14	54	3.23	2.59	18	17.3	28.3	.876	16.2	1.4
4/15	58	2.43	3.08	18.6	17.8	31.2	1.08	20.1	1.64
4/16	62	.53	2.88	16.2	16.6	27.1	1.11	20.6	1.58
4/18	69	5.33	3.82	22.2	23.5	40.6	1.21	21.7	3.33
AHE/2a									
2D3	11	5.33	5.36	9.38	25	39.7	1.27	24	2.87
2C1	16	6.64	7.89	11.1	36.8	64.1	1.82	34.3	4.88
2C10	52	7.6	7.47	11.6	27.9	49.4	1.56	34.2	3.23
2B1	86	5.74	4.46	7.56	25.3	60.4	1.36	25.5	2.41
AHE/3a									
3aD2	7	10.3	16.1	13.3	52.1	40	1.38	46.2	2.54
3aD3	12	8.06	13.6	13.1	52.4	45.9	1.49	49.1	2.47
3aC1	27	9.06	7.73	11.1	44	55.8	1.46	35.4	3.1
3aB1	32	4.64	6.69	9.18	23.9	49.6	1.22	33.9	1.6
SWC/1									
S1/1	2	2.77	8.6	12	30.1	50.9	1.63	39.7	2.69
S1/3	8	2.73	8.97	12.4	32.2	39.8	1.79	36.7	2.76
S1/4	11	7.08	10.8	15.5	37.8	47	1.98	47.8	3.05
S1/5	13	1.82	12.5	14.9	35.2	46.9	2.25	51.3	3.38

A3.3 SIMILARITY MATRICES OF CLUSTER ANALYSES OF BOTTOM SEDIMENTS

Table A3.8 Similarity Matrices for Sand, Silt, and Clay Fractions

Sand	Pb	Cu	Ni	Zn	Mn	Fe	Cr	Organic
Pb	1	.302	.454	.61	.483	.016	.267	.151
Cu		1	.213	.524	.245	.301	.72	.457
Ni			1	.295	.603	.249	.353	.261
Zn				1	.264	.108	.49	.262
Mn					1	.031	.301	.127
Fe						1	.483	.231
Cr							1	.514
Organic								1

Silt	Pb	Cu	Ni	Zn	Mn	Fe	Cr	Organic
Pb	1	.45	.145	.643	.524	.432	.561	.377
Cu		1	.25	.404	.455	.489	.369	.73
Ni			1	.174	.407	.172	.135	.131
Zn				1	.395	.308	.355	.408
Mn					1	.431	.307	.325
Fe						1	.278	.328
Cr							1	.319
Organic								1

Clay	Pb	Cu	Ni	Zn	Mn	Fe	Cr	Organic
Pb	1	.818	.651	.707	.73	.478	.482	.571
Cu		1	.619	.545	.773	.495	.383	.565
Ni			1	.573	.612	.326	.494	.485
Zn				1	.391	.232	.671	.527
Mn					1	.483	.164	.349
Fe						1	.17	.032
Cr							1	.589
Organic								1

Baseline	Pb	Cu	Ni	Zn	Mn	Fe	Cr	Organic
Pb	1	.058	.072	.475	.049	.395	.062	.26
Cu		1	.468	.339	.162	.089	.439	.823
Ni			1	.237	.671	.648	.791	.552
Zn				1	.319	.022	.102	.295
Mn					1	.515	.722	.407
Fe						1	.565	.171
Cr							1	.593
Organic								1

Baseline; Clay fraction data from Saltwater Creek Estuary and Travis Swamp

Table A3.9 Similarity Matrices for Clay fractions of Units D, C, and B

Unit D	Pb	Cu	Ni	Zn	Mn	Fe	Cr	Organic
Pb	1	.616	.467	.715	.822	.655	.443	.243
Cu		1	.085	.417	.663	.32	.093	.051
Ni			1	.563	.478	.309	.588	.404
Zn				1	.524	.438	.581	.122
Mn					1	.358	.437	.216
Fe						1	.16	.055
Cr							1	.236
Organic								1

Unit C	Pb	Cu	Ni	Zn	Mn	Fe	Cr	Organic
Pb	1	.379	.326	.8	.281	.22	.36	.042
Cu		1	.481	.443	.128	.022	.02	.295
Ni			1	.11	.34	.068	.239	.061
Zn				1	.356	0	.515	.183
Mn					1	.101	.451	.191
Fe						1	.022	.161
Cr							1	.294
Organic								1

Unit B	Pb	Cu	Ni	Zn	Mn	Fe	Cr	Organic
Pb	1	.854	.763	.687	.91	.429	.574	.627
Cu		1	.665	.542	.904	.549	.577	.567
Ni			1	.808	.747	.264	.394	.502
Zn				1	.723	.246	.591	.533
Mn					1	.507	.757	.597
Fe						1	.342	.147
Cr							1	.506
Organic								1

A3.4 RAW DATA FROM STUDY OF NON-SALINE WATERS

Table A3.10 Environmental Measurements and Suspended Matter Concentration in the Heathcote River

Date	Water Temp °C	Eh V	pH	Suspended matter µg/ml	Av rainfall mm
26/2/88	13.00	.14	7.20	20.00	3.40
27/4/88	17.00	.14	7.00	24.80	0.00
1/7/88	8.00	.14	7.60	141.00	.10
10/8/88	10.50	.17	7.20	26.40	.37
29/9/88	15.00	.19	7.10	20.90	0.00
7/11/88	13.50	.18	7.10	194.00	4.80
20/12/88	18.50	.15	7.70	26.40	.30
7/2/89	16.50	.13	7.20	36.40	2.20
20/3/89	14.00	.08	7.00	22.50	1.20
3/5/89	13.00	.11	7.00	10.10	1.80
15/6/89	10.00	.15	6.20	9.60	1.10
17/7/89	8.50	.15	6.90	9.60	.03

Table A3.11 Environmental Measurements and Suspended Matter Concentration in the Avon River

Date	Water Temp °C	Eh V	pH	Suspended matter µg/ml	Av. rainfall mm
26/2/88	16.00	.16	7.70	8.00	3.40
27/4/88	17.00	.14	4.70	13.60	0.00
1/7/88	8.50	.18	6.80	10.50	.10
10/8/88	10.00	.20	6.20	8.00	.37
29/9/88	15.00	.18	7.40	6.80	0.00
7/11/88	15.50	.21	7.20	12.40	4.80
20/12/88	20.50	.21	7.60	22.00	.30
7/2/89	18.00	.12	8.20	9.60	2.20
20/3/89	15.00	.10	7.69	15.40	1.20
3/5/89	13.00	.13	6.66	6.60	1.80
15/6/89	9.00	.14	6.40	108.00	1.10
17/7/89	9.00	.15	6.80	6.80	.03

Table A3.12 Environmental Measurements and Suspended Matter Concentration in the City Outfall Drain

Date	Water Temp °C	Eh V	pH	Suspended matter µg/ml	Av. rainfall mm
26/2/88	15.00	.15	7.10	12.00	3.40
27/4/88	17.00	.13	6.70	29.60	0.00
1/7/88	6.50	.15	7.00	17.70	.10
10/8/88	9.50	.17	6.70	9.60	.37
29/9/88	17.00	.19	7.70	6.00	0.00
7/11/88	14.50	.18	6.90	7.60	4.80
20/12/88	21.50	.15	8.90	13.20	.30
7/2/89	18.00	.13	7.14	20.40	2.20
20/3/89	14.50	.08	7.30	12.10	1.20
3/5/89	13.50	.10	7.04	3.90	1.80
15/6/89	10.50	.11	6.80	9.60	1.10
17/7/89	10.50	.10	6.90	4.80	.03

Table A3.13 Environmental Measurements and Suspended Matter Concentration in Pond 5

Date	Water Temp °C	Eh V	pH	Suspended matter µg/ml	Av. rainfall mm
26/2/88	16.00	.15	8.60	80.00	3.40
27/4/88	17.00	.10	6.50	82.00	0.00
1/7/88	6.00	.14	7.80	64.90	.10
10/8/88	9.00	.14	7.20	70.00	.37
29/9/88	14.50	.14	7.10	28.80	0.00
7/11/88	14.50	.15	7.60	80.00	4.80
20/12/88	21.00	.17	7.10	148.00	.30
7/2/89	18.00	.13	8.40	120.00	2.20
20/3/89	15.50	.12	7.91	110.00	1.20
3/5/89	13.00	.09	6.64	73.00	1.80
15/6/89	8.00	.11	7.30	58.00	1.10
17/7/89	7.00	.11	7.90	64.00	.03

Table A3.14 Environmental Measurements and Suspended Matter Concentration in Pond 6

Date	Water Temp °C	Eh V	pH	Suspended matter µg/ml	Av. rainfall mm
26/2/88	16.00	.13	7.90	67.00	3.40
27/4/88	17.00	.10	7.00	68.00	0.00
1/7/88	6.00	.13	7.60	54.20	.10
10/8/88	9.00	.11	7.10	70.00	.37
29/9/88	17.00	.14	8.40	78.80	0.00
7/11/88	15.00	.19	7.80	76.00	4.80
20/12/88	23.00	.16	7.70	50.00	.30
7/2/89	18.00	.11	7.60	76.40	2.20
20/3/89	16.00	.08	8.03	63.00	1.20
3/5/89	13.00	.09	7.55	44.40	1.80
15/6/89	8.50	.13	7.10	47.00	1.10
17/7/89	7.50	.11		58.00	.03

Table A3.15 Heavy Metal Concentrations in the Dissolved Phase of the Heathcote River

Date	Pb ng/ml	Cu ng/ml	Ni ng/ml	Zn ng/ml	Mn ng/ml	Fe ng/ml	Cr ng/ml
26/2/88	.86	3.00	19.00	57.00	59.00	38.00	2.50
27/4/88	<1.5	.50	2.52	16.70	18.70	47.10	UD
1/7/88	.10	.73	1.00	24.80	23.30	UD	5.41
10/8/88	.20	.70	UD	16.00	23.20	-	1.20
29/9/88	.09	.90	UD	11.10	24.10	UD	2.30
7/11/88	.40	1.30	UD	41.90	20.60	95.00	1.60
20/12/88	UD	.49	UD	32.20	56.00	23.40	2.20
7/2/89	.13	.01	UD	48.00	63.90	19.70	1.40
20/3/89	UD	.19	UD	14.60	16.20	23.70	UD
3/5/89	UD	.23	UD	35.80	16.70	27.70	UD
15/6/89	.43	7.90	UD	23.40	32.80	92.00	UD
17/7/89	UD	UD	UD	52.40	34.00	122.00	UD

UD; Undetectable

Table A3.16 Heavy Metal Concentrations in the Dissolved Phase of the Avon River

Date	Pb ng/ml	Cu ng/ml	Ni ng/ml	Zn ng/ml	Mn ng/ml	Fe ng/ml	Cr ng/ml
26/2/88	.53	<1	<.76	5.90	16.00	140.00	.18
27/4/88	.77	.08	UD	3.63	6.33	115.00	UD
1/7/88	<1	.01	UD	3.95	8.11	UD	UD
10/8/88	.30	.40	UD	UD	UD	119.00	UD
29/9/88	.40	.80	UD	UD	7.40	150.00	UD
7/11/88	2.60	3.50	UD	9.20	4.30	501.00	1.20
20/12/88	.53	.49	UD	11.10	29.30	210.00	.57
7/2/89	1.50	.20	UD	4.00	16.20	143.00	.62
20/3/89	1.54	.66	UD	8.23	7.36	141.00	.31
3/5/89	1.10	1.14	UD	15.00	12.90	293.00	.06
15/6/89	1.00	1.30	UD	18.20	13.00	204.00	.18
17/7/89	1.40	1.10	UD	28.20	11.50	206.00	.22

Table A3.17 Heavy Metal Concentrations in the Dissolved Phase of the City Outfall Drain

Date	Pb ng/ml	Cu ng/ml	Ni ng/ml	Zn ng/ml	Mn ng/ml	Fe ng/ml	Cr ng/ml
26/2/88	3.40	2.40	1.20	65.00	82.00	200.00	.53
27/4/88	<1.5	.60	UD	.86	87.80	1.60	UD
1/7/88	.20	.02	1.00	16.30	54.10	UD	3.02
10/8/88	.60	2.50	UD	4.90	92.10	144.00	UD
29/9/88	.10	.60	UD	UD	67.40	36.00	UD
7/11/88	7.20	2.60	UD	108.00	49.80		1.20
20/12/88	.13	.40	UD	1.60	27.00	48.50	.96
7/2/89	UD	.01	UD	7.80	19.20	18.40	.53
20/3/89	1.18	.41	UD	38.40	64.40	256.00	UD
3/5/89	.04	UD	UD	66.50	76.80	253.00	UD
15/6/89	UD	.97	UD	34.20	118.00	467.00	UD
17/7/89	UD	UD	UD	51.80	112.00	569.00	UD

Table A3.18 Heavy Metal Concentrations in the Dissolved Phase of Pond 5

Date	Pb ng/ml	Cu ng/ml	Ni ng/ml	Zn ng/ml	Mn ng/ml	Fe ng/ml	Cr ng/ml
26/2/88	1.30	9.10	34.00	28.00	81.00	120.00	9.70
27/4/88	<1.5	1.20	26.30	26.50	40.60	38.40	9.96
1/7/88	<1	3.63	29.00	13.70	46.60	33.60	8.21
10/8/88	.70	9.50	36.70	UD	38.50	200.00	22.00
29/9/88	.92	8.10	24.20	UD	44.50	141.00	16.70
7/11/88	.40	6.60	29.00	UD	UD	422.00	10.30
20/12/88	UD	5.10	53.00	30.10	UD	129.00	5.50
7/2/89	UD	1.60	29.40	13.60	UD	101.00	3.20
20/3/89	.04	4.27	30.50	17.10	UD	27.70	5.82
3/5/89	UD	5.62	26.50	18.70	33.00	31.90	4.84
15/6/89	UD	3.50	16.50	6.40	36.30	69.40	7.50
17/7/89	4.00	19.60	22.90	34.70	62.20	127.00	17.80

UD; Undetectable

Table A3.19 Heavy Metal Concentrations in the Dissolved Phase of Pond 6

Date	Pb ng/ml	Cu ng/ml	Ni ng/ml	Zn ng/ml	Mn ng/ml	Fe ng/ml	Cr ng/ml
26/2/88	.55	10.00	32.00	13.00	7.00	180.00	14.00
27/4/88	1.00	4.00	19.80	45.50	70.70	180.00	16.80
1/7/88	<1	3.85	68.30	29.10	55.10	91.90	12.10
10/8/88	3.30	17.80	22.40	2.60	51.00		32.50
29/9/88	.70	13.00	33.40	UD	28.60	UD	19.80
7/11/88	.70	7.30	35.00	UD	UD	400.00	12.50
20/12/88	1.50	9.50	39.10	27.50	UD	442.00	11.20
7/2/89	UD	2.80	40.00	22.80	UD	254.00	7.20
20/3/89	1.20	5.65	28.30	13.20	5.80	114.00	11.20
3/5/89	UD	6.28	26.40	16.30	25.30	68.60	6.37
15/6/89	1.30	15.90	17.80	48.90	59.70	214.00	15.80
17/7/89	3.50	22.40	22.90	98.70	66.80	240.00	39.30

Table A3.20 Heavy Metal Concentrations in Total Water of the Heathcote River

Date	Pb ng/ml	Cu ng/ml	Ni ng/ml	Zn ng/ml	Mn ng/ml	Fe ng/ml	Cr ng/ml
26/2/88	4.10	10.00	17.00	78.00	63.00	420.00	2.40
27/4/88	3.80	1.20	2.52	28.00	23.00	499.00	1.21
1/7/88	8.60	4.30	1.00	58.40	34.80	367.00	7.69
10/8/88	2.30	2.90	UD	32.40	31.30	850.00	2.60
29/9/88	2.60	2.40	UD	25.40	28.30	724.00	2.60
7/11/88	31.00	10.80	UD	135.00	60.40	5820.00	11.90
20/12/88	2.60	1.30	UD	56.80	66.50	652.00	4.50
7/2/89	5.20	1.90	UD	52.90	85.50	1009.00	5.10
20/3/89	.32	3.32	.62	25.10	17.40	178.00	UD
3/5/89	1.33	1.85	.67	47.40	18.00	211.00	UD
15/6/89	6.30	41.70	.43	39.60	34.00	416.00	.43
17/7/89	1.70	1.40	UD	63.20	35.30	377.00	1.50

UD; Undetectable

Table A3.21 Heavy Metal Concentrations in Total Water of the Avon River

Date	Pb ng/ml	Cu ng/ml	Ni ng/ml	Zn ng/ml	Mn ng/ml	Fe ng/ml	Cr ng/ml
26/2/88	1.20	<2	.35	9.00	19.00	280.00	.79
27/4/88	1.70	.48	UD	6.61	9.19	294.00	.60
1/7/88	.97	.21	UD	10.20	10.30	257.00	.29
10/8/88	1.50	8.50	UD	9.50	4.70	362.00	1.40
29/9/88	1.30	.90	UD	UD	9.30	449.00	1.20
7/11/88	6.40	4.10	UD	22.40	8.00	761.00	1.70
20/12/88	2.00	.62	UD	25.40	40.10	887.00	1.20
7/2/89	2.90	.40	UD	19.70	23.90	533.00	.75
20/3/89	4.14	1.19	UD	18.20	9.60	496.00	1.10
3/5/89	1.94	1.72	.39	18.50	13.70	476.00	.35
15/6/89	11.50	40.10	4.40	74.40	35.50	3225.00	10.10
17/7/89	2.70	1.10	UD	28.40	12.50	369.00	.57

Table A3.22 Heavy Metal Concentrations in Total Water of the City Outfall Drain

Date	Pb ng/ml	Cu ng/ml	Ni ng/ml	Zn ng/ml	Mn ng/ml	Fe ng/ml	Cr ng/ml
26/2/88	6.80	5.20	.32	90.00	96.00	510.00	1.10
27/4/88	9.30	.30	2.52	7.10	101.00	1185.00	.71
1/7/88	1.90	.62	1.00	36.10	60.60	377.00	3.12
10/8/88	3.90	7.50	UD	30.50	124.00		1.20
29/9/88	2.10	1.20	UD	3.00	75.30	894.00	UD
7/11/88	17.60	5.10	UD	123.00	56.40	749.00	1.60
20/12/88	1.40	.49	UD	12.80	48.00	511.00	1.00
7/2/89	3.40	.50	UD	17.20	23.60	762.00	.62
20/3/89	8.64	2.78	.90	66.20	63.20	761.00	UD
3/5/89	.79	.45	UD	82.80	68.70	578.00	UD
15/6/89	6.70	35.60	UD	59.20	108.00	854.00	.09
17/7/89	21.70	2.30	UD	69.60	111.00	850.00	1.40

Table A3.23 Heavy Metal Concentrations in Total Water of Pond 5

Date	Pb ng/ml	Cu ng/ml	Ni ng/ml	Zn ng/ml	Mn ng/ml	Fe ng/ml	Cr ng/ml
26/2/88	2.20	19.00	40.00	41.00	95.00	380.00	25.00
27/4/88	1.60	5.80	24.00	44.90	65.10	176.00	14.20
1/7/88	2.40	14.60	28.90	49.50	65.90	347.00	30.90
10/8/88	4.40	15.50	28.40	31.90	66.40	306.00	27.70
29/9/88	2.40	10.70	25.90	6.60	55.20	269.00	21.70
7/11/88	10.50	37.80	34.60	86.80	52.60	903.00	130.00
20/12/88	2.50	12.50	43.20	96.20	118.00	208.00	21.60
7/2/89	3.00	11.00	44.50	91.50	143.00	106.00	10.80
20/3/89	2.59	10.30	32.00	28.00	48.90	174.00	17.20
3/5/89	3.17	22.30	32.10	35.30	48.90	258.00	27.40
15/6/89	14.50	40.40	40.20	94.10	62.70	662.00	68.00
17/7/89	10.00	22.90	33.20	81.30	68.60	361.00	42.10

Table A3.24 Heavy Metal Concentrations in Total Water of Pond 6

Date	Pb ng/ml	Cu ng/ml	Ni ng/ml	Zn ng/ml	Mn ng/ml	Fe ng/ml	Cr ng/ml
26/2/88	2.10	21.00	38.00	27.00	79.00	380.00	33.00
27/4/88	3.50	9.90	24.10	65.20	78.60	245.00	21.10
1/7/88	2.20	17.20	27.00	62.40	77.40	367.00	35.00
10/8/88	12.20	23.00	23.40	5.30	68.50	358.00	88.60
29/9/88	3.20	13.10	32.50	16.50	49.60	288.00	25.10
7/11/88	4.80	12.60	32.50	6.10	20.60	424.00	20.60
20/12/88	2.40	10.70	40.70	68.10	97.40	147.00	19.00
7/2/89	3.70	9.40	38.10	75.60	104.00	167.00	15.30
20/3/89	3.67	19.00	33.00	30.30	43.30	246.00	26.10
3/5/89	1.44	10.80	29.30	20.80	36.60	138.00	14.00
15/6/89	14.30	48.60	40.20	117.00	65.10	578.00	58.30
17/7/89	16.10	37.10	32.80	144.00	65.10	514.00	91.80

Table A3.25 Heavy Metal Concentrations in Suspended Matter of the Heathcote River

Date	Pb µg/g	Cu µg/g	Ni µg/g	Zn µg/g	Mn µg/g	Fe µg/g	Cr µg/g
26/2/88	162.00	350.00	0.00	1050.00	200.00	19100.00	-
27/4/88	153.23	28.23	0.00	455.65	173.39	18221.77	48.79
1/7/88	60.28	25.32	0.00	238.30	81.56	2602.84	16.17
10/8/88	79.55	83.33	0.00	621.21	306.82	32196.97	53.03
29/9/88	120.10	71.77	0.00	684.21	200.96	34641.15	14.35
7/11/88	157.73	48.97	0.00	479.90	205.15	29510.31	53.09
20/12/88	98.48	30.68	0.00	931.82	397.73	23810.61	87.12
7/2/89	139.29	51.92	0.00	134.62	593.41	27178.57	101.65
20/3/89	14.40	139.11	27.42	466.67	53.33	6857.78	.00
3/5/89	131.68	160.40	66.34	1148.51	128.71	18148.51	.00
15/6/89	611.46	3520.83	44.79	1687.50	125.00	33750.00	44.79
17/7/89	177.08	145.83	.00	1125.00	135.42	26562.50	156.25

(-, no data)

Table A3.26 Heavy Metal Concentrations in Suspended Matter of the Avon River

Date	Pb µg/g	Cu µg/g	Ni µg/g	Zn µg/g	Mn µg/g	Fe µg/g	Cr µg/g
26/2/88	83.75	.00	43.75	387.50	375.00	17500.00	76.25
27/4/88	68.38	29.71	.00	219.12	210.29	13161.76	44.49
1/7/88	92.38	19.05	.00	595.24	208.57	24476.19	28.00
10/8/88	150.00	1012.50	.00	1187.50	587.50	30375.00	175.00
29/9/88	132.35	14.71	.00	.00	279.41	43970.59	176.47
7/11/88	306.45	48.39	.00	1064.52	298.39	20967.74	40.32
20/12/88	66.82	5.91	.00	650.00	490.91	30772.73	28.64
7/2/89	145.83	20.83	.00	1635.42	802.08	40625.00	13.54
20/3/89	168.83	34.22	.00	647.40	145.45	23051.95	51.30
3/5/89	127.27	87.88	58.79	530.30	121.21	27727.27	44.09
15/6/89	97.22	359.26	40.74	520.37	208.33	27972.22	91.85
17/7/89	191.18	.00	.00	29.41	147.06	23970.59	51.47

Table A3.27 Heavy Metal Concentrations in Suspended Matter of the City Outfall Drain

Date	Pb µg/g	Cu µg/g	Ni µg/g	Zn µg/g	Mn µg/g	Fe µg/g	Cr µg/g
26/2/88	283.33	233.33	0.00	2083.33	1166.67	25833.33	47.50
27/4/88	314.19	0.00	85.14	210.91	445.95	39979.73	23.85
1/7/88	96.05	33.90	.00	1118.64	367.23	21299.44	5.65
10/8/88	343.75	520.83	.00	2666.67	3322.92	-	125.00
29/9/88	333.33	100.00	.00	500.00	1316.67	143000.00	.00
7/11/88	1368.42	328.95	.00	1973.68	868.42	98552.63	52.63
20/12/88	96.21	6.82	.00	848.48	1590.91	35037.88	3.03
7/2/89	166.67	24.02	.00	460.78	215.69	36450.98	4.41
20/3/89	616.53	196.20	74.21	2297.52	-	41735.54	.00
3/5/89	193.85	114.36	.00	4179.49	-	83333.33	.00
15/6/89	697.92	3607.29	.00	2604.17	-	40312.50	9.37
17/7/89	4520.83	479.17	.00	3708.33	-	58541.67	291.67

Table A3.28 Heavy Metal Concentrations in Suspended Matter of Pond 5

Date	Pb µg/g	Cu µg/g	Ni µg/g	Zn µg/g	Mn µg/g	Fe µg/g	Cr µg/g
26/2/88	11.25	123.75	75.00	162.50	175.00	3250.00	191.25
27/4/88	19.51	56.10	0.00	224.39	298.78	1678.05	51.71
1/7/88	36.98	169.03	0.00	551.62	297.38	4828.97	349.61
10/8/88	52.86	85.71	0.00	455.71	398.57	1514.29	81.43
29/9/88	51.39	90.28	59.03	229.17	371.53	4444.44	173.61
7/11/88	126.25	390.00	70.00	1085.00	657.50	6012.50	1496.25
20/12/88	16.89	50.00	0.00	446.62	797.30	533.78	108.78
7/2/89	25.00	78.33	125.83	649.17	1191.67	41.67	63.33
20/3/89	23.15	54.82	13.64	99.09	444.55	1330.00	103.45
3/5/89	43.42	228.49	76.71	227.40	217.81	3097.26	309.04
15/6/89	250.00	636.21	408.62	1512.07	455.17	10217.24	1043.10
17/7/89	93.75	51.56	160.94	728.12	100.00	3656.25	379.69

Table A3.29 Heavy Metal Concentrations in Suspended Matter of Pond 6

Date	Pb µg/g	Cu µg/g	Ni µg/g	Zn µg/g	Mn µg/g	Fe µg/g	Cr µg/g
26/2/88	23.13	164.18	89.55	208.96	1074.63	2985.07	283.58
27/4/88	36.76	86.76	63.24	289.71	116.18	955.88	63.24
1/7/88	40.59	246.31	0.00	614.39	411.44	5075.65	422.51
10/8/88	127.14	74.29	14.29	38.57	250.00	5114.29	801.43
29/9/88	31.73	1.27	0.00	209.39	266.50	3654.82	67.26
7/11/88	53.95	69.74	0.00	80.26	271.05	315.79	106.58
20/12/88	18.00	24.00	32.00	812.00	1948.00	-	156.00
7/2/89	48.43	86.39	0.00	691.10	1361.26	-	106.02
20/3/89	39.21	211.90	74.60	271.43	595.24	2095.24	236.51
3/5/89	32.43	101.80	65.32	101.35	254.50	1563.06	171.85
15/6/89	276.60	695.74	476.60	1448.94	114.89	7744.68	904.26
17/7/89	217.24	253.45	170.69	781.03	-	4724.14	905.17

-; no data

Table A3.30 Similarity Matrices for Heavy Metals in Suspended Matter

Rivers	Pb	Cu	Zn	Mn	Fe	Cr
Pb	1.00	.84	.34	.10	.30	0.00
Cu		1.00	.54	.10	.20	0.00
Zn			1.00	.27	.27	.14
Mn				1.00	.48	.27
Fe					1.00	.41
Cr						1.00

Ponds	Pb	Cu	Zn	Mn	Fe	Cr
Pb	1.00	.82	.74	.33	.69	.80
Cu		1.00	.78	.20	.73	.76
Zn			1.00	.14	.41	.66
Mn				1.00	.62	.20
Fe					1.00	.70
Cr						1.00

Drain	Pb	Cu	Zn	Mn	Fe	Cr
Pb	1.00	.10	.48	.17	.14	.89
Cu		1.00	.28	.30	.10	0.00
Zn			1.00	.40	0.00	.49
Mn				1.00	.30	.14
Fe					1.00	.14
Cr						1.00

APPENDIX 4.0 (Appendix to Chapter 6)

A4.1 HEAVY METAL DATA OF REFERENCE SD-N-1

Table A4.1 Raw SD-N-1 Data analysed by Flame Atomic Absorption Spectroscopy (HF/HNO3 Method)

Pb µg/g	Cu µg/g	Ni µg/g	Zn µg/g	Mn SA µg/g	Mn Aq µg/g	Fe SA %	Fe Aq %	Cr µg/g	ORG %
75.3	61.9	21.9	293	419	428	1.18	1.8	118	8.4
86	64	22.5	378	439	446	1.67	2.04	118	8.7
87.5	67.5	22.9	386	455	448	1.97	2.55	120	8.7
88.4	68	23.7	392	455	466	1.98	2.56	125	8.8
88.6	69.9	24.1	395	458	490	2.31	2.74	128	8.8
91.3	70	24.3	404	463	492	2.35	2.86	128	8.9
91.5	70.2	24.9	404	471	501	2.54	2.89	131	8.9
91.8	70.6	25.3	412	479	501	2.55	2.91	133	9
91.9	71	25.5	416	498	508	2.58	2.93	133	9.4
91.9	71	25.8	422	525	515	2.58	2.94	137	9.6
93.7	72.2	26	422	553	516	2.67	2.94	139	9.6
95.2	72.4	26	423	553	519	2.68	2.94	139	9.6
95.2	73.3	26.2	423	570	520	2.73	2.98	139	10.2
97.5	73.5	26.2	428	575	524	2.83	3.02	140	10.2
98.3	73.8	26.2	432	578	534	2.84	3.06	141	10.3
98.7	74.1	26.4	433	581	534	2.91	3.07	141	10.4
99	74.7	26.6	433	583	538	3.02	3.07	141	10.6
99.6	74.7	26.7	440	594	540	3.06	3.15	142	10.7
100	75	27.3	442	595	541	3.08	3.17	142	10.8
100	75.3	27.3	443	598	548	3.1	3.29	142	10.8
100	75.3	27.6	444	600	549	3.15	3.39	143	11
101	75.8	27.7	444	600	551	3.18	3.41	144	11.1
103	76.3	27.9	451	603	617	3.22	3.56	144	11.2
103	76.3	28.3	458	611	621	3.26	3.69	144	11.3
103	76.3	28.4	466	615		3.29		145	11.5
105	76.4	29.3	467	624		3.42		146	11.6
105	76.7	29.3	471	631		3.46		148	11.8
108	77	30.1	480	632		3.46		148	11.9
109	77.7	30.5	485	635		3.56		150	11.9
112	77.9	32.3	494	641		3.6		155	12
114	78.2	34.9	499	660		3.73		157	12.1
119	78.4	38.8	529	664		3.78			12.1
121	79.4		559						
123	83.6								

Table A4.2 Raw SD-N-1 Data analysed by Flame Atomic Absorption Spectroscopy (HNO3 Method)

Pb µg/g	Cu µg/g	Ni µg/g	Zn µg/g	Mn Aq µg/g	Fe Aq %	Cr µg/g
74.4	59.5	18.2	260	447	2.26	48.8
81.3	69.2	20.5	277	453	2.33	49.1
91.2	70.7	20.7	288	470	2.39	56.3
91.2	70.7	20.8	299	479	2.39	66.5
94.2	73.5	21	325	495	2.48	68.2
95	73.5	21	375	496	2.54	69.5
95	73.5	21.2	381	504	2.6	78.8
95	73.6	21.5	382	508	2.66	85.5
96.5	74.3	21.6	385	509	2.79	88.5
98	74.4	21.7	393	545	2.84	89.2
98.8	74.6	22	402	546	3.07	89.3
101	74.6	22.4	402	546	3.51	89.4
101	74.6	23.5	404	570		91
102	75.5	23.5	406	570		95.9
103	75.9	23.9	407	571		98.2
103	76.3	24.1	409			
103	76.5	24.3	410			
111	76.6	24.9	417			
112	77		422			
113	77.3		437			
114						

Table A4.3 Raw Data Secondary References

	Pb µg/g	Cu µg/g	Ni µg/g	Zn µg/g	Fe SA %	Fe Aq %	Mn SA µg/g	Mn Aq µg/g	Cr µg/g	ORG %
SA1B9										
	3.66	5.58	9.3	19	1.12	1.26	43.2	33.8	24.4	1.09
	3.71	5.67	10.1	19.4	1.3	1.37	53.9	35.1	27.6	1.26
	3.74	5.86	10.2	19.7	1.76	1.41	59.9	39.8	28.5	1.54
	3.93	6.01	11.5	21		1.52		62.1	28.9	1.74
		6.27	11.5	21.4					30.7	
ZT3										
	2.85	5.23	8.2	22.9	1.76	1.45	56.1	37	24.4	1.42
	3.26	5.47	8.52	23.7	1.84	1.52	64.9	47.4	28.4	1.53
	4.86	5.56	8.65	25.7	1.92	1.61	67.1	49.4	28.5	1.59
	5.64	5.84	8.72	28	2.07	1.72	75.3	51	29.7	1.65
		5.84	8.94	33.4	2.12	1.72	76.1	52.5	30.6	1.77
		7.48	9.09	34.5		1.77			31.3	1.92
		7.97	9.86			1.79			34.5	2.04
CT3										
	28.1	19.1	20.1	94.9	3.72	3.54	253	212	67.6	3.69
	31.6	19.4	24.3	118	4.14	3.8	284	220	67.9	3.84
	33.7	20.7	26	123	4.26	3.99	310	221	70.9	3.89
	36.6	22.7	26.3	127	4.54	4.51	328	243	71.5	4.22
	39	24	31.5	174	5.66	4.65	354	272	71.9	4.33
	39.2		32.3	179		4.95	366		84.2	4.78
	40.9		34.1						96.2	5.93
	42.5									

SA, Standard Additions; Aq, aqueous calibration.

Table A4.4 Raw Data of Bayesian Statistical Analysis of Secondary References

Statistic	Pb µg/g	Cu µg/g	Ni µg/g	Zn µg/g	Fe %	Mn µg/g	Cr µg/g	ORGANIC %
SA1B9								
Θ^2	.2	.1	1.7	4.6	.0	14.9	3.7	.0
Vo	38.0	36.0	36.0	36.0	36.0	36.0	36.0	38.0
σ^2o	.2	.1	1.6	4.4	.0	14.1	3.5	.0
S^2	.0	.3	3.7	4.4	.0	594.0	21.4	.3
σ^2	.2	.1	1.6	4.2	.0	28.3	3.7	.0
Xe (t=∞)	.4	.3	1.1	1.8	.2	4.7	1.5	.2
Xe (%)	12.0	5.0	10.5	8.9	13.1	10.5	5.5	12.0
ZT3								
Θ^2	.3	.1	1.2	9.0	.1	16.9	4.5	.0
Vo	34.0	39.0	36.0	36.0	32.0	36.0	36.0	36.0
σ^2o	.3	.1	1.1	8.5	.1	16.0	4.2	.0
S^2	5.2	6.9	1.7	121.0	.1	151.0	117.0	.3
σ^2	.4	.3	1.1	10.7	.0	18.6	6.4	.0
Xe (t=∞)	.6	.4	.8	2.6	.2	3.8	1.8	.1
Xe (%)	14.7	6.2	8.6	9.3	9.6	8.0	5.7	8.6
CT3								
Θ^2	14.1	1.5	12.1	212.0	.4	411.0	27.1	.2
Vo	36.0	36.0	36.0	36.0	35.0	36.0	36.0	35.0
σ^2o	13.3	1.4	11.4	200.0	.3	388.0	25.6	.2
S^2	171.0	18.1	151.0	5545.0	1.5	2376.0	674.0	3.6
σ^2	15.5	1.8	13.7	319.0	.3	419.0	38.9	.3
Xe (t=∞)	2.7	1.2	2.7	14.2	.5	17.9	4.6	.4
Xe (%)	7.5	5.5	9.9	10.5	10.9	7.7	6.1	9.2

Θ^2, "prior" estimate of variance (σ^2); σ^2o, Vo, statistical parameters of equations 1, 2, and 4 of Lindley (1965) (see Chapter 6 for details); σ^2, variance determined by Bayesian Statistics; Xe, error, at 95% confidence, of Secondary References determined by the method of Lindley (1965); Xe (%), Xe expressed as a percentage of the mean X.

A4.3 SOLUTIONS TO EQUATIONS OF LINDLEY (1965)

Equations 1) and 2) (Chapter 6) of Lindley (1965) were solved for σo^2, and Vo by Professor J.J.Deely of Department of Mathematics, University of Canterbury. The calculations are as follows:

Equation 1),

$$E(\Theta) = \sigma o^2 Vo/Vo-2 \qquad (=\Theta^2) \qquad 1)$$

Equation 2),

$$D^2(\Theta) = 2\sigma o^4 Vo^2/(Vo-2)^2(Vo-4) \quad (=var\Theta^2) \qquad 2)$$

Rearrange 2),

$$var\Theta^2 = 2(\sigma o^2 Vo/Vo-2)^2 1/Vo-4 \qquad 3)$$

substitute 1) into 3),

$var\Theta^2 = 2(\Theta^2)^2 1/Vo-4$ and rearrange to get,

$$Vo = 4+2(\Theta^2)^2/var\Theta^2 \qquad A)$$

Rearrange 1),

$\sigma o^2 = \Theta^2(Vo-2)/Vo$,

therefore,

$$\sigma o^2 = \Theta^2(1-2/Vo) \qquad B)$$

From equations A and B the estimate of the true variance σ^2 can be computed by:

$$\sigma^2 = Vo\sigma o^2 + S^2/Vo \div n-2, \qquad C)$$

where n is the number of analyses and S^2 is s^2/n from the

data. The variance of the final estimate of σ^2 can also be computed using:

$$\text{var}\sigma^2 = 2(Vo\sigma o^2+S^2)^2/(Vo+n-2)^2(Vo+n-4).$$

The $\text{var}\sigma^2$ was not calculated in this study.

RADIOCARBON DATING RESULT SHEET

Date: 2/10/87 File: CA/4/1

Charging Category: C

R No. 11511/1 INS No. CR 8366

NZ No. 7448 PR C 3640

Contributor's No. M35/f26 AR

Sample : Shells (Mactra ovata)

Locality : Avon-Heathcote Estuary, Christchurch

Contributor(s) : J.M. Deely

Collection date : 8/8/87 Carbon % XRD Aragonite

Collector's age estimate 150 years BP

Pretreatment :

Gas counting Counting time 1000 min.

RESULTS

A. Age wrt modern standard NZ marine shell (-41 ‰)(note 1)

Based on Libby $T_{1/2}$ (5568 yr)	POST BOMB	±	yr BP (note 2)
Based on new $T_{1/2}$ (5730 yr)	-	±	yr BP (note 3)
Corrected for secular variation (a)	-	±	yr BP (note 4)
(b)	-	-	yr BP (note 5)
Percent modern	120.0	± 0.7	% (note 6)

B. Isotope data and enrichment

$\delta^{13}C$ wrt PDB	-3.6	± 0.1	‰
$\delta^{14}C$ wrt 0.95 NBS Ox. Ac. Std.		±	‰ (note 7)
$\Delta^{14}C$ wrt 0.95 NBS Ox. Ac. Std.		±	‰ (note 8)

Remarks

(Notes PTO)

RADIOCARBON DATING RESULT SHEET Date: 6/10/87 File: CA/4/1

Charging Category: C

R No. 11511/2 INS No. CR 8368

NZ No. 7459 PR B 7512

Contributor's No. M36/f43 AR

Sample : Shells (various species)

Locality : Avon-Heathcote Estuary, Christchurch

Contributor(s) : J.E. Deely

Collection date : 8/8/87 Carbon ____ % XRD Most species Aragonite

Collector's age estimate <200 years B.P.

Pretreatment :

Gas counting Counting time 2000 min.

RESULTS

A. Age wrt modern standard NZ Shell			(-41 °/₀₀)(note 1)
Based on Libby $T_{1/2}$ (5568 yr)	361	± 110	yr BP (note 2)
Based on new $T_{1/2}$ (5730 yr)	371	± 110	yr BP (note 3)
Corrected for secular variation (a)		±	yr BP (note 4)
(b)		-	yr BP (note 5)
Percent modern w.r.t. shell std	95.6	± 1.3	% (note 6)
B. Isotope data and enrichment			
$\delta^{13}C$ wrt PDB	1.47	± 0.1	°/₀₀
$\delta^{14}C$ wrt 0.95 NBS Ox. Ac. Std.		±	°/₀₀ (note 7)
$\Delta^{14}C$ wrt 0.95 NBS Ox. Ac. Std.		±	°/₀₀ (note 8)

Remarks

(Notes PTO)

RADIOCARBON DATING RESULT SHEET Date: 6/10/87 File: CA/4/1

Charging Category: C

R No. 11511/3 INS No. CR 8369

NZ No. 7460 PR B 7514

Contributor's No. M36/f44 AR

Sample : Shells (various species)

Locality : Avon-Heathcote Estuary, Christchurch

Contributor(s) : J.M. Deely

Collection date : 8/8/87 Carbon ____ % XRD assumed all Aragonite

Collector's age estimate 200-1000 years BP

Pretreatment :

Gas counting Counting time 2000 min.

RESULTS

A. Age wrt modern standard NZ shell (-41 °/₀₀)(note 1)

Based on Libby $T_{1/2}$ (5568 yr)	342	± 60	yr BP	(note 2)
Based on new $T_{1/2}$ (5730 yr)	352	± 60	yr BP	(note 3)
Corrected for secular variation (a)		±	yr BP	(note 4)
(b)		-	yr BP	(note 5)
Percent modern	95.8	± 0.7	%	(note 6)

B. Isotope data and enrichment

$\delta^{13}C$ wrt PDB	0.63	± 0.1	°/₀₀	
$\delta^{14}C$ wrt 0.95 NBS Ox. Ac. Std.		±	°/₀₀	(note 7)
$\Delta^{14}C$ wrt 0.95 NBS Ox. Ac. Std.		±	°/₀₀	(note 8)

Remarks

(Notes PTO)

Notes : (1) C-14 ages and standard deviations (based on counting statistics only) are rounded as follows :

0 to 1000 yr, nearest 1
1000 to 2000 yr, nearest 5
2000 to 10,000 yr, nearest 10
10,000 to 20,000 yr, nearest 50
20,000 yr and higher, nearest 100.

Limit-ages and percent modern at the limit are given for 3 standard deviations.

Uncertainty in the C-14 lifetime has been excluded from the statistical calculations.

Present year = 1950 AD

(2) Age used for NZ C-14 age lists.

(3) Godwin (1962), Nat. 195 984.

(4) Clark (1975), Antiquity XLIX 251

(5) Klein et al. (1982), Radiocarbon 24 103

(6) Percent modern = $[A_i/A_0(1 + d)]$ 100

$= [\exp(-age/T_m)]$ 100

(7) $\delta^{14}C$ (age-corrected) = $[(A/A_0') - 1]$ 1000

(8) $\Delta^{14}C$ (age-corrected) = $[(A_i/A_0') - 1]$ 1000

A = sample activity at year of collection, A_0 = 0.95 NBS Ox. Ac. Std. activity, A_0' = A_0 age-corrected to 1958, A_i = A corrected for the isotope effect, d = modern std. correction (∇ 10^{-3}) and T_m is the mean lifetime of ^{14}C (8268 yr).

RADIOCARBON (^{14}C) RESULT SHEET

Date: 4/12/86 File: CA/4/1

Charging Category: X

R No. 11319 INS No. CR 8182

NZ No. 7288 PR B 7366

Contributor's No. M35/f25 AR

Sample : Shells (Chione)

Locality : North New Brighton, Christchurch

Contributor(s) : G.H. Browne

Collection date : 11/4/86 Carbon % XRD <1.5% calcite

Collector's age estimate 1000-3000 years B.P.

Pretreatment :

Gas counting / Counting time 3000 min.

RESULTS

A. Age wrt modern standard	NZ Shell Std	(-41 °/₀₀)	(note 1)
Based on Libby $T_{1/2}$ (5568 yr)	1630	± 50 yr BP	(note 2)
Based on new $T_{1/2}$ (5730 yr)	1670	± 50 yr BP	(note 3)
Corrected for secular variation (a)		± yr BP	(note 4)
(b)		- yr BP	(note 5)
Percent modern	81.7	± 0.5 %	(note 6)
B. Isotope data and enrichment			
$\delta^{13}C$ wrt PDB	-0.08	± 0.1 °/₀₀	
$\delta^{14}C$ wrt 0.95 NBS Ox. Ac. Std.		± °/₀₀	(note 7)
$\Delta^{14}C$ wrt 0.95 NBS Ox. Ac. Std.		± °/₀₀	(note 8)

Remarks

(Notes, PTO)

PLEASE SEND AN AMENDED STATEMENT OF SIGNIFICANCE TO NZGS

Notes : (1) C-14 ages and standard deviations (based on counting statistics only) are rounded as follows :

0 to 1000 yr, nearest 1
1000 to 2000 yr, nearest 5
2000 to 10,000 yr, nearest 10
10,000 to 20,000 yr, nearest 50
20,000 yr and higher, nearest 100.

Limit-ages and percent modern at the limit are given for 3 standard deviations.

Uncertainty in the C-14 lifetime has been excluded from the statistical calculations.

Present year = 1950 AD

(2) Age used for NZ C-14 age lists.

(3) Godwin (1962), Nat. 195 984.

(4) Clark (1975), Antiquity XLIX 251

(5) Klein et al. (1982), Radiocarbon 24 103

(6) Percent modern = $[A_i/A_0(1 + d)]$ 100

$= [\exp(-age/T_m)]$ 100

(7) $\delta^{14}C$ (age-corrected) $= [(A/A_0') - 1]$ 1000

(8) $\Delta^{14}C$ (age-corrected) $= [(A_i/A_0') - 1]$ 1000

A = sample activity at year of collection, A_0 = 0.95 NBS Ox. Ac. Std. activity, A_0' = A_0 age-corrected to 1958, A_i = A corrected for the isotope effect, d = modern std. correction (∇ 10^{-3}) and T_m is the mean lifetime of ^{14}C (8268 yr).

KEY

Original Christchurch area (now the City Centre)

Railway line

Former Mortens Jetty

Former and present Outfalls

Retaining wall

Swamp

0 1km

LEGEND

M.B. McCormacks Bay

ADDITIONAL STREETS/LOCATIONS

1 Acland St
2 Antigua St
3 Armstrong Ave
4 Aynsley Tce
5 Barbadoes St
6 Barrington St
7 Beachville Rd
8 Bells Creek (Gas Works Drain)
9 Bexley Bridge
10 Bower Ave
11 Bricks
12 Bridge St
13 Butler St
14 Canal Reserve
15 Carlton Bridge
16 Carlyle St
17 Cashmere Bridge
18 Caspian St
19 Cathedral Square
20 Catherine St
21 Charlesworth St
22 Colombo St
23 Ebbtide St
24 Ford St
25 Frosts Rd
26 Garlands Road Bridge
27 Glenelg Spur
28 Godwit St
29 Hereford St
30 Idris St
31 Jacksons Rd
32 Jellicoe St
33 Long St
34 Madras St
35 Moabone Point Cave
36 Oxford Tce
37 QE II Park
38 Radley St
39 Rapaki Rd
40 Rat Island
41 Rockinghorse Rd
42 Seaview Rd
43 Torea Lane
44 Tuam St
45 Wainoni Rd
46 Waltham Rd
47 Wigram
48 Wilsons Bridge

FIG. 2 Location Map of the Christchurch area